

WCAP-17788-NP  
Volume 1, Revision 1

December 2019

# **Comprehensive Analysis and Test Program for GSI-191 Closure (PA-SEE-1090)**



**framatome**



UNITED STATES  
NUCLEAR REGULATORY COMMISSION  
WASHINGTON, D.C. 20555-0001

June 13, 2019

MEMORANDUM TO: Mirela Gavrilas, Director  
Division of Safety Systems  
Office of Nuclear Reactor Regulation

FROM: Victor G. Cusumano, Chief /RA/  
Technical Specifications Branch  
Division of Safety Systems  
Office of Nuclear Reactor Regulation

SUBJECT: TECHNICAL EVALUATION REPORT OF IN-VESSEL DEBRIS  
EFFECTS

By letter dated July 17, 2015, the Pressurized Water Reactor (PWR) Owner's Group submitted a licensing topical report, WCAP-17788, "Comprehensive Analysis and Test Program for GSI [Generic Safety Issue]-191 Closure" (Agencywide Documents Access and Management System (ADAMS) Accession No. ML15210A667). WCAP-17788 was intended to support the closure of GSI-191, "Assessment of Debris Accumulation on PWR Sump Performance," and Generic Letter (GL) 2004-02, "Potential Impact of Debris Blockage on Emergency Recirculation During Design Basis Accidents at Pressurized-Water Reactors," dated September 13, 2004 (ADAMS Accession No. ML042360586), by creating a methodology to define an in-vessel fibrous debris limit to respond to in-vessel questions in GL 2004-02.

The review of WCAP-17788 identified several issues that were not readily resolved. As a result, the staff of the U.S. Nuclear Regulatory Commission (NRC) reevaluated the overall significance of the effects of debris on in-vessel blockage considering improvements in understanding gained in recent years. This is in accordance with Office of Nuclear Reactor Regulation efforts to ensure that agency resources are expended on issues commensurate with their safety significance. As part of that evaluation of safety significance, the enclosed technical evaluation report (TER) evaluated the effects of debris on in-vessel blockage against risk thresholds consistent with the Commission's health objectives. The NRC staff determined that the issue is generally of low safety significance.

CONTACTS:	Ashley Smith 301-415-3201	Stephen Smith 301-415-3190	Paul Klein 301-415-3040	Ben Parks 301-415-0979
	Matt Yoder 301-415-4017	Shilp Vasavada 301-415-1228	Andrea Russell 301-415-8553	



In part, GL 2004-02 requested licensees to evaluate in-vessel effects for their plants. The NRC staff is evaluating compliance with Title 10 of the *Code of Federal Regulations* 50.46, "Acceptance Criteria for Emergency Core Cooling Systems for Light-Water Nuclear Power Reactors," also requested in GL 2004-02, separately from the enclosed TER. The information contained in the TER, however, may be useful to staff and licensees while evaluating compliance with that regulation.

Enclosure: Technical Evaluation Report

## SUBJECT: TECHNICAL EVALUATION REPORT OF IN-VESSEL DEBRIS EFFECTS

Dated: June 13, 2019

DISTRIBUTION:

VCusumano, NRR	ASmith, NRR	SSmith, NRR	NON-PUBLIC
SVasavada, NRR	RLukes, NRR	MYoder, NRR	SBloom, NRR
ARussell, NRR	LPerkins, NRR	PKlein, NRR	JDrake, NRR
MReisi-Fard, NRR	JBorromeo, NRR	JDonoghue, NRR	CHoxie, RES
MGavrilas, NRR	BBenney, NRR	TZaki, RES	GCasto, NRR
SBajorek, RES	JStaudenmeier, RES	BParks, NRR	

**ADAMS ACCESSION NO. ML19073A044****\*concurred via e-mail****NRR-106**

OFFICE	NRR/DSS/SRXB	NRR/DSS/STSB	NRR/DMLR/MCCB	NRR/DSS/SNPB
NAME	ASmith*	SSmith*	PKlein*	BParks*
DATE	5/30/2019	5/29/2019	5/31/2019	6/4/2019
OFFICE	NRR/DSS/STSB	NRR/DRA/RILIT: TL (Acting)	NRR/DMLR/MCCB	NRR/DLP/LA
NAME	ARussell*	SVasavada*	MYoder*	DHarrison*
DATE	5/29/2019	6/3/2019	5/31/2019	6/5/2019
OFFICE	QTE	NRR/DSS/SNPB: BC	NRR/DRA/APLB:BC (Acting)	NRR/DSS/SRXB :BC (Acting)
NAME	JDougherty*	RLukes*	MReisi-Fard*	JBorromeo*
DATE	3/21/19	6/10/2019	6/7/2019	6/5/2019
OFFICE	NRR/DMLR/MCCB: BC	RES/DSA/CRAB: BC	NRR/DSS/STSB:BC	
NAME	SBloom*	CHoxie*	VCusumano	
DATE	6/5/2019	5/19/2019	6/13/2019	

**- OFFICIAL RECORD COPY -**

**TECHNICAL EVALUATION REPORT OF  
IN-VESSEL DEBRIS EFFECTS**

WCAP-17788-NP

**Enclosure**  
December 2019  
Volume 1, Revision 1

\*\*\* This record was final approved on 12/12/2019 9:56:16 PM (This statement was added by the PRIME system upon its validation)

## Contents

<b>1.0 EXECUTIVE SUMMARY .....</b>	<b>- 2 -</b>
<b>2.0 LIST OF ACRONYMS .....</b>	<b>- 3 -</b>
<b>3.0 INTRODUCTION.....</b>	<b>- 4 -</b>
<b>4.0 BACKGROUND.....</b>	<b>- 6 -</b>
4.1 Overview of WCAP-17788.....	- 8 -
<b>5.0 TECHNICAL EVALUATION .....</b>	<b>- 8 -</b>
5.1 System Description.....	- 11 -
5.1.1 Key Parameters.....	- 12 -
5.2 Sequence of Events .....	- 13 -
5.2.1 Availability of Emergency Core Cooling System Primary Flowpath .....	- 13 -
5.2.1.1 Cold-Leg Break .....	- 15 -
5.2.1.1.1 Debris Collection at the Core Inlet .....	- 18 -
5.2.1.1.2 Boric Acid Precipitation .....	- 20 -
5.2.1.1.3 Debris Suspended in the Core .....	- 22 -
5.2.1.1.4 Local Collection of Debris .....	- 23 -
5.2.1.1.5 Concentration of Particulate Debris .....	- 23 -
5.2.1.1.6 Conclusions for the Cold-Leg Break .....	- 25 -
5.2.1.2 Hot-Leg Break.....	- 26 -
5.2.1.2.1 Fiber Penetration .....	- 28 -
5.2.1.2.2 Boric Acid Precipitation .....	- 30 -
5.2.1.2.3 Conclusions for the Hot-Leg Break .....	- 30 -
5.2.1.3 Upper Plenum Injection Plants.....	- 31 -
5.2.1.3.1 Conclusions for Upper Plenum Injection Plants.....	- 32 -
5.2.1.4 Debris Generation and Transport.....	- 33 -
5.2.1.5 Chemical Effects .....	- 34 -
5.2.1.5.1 Testing .....	- 34 -
5.2.1.5.2 Test Results—Precipitation Timing.....	- 37 -
5.2.1.5.3 Staff Analysis of Precipitate Timing .....	- 38 -
5.2.1.5.4 Chemical Deposits on Fuel .....	- 39 -
5.2.1.6 Conclusion—Availability of Primary Flowpath.....	- 39 -
5.3 Defense in Depth.....	- 39 -

5.3.1	Containment .....	- 40 -
5.3.2	Operator Actions .....	- 40 -
5.3.3	Alternate Flowpaths.....	- 40 -
5.3.3.1	Background .....	- 41 -
5.3.3.2	Simplifying Assumptions .....	- 41 -
5.3.3.3	Description of Analyses.....	- 42 -
5.3.3.4	Analytic Methods.....	- 44 -
5.3.3.5	Conservative Assumptions.....	- 44 -
5.3.3.6	Results .....	- 45 -
5.4	TRACE Sensitivity Studies .....	- 46 -
5.4.1	CLB .....	- 47 -
5.4.1.1	Westinghouse Upflow Plant .....	- 48 -
5.4.1.1.1	<i>Blockage at the Lower Core Plate (99 percent)</i> .....	- 49 -
5.4.1.1.2	<i>Blockage at the Lower Core Plate (99.5 and 99.9 percent)</i> .....	- 49 -
5.4.1.1.3	<i>Blockage at the Fuel Inlet Nozzles (99 and 100 Percent)</i> .....	- 49 -
5.4.1.1.4	<i>Blockage at the Fuel Inlet Nozzle with Delayed HLSO (100 percent)</i> ....	- 50 -
5.4.1.1.5	<i>Core Power Sensitivity</i> .....	- 50 -
5.4.1.1.6	<i>Axial Power Shape Sensitivities</i> .....	- 50 -
5.4.1.1.7	<i>Large Split Break at Top of CL</i> .....	- 50 -
5.4.1.2	Combustion Engineering Plant.....	- 51 -
5.4.1.3	TRACE Study Applicability to the PWR Fleet .....	- 51 -
5.4.2	HLB .....	- 52 -
5.4.2.1	Westinghouse Upflow Plant .....	- 52 -
5.4.2.2	Combustion Engineering Plant.....	- 53 -
5.4.3	Applicability to the Pressurized Water Reactor Fleet .....	- 53 -
5.5	Integrated Decisionmaking .....	- 54 -
5.5.1	Determination of Safety Significance .....	- 54 -
5.5.2	Risk Insights – Initiating Event (LOCA) Frequencies .....	- 55 -
5.5.3	Safety Margins .....	- 57 -
6.0	<b>CONCLUSION</b> .....	- 59 -
7.0	<b>REFERENCES</b> .....	- 60 -

## 1.0 EXECUTIVE SUMMARY

Generic Safety Issue (GSI)-191, "Assessment of Debris Accumulation on PWR [pressurized water reactor] Sump Performance," is a longstanding issue and a brief background of the issue is included in this technical evaluation report (TER). Initial efforts by industry and the U.S. Nuclear Regulatory Commission (NRC) evaluated sump strainer blockage. More recent testing and analysis focused on the potential for fine debris to pass through the sump strainer and block the reactor vessel (RV) core inlet (in-vessel downstream effects (IVDEs)). The NRC staff's safety evaluation (SE) of the initial Pressurized Water Reactor Owner's Group (PWROG) fuel assembly (FA) test program in WCAP-16793-NP-A, Revision 2, "Evaluation of Long Term Cooling Considering Particulate, Fibrous and Chemical Debris in the Recirculating Fluid," issued July 2013 (1) resulted in a core fiber limit that permitted approximately one third of operating PWRs to successfully demonstrate long-term core cooling (LTCC).

A second PWROG in-vessel testing and analysis program, described in WCAP-17788, "Comprehensive Analysis and Test Program for GSI-191 Closure," submitted July 2015 (2), used a design specific approach and considered phenomena timing to justify higher plant specific in vessel fiber amounts. The NRC staff reviewed WCAP-17788 but did not complete its review or determine that WCAP-17788 could be approved for use by licensees. However, during its review of WCAP-17788, the NRC staff identified a significant amount of evidence indicating that potential IVDEs have low safety significance.

The evaluation documented in this TER combines the evidence in WCAP-17788 with the NRC staff's independent analyses and evaluations to provide a more definitive conclusion regarding the safety significance of IVDEs. The staff used risk insights to differentiate the type of evaluation performed based on the likelihood of a break size. For more likely (smaller) breaks, mechanistic analyses for some of the highest fiber plants showed successful mitigation of IVDEs. For less likely (larger) breaks, the NRC staff established that the safety significance is low by considering the low initiating event frequencies and thermal hydraulic (TH) analyses which show that even in the case of substantial core inlet blockage, alternate flow paths (AFPs) through the core barrel-baffle region should be effective for all operating plant designs. All evidence considered indicated that IVDEs are unlikely to compromise LTCC following a loss-of-coolant accident (LOCA).

The staff evaluation considered differences in plant designs, and the differing system responses associated with various break locations. The staff considered cold leg (CL) and hot leg (HL) breaks separately because of differences in plant response and issues (e.g., boric acid precipitation (BAP)) that are more significant for certain types of breaks. Plants with upper plenum injection (UPI) were also considered separately because of their unique design features. The timing of chemical precipitation was considered in relation to the timing of post-LOCA actions. FA tests have shown that higher fiber quantities can be tolerated if no precipitates are present, while actions such as switching to HL recirculation would mitigate the impact of any precipitates by bypassing any blockage and potentially disrupting bed formation at the core inlet.

This TER applied a novel approach to conclude that the safety significance of IVDEs is low since post LOCA debris is unlikely to result in a loss of LTCC. It is not intended to establish compliance with existing regulations (i.e., Title 10 of the *Code of Federal Regulations* (10 CFR) 50.46, "Acceptance Criteria for Emergency Core Cooling Systems for Light Water Nuclear Power Reactors") (3). The NRC staff is evaluating compliance in an effort separate from this TER. The information contained in the TER, however, may be useful to staff and licensees while evaluating compliance with that regulation.

## 2.0 LIST OF ACRONYMS

ADAMS	Agencywide Documents Access and Management System
AFP	alternate flow path
ANL	Argonne National Laboratory
ANS	American Nuclear Society
ANSI	American National Standards Institute
B&W	Babcock & Wilcox
BAP	boric acid precipitation
BB	barrel/baffle
BN	bottom nozzle
BWNT	Babcock & Wilcox Nuclear Technologies
CDF	Core Damage Frequency
CE	Combustion Engineering
CFR	<i>Code of Federal Regulations</i>
CL	cold leg(s)
CLB	cold-leg break(s)
CSS	containment spray system
CVCS	chemical and volume control system
DC	downcomer
DEGB	double-ended guillotine break
DID	defense-in-depth
ECCS	emergency core cooling system
EM	evaluation model
EPRI	Electric Power Research Institute
F	Fahrenheit
FA	fuel assembly
g/FA	grams per fuel assembly
GL	Generic Letter
GSI	Generic Safety Issue
HPI	high pressure injection
HL	hot leg
HLB	hot-leg break
HLSO	hot-leg switchover
IBOB	initial set of autoclave tests with debris not in mesh bags
IVDE	in-vessel downstream effects
LOCA	loss-of-coolant accident
LOCADM	Loss-of-Coolant Accident Deposition Model
LP	lower plenum
LTCC	long-term core cooling
NRC	Nuclear Regulatory Commission
NRR	Office of Nuclear Reactor Regulation
PCT	peak cladding temperature
psi	pounds per square inch
PTFE	polytetrafluoroethylene
PWR	pressurized water reactor
PWROG	Pressurized Water Reactor Owners Group
RAI	request for additional information
RCS	reactor coolant system

RES	Office of Nuclear Regulatory Research
RG	Regulatory Guide
RLBLOCA	realistic large-break LOCA
RV	reactor vessel
RWST	refueling water storage tank
SE	safety evaluation
SG	steam generator(s)
SI	safety injection
SSO	sump switchover
STB	sodium tetraborate
STP	South Texas Project
TER	technical evaluation report
TH	thermal-hydraulic(s)
TSP	trisodium phosphate
UP	upper plenum
UPI	upper plenum injection
WCAP	Westinghouse Technical Report Number Preface (formerly Westinghouse Commercial Atomic Power)
ZOI	zone of influence

### **3.0 INTRODUCTION**

Each operating PWR licensee is required to demonstrate that LTCC can be maintained as required by 10 CFR 50.46, considering that debris may have an impact on system function. This provides assurance that the emergency core cooling system (ECCS) strainers will function adequately, that the ECCS and containment spray system (CSS) pump net positive suction head margins are maintained, and that downstream components do not become blocked or damaged by debris that may pass through the strainer.

The NRC staff issued Generic Letter (GL) 2004-02, "Potential Impact of Debris Blockage on Emergency Recirculation During Design Basis Accidents at Pressurized Water Reactors," dated September 13, 2004 (4) to request PWR licensees to evaluate the effects of debris on LTCC as stated in 10 CFR 50.46(b)(5). Specifically, 10 CFR 50.46(b)(5) requires that the calculated core temperature shall be maintained at an acceptably low value and decay heat shall be removed for the extended period of time required by the long-lived radioactivity remaining in the core, following the initial system transient that results from a primary system coolant pipe break. Information in GL 2004-02 summarizes applicable operating experience and previous NRC generic communications, including GSI-191. Considered together, GL 2004-02, GSI-191, and the operating experience referenced within these documents, describe the impact that debris can have on LTCC.

The industry response to GL 2004-02 included: (1) substantial improvements to plant safety via ECCS recirculation sump design modifications and enhancements to containment cleanliness and (2) increases in phenomenological understanding of the various issues associated with LTCC when considering the presence of debris. Examples of the former include the installation of significantly larger ECCS suction strainers and reductions of potential debris sources in PWR containments. Examples of the latter include a large body of experimental testing, advances in investigating the risk significance through probabilistic risk analysis, and investigation of downstream effects using computer codes for TH analysis. However, IVDEs remain unresolved



for approximately two-thirds of the PWR fleet. This report evaluates the overall safety significance of IVDEs.

The NRC staff conducted this technical evaluation in accordance with Office of Nuclear Reactor Regulation (NRR) efforts to ensure that in expending agency resources, the staff gives priority to issues in accordance with their safety significance (see Section 5.5). Given the ongoing technical issues with portions of the TH analysis in WCAP-17788, the staff reevaluated the overall significance of the effects of debris on in-vessel blockage, considering improvements in understanding gained in recent years. Alternative means of demonstrating ECCS performance and compliance with 10 CFR 50.46, as requested in GL 2004-02, are being developed separately, and may be informed by this evaluation.

The NRC staff used an integrated decisionmaking process to make its conclusions regarding IVDEs. This TER relies on engineering judgment, and qualitative and quantitative evidence, including risk insights. The staff approach is provided within the following sections of the TER:

- Section 4.0, "Background," provides an overview of the GSI-191 history.
- Section 5.0, "Technical Evaluation," describes the scenario that requires evaluation of IVDEs at a high level.
- Section 5.1, "System Description," describes the initial plant response to a large LOCA. This section also includes the key parameters that affect the reliability of the primary flow path and/or DID risk insights.
- Section 5.2, "Sequence of Events," describes phenomena that apply to all LOCA scenarios. It also describes how hot-leg breaks (HLBs) and cold-leg breaks (CLBs) affect the system response for typical PWR designs and UPI designs. This section evaluates chemical effects and subscale FA testing and associated analyses. Finally, this section provides the basis for the staff conclusion that the primary coolant flow path (through the fuel inlet nozzles) will provide adequate LTCC.
- Section 5.3, "Defense in Depth (DID)," discusses plant options to provide LTCC if debris completely blocks the core inlet. The DID topics include containment, operator actions, and AFPs.
- Section 5.4, "TRACE Sensitivity Studies," provides a summary of supplemental NRC calculations.
- Section 5.5, "Integrated Decisionmaking," defines the criterion NRC staff used to determine safety significance. Section 5.5 also establishes an expected frequency for initiating events that could challenge LTCC due to IVDEs. Finally, Section 5.5 considers margins that provide confidence that the scenarios that are considered to successfully maintain LTCC through the design flow path will be successful.

In addition to the testing and analysis performed by the PWROG in support of WCAP-17788, the NRC staff used additional information and engineering judgment to inform the TER conclusions, as summarized below.

- In WCAP-17788, the PWROG referred to heated rod testing (5) and brine testing (6). The staff reviewed these test programs to determine the extent to which the information

from them could be used in the TER. The test programs demonstrated phenomenological behavior and are referred to solely in this respect.

- The NRC staff used a combination of information from WCAP-17788 and independent NRC staff TRACE TH analyses to reach the conclusions in this TER. The WCAP-17788 analyses were performed using computer codes approved for some aspects of LOCA analysis, but not specifically for application to LTCC. The novelty of the application led to significant questions during the WCAP-17788 review. These issues and the staff approach for addressing them are discussed further in Section 5.3.3. The analyses were not typical of licensing basis LOCA calculations in that they were not plant specific and lacked rigorous qualification for some key phenomena in the models. The staff determined that the results are representative of the classes of plants being modeled. The staff used the analyses to determine acceptable HLB fibrous debris loads, demonstrate typical flow patterns within the RV, and demonstrate AFP viability. The staff considers the use of the WCAP-17788 analysis results, in combination with the independent NRC staff TRACE results, sufficient to support the TER conclusions.

This TER is an evaluation of the general safety significance of IVDEs. The staff believes this analysis is significantly conservative compared to typical operating US PWRs, but it is not an evaluation of any specific plant. It does not address methods for plants to demonstrate compliance with regulations or define licensing basis parameters for the IVDE issue.

#### **4.0 BACKGROUND**

As discussed above, GL 2004-02 required plants to evaluate the effects of debris on LTCC as defined in 10 CFR 50.46.

In the NRC document, "Revised Content Guide for Generic Letter 2004-02 Supplemental Responses," issued November 2007 (7), the NRC staff identified several areas for licensees to evaluate to ensure that plants have the ability to mitigate LOCAs. All plants performed evaluations to address the areas delineated in the content guide. The technical areas of the content guide fall into two general categories, strainer and downstream effects. The downstream effects are further split into in-vessel effects and effects on other equipment. Industry developed guidance to address evaluation of the strainer and downstream effects on equipment (Nuclear Energy Institute 04-07, Volume 1, "Pressurized Water Reactor Sump Performance Evaluation Methodology," issued December 31, 2004 (8), and WCAP-16406, Revision 1, "Evaluation of Downstream Sump Debris Effects in Support of GSI 191," issued March 2008 (9)). The NRC endorsed this guidance with modifications.

All licensees addressed aspects of the effects of debris on LOCA mitigation. For example, all operating plants installed larger strainers and implemented actions to limit the introduction of debris into containment, and to ensure that debris is removed from containment prior to restarting units. The upgraded strainers installed in the plants have larger surface areas to accommodate debris that may arrive and have smaller screen openings when compared to earlier strainer designs. These smaller openings decrease the size distribution of debris that may pass downstream and enter the reactor core or affect other equipment.

Most PWRs provided sufficient information to demonstrate that their strainers will function adequately under conditions caused by the most challenging LOCAs for their plant. A few are still completing evaluations, and some are supplementing deterministic evaluations with

risk-informed analyses. All licensees have evaluated ex-vessel downstream effects and used NRC approved WCAP-16406-P-A (9), to evaluate the effects of debris on pumps, valves, spray nozzles, orifices, and instrumentation.

Enclosure 1 to SECY-12-0093, "Closure Options for Generic Safety Issue-191, Assessment of Debris Accumulation on Pressurized-Water Reactor Sump Performance," dated July 9, 2012, (10) provides a history of GSI-191. In the staff requirements memorandum (SRM) (11) associated with SECY-12-0093, the Commission directed the NRC staff to use risk insights to close GL 2004-02. The SRM also stated that based on plant actions there is adequate DID to allow the plants time to demonstrate compliance with the regulations. Industry continued testing and analysis to demonstrate that in-vessel debris loads are acceptable and to show acceptable strainer performance. In accordance with the SRM, approximately six licensees elected to use risk-information to show acceptable system performance.

Industry also developed guidance (WCAP-16793-NP-A) (1) for the evaluation of the effects of debris in the RV on LTCC. The NRC approved this guidance in an SE (12). The debris limits approved in the guidance were based on bounding assumptions that cover all plant designs. WCAP-16793 was able to be used by 19 PWR units to conclude that in-vessel debris would not inhibit LTCC. The NRC staff is aware of five additional "low fiber" units that could use the WCAP-16793 guidance to demonstrate acceptable in-vessel performance but have chosen not to in order to gain larger margin to debris limits. The NRC staff recognizes that the WCAP-16793 limits are conservative because the methods used to develop them were greatly simplified to reduce resource expenditure and to assure that test conditions bounded the PWR fleet. Two additional units performed plant-specific TH analyses to demonstrate that LTCC would be assured, even if a greater amount of debris than approved in WCAP-16793-NP-A was transported to the core (13).

The licensees for the remaining units have calculated, or assumed, that the amounts of debris that will pass through the strainer and enter the reactor coolant system (RCS) are greater than the approved WCAP-16793 limit. The PWROG developed and submitted WCAP-17788 (2) to demonstrate on a plant-specific basis that greater amounts of debris in the core would not adversely affect LTCC. WCAP-17788 incorporated results from FA testing, chemical effects testing, TH analysis, and additional mathematical modeling. It also referred to other work that increased the knowledge of the effects of debris on LTCC, particularly in the RV.

WCAP-17788 evaluated chemical effects, HLBs, and CLBs separately. Instead of using a bounding analysis as in WCAP-16793-NP-A, the PWROG used design-specific information to show that larger amounts of debris could be accommodated without inhibiting LTCC. The PWROG differentiated the analyses between four reactor designs and accounted for differences in fuel design. The method also allowed plants to consider plant-specific design characteristics such as ECCS flow rates, strainer size, chemical effects, and the number of FAs in the core. The analyses made bounding assumptions for some of the inputs like decay heat curves, timing of switchover to recirculation, FA flow velocity, and debris mixture arriving at the core. The analyses relied on a relatively complex TH analysis to demonstrate that LTCC could be maintained when the core inlet flow was impeded by debris following switchover to sump recirculation. The analyses also assumed that debris eventually completely blocked the core inlet.

#### 4.1 Overview of WCAP-17788

The NRC staff did not complete its review of WCAP-17788, and thus, it is not approved for use. However, the NRC staff relied on the analyses, evaluations, and experimental data submitted in WCAP-17788 to support its evaluation of the safety significance of IVDEs. WCAP-17788 proposed a methodology to use plant-specific analyses to determine in-vessel debris amounts for each plant based on plant-specific characteristics (e.g., plant-specific decay heat, strainer characteristics, debris transported to the strainer, flow rates, time of sump recirculation, activation of AFPs, formation of chemical precipitates, and implementation of measures to prevent BAP). Once the mass of fiber entering the RV is established, it is compared to an acceptance criterion calculated for each plant and fuel design to determine if the calculated fiber load would inhibit LTCC.

The NRC staff reviewed WCAP-17788 and developed numerous requests for additional information (RAIs), especially about the TH analysis. The PWROG used computer codes used in ECCS evaluation models (EMs) that had been found acceptable for short-term system response analysis and attempted to determine a bounding peak cladding temperature (PCT) to demonstrate LTCC adequacy. The staff found that the codes used for the analyses, while previously approved for short-term LOCA analyses, had not been accepted by the NRC staff to evaluate the phenomena associated with LTCC including predicting a PCT to demonstrate adequate LTCC. In some cases, the results indicated nonphysical behavior. To allow plants to resolve the issues individually despite these uncertainties, the NRC staff drafted limitations on the use of WCAP-17788. These limitations would have required significant plant-specific analyses.

#### 5.0 TECHNICAL EVALUATION

The scenario of relevance for evaluating IVDEs is initiated by a primary coolant system pipe rupture or break that leads to a LOCA. Because reactor coolant is discharged through the pipe break, debris is generated within containment. Although the ECCS is initially aligned to a reservoir (e.g., borated water storage tank or refueling water storage tank (RWST)), once the liquid in the reservoir is depleted, the ECCS suction must be realigned for recirculation by switching the source from the depleted reservoir to the containment sump (i.e., sump switchover (SSO)), which collects primary system liquid that has spilled out of the pipe break or collected from containment spray.

Under recirculation cooling, the coolant that spills out of the break and returns to the containment sump can pick up debris dislodged by the initial pipe break, as well as other debris that may be in containment. The system includes a strainer that is intended to collect most of the debris, but some debris will pass through the strainer, and be pumped into the RCS. Once within the reactor, the debris will transport through the RV. Design features like FA debris filters may collect some of the debris, while other debris may settle in more stagnant regions of the system. If significant amounts of debris collect at the debris filters, the flow resistance at the core inlet may increase, challenging the adequacy of LTCC.

The fluid initially present in the RCS is borated water. Injected emergency coolant is also borated water. Coolant flows out of the break and containment spray interacts with plant materials as it is transported through the containment to the sump, creating a pool with additional dissolved species. Chemical effects include the formation of precipitates and other

chemical products that could be filtered by a fibrous debris bed and further impair the flow of coolant needed for core cooling. An additional concern in the core region for CLBs is the potential for boric acid to concentrate due to boiling associated with the decay heat of the fuel, potentially resulting in BAP. A key mitigating measure is the use of HL switchover (HLSO) (or equivalent) after a period of time to flush the core by injecting coolant into the HL, rather than the CL. HLSO (or equivalent) is required by all PWR Emergency Operating Procedures with its timing dependent on plant-specific evaluations.

WCAP-16793 stated that the following criteria must be met to ensure that debris in the core will not adversely affect LTCC:

- Adequate flow for decay heat removal is supplied to the core
- BAP is prevented

The staff agrees that if these are met, LTCC will be successful.

The method used by the staff to evaluate this issue includes the premise that it is unlikely a LOCA large enough to generate and transport enough debris to the core to prevent LTCC will occur. The evaluation considered the low probability of the initiating event in combination with the low likelihood of the formation of a debris bed across the entire core. Sections 5.2.1 and 5.5.2 discuss these parameters.

The NRC staff also has significant knowledge of how the system will respond to varying amounts of debris (or resistance to flow) at the core inlet, including complete blockage at the fuel inlets. The knowledge base for these conditions consists of test and analytical information. In some cases, the test results were used as inputs to TH analyses. Section 5.2.1 discusses this information.

Table 1 below lists some of the major phenomena associated with the evaluation of IVDEs. The table is designed to demonstrate the differences or margins between the assumptions used in the safety significance evaluation and the expected realistic behavior. To the extent possible, the phenomena are listed sequentially as a LOCA scenario would progress in the plant. Many of the phenomena overlap in time.

Table 1: LOCA Phenomena

Attribute	Assumption	Most Probable		Margin	Sequence of Events
LOCA Size	6-inch	<6-inch		Less debris is likely	Initial Recovery
Recirculation Switchover Time	20 minutes	>30 minutes		More debris settles before reaching sump, less debris, lower decay heat	Switchover and Early Recirculation
Unqualified Coating Failure	100% Fine	<100%	Time dependent	Some fail as chips; less debris transports	
Debris Transport	100% Fines Transport	Some fines trapped, including debris recirculating from CS and break		<100% transports	
Fiber Penetration	15%	<15%, decreases with debris amount		Depends on plant design	
Core Inlet Fiber Bed	Uniform	Non-Uniform		More debris required to block core	
FA Debris Testing	Conservative flow, particulate amount, particulate sizing	Higher flow, different particulate characteristics		Debris limits from testing are conservative	Early Recirculation to Long-Term
TH Analysis for Debris Limit	Assume instantaneous blockage	Slow increase in core inlet resistance		Additional conservatism in debris limits	
Chemical Effects Timing	6 Hours	≥24 Hours		Core inlet unblocked at fiber limit w/o chemical effects, lower decay heat when AFP is sole flowpath	Long-Term Effects
Hot Leg Switchover Timing	24 Hours Maximum	Plant specific, most less than 10 hours		Consider actual plant timing, bypasses debris bed	

## 5.1 System Description

This description applies to all LOCA locations. There are two separate categories for LOCA break locations depending on whether the break is upstream or downstream of the core (CL side or HL side). The break locations are called HLBs and CLBs. Most plant responses are similar for both categories. Because of differences in plant response to breaks on the hot and cold side of the RCS, HLBs and CLBs are evaluated separately. The system responses to HLBs and CLBs are primarily described in Section 5.2. However, aspects of the LOCA response are discussed throughout this document.

The initial plant response for LOCAs is similar regardless of whether they occur on the HL or CL side of the RCS. Following a large LOCA, the CSS is actuated to suppress containment building pressure, and the ECCS is actuated to replenish liquid in the core and remove decay heat. Some breaks, depending on the break size and the plant setpoint, will not initiate CSS. Initially, the water source is from stored locations (e.g., the RWST). The boric water from these stored locations refloods the core within a few minutes, decreasing the cladding temperatures to within a few degrees of saturation. Water that is pumped into the RV is discharged through the break into containment, where it collects on the containment building basement floor and in the ECCS sump(s). The time required for the stored water to be depleted depends on the size of the break, the volume of fluid in the tank, and the ECCS and CSS pump capacities. This coolant injection phase can end as early as 20 minutes following the initiating event, if maximum ECCS and CSS flow and minimal stored water volumes are assumed.

After the stored water supply is exhausted, the CSS and ECCS are realigned to draw coolant from the containment sump. The coolant discharged from the RCS and CSS is recirculated into the RCS to provide for continued LTCC without the need for additional cooling water. Most plant responses are similar for HLBs and CLBs, however, Westinghouse 2-loop plants have a significantly different ECCS design known as UPI. Section 5.2.1 describes the responses of the different plant types to breaks in different locations.

Debris-laden coolant may begin to enter the RCS once the ECCS suction source is switched from the RWST to the containment sump. The amount of debris that enters the RCS depends on the filtering efficiency of the strainer, debris generation amounts, ECCS configuration, break location, amount of flow through the CSS, and the amount of time coolant is being drawn from the sump. Some debris that enters the RCS will reach the RV.

During CL recirculation, the flow transports debris through the downcomer (DC) into the lower plenum (LP) and into the core through the core inlet support region. After recirculation is switched to the HL, flow transports debris into the UP and into the top of the core. Depending on the break location and the injection location, some debris may flow out of the break.

Debris may collect at the bottom nozzle (BN) of the FA, causing resistance to flow. In some cases, it may collect at spacer grids higher in the FA. Ultimately, if enough debris is collected on the BNs, flow through the core inlet could be impeded, compromising LTCC.

All U.S. PWRs have AFPs in the RV that provide a path for coolant to reach the core if the core inlet becomes completely blocked with debris. Examples of AFPs include the barrel baffle (BB) region, pressure relief holes, upper head spray nozzles, and flow over the top of the steam generator (SG) tubes. The types of AFPs and resultant amount of flow area they provide is plant-specific.

### 5.1.1 Key Parameters

The NRC staff reviewed the effects of debris on LTCC with respect to debris in the RCS for the current operating fleet of PWRs in the U.S. The review is based on inputs in WCAP-17788, information provided by licensees, and other information available. It is considered representative of US PWRs, if not necessarily bounding. The following are the key parameters considered by the staff as they evaluated the general safety significance of the issues. Consideration of these parameters may be useful as licensees and staff evaluate plant-specific compliance.

- (1) Plants have a method of diluting the coolant in the core by implementing HLSO or equivalent action. This addresses the potential for BAP and concentration of other debris types in the reactor and reduces the potential for chemical effects to result in complete blockage due to a debris bed at the core inlet.
  - (a) To allow the [ ] CLB limit, plants other than UPI initiate HLSO before chemicals may form as per Volume 5 of WCAP-17788 (14). See Section 5.2.1.5.
  - (b) To prevent excessive concentration of particulate debris in the core, HLSO is initiated within 24 hours. See Section 5.2.1.1.3.
  - (c) To prevent BAP, plants initiate HLSO in accordance with their licensing basis. See Section 5.2.1.1.2.
- (2) Chemical effects timing ( $t_{chem}$ ) relative to the earliest time that complete core blockage can occur while not compromising LTCC ( $t_{block}$ ). See Sections 5.2.1.5 and 5.3.3.3.
- (3) Plant-specific post-LOCA environment is consistent with WCAP-17788 Test Group. See Section 5.2.1.5.
- (4) Earliest time to swap to recirculation. See Section 5.3.3.2.
- (5) Particulate debris amounts reaching the core pertaining to CLB. See Section 5.2.1.1.5.
- (6) Fibrous debris amounts reaching the core pertaining to CLB and HLB. See Sections 5.2.1.1, 5.2.1.2, and 5.3.3.6.
- (7) Minimum ECCS flow. See Section 5.3.3.5.
- (8) FA debris capture characteristics as evaluated in WCAP-17788.
- (9) AFP resistance values. See Section 5.3.3.2.
- (10) Available driving head for the CLB. See Section 5.2.1.1.1.
- (11) RCS liquid mass. See Section 5.2.1.1.5.
- (12) LOCADM results. See Section 5.2.1.5.4.
- (13) LOCA frequency. See Section 5.5.2.

These key parameters are considered essential considerations for the NRC staff's safety significance determination. Some of these parameters, or others not listed here, may be important to individual licensees' LTCC adequacy evaluations.



## 5.2 Sequence of Events

This section describes phenomena that apply to all LOCA scenarios. It also describes how HLBs and CLBs affect the system response for typical PWR designs and UPI designs. Finally, this section provides the basis for the staff conclusion that it is unlikely the primary coolant flowpath (through the fuel inlet nozzles) will become blocked to an extent that would compromise the adequacy of LTCC.

The break size and location govern the characteristics of the initial system response, as well as the amount of debris generated. These must be considered in the IVDE evaluation.

The IVDEs associated with larger breaks are assumed to be more challenging to mitigate than smaller breaks. A complete, double-ended guillotine break (DEGB) would have the highest energy discharge and the greatest potential to generate the most debris. In addition, the coolant pressure and inventory are lost most quickly following the largest break, and the source of pumped injection flow is hence depleted the most quickly, leading to the earliest SSO time. These dynamics lead to a scenario in which recirculating coolant would have the greatest concentration of debris, and the debris-laden coolant would be delivered to the core at the earliest time, while the core decay heat levels remain high. The resulting scenario would require the greatest coolant flow rate, yet the high concentration of debris would have the highest likelihood of causing a blockage that could inhibit adequate core cooling.

Smaller breaks, by comparison, would tend to generate less debris and deplete the source of injectable coolant more slowly. As a result, the recirculation would begin later, and would feature a lower concentration of debris. Longer times to recirculation also provide additional time for debris to settle in the post-LOCA sump pool.

Based on the evaluation described above, the NRC staff determined that the following assumptions were reasonable to use when evaluating the safety significance of IVDEs:

- Break size and SSO time are inversely correlated; larger breaks would be associated with faster switchover to recirculation, and smaller breaks would allow for SSO when the decay heat has dissipated more.
- Break size and debris generation are directly correlated; larger breaks discharge coolant at a faster rate resulting in more damaging jets and greater damage to materials in containment.

### 5.2.1 Availability of Emergency Core Cooling System Primary Flowpath

The analyses in WCAP-17788, Volume 3 (15) and Volume 4 (16), as well as the earlier work documented in WCAP-16793-NP-A, conservatively assumed that debris would collect uniformly at the core inlet because that results in the greatest headloss for a given amount of debris. However, the debris bed is realistically expected to collect non-uniformly for reasons described below. As a result, the amount of debris required to completely block the core inlet would be greater than that assumed in the analyses.

If a debris bed does not form at the core inlet or other locations that affect cooling, current LTCC analyses remain applicable. However, based on testing (WCAP-16793-NP-A (1) and WCAP-17788 (2)), it was determined that a fiber bed could form at FA inlets. This testing was

conducted with a single FA or portion of an FA and assumed uniform flow into all areas of the core.

WCAP-17788 established debris limits of [ ]. The HLB debris limit is based on subscale FA testing and the TH analyses performed for WCAP-17788. The CLB limit applies to all RCS designs. The HLB fiber amount referenced in this section is based on the combined RCS and fuel design with the smallest debris limit. These debris limits assume that the debris bed forms uniformly as it did during reduced-scale FA testing performed as part of the WCAP-17788 analyses.

The PWROG TH analysis and the NRC TRACE evaluations (See Section 5.4) predict significant variations in flow rate and direction at the core inlet, which will prevent the deposition of a uniform debris bed. This makes complete blockage of the core inlet less likely. The flow in the center of the core will be up (from the LP to the core), while the flow at the periphery will be down, (from the core to the LP). The patterns are caused by higher decay heat in the central core and relatively low decay heat in the periphery. Contributing to this flow pattern is the downward flow entering the LP from the DC. These flow patterns will cause the deposition of fiber at the center of the core inlet first. As debris builds in the areas with upward flow, some flow redistribution to the periphery may occur.

Other influences on flow will tend to prevent uniform flow to the core. For example, the lower core plate, core support plate, and other hardware within the LP disturb the flow patterns at the core inlet. These contribute to non-uniform arrival of flow and debris at the core inlet. This phenomenon was observed during brine testing (PWROG-15091, "Subscale Brine Test Program Report," dated November 30, 2015 (6)) in which it was difficult to form a uniform bed at the FA inlet.

The NRC staff observed similar non-uniform debris bed formation during several strainer tests, which provides evidence that similar behavior will occur at the core inlet (17) (18) (19). The velocities approaching the disks in most strainers are non-uniform because the plenum that collects the flow that passes through the perforated disks is hydraulically closer to some surfaces than others. The velocities closer to the plenums are higher. The velocity profile determines the degree of non-uniformity. Greater disruptive forces are present for the in-vessel case. Some of the flow is down, or away from the core inlet. This prevents deposition of debris in those areas. The flow velocity at the core inlet can vary considerably depending on the ECCS design and the break location. CLB flow velocities are low, while HLB velocities can be much higher if all pumps are injecting. CLB average core inlet velocities are similar to strainer approach velocities. HLB velocities are generally higher.

The staff considered that chemical precipitates in the debris bed could cause the bed to deposit more uniformly over the core inlet by increasing the differential pressure across the bed and causing flow to be redirected. However, as discussed in Section 5.2.1.5, precipitation is expected to occur later in the transient. By the time precipitates may form, the debris will be depleted from the pool so that further transport to the core inlet is significantly reduced.

Testing for WCAP-17788 indicates that the debris deposited at the core inlet would not cause a significant resistance to flow until the fiber limit is approached. This is consistent with testing from WCAP-16793 that showed there was a threshold fiber amount below which significant headloss would not occur. Therefore, significant redistribution of the debris will not occur early in the scenario. The design of the PWR core also permits crossflow between FAs which allows

some equalization of the differential pressure in the areas where debris is deposited under the low-velocity conditions following a LOCA.

When considering a full core relative to the subscale testing, it is expected to take more debris than the limits in WCAP-17788 to prevent coolant from reaching the core. In the event the core inlet accumulates enough debris to stop flow, AFPs are available to provide adequate core cooling. Section 5.3.3 discusses these AFPs. The debris limits assume that chemical effects have not occurred. Section 5.2.1.5 discusses chemical effects. In addition, once a plant initiates HL recirculation or a similar BAP prevention action, adequate LTCC is maintained. HL recirculation is also likely to dislodge portions of the debris that may collect at the core inlet.

The NRC staff considers the assumption that all debris passing through the strainer reaches the core inlet to be conservative. For breaks large enough to initiate the CSS, the amount of fiber reaching the core inlet would be reduced by the amount of fiber diverted to the CSS. For smaller breaks, the CSS may not initiate; however, the overall amount of debris generated would be less.

Evaluations conducted by the PWROG and the NRC demonstrated that even a very small open flow area at the core inlet will allow adequate coolant to enter the core. One evaluation conducted for WCAP-16793-NP-A (1), Appendix B, showed that up to 99.4 percent of the inlet could be blocked and flow to ensure core cooling would still be adequate. Calculations performed by the NRC Office of Nuclear Regulatory Research (RES) confirmed this evaluation (20). Later, more detailed TH evaluations performed by RES showed that 99 percent of the flow area could be blocked for HLBs and CLBs while ensuring adequate flow and prevention of BAP (21). This 99 percent flow area was converted to a core inlet resistance and applied uniformly over the core inlet area in the RES model.

An additional source of information regarding debris bed formation at the core inlet is testing conducted for WCAP-17360-P, "Small Scale Unbuffered and Buffered Boric Acid Nucleate Boiling Heat Transfer Tests with Sump Debris in a Vertical 3x3 Rod Bundle," dated May 31, 2012 (5). This WCAP discusses 3x3 heated rod bundle testing that was conducted with fibrous and particulate debris. The BN and first spacer grid provided the most likely places for debris to be captured. Capture of fibrous debris at spacer grids was observed during testing for WCAP-16793. During the heated rod testing, there was no debris capture at the spacer grids except for a small amount of debris captured between the outer surface of the grid and the test column. Although the testing did not include a prototypical geometry at the approach to the fuel, the test results suggest that turbulence may help to inhibit debris bed formation. The heated rod testing provided qualitative evidence that turbulence will tend to prevent debris bed formation, especially at spacer grids.

As part of a DID analysis, the NRC staff considered how the LOCA response would evolve if a high-resistance debris bed were to form at the core inlet. Section 5.3.3 discusses the availability of AFPs that bypass the normal core inlet.

#### 5.2.1.1 Cold-Leg Break

Following a CLB, for all PWR designs except UPI, the ECCS is injected into the CL and flows down the DC into the LP and up into the core. Only the flow necessary to make up for inventory in the core region lost to boil-off enters the core. The rest of the flow goes out of the break in the CL and spills back to the sump. The amount of debris reaching the core inlet for the CLB is

much less than for the HLB because most of the debris flows out the break. For the CLB, the force driving the coolant into the core is the manometric balance between: (1) the level in the CL (up to the break elevation) and DC, and (2) the level in the core. As the water boils out of the core it is replaced because of the gravity head in the DC. There are also flow losses from liquid and vapor flows. The amount of coolant required to replace the boil-off is higher at the beginning of the event and is reduced as decay heat decreases. Flow to the CSS does not enter the core and is returned to the sump with any entrained debris.

For a CLB, when injection is switched to the HL, the discharge of the ECCS pumps is aligned to the UP (with pressure limited by the height of the SG tubes). This flow will reverse the flow at the core inlet, flush concentrated debris and boric acid from the core, and disrupt any debris bed at the core inlet.

The NRC staff determined that it is unlikely for a debris bed to form across the entire core inlet following a CLB. Circulating currents will prevent or limit debris deposition at the core periphery. Maintaining a small open area at the core inlet will assure adequate flow to cool the core. The concepts outlined here are the same as those discussed in Section 5.2.1 and are not repeated in detail.

The PWROG submitted an evaluation of the effects of debris on a CLB in WCAP-17788 and updated the evaluation with supplemental information. This establishes a basis for a debris limit for the CLB case. In the analysis, the AFP credited in the HLB was assumed to be unavailable, and all flow to the core was assumed to flow through the core inlet. The CLB debris limit was set at [ ].

Boiling in the core is vigorous at the beginning of recirculation, which results in sufficient liquid carryover to limit the buildup of boric acid in the RV and adequate mixing in the RV to maintain homogeneous boron concentration. The WCAP-17788 TH analysis shows upflow in the center of the core and downflow in the periphery. TRACE studies predict similar flow patterns at the core inlet (see Section 5.4). The circulating currents result in the transport of boron from the core region to the LP. The boron concentration in the core may increase until the density of the fluid in the core is high enough to result in density driven convection between the core and LP. As boiling decreases, convection can become the dominant mixing mechanism. If the boron concentration in the RV becomes too high, boron precipitation could occur which would affect the ability to cool the fuel. The TRACE studies also predict that mixing between the core and LP will occur. The LP provides a volume for dilution of boric acid and other debris that may be suspended in the core.

Debris will begin to arrive at the core inlet shortly after recirculation begins and most debris will reach the core inlet within a few hours. Most will arrive relatively early because the strainer will become more efficient at filtering over time as debris collects on it. Debris will also be removed because of collection in the core or settling elsewhere throughout the sump or RCS.

The following topics are addressed to evaluate the debris limit of [ ].

- debris collection at the core inlet
  - resulting in increased pressure losses
  - preventing transport of high-concentration boron solution from the core to the LP

- debris suspended in the liquid phase
  - increasing pressure losses through the inner RV because of changes in fluid properties and two-phase flow characteristics and changes in heat transfer processes
  - causing early BAP because of reduced liquid inventory, reduced liquid carryover, or changes to the precipitation mode or precipitation location
- debris deposition on spacer grids in the core increasing frictional losses or reducing heat transfer

Note that UPI plants are treated differently because of the location of the ECCS injection. Section 5.2.1.3 discusses UPI plants.

A greater amount of debris generation is required to inhibit flow for a CLB than for a HLB. This is based on the distribution of flow after it passes through the strainer. For a HLB, all ECCS is pumped through the core. For a CLB, only the volume of water required to replace that boiled out of the core flows to the core inlet. The remainder of the flow goes out the break, and with it any debris that is entrained in the flow. The debris that flows out of the break is returned to the sump pool and has an opportunity to enter the ECCS again. However, testing has shown that the filtration efficiency of the strainer for fiber increases quickly as fiber is captured on the strainer surface.

As an example, South Texas Project (STP) performed studies to determine how much debris could arrive at the core inlet under various conditions. STP has among the highest fiber amounts in containment compared to the other U.S. PWRs because it uses only fibrous insulation in its containment. The studies were based on strainer penetration test results and modeling of the flow as it circulated through the strainer, the ECCS, and the CSS. The model found that for a design basis case with a single failure (one train of ECCS and CSS running), 376 grams of fiber would arrive at the core inlet. Without CSS (only low-head safety injection and high-head safety injection running), the value was 539 grams. For a single low-head safety injection pump running using the most conservative penetration results, the debris amount arriving at the core was 1,119 grams. This amount of debris is assumed to be evenly distributed among 193 FAs. The FA loading for the single low-head safety injection case is very low at 5.8 g/FA. The NRC staff noted that it is unlikely that only a single low-head safety injection pump would be operating during recirculation, but even if that is the case, the debris loading is well below the level of concern. Pumps may be secured to reduce flow through the strainers, but this is generally done at a time when most of the debris has been removed from the sump fluid by filtering. As can be seen above, the more realistic cases have lower debris amounts.

STP also performed beyond design basis sensitivity studies to determine the most challenging flow configuration for CLB in-vessel debris. STP established a strainer debris limit of 192 pounds of fine fiber based on strainer headloss testing. LOCAs that resulted in greater than 192 pounds of fine fiber at the strainer were assumed to contribute to core damage. As shown in the analysis for the license amendment request (13), 192 pounds of fine fiber could result from a 12.8-inch DEGB. However, most breaks generating this much fiber were significantly larger. A few of the largest breaks at STP could result in fine fiber amounts of up to 830 pounds.

The beyond design basis sensitivity studies were based on fine fiber debris loads at the strainer of 192 pounds (design basis limit) and 800 pounds. The 800-pound value is representative of the amount of fine fiber that can arrive at the strainer from the largest LOCA breaks at STP. The sensitivity studies demonstrated that even with the largest strainer fiber loading and overly conservative flow conditions, the CLB limit was not reached for STP. It was determined that lower strainer flow rates resulted in higher core debris amounts. For example, the highest debris amount was calculated assuming one-half high-head safety injection flow and no other pumps in service. The result was 2,400 grams of fiber at the core. For STP, this results in 12.4 g/FA. It was further determined that the highest core loading would occur with the largest number of strainers in service with the lowest possible flow through each.

Vogtle Electric Generating Plant performed a similar evaluation for the CLB, also using plant-specific penetration testing and modeling. Vogtle is also a very high-fiber plant. Instead of using a plant-specific debris amount in the testing, a theoretical strainer debris bed thickness of one inch was attained for each test by batching in small amounts of fiber. Testing demonstrated that additional debris did not penetrate the strainer, even before the one-inch threshold was reached. Most of the fiber penetrated the strainer early in each test when the debris load was low. Vogtle calculated that 13 g/FA of fiber would arrive at the core inlet for the CLB under the most limiting design basis conditions for pump and strainer operating combinations. As a comparison, for the Vogtle HLB case, 91 g/FA of fiber was calculated to reach the core. Note that STP did not calculate a HLB fiber amount, but conservatively assumed that the core was completely blocked relatively early in the event.

Plants have different design configurations that will affect the amount of fiber that may reach the core following a CLB. However, the STP study and the Vogtle results demonstrate that small breaks do not generate enough debris to inhibit LTCC following a CLB. These examples provide evidence that even the largest CLBs in high-fiber plants are unlikely to result in greater than [ ] fibrous debris at the core inlet. Also, because debris deposition at the core inlet will be non-uniform, it is very unlikely that debris at the core inlet will inhibit LTCC following a CLB. In conclusion, even the largest DEGB is unlikely to generate enough debris to approach the [ ] CLB limit presented in WCAP-17788 and a large CLB is predicted to occur very infrequently (see Section 5.5.2).

#### 5.2.1.1.1 Debris Collection at the Core Inlet

The fluid velocity profile across the core inlet varies depending on the relative power of the fuel. The flow patterns at the core inlet will deposit debris close to the center of the core but not at the periphery. Boiling and circulating flows will prevent a uniform debris bed from forming across the entire core inlet for the debris amounts determined by testing. Therefore, mixing between the core and LP are unlikely to be inhibited during the LOCA recovery (see Section 5.2.1). Even with an increase in density in the core region, which was not modeled by industry analyses, the recirculating currents will continue as decay heat decreases and boron concentrates in the core region. This conclusion is supported by TRACE simulations (21) that included the effects of boric acid concentration in the core. Section 5.4 discusses TRACE calculations.

The TH analysis in WCAP-17788 becomes unreliable once decay heat decreases to the point where boron concentration in the core increases because of limitations of the code in accommodating buoyancy-driven flow. The TH analysis shows that the steam quality exiting the

RV remains below 0.8 before the switchover to sump recirculation and that this ensures that boron solutes will not concentrate in the core up to that point.

The driving force for water entering the core is the manometric balance between the DC region of the RV and the core region. The head from the DC must overcome liquid and vapor flow losses on the core side as well as any headloss caused by debris and density difference resulting from concentration of boric acid or other debris in the core region.

The SE for WCAP-16793-NP-A found that at less than 15 g/FA, flow to the core would continue for the HLB condition, even if chemical precipitates were present. For the CLB, the staff found that LTCC would be assured for plants that meet the HLB criterion of 15 g/FA, but this finding did not address the effects of BAP. The staff finding also assumed that the maximum fibrous debris load arriving at the core inlet for the CLB would be roughly half of the HLB amount.

For this TER, it is assumed that chemical effects, discussed in Section 5.2.1.5, are delayed until after the licensee implements HLSO (or equivalent). WCAP-16793-NP-A testing found that under CLB flows, the deposition of fibrous and particulate debris at the FA inlet resulted in very low headloss. These headlosses were found to be much lower than those occurring when chemical precipitates were included. The CLB testing for WCAP-16793-NP-A (see WCAP-17057-P, Revision 1, "GSI-191 Fuel Assembly Test Report for PWROG," issued September 2011 (22)) included several tests with a fiber loading of [ ] and varying amounts of particulate. The tests included chemical precipitates. During the testing, headlosses were allowed to stabilize and were recorded before chemical debris was added to the test. The highest non-chemical headloss recorded during the testing was [ ]. The PWROG stated that the available driving head for all plants is greater than this value. [ ]

[ ]. Information provided by the PWROG indicates that the driving head calculation was based on a reactor design that has 14-foot FAs while all other designs have 12-foot FAs. The DC for the example plant was stated to be similar to the designs that have 12-foot FAs. This indicates that the calculation has about 2 feet of margin for most plants (approximately 1 psi).

The PWROG also performed small scale boiling rod bundle tests that included fibrous and particulate debris. These tests were performed and documented in WCAP-17360 (5). The testing used a vertical 3x3 rod bundle that had dimensions and materials like those of PWR fuel. The rods were heated to achieve boiling conditions similar to those expected after a large CLB. During the rod bundle tests no debris bed formed at the fuel inlet. The debris was observed to pass through the BN and settle on top of the nozzle or pass into the heated core region. WCAP-17360 determined that the boiling conditions downstream of the FA inlet produce instabilities that inhibit debris bed formation. A small amount of fiber was observed to collect at the outer edge of the spacer grids (between the grids and the test column). The rod bundle testing was not conducted with a prototypical FA or LP, so it cannot be definitively relied on as applicable to a full core. However, it does provide evidence that turbulence from boiling will prevent significant amounts of debris from collecting at the spacer grids.

The rod bundle tests demonstrated that density-driven flow occurs in the boiling condition through observation of temperature stratification in pure water tests and mixing of fluid, as determined by relative temperature between the simulated core and LP, for tests that included boric acid. Additional evidence of mixing was obtained by sampling the water in the simulated

LP. Maintaining the LP as a mixing volume reduces the concentration of boric acid and other debris in the core making BAP less likely and delaying its onset.

Previous studies performed by the PWROG for WCAP-16793 and RES showed that for the CLB, a single open FA provides adequate coolant to maintain LTCC.

The following events are each unlikely as discussed above:

- (1) Large CLB LOCA
- (2) Transport of fibrous debris more than the analyzed limit (based on a uniform debris bed)
- (3) Formation of a uniform debris bed

Considering the above, it is very unlikely that a high resistance debris bed will form at the core inlet such that flow into the core will be prevented. Therefore, the potential for a loss of LTCC because of debris in the core is of low safety significance for the CLB. The initiation of HL injection or an equivalent action is assumed before chemical effects may occur. HL injection bypasses the debris bed at the core inlet before headlosses resulting from chemical effects exceed the available driving head and flushes concentrated debris and boric acid from the core.

#### 5.2.1.1.2 Boric Acid Precipitation

The PWROG performed SKBOR studies to estimate the effects of debris buildup at the core inlet on BAP. The simulations reflected conditions typical of design-basis safety analyses. A case was performed as a baseline assuming no core blockage and 50 percent mixing with the LP. Sensitivity cases assumed 100 percent mixing availability with the LP but assumed percentages of core inlet blockage varying from 0 to 75 percent. The study found that the cases with 0, 25, and 50 percent blockages took longer to reach the boric acid solubility limit than the baseline. The 75 percent blockage case reached the BAP limit faster than the baseline. Therefore, it was concluded that greater blockage leads to delays in the exchange flow between the core and LP.

The study demonstrated that up to 50 percent of the core inlet can be blocked with debris before the flow exchange between the core and LP will be inhibited such that the licensing basis assumption of crediting 50 percent of the LP volume becomes questionable. The SKBOR studies are conservative because of the application of conditions used in design basis safety analyses. Based on the SKBOR studies, WCAP-17788 states that a relatively low steam quality (less than 80 percent) allows a significant amount of the boron to be removed from the core via entrainment and that this will delay the onset of BAP compared to most of the SKBOR cases in the study. The PWROG performed an SKBOR study that demonstrated a steam quality of 0.95 would result in significant boron concentration in the core, but that the concentration would never exceed the precipitation limit. Higher steam qualities resulted in eventual precipitation. These studies assumed that 50 percent of the LP was available for dilution of the boron.

The findings from the SKBOR studies are consistent with the trends found in TRACE studies of BAP completed by RES (21). The TRACE studies are discussed in Section 5.4. TRACE found that BAP would be delayed significantly longer than in the SKBOR studies conducted by the PWROG.



The PWROG conducted a brine test program described in PWROG-15091-P, "Subscale Brine Test Program Report," dated November 30, 2015 (6). The testing was conducted to learn more about density-driven mass transport between the core and the LP with and without debris present at the FA inlet. The test program demonstrated the fluid exchange and showed that highly resistive debris beds cannot form at the core inlet at the established CLB in-vessel fiber debris limit. The program did not consider chemical effects because it was assumed that HL recirculation would be initiated before chemical precipitation. Testing included conditions expected to occur following a CLB and considered both Westinghouse and AREVA core inlet geometries.

Fibrous debris ranges for the testing represented 2.5 to 22.5 g/FA. Some of the tests included particulate, but it was ultimately determined that the amount of particulate included did not significantly affect the test results or differential pressure across the debris bed for the tested conditions. The results from the brine testing were consistent with the subscale headloss testing that found that [ ].

The brine testing demonstrated that the exchange flow rate (between the simulated core and LP volumes) was influenced by the amount of fiber included in the test. Larger fiber amounts blocked more open areas in the BN. Under the test conditions, the relative timing of the debris injection, the flow velocity into the FA, and the increase in density of fluid in the core region affected the ability of a debris bed to form. If a debris bed formed, the exchange between the modeled core and LP regions stopped but was reestablished when the density of the fluid in the core increased or when the flow from the LP to the core decreased and the debris bed was disrupted. The brine testing provides evidence that exchange flow can take place, even if a relatively low resistance debris bed forms at the core inlet.

The NRC staff noted that the brine test results and the results of FA testing for WCAP-16793-NP-A had different headloss values for similar fibrous debris loads. The PWROG stated that the results from the brine testing and other FA tests had different headlosses because the test methods were different. It was noted that higher in-bed particulate loads can result in higher headlosses and that the tests being compared might not have similar particulate loads because the WCAP-16793-NP-A tests used a recirculating flowpath while the brine testing used a once-through system. Some of the particulate in the brine testing might have passed through the fuel inlet and avoided capture in the debris bed. The PWROG also noted that both test programs support the assertion that a [ ] limit will not result in a significant headloss at the core inlet.

The staff concluded that the headlosses that may occur at debris loads below the fiber limit are relatively low before the arrival of chemical precipitates and that both test programs demonstrated this.

Based on the SKBOR studies and the brine testing discussed in this section, and the TRACE results presented in Section 5.4, the NRC staff determined that debris effects do not invalidate the current licensing bases or HLSO times for operating PWRs. The analyses indicate that BAP may be of lower risk than was previously thought. However, changes to a plant's licensing basis that draw on these insights would have to be justified on a plant-specific basis. In addition, maintaining HLSO (or equivalent) is important to ensure continued LTCC by flushing concentrated debris from the core and to decrease the probability that chemical precipitates cause a significant increase in headloss.

#### 5.2.1.1.3 Debris Suspended in the Core

The effects of debris in the core for the HLB are expected to be bounded by those that will occur during the CLB. This section includes some discussion of HLB behavior, but the behavior following a HLB should be similar to that following a CLB, except for the amount of debris present.

Debris that passes through the core inlet or enters through an AFP will reach the core and UP. Debris in the core can affect fluid and heat transfer properties of the fluid. Because the CLB initially has the core in a boiling pot mode, any debris that reaches the heated core is assumed to stay there. For the HLB, much of the debris is flushed from the core making the CLB limiting. For the CLB, debris can concentrate in the core, similar to the way boric acid can. Most fibrous debris will reach the core in the first few hours of the event, and most particulate debris will arrive much later because most transportable particulate debris is failed unqualified coatings. The amount of fibrous debris reaching the core is much less than the amount of particulate debris that may reach the core. For the HLB, the amount of fiber that reaches the core may be greater than for the CLB. However, before significant core blockage, some of the fibrous debris will be flushed from the core. The amount of fibrous debris that may reach the core is an order of magnitude less than the potential particulate debris.

Electric Power Research Institute (EPRI) testing, described in EPRI 1011753, "Design Basis Accident Testing of Pressurized Water Reactor Unqualified Original Equipment Manufacturer Coatings," dated September 30, 2005 (23), demonstrated that most unqualified coatings will fail after 24 hours. Early in the event, boiling maintains turbulence in the core and keeps debris well mixed. After a few hours, depending on plant-specific procedures, plants initiate actions, like HLSO (or equivalent), to flush concentrated boric acid from the core. This action will also flush debris from the core. Because most of the debris that may enter the core following a CLB cannot arrive until after HLSO (or equivalent), the amount of debris in the core is relatively small, minimizing the effects of debris on fluid and heat transfer properties. Section 5.2.1.1.5 discusses in more detail coatings failures, particulate debris, coatings failure timing, and debris characteristics.

Rod bundle testing demonstrated that debris in the heated region remained well mixed with the fluid. [

]. Some deposition of debris at the outer edge of the spacer grids was observed. Similar behavior is expected for the HLB. The TH analyses discussed above demonstrate that circulating currents are present following a CLB. The currents assist with keeping debris and boric acid well mixed in the core.

Debris suspended in the core may have an influence on fluid properties and displace liquid in the core. WCAP-17788 assumed a 5 percent mass limit on the debris in the core. The increase in density from this amount of debris was determined to have a small effect on headloss. The effects on fluid viscosity and surface tension were also determined to be small. The rod bundle testing was referenced to show that bubbly flow observed in the testing was not significantly affected by the addition of debris.

Debris suspended in the core may also affect fluid heat transfer properties. Rod bundle testing validated that no major degradation of heat transfer occurred. Open literature, provided as

references in WCAP-17788, indicates that limited amounts of particulate debris suspended in fluid will improve heat transfer.

Debris in the core could affect BAP by displacing liquid and reducing the liquid volume available for mixing. Based on the small amount of liquid displaced, any changes to the rate of boron buildup in the core will be negligible. The 3x3 rod bundle testing also provided evidence that precipitation modes, and boric acid transport and mixing phenomena, are not negatively affected by debris in the core.

#### 5.2.1.1.4 Local Collection of Debris

The rod bundle testing demonstrated that significant collection of fiber at the spacer grids is unlikely. However, should debris become trapped in the spacer grids, the effects would be limited to local areas. WCAP-16793-NP-A, Revision 2 (1) evaluated complete blockage around a fuel rod at a spacer grid and demonstrated that axial conduction would allow the fuel cladding to remain at acceptably low temperatures. In addition, the 3x3 rod bundle testing did not identify any significant collection of debris at the spacer grids, even with a relatively high fibrous debris load equivalent to 150 g/FA. The open lattice fuel design for PWRs permits crossflow between assemblies, which will allow flow around localized blockages. This section applies to HLBs and CLBs.

#### 5.2.1.1.5 Concentration of Particulate Debris

The NRC staff evaluated the different categories of coatings and other particulate debris sources to assess the potential effects of particulate debris. The three coating categories evaluated are qualified coatings, degraded qualified coatings, and unqualified coatings. The evaluation of coatings depends on failure timing to demonstrate that an excessive amount of particulate debris will not concentrate in the core following a CLB. For a HLB, the coatings and other particulate debris are not expected to concentrate because there is significant excess flow through the core that will flush debris as it exits the reactor.

Similar to boric acid, debris may concentrate in the core during a CLB because water boils away and particulate debris remains behind. Because there is not significant empirical data for particulate filtration by sump strainers, it is assumed all particulate debris passing through the strainer arrives at the core. In addition, filtering at the core inlet is not assumed.

All qualified, unqualified, and degraded coatings within the ZOI are assumed to fail immediately as fine particulate that is transported to the core. Based on the review of individual plant submittals in response to GL 2004-02, the approximate range for ZOI coatings amounts is 100 to 2,000 pounds. Qualified coatings outside the ZOI are assumed to remain intact and attached to the substrate. They do not contribute to the debris source term at any time during the LOCA recovery.

Unqualified coatings are assumed to fail as particulate debris. This category of coating is generally the largest contributor to the fine particulate debris source term. Some plants consider degraded qualified coatings to be unqualified. Based on the review of individual plant submittals in response to GL 2004-02, the amount of unqualified coating debris ranges from less than 100 pounds to 20,000 pounds. Based on the EPRI testing discussed below, it is estimated that less than 10 percent of the unqualified coatings will fail before 24 hours. Therefore, it is assumed that 10 percent of the unqualified coatings are available for transport to

the core before the initiation of HLSO (or equivalent), which occurs within 24 hours after the initiating LOCA. Once HLSO (or equivalent) is initiated, the core will be flushed of concentrated boric acid and particulate debris.

Degraded qualified epoxy coatings outside the ZOI are assumed to fail as chips. The chips are assumed to settle or be captured by the strainer and not be available to transport to the core. Degraded qualified inorganic zinc outside the ZOI is assumed to fail in particulate form. This particulate is assumed to be available to transport to the core, but the degradation of this coating category into particulate is estimated to take longer than 24 hours so it would not be transported to the core before HLSO. Many plants did not differentiate between degraded qualified coatings and unqualified coatings in their analyses. For these plants, the unqualified coating term is conservative with respect to the amount of particulate debris that may pass downstream of the strainer. The basis for the assumed debris characteristics of the degraded qualified coatings is testing performed by Keeler & Long. (24)

Unqualified coatings make the most significant contribution to amounts of particulate debris in the core. To evaluate the potential effects of particulate debris in the heated core, the NRC staff referred to an EPRI report that discusses the behavior of unqualified coatings when exposed to post-LOCA conditions (23).

In addition to coatings, particulate debris can originate from latent debris and particulate type insulations. According to NRC guidance, the assumption for the mass of latent particulate is generally 170 pounds (8). Guidance also recommends plants to confirm their latent debris amounts. Plants identified a range of latent particulate, with the largest amount assumed to be 500 pounds.

Most plants do not have a significant particulate insulation source term. However, one licensee determined that 2,200 pounds of calcium silicate insulation could be generated by a limiting break. This plant has the largest particulate source term when calculated, as discussed below.

To estimate the amount of particulate debris that might transport and collect in the core during a CLB, the NRC staff used information provided by licensees in their responses to GL 2004-02. The staff summed 100 percent of the ZOI generated coatings, 100 percent of the latent particulate, 100 percent of the particulate insulation debris calculated to reach the strainer, and 10 percent of the total unqualified coatings. A few plants were estimated to have maximum values of particulate that could reach the core between 2,500 and 3,000 pounds. These values are considered realistic for the worst breaks, and therefore conservative for other breaks. The largest calculated particulate amount calculated by the staff was 2,910 pounds.

The staff assumed that 2,910 pounds of particulate would be mixed with the coolant in the core and LP regions. Mixing between the regions is discussed in the CLB discussion in Section 5.2.1.1. The amount of liquid in the core and LP is assumed to be 60,480 pounds based on 50 percent voiding in the core and 100 percent of the LP volume available for the Westinghouse 3-loop reactor design. If the entire mass of particulate is mixed in the LP and core region, the mass ratio is 4.8 percent particulate to liquid. A 3-loop Westinghouse design was used to determine the fluid mass because it has smaller volumes for the LP and active core regions than the 4-loop Westinghouse reactor design. The 3-loop and 4-loop Westinghouse designs are considered as representative of the PWR fleet. The 2-loop Westinghouse designs have smaller RCS volumes but use injection into the UP, which reduces the concern with concentration of debris in the core. The staff verified that the maximum particulate mass for the

2-loop plants is less than 1,000 pounds so the mass ratio for these plants is limited to about 2 percent considering the smaller volumes for these plants.

For design-basis BAP calculations, 50 percent of the UP volume, up to the bottom of the HL, is typically credited. This volume was ignored for the particulate debris calculation and provides margin in the calculation.

The debris amounts in the example above are realistic maximum debris generation values for the limiting plant in the fleet. The amounts of debris generated were calculated for the worst-case breaks using accepted methods that are considered conservative. Other breaks, especially smaller, more likely breaks, would result in less debris. Also, a low liquid mass was used in the calculation by choosing a plant design with low volume core and LP regions (except for UPI plants discussed above) and assuming a high void fraction for the core region. Therefore, the calculated mass ratio is considered a conservatively high value for the fleet. Almost all breaks would generate significantly less particulate debris. In addition, the amount of particulate assumed to reach the core is based on 100 percent transport. It is likely that some would not reach the strainer or would settle in the LP, be filtered by the strainer, or be filtered at the core inlet. The latent particulate is a relatively small portion of the source term for the plants with a large amount of particulate, but a significant amount of this source would settle because of its larger size.

WCAP-17788 evaluated a limit of 5 percent by mass particulate to liquid in the core. The final evaluation of this issue was included in the Westinghouse response to Request for Additional Information (RAI) 1.3 by letter dated September 28, 2018 (25). The NRC staff found the evaluation to reasonably address the potential issues that could result from particulate suspended in the core.

Once HLSO (or equivalent) is initiated, any debris that has collected in the core will be diluted by mixing the coolant in the reactor back into the sump. Therefore, it is important that plants perform HLSO within 24 hours to prevent excessive unqualified coatings from concentrating in the core.

#### 5.2.1.1.6 Conclusions for the Cold-Log Break

Based on the discussion above, the staff concludes that the [ ] fiber limit for the CLB is acceptable and that flow to the core will be maintained with this debris load if chemical precipitates do not deposit or form on the debris bed. The probability of any PWR accumulating [ ] at the core inlet is very low because of the low volume of flow, and therefore the low amount of debris that approaches the core inlet during a CLB. If more than [ ] is transported to the core inlet, the formation of a uniform bed is unlikely, and flow to the core will likely continue. The actual debris amount that might result in preventing adequate flow to the core is not defined because testing is based on a uniform debris bed. If the core inlet becomes completely blocked, AFPs will allow flow to reach the core. There is adequate DID to assure LTCC following a CLB for the current operating fleet of PWRs.

Current plant licensing bases for BAP do not need to be revisited because of the effects of debris on LTCC. Analyses performed in WCAP-17788 and TRACE (21) show that boric acid will not concentrate to the point of precipitation in areas important to support cooling.

The collection of debris in the heated core will not significantly affect LTCC. The amount of debris that enters the core following a CLB is limited by the amount of debris available before the initiation of HL injection (or equivalent) and the low amount of flow entering the core. A large amount of particulate debris may be available, but this debris will not become transportable until after HLSO is initiated. This prevents the concentration of significant amounts of debris in the core. Filtering by the strainer also reduces the amount of debris that may enter the core.

Local collection of debris (at spacer grids) will not adversely affect cooling of the fuel as demonstrated by calculations for WCAP-16793-NP-A.

Flow from HL injection (or equivalent) is expected to be initiated prior to BAP. Complete blockage of the core inlet is not expected for plants that initiate HL injection (or equivalent) before the formation of chemical precipitates.

#### 5.2.1.2 Hot-Leg Break

Following a HLB LOCA, for all PWR designs except UPI, the ECCS is injected into the CL and flows down the DC, into the LP, and up through the core. All the injected flow passes through the core. All debris that bypasses the strainer and is pumped by the ECCS will arrive at the core inlet and may collect there causing an increased resistance to flow through this path. The driving head available for this scenario is the ECCS pump discharge as limited by the height of the SG tubes. If the core inlet resistance increases significantly because of debris, AFPs will become activated to allow coolant to reach the core and remove decay heat, helping to maintain LTCC. Flow to the CSS does not enter the core and debris in that stream returns to the sump.

After a few hours, PWRs change the injection path to prevent the buildup of boric acid in the core following a CLB. This action is taken following all large LOCAs because the operators may not be able to determine if the break is on the hot or cold side of the RCS. The injection is switched to the HL or a combination of the HL and CL. For a HLB, this injects coolant into the UP where it can drain into the core to provide cooling. Excess flow spills out of the break in the HL and returns to the sump.

To determine the approximate size of a break that could result in significant debris at the core inlet, the NRC staff used information from several sources. First, a debris limit of [ ] was assumed. This is taken from the WCAP-17788 analysis for the most conservative fuel and plant design combination and applies only to the HLB scenario. Debris limits for the HLB were calculated to be between [ ] depending on the fuel and reactor design combination. Some combinations could have accommodated more, but [ ] represents the maximum debris amount tested for WCAP-17788. [ ]

].

Table 2 of Section 5.3.3.6 lists the HLB fibrous debris limits for the various RCS design and fuel type combinations. Section 5.2.1.1 discusses CLBs.

Although the staff did not accept the WCAP-17788 analysis that determined the fiber limits, the staff considered that the limits were established at limiting flow, particulate size, and particulate to fiber ratios. The staff also compared the fibrous debris limits from WCAP-17788 to test

results from WCAP-16793. The fiber limits from WCAP-17788 testing are lower than those in tests that WCAP-16793 indicate as acceptable. Even with significantly higher fiber amounts included, test results from WCAP-16793 indicate that the WCAP-17788 limits are conservative.

The NRC staff assumed that information from the STP submittal could be used to estimate the HLB size that would generate and transport enough fibrous debris to reach the acceptance limit. Plants that have less fibrous insulation installed in the containment are of lesser concern and are bounded by plants with large amounts. The choice of STP as the example plant is reasonable because of the large amount of fibrous insulation, the large number of breaks evaluated around the break size of interest, and the use of the largest debris amount from the subset of breaks available at the given size. STP provided debris generation and transport information for all welds that could fail and result in a LOCA as part of a risk-informed license amendment request to resolve GSI-191 (13). The staff considers STP representative of the most challenging plants with respect to the generation and transport of fibrous debris to the strainer.

To determine the maximum amount of fiber that can arrive at the strainer and still meet the most conservative fiber limit, the staff considered a plant with the minimum number of FAs (157) and an 85 percent filter efficiency at the strainers. For these conditions, the maximum fiber allowed at the core inlet is 3,202.8 grams or 7.1 pounds (20.4 grams of fiber multiplied by 157 FAs.) Using an 85 percent filter efficiency for the strainer, this implies that 47 pounds of fiber can arrive at the strainer. (UPI plants have fewer FAs but are evaluated in a different way. See Section 5.2.1.3.)

The smallest break at STP that results in 47 pounds of fibrous debris at the strainer is a 6-inch DEGB (5.19-inch inner diameter). The STP debris loading includes 28.5 pounds of latent fiber. Therefore, for this case, 16.5 pounds of break generated fiber are transported to the strainer. Some 6-inch breaks generate more fibrous debris, and some generate less. The range of fibrous debris loads at the strainer for all 6-inch breaks is 29 to 63 pounds.

The next smaller break in the STP analysis is on a 4-inch pipe. The limiting 4-inch break transported about 38 pounds of fiber to the strainer. All other 4-inch breaks resulted in less fiber at the strainers.

A fiber pass through of 15 percent (85 percent filter efficiency) is realistic and biased conservative based on the data that licensees have provided to the NRC. Section 5.2.1.2.1 discusses strainer penetration in further detail. The value is based on testing that used 100 percent fine fiber inserted upstream of the strainer and used realistic or conservative flow rates and other test methods. The data provided strainer filter efficiency for a range of debris loads. The NRC staff does not have a large database of penetration testing that is useful for calculating penetration values at relatively low fiber amounts. Most early penetration testing was performed to determine the maximum amount of fiber that can penetrate the strainer considering a plant's maximum debris load. There is some uncertainty associated with the 15 percent penetration value because of the many different strainer configurations (size, number of strainers, flow velocity, and other factors) throughout the PWR fleet. The evaluation of the smallest break size that could generate enough debris to cause in-vessel issues is centered on a relatively small fiber amount. As the amount of fiber at the strainer increases, filtration efficiency increases.

For this evaluation, the pipe break that could result in a problematic debris amount for the most limiting HLB conditions is assumed to be a DEGB of a 6-inch pipe on the hot side of the RCS. Such breaks are predicted to occur infrequently (see Section 5.5.2). Smaller, more likely breaks, will be less challenging to the fuel than analyses conducted by the PWROG and NRC indicate. Smaller breaks result in lower ECCS injection flow rates.

Also, as discussed above CSS may not be initiated for some plants for small breaks. The lower injection flows delay the switchover to recirculation. The WCAP-17788 analyses assumed an early switchover based on the largest LOCAs. Early switchover results in a higher decay heat assumption that is more challenging to fuel temperatures. Delaying the switchover to recirculation would result in a decrease in decay heat and require less flow to maintain LTCC. This provides margin in the analyses.

Subscale FA testing performed for WCAP-17788 found that headloss across debris at the core inlet will vary depending on the size and amount of particulate debris arriving at the core inlet. The fibrous debris limit was established using a conservative size distribution and amount for particulate debris. Small amounts of particulate result in an uncompact bed with low headloss. Excessive amounts of particulate result in an unstable bed and bed breakthrough at the fiber amounts tested. Flow also affected debris bed formation, with higher flow rates resulting in bed breakthrough. The fiber limits determined by testing were based on the most limiting conditions for the parameters studied. Alternate conditions will result in higher fiber loads required to reach the same headloss.

The analysis discussed in this section is considered realistic or conservative for the following reasons:

- It used debris loads representative of a very high fiber plant
- It used a realistic to conservative strainer filtering value
- It used the most limiting fiber limit for 2 FA types and 4 plant design categories
- It used the smallest number of FAs for applicable plant designs
- Other margins discussed in this section and throughout the document apply

#### 5.2.1.2.1 Fiber Penetration

There is a significant database that can be used to determine plant-specific total fiber penetration amounts or total amounts per specific strainer area. Early testing did not gather periodic data to determine the penetration behavior for fiber, but simply collected a total amount at the end of the test. More recent testing collected fiber downstream of the strainer at frequent intervals. Information from this testing has been used to determine how fiber penetration changes over time or with strainer debris load.

Penetration data indicates that the percentage of debris that passes downstream of the strainer at any time is related to the debris load on the strainer. Penetration percentage values taken only at the end of the test are not meaningful except to the specific condition tested or to determine a maximum fiber penetration value for a specific plant. The NRC staff has a limited database of strainer penetration testing that can be used to determine time or load dependent



strainer penetration amounts. Figure 1 below (from the Vogtle test program) illustrates that fiber penetration decreases as debris amount on the sump strainer increases (26).

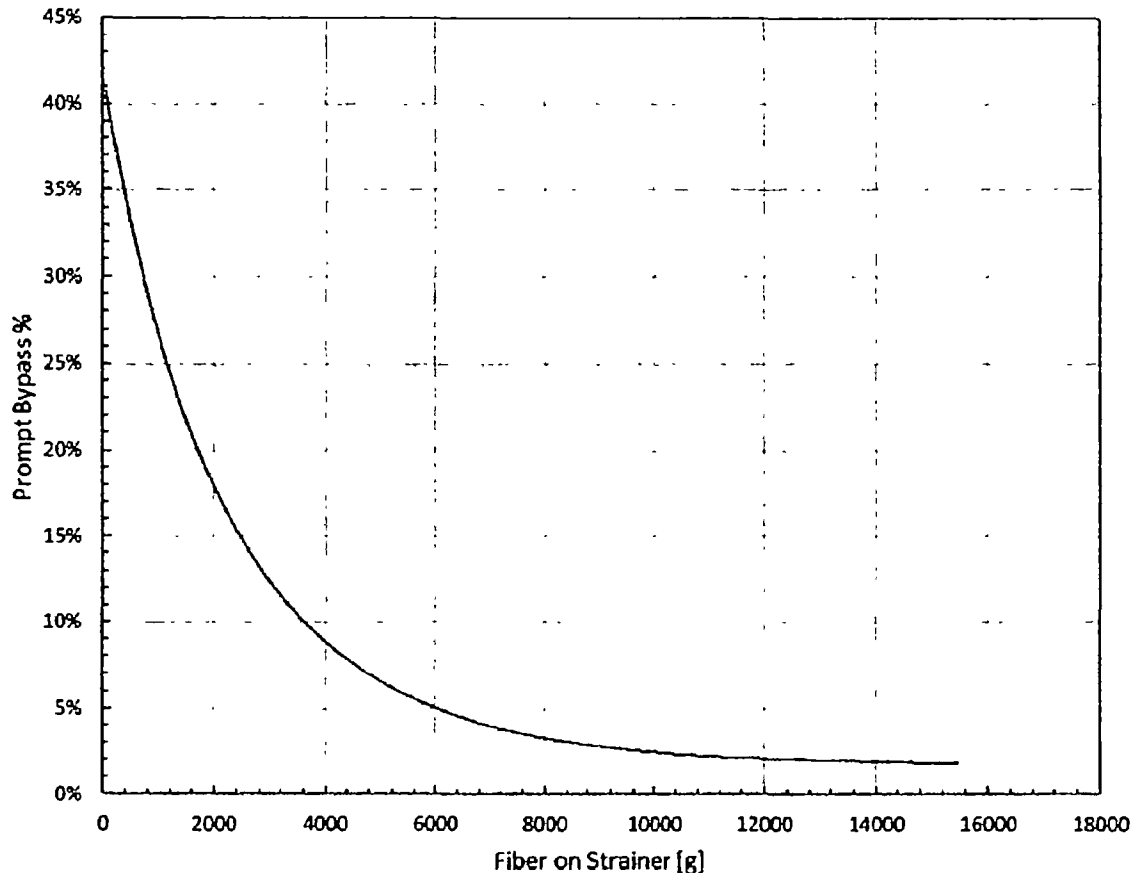


Figure 1 - Fiber Penetration as a Function of Debris Load

The staff used information from six recent strainer penetration test programs that have more refined information based on frequent downstream debris collection. Each program performed several tests to gain understanding into the factors that affect penetration. The staff determined that fiber penetration amount decreases quickly with fiber buildup on the strainer as shown in the figure above. Relatively smaller breaks may be almost as challenging for downstream effects as larger breaks because the debris initially arriving at the strainer increases the filtration efficiency.

The evaluation for the 6-inch HLB in this TER considered the results from these six penetration test programs because they were the only relevant information available to the staff. The staff used a value for penetration that was conservative with respect to the available data for the debris load considered for the case. Some plants may have plant-specific strainer configurations that would allow greater penetration at the specific debris load considered. However, two of the units with recent testing have very large strainer areas (one is the largest strainer installed in any U.S. PWR) making it likely that the data would be conservative with respect to the fleet. Other considerations like approach velocity and strainer perforation size

can influence penetration values. The amount of fiber that reaches the core also depends on plant configuration, including the number of strainers, and how the operating ECCS and CSS pumps are aligned to the strainers. For example, any debris that is returned to the sump via the CSS or flows out of the break, returns to the sump and may be removed by filtering on the strainer. If CSS does not initiate or a plant has lower ECCS flow, more debris is delivered to the core before the strainer efficiency increases.

The amounts of debris transported to the core for the CLB are less than for the HLB because most of the ECCS flow spills out the break in the CL. WCAP-17788 assumed that less than [ ] of fibrous debris would arrive in the heated core and at the core inlet combined for the HLB. The Vogtle study discussed above is for a very high fiber plant. This study indicates that 90 g/FA could reach the core under limiting conditions for Vogtle. Sections 5.2.1.1.3, 5.2.1.1.4, and 5.2.1.1.5 in the CLB section discuss debris suspended in the core.

Considering available data and variations in plant strainer parameters, the penetration value used by the staff is conservative for most or all plants in the U.S. PWR fleet.

#### 5.2.1.2.2 Boric Acid Precipitation

BAP has historically been evaluated with respect to CLBs (Section 5.2.1.1.2 above discusses the potential for BAP to occur following a CLB). However, if debris collects at the core inlet following a HLB, to the extent that flow into the core is significantly reduced, conditions similar to those in a CLB could occur. The staff considered the conditions following a HLB and determined that the potential for BAP was bounded by the CLB conditions. For a HLB, the coolant delivered to the core before a significant amount of debris arrives is much greater than that needed to replace coolant lost to boiling. This excess flow flushes boric acid and other debris from the core more than during a CLB. Flushing of the core will continue unless a significantly resistant debris bed forms at the core inlet. Even if a resistant debris bed forms and begins to inhibit flow through the core inlet, coolant is redirected to the core through AFPs. The flow delivered to the core exceeds that required to replace boil off and the fluid in the core is well mixed by convective currents and boiling. Therefore, boric acid is removed from the core such that the concentration required for precipitation will not be approached.

#### 5.2.1.2.3 Conclusions for the Hot-Leg Break

The combination of the low frequency of a break that could generate and transport enough debris to challenge LTCC, and the conclusion that a debris bed that could block core inlet flow is unlikely to form implies that it is very unlikely that debris would adversely affect LTCC.

Based on the discussion above, the staff concludes that the fiber limits from WCAP-17788 (also listed in

Table 2 in Section 5.3.3.6) are acceptable metrics to assist in evaluating the acceptability of HLB debris amounts. Flow to the core will be maintained with these debris loads if chemical precipitates do not deposit or form on the debris bed. If a limited amount of fiber greater than the design-specific limit is transported to the core inlet, a uniform bed is unlikely to form and flow to the core will continue. The actual debris amount that might result in preventing adequate flow to the core is not defined. If the core inlet becomes completely blocked, AFPs will allow flow to

reach the core as described in Section 5.3.3. There is adequate DID to assure enough flow to maintain LTCC following a HLB for the current operating fleet of PWRs that demonstrate acceptable fiber amounts at the core inlet.

Considering the above, the NRC staff concludes that it is very unlikely that debris in the RV, generated by a HLB, would inhibit LTCC for the current operating PWR fleet. In addition, the BAP evaluation for the CLB is limiting with respect to the HLB, so BAP is not a concern for the HLB.

#### 5.2.1.3 Upper Plenum Injection Plants

The UPI plants have an ECCS configuration unlike other PWR designs. The operating fleet has five UPI units (R.E. Ginna Nuclear Power Plant; Prairie Island Nuclear Generating Plant, Units 1 and 2; and Point Beach Nuclear Plant, Units 1 and 2). The ECCS initially injects directly to the UP, above the core via an independent nozzle. All fluid and entrained debris are available to enter the top of the core. The initial injection into the UP is similar to HL injection for a typical PWR. Therefore, a HLB for the UPI design is like the CLB for other plants and most of the flow goes out the break in the HL. The core inlet for ECCS injection and initial recirculation is at the top of the core instead of at the bottom of the core.

The top of the core is not likely to become blocked with debris because of the turbulence caused by boiling and steam exiting the core. The steam exiting the core will impact structures above the core exit and add to the turbulence. For a HLB, most of the coolant spills out the break. For a CLB, the coolant flows through the core and out the break. Therefore, debris enters the core region with the flow. The effects of turbulence on the formation of debris beds were discussed above for typical PWR designs. Turbulence is much greater for the UPI design because coolant enters the reactor at the top of the core where the velocity of steam exiting the core is relatively high. Because the top of the core is unlikely to become blocked, cooling is maintained during injection into the UP.

UPI plants use something similar to HLSO to prevent BAP following a HLB. Instead of switching injection from the CL to the HL, UPI plants switch from UPI to CL injection, or a combination of UPI and CL injection. The switch to CL injection occurs several hours after the initiating LOCA. If the break is in the hot side, the switch to CL injection will flush concentrated debris and boric acid from the core. If the break is in the cold side, coolant injected into the CL will flow into the core via the DC and LP and only the coolant required to make up for boil off enters the core. By the time a UPI plant switches to CL injection, debris in the sump will be depleted so it is unlikely that a debris bed will form at the core inlet. Because of the unique design of UPI plants, it is not critical that the switch to CL injection be initiated before chemical precipitates may form. This is because a filtering bed is unlikely to form at the top of the core where injection occurs. However, it is important that CL injection is initiated to flush concentrated debris and boron from the core.

Once injection is switched to the CL, debris remaining in the sump may be pumped to the core inlet. The injection into the CL can provide pressure up to the shut off head of the ECCS pumps (as limited by the height of the SG tubes) if the break is in the HL. For this condition, WCAP-16793-NP-A and the associated staff SE accepted a fibrous debris load of up to 15 g/FA at the core inlet, even when chemical effects are included in the debris headloss.

The switchover to CL recirculation takes place several hours after the LOCA; therefore, it is possible for chemical precipitates to form and filter on any debris bed. By this time, filtering on the strainer, settling, or deposition in the core will have removed most of the fibrous debris from the sump. A small amount of fiber may be suspended in the pool and transported to the strainer. Most of this will be captured on the debris bed on the strainer, but a small amount may penetrate and transport to the fuel inlet nozzles. As discussed in Section 5.2.1, a continuous bed is not expected to form at the core inlet, especially with the limited amount of fibrous debris arriving at the bottom of the core for this scenario. The debris amounts likely to arrive at the core inlet this late in the scenario are much less than 15 g/FA because the source term in the pool has been reduced to almost zero by the time CL injection is initiated.

After switchover to CL injection, for a CLB, coolant is delivered to the core only by the head resulting from the manometric balance between the core and the DC. This is similar to the CLB with CL injection in other PWR designs, but it occurs for UPI designs only after the switchover to CL recirculation. For UPI plant CLBs, after switchover to CL injection, only the coolant required to make up for boil off enters the core. The remainder of the coolant with any entrained debris flows out the break. Because the switch to CL injection is relatively late in the LOCA scenario, chemical precipitation may occur. For this condition, WCAP-16793-NP-A did not conclude that a debris limit of 15 g/FA was justified. After chemical effects are included in the debris headloss, testing shows that the headlosses for the CLB flow rates can increase by 1 psi above non-chemical headlosses for tests that included fiber of [ ]. This headloss could encroach on the available driving head for CL recirculation for the UPI plants. However, because the break is in the CL and most of the debris will have been deposited on the strainer before the initiation of CL injection, the amount of debris reaching the core inlet is much less than for the HLB.

The largest source of fiber may be that from erosion of larger pieces that have settled in the pool. Most of this erosion occurs relatively early in the event and decreases with time. Erosion is a relatively small source of fiber and the eroded fines are likely filtered by the sump strainer/debris bed. Most of the fluid injected into the CL flows out of the break and back to the sump where it is filtered at the strainer before being recirculated back to the core. Because the amount of fiber in the pool has been depleted by the time CL recirculation is initiated and the majority of any debris that penetrates the strainer flows out the break, the quantity of fiber reaching the core inlet for a CLB is much lower than for the HLB considered in WCAP-16793-NP-A. The amount of fiber reaching the core inlet is unlikely to have a measurable effect on headloss or flow at the core inlet.

#### 5.2.1.3.1 Conclusions for Upper Plenum Injection Plants

Because of the unique design of the ECCS for UPI plants, a debris bed will not inhibit flow into the core. The initial injection is into the UP where turbulence will prevent a bed from forming. By the time a UPI plant switches to CL injection, the amount of fiber that may be transported from the pool to the strainer is very small and the filtration efficiency of the strainer is high

because of the debris bed deposited on it. Therefore, the amount of fiber reaching the core inlet (FA BNs) will not affect LTCC.

#### 5.2.1.4 Debris Generation and Transport

This section discusses margin related to debris generation and transport. It provides details, especially for the aspects of the analyses that are more complex. The margins are summarized in Section 5.5.3.

The most likely breaks are smaller breaks that are less challenging to mitigate from several perspectives. Reasons for this are discussed below with respect to specific parameters that are considered in the evaluation. In addition to those, smaller breaks result in lower required ECCS makeup flow. The injected sources are available for a longer period and decay heat is lower when the system is switched to recirculation. Lower decay heat allows for lower flows to make up for coolant lost to boil off and greater time for operators to respond to debris blockage.

Debris generation values used by licensees in their analyses are for the most challenging breaks for strainer performance. The methodology used to determine debris generation amounts contains conservatism, but also uncertainty. The staff determined that the methodology is generally conservative, with few exceptions. However, the use of the debris generation values from the most challenging breaks clearly results in a substantially conservative bias because of the very low frequency associated with these breaks. The smaller, more likely breaks will result in much lower debris generation and reduced challenges to LTCC.

The transport assumptions used in this evaluation and by licensees are based on approved guidance that is considered conservative. The assumptions about transport and debris characteristics are chosen to maximize the amount of debris arriving at the strainer. In addition, the debris amounts represent the bounding breaks for each debris type.

The debris characteristics assumed for the transport evaluation are chosen to increase the probability that debris will be transported to the strainer. Coating particulate is assumed to be 10-micron particles that are suspended in the fluid. Testing has shown that the coatings will fail in a range of sizes and that some of the particulate will be large enough that it will settle in the sump pool or LP of the reactor. Fine fiber is assumed to be individual strands that remain suspended in the coolant. Clumps of fiber in larger size ranges are assumed to be the smallest size within the range, making them more likely to be predicted to transport.

Fluid velocities and turbulence used in transport calculations are based on flows and coolant entering the pool that are developed from the largest breaks and maximized turbulence from fluid falling into the pool. Smaller breaks would result in lower flow rates, and reduced turbulence from water falling into the pool, and they might not result in flow from the CSS if CSS is not initiated. The lower flow rates and reduced turbulence would result in increased debris settling. In addition, lower flow rates result in delayed switchover to recirculation because the RWST is depleted more slowly. The delayed switchover allows more time for debris to settle in a relatively stagnant pool. A smaller break can also result in lower flow rates to the RCS and a higher CSS to ECCS flow ratio. The higher flow ratio results in the return of more fluid to the sump, which allows any entrained debris to pass through the strainer again with the potential for filtering.

The transport evaluation assumes that particulate is not filtered but continues to recirculate until it reaches the core and remains there. Testing has demonstrated that some particulate is deposited on fiber beds relatively early. As the debris bed becomes denser, the amount of particulate filtered increases. Some particulate would also settle or deposit on surfaces. Early in the scenario, the conservatism associated with the assumption that particulate debris is not filtered may be small.

Credit is not given for the capture of fine debris on interceptors, walls, or other structures in containment or within the RV. These structures would capture some fine debris.

It is assumed that all fibrous debris is captured at the core inlet for both the CLB and HLB cases. Some of the fiber will pass through the core inlet and remain in the heated core region or exit the core with excess flow (for the HLB). The amount of fiber assumed trapped at the core inlet is conservative.

Testing conducted for a new reactor design demonstrated that some fiber will settle in the LP and not be available for transport to the core inlet. Settling of fiber is not credited.

Therefore, the amounts of fiber and particulate used for this evaluation are conservative.

#### 5.2.1.5 Chemical Effects

Volume 5 of WCAP-17788 contains the in-vessel chemical effects evaluation (14). The following discussion summarizes the PWROG in-vessel chemical effects testing and the NRC staff evaluation. For greater detail, the draft NRC staff SE for Volume 5 is non-publicly available in ADAMS (27). The following discussion provides a high-level summary of the PWROG chemical effects testing and the NRC staff evaluation. Section 5.2.1.2 of this report gives an overview of the WCAP-17788 methodology, including how chemical effects were considered for a HLB.

##### 5.2.1.5.1 Testing

PWROG survey data were used to create post-LOCA plant materials and sump chemistry inputs for the test plan. The plant materials input consisted of metals (including aluminum and galvanized steel), insulation materials, fire barrier material, and concrete. The fibrous and particulate insulation materials included calcium silicate, E-glass (fiberglass), silica powder, mineral wool, microporous insulation, and aluminum silicate. Fire barrier material included Interam™. The sump chemistry inputs included the projected post-LOCA temperature profile, sump pool volume, pool alkalinity (pH), and buffer type. The temperature profiles were based on either a post-LOCA temperature profile provided by a plant or were estimated using temperature data provided by the plants with their survey responses.

Testing was performed with independently controlled 60-liter capacity stainless steel autoclaves (pressure vessels). Two resistive heater bands were mounted on the outside of each vessel to provide the heating for the elevated test temperatures. One of these heating bands was located near the bottom of the autoclave to promote convection and more uniform temperatures. The test set-up included means to introduce pressurized air and to vent air. A stainless-steel sampling line was located at approximately the mid-height of the autoclave vessel to avoid sampling either easily settled materials or floating materials in the fluid samples. The autoclave assemblies also included pressure gauges and pressure relief valves. Thermocouples provided temperature measurement of the test fluid. A computerized data system used feedback from the thermocouples to automatically control the temperature of the autoclaves to a

pre-determined profile specific to the test group. Metallic test coupons were suspended from the top of the autoclave using polytetrafluoroethylene (PTFE) cord material to electrically isolate the coupon from the stainless-steel autoclave. Depending on the type of autoclave test, fibrous and particulate debris were either placed in a bag to constrain the loose debris (i.e., "in-bag" tests) or were freely dispersed within the autoclave test fluid (i.e., initial battery out of bag ("IBOB") and "out-of-bag" tests).

The NRC staff visited the Westinghouse laboratory in Churchill, Pennsylvania in May 2013 and November 2013 to witness testing and to discuss the test methodology and preliminary results. The visits were intended to improve staff understanding of the tests to better support a review of the WCAP-17788 submittal. The NRC staff trip report dated June 10, 2013 (28) is available in ADAMS. The NRC staff trip report dated December 24, 2013 (29) is non-publicly available in ADAMS.

The initial autoclave water chemistry included representative amounts of boric acid for all tests. Autoclave test pH depended on the plant-specific conditions. For tests that used a sodium hydroxide (NaOH) buffer, pH adjustment occurred before insertion of the test materials into the autoclaves since NaOH is inducted into the containment spray immediately following a LOCA. Therefore, the pH for plant groups with NaOH was constant throughout each test except for any small changes caused by debris reactions. For plants-specific tests using sodium tetraborate (STB) or trisodium phosphate (TSP) buffers, the sodium carbonate and the buffer were added after the coupons had been exposed to the lower of either the maximum test temperature or 200 degrees Fahrenheit (°F) for 30 minutes. This sequencing is intended to expose the test materials to a more representative initial acidic plant pH before buffer dissolution. In the event of a LOCA, the sump pool pH for plants with STB buffering increases as STB is either dissolved from retention baskets or is introduced from melting ice (in the case of plants with ice condensers). For plants with TSP buffering, the pool pH following a LOCA increases as TSP dissolves from retention baskets. Following the addition of buffer and carbonate, the autoclaves are pressurized with air (approximately 30-50 psig) and controlled to a temperature profile specific to the test group.

Fluid samples were taken from the autoclave tests at various times and were immediately placed in an oven at a predetermined temperature lower than that of the autoclave. The exact oven temperature was dependent on the autoclave fluid temperature at the time of sampling. The temperature difference between the autoclave temperature and the oven temperature was intended to simulate the temperature drop of sump fluid passing through a heat exchanger before entering the RV. After a minimum oven hold time of 1 hour, the samples were analyzed by performing vacuum filtration (to determine filtration times for each sample) and by turbidity measurement.

Vacuum filtration was used to determine the specific timing of the chemical precipitate product. As a screening criterion, the PWROG established a filtration time (drain time) threshold value of 100 seconds for 50 milliliters of fluid to indicate the possible presence of chemical precipitates in the test fluid. The vacuum filter membranes used were a 1.0-micron pore size PTFE fiber filter designed for high-temperature filtration.

The PWROG hot filtration test objective was to detect the presence of any chemical products that could cause high pressure drops across a fiber bed in the RV during the initial 24 hours following a LOCA. Since drain times can vary for a variety of reasons not related to chemical precipitates, the PWROG selected a 100 second drain time as the screening threshold for chemical effects based on earlier testing performed by Westinghouse and experience with the

first six WCAP-17788 test groups. The 100 second threshold value resulted in identification of chemical precipitates and generated false positives, when drain times exceeded 100 seconds as a result of non-chemical debris. Tests with drain times exceeding 100 seconds and uncertainty about the cause of the longer drain times were then sorted out by further experimentation (e.g., bench tests). In Section 7.1 of Volume 5 of WCAP-17788, the PWROG later evaluated and confirmed the appropriateness of a 100 second drain time threshold value. The NRC staff also evaluated the filtration test 100 second drain time threshold for chemical effects screening. The staff reviewed the filtration test results and found the 100 second drain (filtration) time acceptable as a screening threshold as discussed in the draft SE. Based on the information provided by the PWROG, the staff found the temperature profiles and oven cooling before hot filtering that were used in the test program to be acceptable.

The Volume 5 test results showed that aluminum precipitates were the cause for high drain times related to chemical effects. Finding aluminum-based precipitates to be the dominant contributor to post-LOCA chemical effects in PWR environments is consistent with previous testing results, including NUREG/CR-6913, "Chemical Effects Head-Loss Research in Support of Generic Safety Issue 191," issued December 2006 (30); "NUREG/CR-6914, Volume 2, "Integrated Chemical Effects Test Project," issued September 2006 (31); and WCAP-16530-NP-A, "Evaluation of Post-Accident Chemical Effects in Containment Sump Fluids to Support GSI-191," issued March 2008 (32). This is also consistent with NRC staff observations from many vertical loop and strainer chemical effect headloss tests performed at five different strainer vendor facilities, including tests with addition of pre-mixed WCAP-16530-NP-A precipitates and tests in which dissolved chemicals were added and precipitation occurred in the test loop (33).

The NRC staff finds the aluminum precipitation boundary identified in Section 7 of Volume 5 of WCAP-17788 to be an acceptable prediction tool for chemical precipitation within 24 hours of a LOCA. The staff compared Argonne National Laboratory (ANL) and WCAP-17788, Volume 5, solubility predictions at various pH and temperatures. Although the ANL solubility equations (34) are more conservative at all temperatures of interest when the pH is less than 8.5, the ANL equations over-predict solubility for the high pH tests that can be representative of plants that add NaOH to the containment spray following a LOCA. The WCAP-17788 precipitation boundary predicted all cases of aluminum precipitation in Volume 5 testing, except for Test Group 41, which was not representative of a plant condition. In contrast to the one test group exception, however, there were 39 test samples where the aluminum precipitation boundary predicted chemical effects but there was no evidence of precipitation from subsequent filtration testing. In addition, there were 38 test samples where the precipitation boundary predicted precipitation and it was detected during filtration testing. These numbers indicate that the precipitation boundary function proposed in Volume 5 is conservative within the 24-hour post-LOCA time frame of interest.

Although the NRC finds the aluminum precipitation boundary function identified in WCAP-17788, Volume 5, Section 7, to be conservative, the staff also recognizes there is inherent uncertainty associated with a predictive solubility tool. The PWROG addressed the uncertainty in the solubility boundary by proposing that plants retain margin to the boundary, as shown in Table RAI 5.13-1 (35). PWROG guidance in Section 7.6 indicates that plants that have changed material quantities from the test group can demonstrate that the change is acceptable by either (1) showing that the actual plant conditions reduce precipitation risk relative to the test, or (2) demonstrating that there is still sufficient margin to precipitation if the deviation from the test condition results in an increase in the risk of precipitation. The NRC staff finds the



PWROG guidance related to the margin to precipitation values acceptable since it accounts for potential errors in temperature, pH, and inductively-coupled plasma mass spectrometer measurements in a conservative manner.

Based on the considerations summarized above and discussed in more detail in the draft SE, the NRC staff finds the overall technical approach in Volume 5 of WCAP-17788-P to be acceptable for determining short term (within 24 hours following a LOCA) chemical effects in the RV since this approach used representative test conditions, accounted for uncertainties, and had an overall test approach that was effective in detecting chemical precipitation.

#### 5.2.1.5.2 Test Results—Precipitation Timing

The overall WCAP-17788 methodology relies on the time to chemical precipitation being longer than the minimum time at which AFPs into the core can accommodate complete core inlet blockage. WCAP-17788 expresses success as  $t_{chem} > t_{block}$ . Section 5.3.3 further describes  $t_{block}$ . Volume 1 of WCAP-17788 states that  $t_{block}$  is less than 6 hours for all plant designs (36). At that point, flow through AFPs into the core is sufficient for LTCC according to the WCAP-17788 analysis. The autoclave and filtration testing performed for Volume 5 showed that a 6-hour precipitation timing is conservative for almost all PWRs.

Figure 2 shows the timing of chemical precipitation based on the WCAP-17788, Volume 5, PWR test group data. One test group with plant representative conditions had precipitation earlier than 6 hours.

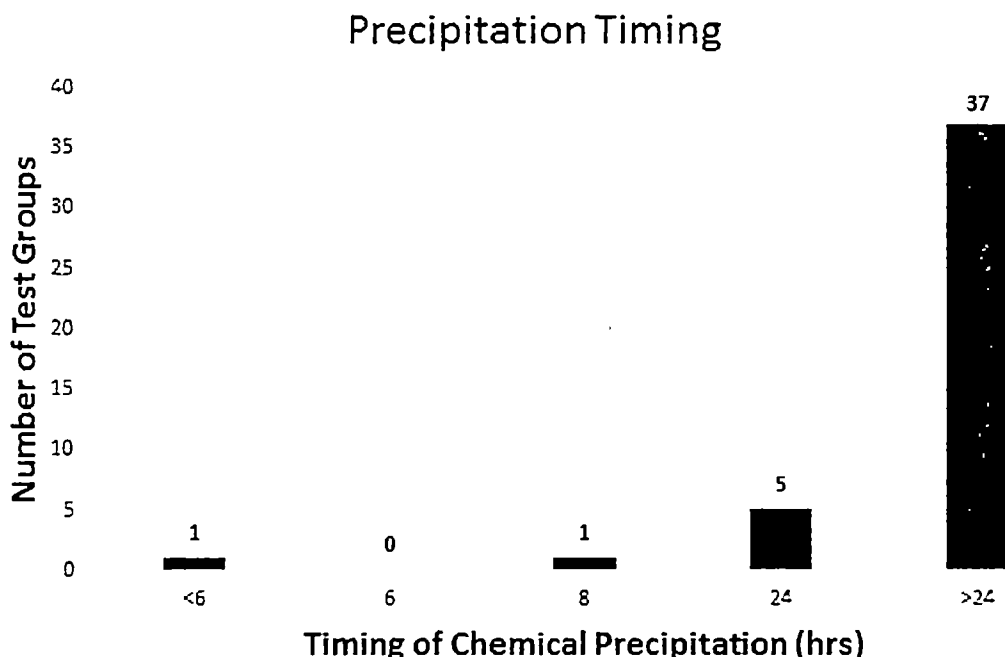


Figure 2: Timing of Chemical Precipitation for WCAP-17788 Test Groups

For the remaining test groups, the NRC staff concluded that one test group may have experienced precipitation as early as 8 hours, although the PWROG concluded that precipitation did not occur until 24 hours for this group based on the mass of aluminum on the filter paper. Five other test groups showed evidence of precipitation in the 24-hour samples. One of these five test groups with precipitation at 24 hours only performed an "out of bag" test with plant representative amounts of debris. Earlier "in bag" tests with extra aluminum margin had early chemical effects. The plant-representative "out of bag" test contained about 2/3 of the aluminum coupon surface area compared to the earlier "in bag" tests with early chemical effects.

No precipitation was detected up through the 24-hour sampling time for 37 of 44 test groups.

#### 5.2.1.5.3 Staff Analysis of Precipitate Timing

The NRC staff used the results from the WCAP-17788, Volume 5, chemical effects testing to consider precipitation timing and other post-LOCA operator actions that could impact the integrity of a fibrous debris bed at the core inlet. The NRC staff compared chemical precipitation timing to the time when safety injection flow paths are modified (e.g., switching to HL injection or the equivalent) to preclude BAP. Switching safety injection to the HL, injecting simultaneously into the HL and CL, or an equivalent modified flow path (for some plant designs) before chemical precipitation is expected to reduce the probability of a high resistance debris bed forming at the core inlet. The NRC staff observed during the brine testing (6) that a reduction in flow allowed the buoyancy-driven circulation to disrupt the debris bed. This suggests that HLSO could disrupt a debris bed at the core inlet.

The NRC staff evaluation focused the timing evaluation on the seven test groups (representing nine units) that confirmed chemical precipitation during the WCAP-17788, Volume 5, testing. One test group (two units) with confirmed chemical precipitates before 6 hours represents a two-unit, low fiber plant that has closed out in-vessel concerns under the conservative fiber limits established by the NRC staff in the SE for WCAP-16793. Therefore, assuming chemical precipitates arrive at the core inlet at this plant earlier than 6 hours, there is insufficient fiber to form a bed capable of blocking flow at the core inlet. This plant calculated a post-LOCA in-vessel fiber quantity of approximately 10 g/FA, significantly less than the 15 g/FA acceptance criterion the NRC staff approved in the WCAP-16793-NP-A SE. The staff approved the 15 g/FA limit since FA testing showed that the pressure drop from this quantity of fiber, with particulate and chemical precipitates, is acceptable. The single FA tests were designed to promote uniform flow to the bottom of the FA to ensure that a fiber bed was formed. This plant design also has UPI following a LOCA. Fiber bed formation at the top of a UPI plant core following a LOCA is not expected because of turbulence from boiling (see Section 5.2.1.3).

Other than the units discussed above, the results from the next earliest test group indicated that precipitation may have occurred as early as 8 hours. The staff notes that the PWROG considered the confirmed precipitation time for this plant to be 24 hours. This plant switches to HL injection no later than 6.5 hours following a LOCA.

One additional test group (one unit) with confirmed chemical effects at 24 hours using plant-representative conditions, had early chemical effects during initial "in bag" testing (with greater than representative materials, including aluminum surface area). The final "out of bag" test for this group was performed with representative amounts of calcium silicate, fiberglass,

and aluminum. This plant switches to simultaneous injection in the HL between 5.5 and 6.5 hours after a LOCA. Without a plant representative "in bag" test, the staff is uncertain if precipitation would occur before HLSO since previous tests for this group showed "in bag" testing produced earlier chemical effects than "out of bag" tests.

Four other test groups confirmed chemical precipitation at 24 hours. Three of the four groups have a maximum time before safety injection flow into the HL (or other flow injection into the RV) to prevent boron precipitation equal to 6.5 hours. The final unit that confirmed precipitation at 24 hours has a HL injection time of 14 hours following a LOCA.

The remaining 37 test groups did not detect precipitation within the 24-hour test period. Each of these plants is expected to flush the core within 24 hours following the assumed LOCA, thereby increasing the probability that any bed on the core inlet would be disrupted before chemical precipitation.

#### 5.2.1.5.4 Chemical Deposits on Fuel

The staff previously evaluated the effects of chemical deposits on fuel cladding as part of its SE of WCAP-16793-NP-A. That SE explains why the NRC staff approved the use of the Loss-of-Coolant Accident Deposition Model (LOCADM) to evaluate deposits on fuel following a LOCA. The NRC staff reviewed LOCADM analyses for the 21 units that have closed GL 2004-02 and none of these units have results that challenge the 800 °F or 50-mil thick deposit acceptance criteria. This includes units with high fiber loading. LOCADM is a tool developed by the PWROG that can be used to validate that chemical deposits will not prevent adequate LTCC.

#### 5.2.1.6 Conclusion—Availability of Primary Flowpath

The staff concludes that following a LOCA, debris is not expected to completely block the normal ECCS flowpath through the core and prevent adequate LTCC. This is supported by testing and analysis that, taken as a whole, make this an implausible event. This conclusion considers the timing of events, understanding of the TH behavior of the system, and safety margins in the analyses. Should the primary flowpath through the core inlet become blocked, the staff considered DID offered by AFPs and other considerations. Section 5.3 describes these in more detail.

### 5.3 Defense in Depth

In the preceding sections, the NRC staff developed a basis to conclude that a core-wide inlet blockage arising from IVDEs following a postulated LOCA is an unlikely scenario. If, however, the core inlet became completely blocked with a high resistance debris bed, the NRC staff identified multiple mitigation features to provide LTCC, or to assure that the potential inhibition of LTCC does not lead to unacceptable public health and safety consequences. Since the NRC

staff determined that a core-wide inlet blockage is unlikely, these are considered DID. The sections below evaluate each DID mechanism identified by the staff.

### 5.3.1 Containment

Blockage at the core inlet does not affect the ability of the CSS to depressurize and remove heat from the containment. Therefore, the failure of containment is not expected to result from an in-vessel blockage and the containment barrier is assumed to remain intact to provide DID for the IVDEs under consideration in this TER. The staff recognizes that the debris being evaluated for in-vessel blockage can also block the ECCS strainers that supply water to the CSS. However, this evaluation assumes acceptable strainer performance has been demonstrated. The staff evaluates strainer performance separately.

The staff considered that a loss of LTCC could result in core damage that might affect strainers located close to the RV if the vessel is breached due to molten fuel reaching the lower head. The staff determined that few plants have with this configuration, and some of these have remote strainers in addition to the ones near the RV. The staff also determined that even if the core inlet is blocked, coolant delivered to the LP will reduce the potential for molten fuel to reach the lower head and for vessel breach. Therefore, it is unlikely that IVDEs would cause strainer failure and CSS will remain functional.

### 5.3.2 Operator Actions

All PWRs use HLSO or a similar action to prevent the buildup of boric acid in the core. In response to the issue of the effects of debris on LTCC, PWRs have initiated plant-specific actions to monitor for, and respond to, loss of flow to the core. HLSO is one of the actions that the plants use to inject coolant via a flowpath that is not blocked with debris (injection to the top of the core). Use of HL injection will also tend to disrupt any bed formed at the core inlet by reversing flow through the core. This will be more effective for CLBs, although reducing or stopping flow to the core inlet was shown to remove debris beds from the BN for low-resistance beds.

In addition, industry developed actions that include monitoring and responding to blockage at the core inlet. These measures include monitoring core exit thermocouples, reactor levels, and containment radiation levels from the control room. If core blockage is detected, the plant operators have multiple options to mitigate the condition. Mitigative measures include refilling the RWST and injecting via different flowpaths, reducing RCS pressure, restarting reactor coolant pumps, and initiating early HL injection. Therefore, in the unlikely event that a LOCA occurs, a high-resistance debris bed forms at the core inlet, and AFPs are not successful in providing flow to the core, operator action options exist to maintain LTCC.

### 5.3.3 Alternate Flowpaths

If the core inlet becomes completely blocked, each plant has AFPs to provide coolant to the core for LTCC purposes. These AFPs include design features such as flow passages in the BB region, upper head spray nozzles, and pressure relief holes between the BB region and the core

periphery. A series of TH analyses described in Volume 4 of WCAP-17788 (16) and associated RAI responses (37) (38) (39) evaluates the efficacy of the AFPs to provide LTCC.

The material described in this section relates to debris accumulating at the core inlet (specifically, the BN or spacer grid) after a HLB. Another consideration is that debris present in the coolant not captured at the core inlet, passes through the AFPs, and continues to the heated core region. This can happen in two ways: (1) resistance at the inlet builds to the point where AFPs are activated, directing flow through the AFP to the core or (2) operator action occurs to initiate HLSO, in which a fraction of the ECCS flow is transferred from the CL to the HL to mitigate possible BAP. The combined amount of fibrous debris that can accumulate at the core inlet and within the core without affecting LTCC is assumed to be [ ], which is discussed in Volume 1, Section 6.4, of WCAP-17788. The staff evaluated in-core fibrous and particulate debris as described in Section 5.2.1.1.3 of this TER. The remainder of this section considers the effect of debris blocking the core inlet.

#### 5.3.3.1 Background

Once a plant depletes its injectable inventory, its ECCS is aligned for recirculation via SSO. At that point, fibrous and particulate debris may enter the RCS. Such debris may collect at the core inlet as the recirculating coolant travels from the LP into the core. Over time, as debris continues to collect, the hydraulic resistance at the core inlet will increase. The presence of chemical effects, such as precipitates, may also contribute to increased inlet flow resistance. If the flow resistance continues to increase, a greater fraction of liquid will enter the core through the AFPs as opposed to the core inlet. If the core inlet becomes completely blocked, the AFPs become the sole source of liquid entering the core to replace that which is boiled off or spilled out of the break.

Many variables can influence the scenario described above, including the following:

- the depletion time of the source of injectable emergency coolant,
- 
- the amount of debris entering the RCS,
- the fraction of that debris that can be transported to the core inlet,
- the amount by which the hydraulic resistance at the core inlet increases over time,
- the ability of, and time at which, transported debris may cause a complete core inlet blockage

The scenario is further complicated by plant-specific considerations, including design features such as flow connections between the BB and core regions or ECCS flow capacities, and the particular operating characteristics (e.g., core power distribution) at the time of the initiating event.

#### 5.3.3.2 Simplifying Assumptions

To distill this complex scenario into a tractable problem, the PWROG made several simplifying assumptions in evaluating the efficacy of the AFPs. Some of these assumptions are summarized below:

- break location – The AFP analyses simulated a HLB because it results in the largest fraction of recirculating ECCS flow traveling to the core inlet, where debris could then collect to form a bed.
- SSO time – The AFP analyses assumed that SSO would occur 20 minutes following the initiating event. This is intended to represent a bounding minimum that would cause most debris to be transported into the RCS early, while the decay heat remains high.
- core operating characteristics – The AFP analyses assumed the limiting FA was operating with a top-peaked power shape, similar to that assumed in small-break LOCA analyses, to maximize a second heatup if the core uncovers during a core inlet blockage.
- reactor design differences – Four separate sets of analyses make up the AFP analyses, each set intended to represent a different class of operating PWR reactors. These included: (1) an upflow-configured, 4-loop Westinghouse plant, (2) a downflow configured, 3-loop Westinghouse plant, (3) a Combustion Engineering (CE) plant, and (4) a Babcock & Wilcox (B&W) plant.
- analytic methods – The AFP analyses were performed using EMs that were derived from NRC-approved EMs used to analyze short-term ECCS performance.
- AFP treatment – Each class of plant has different AFPs that were modeled. The AFP resistances were hand calculated using physical plant geometry and, via scaling analyses, were adjusted to ensure that core power was considered as well (see below).

The treatment of rated thermal power level also warrants additional discussion. In WCAP-17788, the thermal power levels selected for each category were not necessarily bounding for each plant in that category. Instead, the PWROG intended to account for variations in core power in the way that the AFP resistances were modeled. The PWROG's response to RAI 4.2 (38) provided a scaling analysis to demonstrate that the core power was considered by scaling the AFP resistance for the modeled plant. Although the NRC staff did not review this RAI response in sufficient detail to make a regulatory finding, it provides information to indicate that the analyses included a means to account for variations in core power level without modeling an explicitly bounding, high-power level.

Although these simplifying assumptions enabled a reasonably consistent set of analyses among the four design classes, it should be noted that the CE analyses were performed using slightly different approaches, in some cases, because the minimum ECCS flow per FA is lower than for the other plants. As appropriate, the sections below note these differences. Furthermore, because the CE plant analyses used a different, and generally less limiting, set of assumptions, the NRC staff performed supplemental analyses for the CE plants using the TRACE computer code, as discussed in Section 5.4.

#### 5.3.3.3 Description of Analyses

The goal of the WCAP-17788 analyses in Volume 4 (16) was to determine if AFPs were adequate to maintain LTCC after switchover to recirculation and formation of a debris bed blocking the core inlet. While 10 CFR 50.46(b)(5) requires that the core be maintained "at an acceptably low value" to remove decay heat from the core, the PWROG opted for an

acceptance criterion of 800 °F as a more quantitative, acceptably low value to show that LTCC is not compromised.

In this TER, however, the NRC staff evaluated the AFP analyses differently. The NRC staff considered the AFP analyses, insofar as the analyses provided evidence that the AFPs would ensure LTCC if a complete core inlet blockage occurred. It should be noted that, while the AFP analyses were performed using methods based on NRC-approved models, the analytic results were not considered to provide an exact prediction of the PCT, or to provide a bounding prediction of behavior for the entire PWR fleet. As discussed below, some parameters, such as the assumed plant power level, do not bound all plants in the category analyzed. However, the NRC staff considers the analyses to establish the concept that the AFPs can provide an additional means to cool the core thus preventing core damage beyond that which occurs during the blowdown and recovery phases of the event. The NRC staff determined that this conclusion is appropriate, given the low likelihood of complete core blockage following the already unlikely initiating event.

The AFP analyses described in WCAP-17788 include three variables<sup>1</sup> that characterize the effects of debris blockages at the core:

- (1)  $K_{max}$  is the maximum resistance due to fibrous and particulate debris bed formation that can be tolerated at the core inlet. This value is compared to results of subscale headloss testing to establish an upper bound of the amount of fibrous debris that can be tolerated at the core inlet. A  $K_{max}$  value corresponding to the headloss testing results for each FA was applied beginning at the SSO time, although the CE analyses modeled  $K_{max}$  as a piecewise linear ramp beginning 800 seconds after the SSO time. This difference was justified in the response to RAI 4.26 (39). In actuality,  $K_{max}$  is a function of ECCS flow rate. The limiting cases are derived from the lowest ECCS flow rates.
- (2)  $t_{block}$  is the earliest time that complete core blockage can occur while not compromising LTCC. While  $K_{max}$  was applied at SSO time (except for the CE analyses identified above), the core inlet flow resistance was increased to a prohibitively high value to prevent flow through the core inlet and establish the AFPs as the primary source of core cooling. For the CE plants, the analysis for  $t_{block}$  was separate from the  $K_{max}$  analysis.
- (3)  $t_{chem}$  is the time at which chemical precipitates form, as determined by autoclave testing. The methodology assumes that after  $t_{chem}$ , the resistance through the debris bed is greatly increased because of chemical precipitate formation. Due to this increased resistance, the WCAP-17788 methodology requires the timing of complete core blockage,  $t_{block}$ , to be less than the timing of chemical precipitates,  $t_{chem}$ . If  $t_{chem}$  is less than  $t_{block}$ , then the method in WCAP-17788 is not valid and further analysis is needed.

To simplify the calculations and provide margin, the  $K_{max}$  values were determined at limiting conditions as discussed above. The  $K_{max}$  values are converted to debris limits as described in Volume 6 of WCAP-17788 (40) and discussed further in Section 5.2.1.2.

---

<sup>1</sup> In a separate series of analyses, the PWROG also evaluated the parameters  $K_{split}$  and  $m_{split}$ , which related to the core inlet flow resistances and flow rates required to divert flow into the AFPs, but these are not evaluated in detail in this TER. They merely assure that, at any given ECCS flow rate, some portion of flow will divert to the AFPs as the core becomes blocked.

The  $K_{max}$  and  $t_{block}$  values are determined iteratively. That is, for  $K_{max}$ , the value was increased until the PCT limit was approached when the resistance was applied at SSO (except for the CE analysis which is discussed above). For  $t_{block}$ , the time of application of a near infinite resistance was decreased until the PCT limit was approached.

#### 5.3.3.4 Analytic Methods

The PWROG used three separate computer codes to perform the AFP analyses:

- (1) The Westinghouse upflow and downflow analyses were performed using WCOBRA/TRAC. The NRC staff approved this code for use as a part of the Westinghouse Code Qualification Document (41) and Automated Statistical Treatment of Uncertainty Method (ASTRUM (42)) ECCS EMs.
- (2) The CE analyses were performed using S-RELAP5. The NRC staff approved S-RELAP5 for use, among other analytic methods, as a part of the Realistic Large-Break LOCA (RLBLOCA) EM documented in EMF-2103(P)(A), Revision 1, "Realistic Large Break LOCA Methodology for Pressurized Water Reactors," issued January 2015 (43), and Revision 3, issued June 2016 (44).
- (3) The B&W analyses were performed using RELAP5/Mod2-B&W (R5M2BW) (45). The NRC staff approved R5M2BW for use, among other analytic methods, as a part of the Babcock & Wilcox Nuclear Technologies (BWNT) LOCA EM (46).

WCOBRA/TRAC and S-RELAP5 are approved as elements of realistic ECCS EMs, in which the computer code is applied with a statistical methodology that accounts for uncertainties, while R5M2BW is approved as an element of an EM conforming to 10 CFR Part 50, Appendix K, "ECCS Evaluation Models," in which the EM relies on a series of bounding, conservative assumptions to account for uncertainties in the results. Regardless of the computer code however, all the AFP evaluations were performed in a deterministic sense, with reliance on conservative assumptions to offset the effects that uncertainties could have on the predicted results. No attempt was made to quantify uncertainties using the statistical features of the Code Qualification Document, ASTRUM, or RLBLOCA.

#### 5.3.3.5 Conservative Assumptions

As described above, these analyses relied on a set of generally conservative modeling assumptions to offset some uncertainties that were not explicitly addressed. While this evaluation is not intended to review these conservatisms exhaustively, examples include the following:

- Decay heat was modeled similar to the requirements in 10 CFR Part 50, Appendix K. The Westinghouse upflow and downflow analyses, as well as the B&W analyses, used the 1971 American Nuclear Society (ANS) Proposed Standard, "Decay Energy Release Rates Following Shutdown of Uranium Fueled Thermal Reactors" (47) with a 1.2 multiplier. The CE analyses for  $t_{block}$  used the 1979 standard American National Standards Institute (ANSI)/ANS-5.1-1979, "Decay Heat Power in Light Water Reactors" (48), for decay heat with a 1.1 multiplier, while the CE  $K_{max}$  analyses used the 1979 ANS standard for decay heat with a 1.2 multiplier.



- Owing to variability in conceivable ECCS recirculation flow rates, the PWROG studied a range of flow rates on a per-FA basis. The limiting results for the  $K_{max}/t_{block}$  analyses were obtained from minimum recirculation flows, which are the basis for this evaluation.
- For the limiting analyses summarized in Section 5.3.3.6,  $K_{max}$  was applied at the time of SSO, with the exception of the CE  $K_{max}$  analysis, which applied a piecewise linear ramp beginning at 2,000 seconds (i.e., 800 seconds after SSO time, as described in the response to RAI 4.26 (39)). The response to RAI 4.26 also showed a reasonable amount of conservatism in the CE  $K_{max}$  modeling approach.
- For the Westinghouse upflow and downflow analyses, as well as the CE analyses, a complete blockage was modeled instantaneously at  $t_{block}$ . This is conservative because a debris bed would take time to build at the core inlet, especially to the point where inlet blockage occurs. Modeling these blockages with a more gradual ramp would result in earlier establishment of the AFPs and could even prevent a secondary heatup. However, instantaneous blockages were modeled to obviate the need to justify a particular time-dependent ramp of the core inlet flow resistance.
- Because the B&W plants have low resistance AFPs, resulting in greater coolability, they were evaluated assuming a complete blockage at the core inlet beginning at the time of SSO.

#### 5.3.3.6 Results

In aggregate, the limiting analyses for each plant indicated that, if the core inlet blocked with a finite amount of fibrous and particulate debris at SSO, followed by a complete blockage at some later time, a secondary cladding heatup would occur. In the Westinghouse analyses for  $K_{max}$ , the heatup occurred coincident with the application of the  $K_{max}$  blockage at the time of SSO. In the Westinghouse  $t_{block}$  analyses, a heatup of similar magnitude occurred with a complete core blockage at time  $t_{block}$ . In both cases,  $K_{max}$  and  $t_{block}$  were modeled to ensure that PCT did not exceed 800 °F. In the CE analyses, there was not a significant heatup in the  $K_{max}$  analysis, but there was a heatup to about 545 °F after  $t_{block}$ . Meanwhile, the B&W analyses indicated that, because of the ample flow communication between the BB and core region for that category of plants, LTCC would be assured with no secondary heatup, even if the core inlet is completely blocked at the time of SSO. Altogether, the analytic results indicate that the AFPs are an available source of DID, in the unlikely event that the entire core becomes blocked with debris. The limiting results from the analyses in WCAP-17788 are summarized in

*Table 2.*

In WCAP-17788, Volume 4, and in response to NRC staff RAIs, the PWROG also performed sensitivity studies, which demonstrated the conservative nature of the analyses. For example, for the Westinghouse upflow analyses, the PWROG also simulated a linear ramp in core inlet flow resistance in two cases. These cases illustrated more benign system behavior compared to the  $K_{max}$  analyses, and the PWROG stated that these linear ramp cases were more realistic regarding the timing at which debris is expected to arrive at the core inlet. As discussed elsewhere in this TER, the NRC staff agrees with this assessment because the debris would

require transport to the core from the sump, such that an instantaneous blockage at the time of SSO is unlikely.

Table 2: Debris Limits and the Associated  $t_{\text{block}}$

Plant Design	Fuel Type	Debris Limit (g/FA)	$t_{\text{block}}$ (min)	PCT (°F)
Westinghouse Upflow	Westinghouse	[ ]	143	≈780
	Framatome	[ ]		
Westinghouse Downflow	Westinghouse	[ ]	260	≈790
	Framatome	[ ]		
CE	Westinghouse	[ ]	333	≈545
	Framatome	[ ]		
B&W	Westinghouse	[ ]	20	+
	Framatome	[ ]		

\*These represent maximum values based on the debris load tested.

\*The B&W analysis did not indicate a secondary cladding heatup

As discussed in Section 5.3.3.3, the PWROG applied a PCT acceptance criterion of 800 °F or less to demonstrate adequate LTCC. The NRC staff did not find that the results demonstrated, with high probability, that LTCC would be ensured. However, the NRC staff accepts the analyses as a demonstration that AFPs provide a measure of DID. The specific results are quantified above to illustrate the variability among analyses, as well as to correlate the results to in-plant debris limits, specific  $t_{\text{block}}$  values, and to provide a comparison to the TRACE supplemental analyses (21) discussed in Section 5.4.

These analyses assume that in-vessel debris is limited to a value that would correspond to a core inlet flow resistance that was modeled as  $K_{\text{max}}$  for each plant type. The PWROG performed subscale headloss testing, as described in Section 6 of Volume 1 of WCAP-17788, to correlate specific fiber limits to the  $K_{\text{max}}$  values modeled in the AFP analyses.

Tables 6-3 and 6-5 of WCAP-17788, Volume 1, provide these fiber limits, which are summarized above in

Table 2.

#### 5.4 TRACE Sensitivity Studies

RES conducted TRACE analyses (21) to explore the effects of debris on LTCC. These analyses apply to both HLB and CLB conditions. Details of the various studies performed are shown in Table 3. None of these are confirmatory calculations in the traditional sense in that they were not intended to validate or verify specific industry results. The first two columns include studies performed in the 2015/2016 timeframe. They were completed before WCAP-17788 was submitted to the NRC for review. The second two columns are a result of the current effort to aid in determining the safety significance of IVDEs.

As shown in Table 3, the TRACE analyses were performed for two specific plant models that are representative of or conservative compared to the operating PWR fleet. Modeling was not performed using plant-specific conditions but used realistic inputs and assumptions to provide insights regarding LTCC behavior considering the effects of debris. The analyses also provided

insights into how changes in important assumptions affect behavior. The analyses show that flow within the core and LP regions will promote non-uniform debris distribution at the core inlet. They also show that liquid entrainment will limit the concentration of boric acid within the core region such that BAP is not a concern if licensees implement CL injection as required in their licensing bases. The TRACE work provides a separate and independent source of knowledge regarding the effect of IVDEs on LTCC.

Table 3: TRACE Sensitivity Studies

	CLB BAP	HLB BAP/AFP	HLB/AFP	CLB/AFP
Purpose	Evaluate effects of debris buildup at core inlet on BAP	Evaluate effects of debris buildup at core inlet on BAP and LTCC	Evaluate PWROG conservatisms	Evaluate PWROG conservatisms
Model	DEG, 4-loop W upflow, mid-peaked axial, ANS 79		DEG, CE, top-peaked axial, ANS 79	
Cases/ Sensitivities	- 99-99.9% blocked LCP - 99-100% blocked nozzle - HLSO time, decay heat, axial skew	- 99.5-100% blocked core inlet	- Decay heat - Bypass - Blockage timing - Rate of blockage - HPI flow	- Base case only

#### 5.4.1 CLB

For the CLB, the TRACE analyses address both the effects of blockage at the core inlet and the potential for BAP.

The TRACE runs conducted by RES (21) for the CLB indicate that it is unlikely for BAP to occur, or for LTCC to be inhibited because of a loss of flow, even if a debris bed forms at the core inlet. TRACE runs were performed for a Westinghouse 4-loop upflow design PWR and a CE design PWR. The majority of the CLB analyses were conducted for the Westinghouse design and the discussions in this section concentrate on those analyses. The staff concluded that for the CLB, the mechanical design of the reactor would not have a large influence on the analysis.

In the Westinghouse simulations, TRACE was modified to account for higher densities and viscosities that occur because of the concentration of boric acid within the core region following a CLB. The TRACE runs confirmed the temperature driven circulation patterns that were demonstrated in industry modeling. The simulations assumed that recirculation started at 1,200 seconds to ensure the use of high decay heat values. Several cases were run. A

reference case that assumed no blockage was performed for comparison to the cases that simulated blockage. The reference case and most other cases assumed a mid-core peak and nominal decay heat based on the 1979 ANS draft Standard ANS-5.1/N18.5, "Decay Energy Release Rates Following Shutdown of Uranium Fueled Thermal Reactors" (48). The reference case found that up until about 10,000 seconds, the boric acid concentration in the core region was limited because of entrainment of liquid in the steam flowing to the SGs. As decay heat (and entrainment) decreased, the concentration of boric acid in the core increased. The concentration of boric acid in the core and LP was uniform. Mixing with the LP was caused by the upflow in the central core and downflow in the periphery. The difference in boric acid concentration between the two volumes was not significant enough to cause buoyancy-driven circulation. However, the boric acid concentration in the LP remained slightly lower than that in the core. It was assumed that HL injection was initiated at 6 hours, which eliminated the increase of boric acid concentration in the core. The baseline simulation was continued to 7.5 hours, at which time the core was covered, and boric acid concentrations returned to low levels.

#### 5.4.1.1 Westinghouse Upflow Plant

The following list includes the reference case assumptions for the Westinghouse Upflow Plant TRACE CLB analysis.

- DEGB of the CL
- No debris blockage
- SSO at 20 minutes
- Blockage applied from 1,200 seconds to attain full resistance at 5,000 seconds, linear ramp
- HLSO at 6 hours
- Nominal decay heat
- End of simulation at 7.5 hours
- Flat axial power peaked at mid-core
- 212 °F recirculation temperature

Additional TRACE cases simulated progressively increasing levels of debris blockage. The blockage was simulated at the lower core plate, below the area where blockage would occur in the plant. This is a conservative scenario because simulating the blockage at this location prevents flow through the AFPs credited in the PWROG analyses for the HLB from WCAP-17788. Other sensitivity studies, discussed later in this section, applied blockage at the core inlet which allows flow to the AFPs. The blockage was applied by "closing valves" to the assumed blocked area. RES checked the resistance ( $k/A^2$ ) value for the valves against the expected debris resistance value to ensure the modeling was valid. The blockage was applied over time starting at 1,200 seconds and was ramped to the full blockage for the case being run

over the next 3,800 seconds, or just longer than an hour, which is considered reasonable. The full blockage value for the case was assumed to occur at 5,000 seconds.

Each of the sensitivity studies for the Westinghouse upflow plant are summarized in the following sections.

#### 5.4.1.1.1 Blockage at the Lower Core Plate (99 percent)

In the case where 99 percent of the core area was blocked, the core remained covered and no temperature excursions occurred. Boric acid concentration was elevated but remained well below the concentration where BAP could occur. Localized BAP was observed only in the UH in areas where trapped fluid boiled away leaving the boric acid solids behind. There was no BAP predicted at the core inlet, BB regions, or areas that could impede coolant flow to the core. The simulation of HLSO effectively ended the transient, even when the resistance at the lower core plate was assumed to remain in place.

#### 5.4.1.1.2 Blockage at the Lower Core Plate (99.5 and 99.9 percent)

The case for 99.5 percent blockage had slightly elevated boron concentration compared to the 99 percent case, but LTCC was maintained. Cases where core inlet blockage exceeded 99.9 percent resulted in cladding heat up as blockage at the core inlet prevented adequate coolant from entering the core. In this simulation, boric acid concentration in the core was found to be below the precipitation limit, even when the PCT excursion occurred. This finding implies that fuel failure caused by loss of coolant flow will occur before failures caused by BAP. The boric acid concentration did not approach the solubility limit in any of the blockage sensitivity studies.

#### 5.4.1.1.3 Blockage at the Fuel Inlet Nozzles (99 and 100 Percent)

The TRACE simulations investigated the effect of debris blockage location by simulating blockage at the fuel inlet nozzles instead of the lower core plate. Blockage at this location prevents (or reduces) coolant flow entering the core directly but allows flow to the BB region. A 99 percent blockage was applied at the fuel inlet nozzles. Results of this simulation showed that LTCC continued and boric acid concentration remained well below precipitation limits. Flow from the BB region into the core near the top nozzles mixed with the coolant in the core and diluted boric acid in the core.

For the 100 percent blockage case, the only flowpath to the core was through the BB region. Core coolability was maintained and boric acid concentration was maintained well below the BAP limit. Flow through the BB region and into the core exceeded boil off from decay heat. Because of the low resistance assumed at the core inlet in WCAP-17788 CLB cases, flow through the BB region was not credited to ensure LTCC. The identification of the BB flowpath by the TRACE simulations indicates that the diverse flowpaths credited for the HLB can also provide the required flow for the CLB. The flow is through the same pathways credited for the HLB analysis, so all reactor designs evaluated have flowpaths available to allow LTCC for a CLB if the core inlet becomes completely blocked.

#### 5.4.1.1.4 Blockage at the Fuel Inlet Nozzle with Delayed HLSO (100 percent)

A case was run to evaluate the effects of a much later switchover to HL injection. Instead of assuming 6 hours for the initiation of HL injection, the case was run for 36 hours. The case assumed 100 percent blockage at the FA inlet. The boric acid concentration increased over time but did not exceed the solubility limit. The concentration plateaued at around 30 hours. The boric acid in the core remained well mixed. Some precipitation was predicted in the UP after 30 hours. This likely resulted in maintaining the core concentration below the solubility limit.

#### 5.4.1.1.5 Core Power Sensitivity

A sensitivity case using Appendix K decay heat assumptions was run by increasing the reference case decay heat by 30 percent. A 99 percent blockage was assumed at the lower core plate. The higher power case resulted in a more highly voided core and UP, but no heatup occurred. Compared to the similar case at the reference decay heat value, the boric acid concentrations were significantly lower and the rate of increase in concentration remained low for a longer time. This is caused by entrainment of the boric acid in the liquid exiting the core.

#### 5.4.1.1.6 Axial Power Shape Sensitivities

Top and bottom skewed axial power shape cases were run. Both cases assumed 99 percent blockage at the lower core plate. There were differences in the very early PCT results during blowdown and reflood, but the LTCC results were very similar.

An interesting result from the decay heat sensitivity is that higher decay heat results in lower boric acid concentrations. Greater liquid entrainment resulted in more boric acid removal from the core. This is counterintuitive unless entrainment, which is not credited for design basis calculations, is considered. The TRACE simulations also provide more realistic results than the SKBOR methodology discussed in Section 5.2.1.1.2 in that they account for the physical effects of liquid carryover in the steam and for viscosity and density changes resulting from concentrated boric acid.

#### 5.4.1.1.7 Large Split Break at Top of CL

A sensitivity case was run to examine the effects of a split break at the top of the CL. The results were like those of the DEGB cases.

For all Westinghouse CLB cases, there is liquid carryover at the beginning of the event so that the buildup of boron in the core region is limited. Later in the event, boron may begin to concentrate in the core. However, the increased density of boric acid in the core region will promote buoyancy driven convection and mixing with the LP. This convection, convection caused by heating of the fluid, and the agitation caused by boiling results in mixing within the core and between the core and LP. Early in the LOCA recovery, heat-driven convection and boiling will drive the mixing. Later, convection resulting from density increases from boron concentration may become more dominant.

#### 5.4.1.2 Combustion Engineering Plant

The CE cases were run mainly to gain understanding of the behavior of the CE design following an HLB. The CE cases did not model concentration of boric acid in the core. The single CLB case run for the CE design used a decay heat multiplier of 1.1 times the ANS 1979 decay heat curve and a top peaked axial power shape. The case simulated full core blockage at 20,000 seconds. No cladding heatup was predicted. This case shows that the AFPs can provide cooling for the CE design even if a full core blockage occurs. The conclusion is valid for the conditions simulated but is dependent on several variables including the time blockage occurs.

#### 5.4.1.3 TRACE Study Applicability to the PWR Fleet

The Westinghouse and CE HLB TRACE studies are discussed in Section 5.4.2.

Applicability of the BAP TRACE study to the PWR fleet considered the following:

- The TRACE runs modeled only two reactor designs (Westinghouse 4-loop upflow and CE), and most of the CLB cases were run for the Westinghouse upflow design.
- The boron concentration aspects of the model were validated to Primärkreislauf-Versuchsanlage (commonly known as PKL) data with good correlation, but additional validation of modeling for boron concentration and density was not performed because of a lack of available data. See Section 4 of the TRACE report (49). Other parts of the model were more rigorously validated.
- The simulations did not use design-basis assumptions but performed sensitivity studies to understand how assumptions can affect the results. On the other hand, the studies considered core inlet blockage, which has not been considered in design-basis calculations.
- The results are not considered design basis type calculations, but they indicate that BAP is much less likely to occur than previously postulated and provide independent information regarding the PWROG calculations for core cooling and BAP.

The TRACE results also identified that circulatory currents are present within the RV. These currents will prevent uniform debris bed formation at the core inlet. The PWROG simulations showed that these currents were present early in the LOCA recovery period but, unlike the TRACE studies, did not attempt to demonstrate that they would be present later in the recovery because the concentration of boric acid in the core was not modeled.

RES concluded that the qualitative results of the TRACE analysis should be applicable to all plants that have bypass holes that will not become blocked by debris. UPI plants are significantly different so are not comparable. Variations in key plant parameters will affect the quantitative results. Westinghouse and B&W designs have core bypass flow paths that are qualitatively similar to those of the CE plants. B&W and some Westinghouse designs have AFPs that connect the bypass region to the core at lower elevations so that coolant can enter the core without filling up the entire bypass flow volume. The BAP results from the Westinghouse plant CLB TRACE analysis are applicable to the CE and B&W plants since there are significant mixing volumes above the core and in the HLs for all designs. The CLB debris

limits are the same for all fuel and reactor designs and the response of the system is similar enough for the results to be considered applicable.

The NRC staff considers the Westinghouse plant selected for boric acid concentration studies conservative relative to the PWR fleet due to its upflow configuration in the core bypass region. The upflow design reduces the mixing volume available for dilution of boric acid. The design also delays flow from the AFP to the core if a 100 percent blockage at the core inlet nozzles occurs because the BB must fill to the top before flow to the core is established.

The Westinghouse CLB TRACE analysis found that core uncover occurs before BAP takes place. Because core uncover is the central issue during long-term cooling, additional calculations were made for the representative CE plant. These calculations showed that even with a conservative blockage at the fuel inlet nozzles, uncover is not expected to occur for this design, similar to the Westinghouse plant findings. The calculations and sensitivity studies performed in the TRACE report indicate that even with a highly conservative blockage at the core inlet nozzles, neither core uncover nor BAP is expected for the CLB case.

In the unlikely event that the fuel inlets become completely blocked, TRACE simulations show that the BB will fill with coolant and coolant will flow into the core via AFPs. TRACE demonstrates that the core remains covered. The AFP through the BB region that was credited for the HLB (see Section 5.3.3) is also viable for the CLB, although industry analyses for the CLB do not credit it.

#### 5.4.2 HLB

RES performed a series of HLB sensitivity studies using the TRACE code for both the Westinghouse upflow and CE plant categories as described below.

##### 5.4.2.1 Westinghouse Upflow Plant

RES performed Westinghouse upflow sensitivity studies to determine if a break in the HL could result in high boric acid concentrations in the core and RV. The plant selected for simulations was a Westinghouse four loop PWR with a core power of 3,411 megawatts thermal. The plant model (representative of the Seabrook Station) is an upflow plant, meaning that core bypass flow enters the BB region near the core inlet and exits near the fuel top nozzle elevation. No communication was modeled between the BB region and the active core. This configuration is assumed to be conservative for investigations involving core inlet blockage with debris. Coolant cannot reach the core unless it flows completely through the BB region and back into the core near the core exit, unless it flows through the high-resistance path of the debris.

For the HLB calculations, the blockage was simulated to occur at the bottom fuel nozzles using a resistance ramped from 1,200 to 5,000 seconds. The total blockage ranged from 99 percent to 100 percent. At 100 percent blockage, no flow could go directly into the bottom of the core, and any coolant reaching the core was forced to flow through the BB region and enter at the top of the core. While the BB region filled, sufficient inventory remained in the core region so that the rods remained covered and cladding temperatures remained at saturation temperature. After the BB region refilled, sufficient coolant entered at the top of the core to maintain core coverage and prevent cladding heat up.



At 100 percent blockage, the core boric acid concentration was only slightly greater than that obtained in the calculations with 99.5 percent blockage or less. Flow through the BB region was sufficient to remove decay heat and keep the two-phase level at the HL elevation.

Both HL calculations (99.5 and 100 percent blockages) maintain the two-phase level to the level of the HL, and as a result the carryover fraction is nearly 1.0. This is because when the two-phase level is at the level of the HL, coolant can easily flow into the HL and to the break. Essentially, the vessel is "full" and a mass balance exists, and the total ECCS flow is matched by the total flow out of the vessel. Excess coolant simply flows to the break. Thus, the HL calculations do not indicate the minimum amount of carryover necessary to prevent boron precipitation.

#### 5.4.2.2 Combustion Engineering Plant

This section compares a TRACE analysis for CE to the PWROG analysis that used S-RELAP5. Objectives include: (1) determining how the dependence of the long-term core depression and heatup varies with core blockage ramp times, (2) determining whether there is a ramp rate that would preclude a core uncover and heatup altogether, and (3) understanding the sensitivity of the results to assumptions about key parameters and boundary conditions.

The TRACE plant model used for these calculations is similar to the St. Lucie Plant. The analyzed event consists of a double-ended guillotine HLB with only high-pressure injection (HPI) available and a containment pressure of 1 atmosphere during long-term cooling. The core inlet is assumed to be completely blocked by debris at some point in time and core cooling water must flow through the core bypass flow path and empty into the top of the core. Sensitivity calculations include varying key input parameters and assumptions including decay heat, bypass flow resistance, HPI flow rate, core blockage time, and blockage rate.

The analyses showed that there is no significant fuel heatup in the long term as the result of core blockage. Sensitivity calculations showed that decay heat, bypass flow resistance, HPI flow rate, core blockage time, and blockage rate could be changed significantly with little sensitivity to the core level after the blockage. The results are qualitatively similar to those of the PWROG analysis.

#### 5.4.3 Applicability to the Pressurized Water Reactor Fleet

TRACE sensitivity studies were not performed for the Westinghouse downflow or B&W plant categories. The qualitative results of this analysis should be applicable to all plants that have bypass holes large enough to not be blocked by debris after the switchover to sump recirculation. WCAP-17788 tested openings down to ¼-inch to demonstrate that these sized openings would not become blocked with debris. Openings less than ¼-inch were not credited in the WCAP-17788 analyses. Modeling of different plant designs would reveal quantitative differences that depend on the details of the key plant parameters such as specific plant dimensions, core power, bypass resistance, and ECCS flow rate. However, based on the industry TH analyses and the TRACE studies performed for the Westinghouse upflow and CE plants and the similarities in PWR designs, the NRC staff does not believe that additional TRACE studies are necessary.

## 5.5 Integrated Decisionmaking

### 5.5.1 Determination of Safety Significance

The NRC staff prepared this TER using integrated decisionmaking which includes an assessment of traditional engineering evaluations and probabilistic information. Integrated decisionmaking considers information from a variety of sources including risk insights, traditional engineering evaluations and insights, operational experience and historical plant performance, engineering judgment, and current regulatory requirements. In addition, evaluation of DID and safety margins are an important part of the integrated decisionmaking process.

While a quantitative analysis of the risk associated with IVDEs following a hypothetical LOCA at each U.S. PWR is impractical, the NRC staff combined risk insights with its engineering evaluation, including the low initiating frequency of LOCAs that can challenge LTCC via IVDEs to determine the safety significance of IVDEs. This section discusses the NRC programs that were used to evaluate the safety significance of the issue.

The NRC staff considered guidance that is presented in: LIC-504, Revision 4, "Integrated Risk-Informed Decision-Making Process for Emergent Issues" (50); NUREG/BR-0058, Regulatory Analysis Guidelines of the U.S. Nuclear Regulatory Commission (51); RG 1.174, Revision 3, "An Approach for Using Probabilistic Risk Assessment in Risk-Informed Decisions on Plant-Specific Changes to the Licensing Basis," January 2018 (52); and the Significance Determination Process (SDP) (IMC 0609) (53). Table 4 provides a summary of the risk metrics associated with those programs. The guidelines for assessing risk in the established programs discussed in Table 4 were derived from the Commission's Safety Goal Quantitative Health Objectives (QHOs) and the values were selected to be consistent with the Safety Goal QHOs (see, for example, SECY 97-077, (54)). All these processes use integrated decisionmaking and include considerations of DID and safety margin in addition to risk information to assess appropriate regulatory response relevant to the process (e.g., reactive inspection, license amendment request approval, etc.). As described in NRC guidance, each of these processes are tailored to the context of their regulatory use. For this reason, the extent to which they use the risk assessment in conjunction with the other elements of integrated decisionmaking varies. Further, the risk assessments used for these processes vary in scope, level of detail, and technical rigor.

For example, RG 1.174 is used to evaluate plant licensing changes. In this process, the change in risk and its comparison against risk acceptance guidelines is one of five key principles that are considered by staff in its evaluation. NRC guidance for performing regulatory analysis for substantial safety enhancements includes risk thresholds for identification of such enhancements (51). The thresholds are starting points and the evaluation includes consideration of available safety margins and DID, which together with the thresholds influence staff decisions. LIC-504 is NRC staff guidance for evaluating emergent issues and refers to the same five key principles defined in RG 1.174 as important inputs to be used in addition to risk values calculated in the process. The SDP uses PRA analyses to evaluate the change in risk resulting from a degraded condition associated with a licensee performance deficiency and relates the significance to established thresholds. The SDP process also includes consideration of qualitative factors as part of the assessment and consideration of safety margins and DID is prominent in cases where the impact of the performance deficiency cannot be readily captured

using PRA analyses. The values in Table 4 are simplified representations of the thresholds from these processes.

Table 4: Risk Metric

Reference	Risk Metric ( $\Delta$ CDF/Rx Year)				
	Lower Risk 10 <sup>-7</sup> or Lower	10 <sup>-7</sup> - 10 <sup>-8</sup>	10 <sup>-8</sup> - 10 <sup>-5</sup>	10 <sup>-5</sup> - 10 <sup>-4</sup>	Greater Risk 10 <sup>-4</sup> or Higher
RG 1.174	Acceptable		Evaluate	Unacceptable	
SDP	Green		White	Yellow	Red
LIC-504	No Action	Evaluate (Shut Down if CDF > 10 <sup>-3</sup> )			
NUREG/BR-0058	No Action			Evaluate	Take Action

As stated above, the NRC staff did not quantify the risk attributable to IVDEs following a LOCA. However, as discussed in Section 5.5.2 the staff determined that the order of magnitude of the occurrence frequency of LOCAs that can challenge LTCC via IVDEs would be 1 x 10<sup>-8</sup> per year or less. Assuming that an initiating event (LOCA) that can challenge LTCC via IVDEs leads directly to core damage will result in an order of magnitude of 1 x 10<sup>-8</sup> per year or less for core damage frequency. This is consistent with the low end of the quantified risk spectrum for existing NRC programs and corresponding guidance referenced in Section 5.5.1. Additionally, given the high probability of the containment remaining intact following a LOCA including IVDEs, an increase in the frequency of large early releases attributable to IVDEs is not expected (see Section 5.3.1).

Therefore, based on its evaluation summarized in this TER, including the low initiating frequency of LOCAs consequential enough to challenge LTCC via IVDEs (see Section 5.5.2), DID, and the available safety margins, the staff concludes that a quantitative assessment would indicate that the core damage frequency attributable to the types of IVDEs considered in this TER are of low safety significance. Using integrated decisionmaking, the evidence considered by the staff indicates that the safety significance associated with IVDEs is expected to be in the acceptable range for several existing NRC processes shown in Table 4.

The safety significance approach followed in this TER has not been evaluated for use outside the TER. Therefore, it should not be used on a generic basis unless specifically evaluated for such a use.

#### 5.5.2 Risk Insights – Initiating Event (LOCA) Frequencies

Although the NRC staff did not quantify the risk attributable to IVDEs following a LOCA, it sought to understand the frequency of such occurrences to inform its decisionmaking. To do so, the staff sought to determine an order of magnitude estimate for initiating frequency of LOCAs that can challenge LTCC via IVDEs based on the engineering analyses discussed in Section 5.2 of this TER.

The NRC staff's evaluation of the information presented by STP (13) determined that debris generation from a DEGB of a 6 inch or larger pipe on the HL side could result in a fibrous debris bed achieving the threshold limit for challenging LTCC via IVDEs. Section 5.2.1.2 explains how the fiber amount associated with the 6-inch pipe break was determined to be applicable on a generic basis. The 6-inch pipes of interest at STP have an inner diameter of 5.19 inches.

Therefore, the staff sought to determine an order of magnitude estimate for LOCA initiating frequency for breaks 5 inches and larger. Table 7.7 of NUREG-1829, "Estimating Loss-of-Coolant Accident (LOCA) Frequencies Through the Elicitation Process," issued April 2008 (55), provides the mean initiating LOCA frequencies for different break categories (each of which corresponds to an effective break size) based on 40-year plant operation. The staff considers the 40-year frequency estimates to be applicable to plants that are operating beyond 40 years. Those values include both piping and non-piping contributions. Table 7.2 of NUREG-1829 provides the ratio of non-piping to piping contributions for each break category. The non-piping contribution is based on the LOCA initiating frequency estimates at the time of the expert elicitation in NUREG-1829. However, based on information in Sections 6.3.4 and 7.2 of NUREG-1829, the non-piping contribution is expected to remain the same or "decrease somewhat." Therefore, the ratio of non-piping to piping contributions for each break category in Table 7.2 were used because they were considered applicable to determining the order of magnitude estimate desired for this evaluation. The resulting initiating frequency for all LOCAs 5-inches or greater is approximately  $2 \times 10^{-5}$  per year as determined by staff calculations. The corresponding value for the arithmetic mean estimates for 40-year plant operation using information from Table 7.11 of NUREG-1829 is approximately  $6 \times 10^{-5}$  per year. Therefore, in both cases, the order of magnitude of relevant breaks is  $10^{-5}$  per year.<sup>a</sup> These estimates are for all piping 5-inches or larger regardless of its location in the RCS.

Since breaks in piping 5 inches or larger on the HL side are consequential to this TER, a refined order of magnitude estimate of the initiating frequency was determined using the expert elicitation data from NUREG-1829 (56). The expert elicitation data were aggregated to determine the initiating frequency of 5 inch or larger breaks in the HL as well as piping connected to the HL such as the surge line. The result is based on the values for 40 years of operation. The overconfidence adjustment derived based on Tables 7.1 and 7.7 in NUREG-1829 was applied. The refined estimate for the initiating frequency for all LOCAs 5 inches and greater on the HL side (i.e., the HL as well as piping connected to the HL) is approximately  $1.5 \times 10^{-6}$  per year (i.e., the order of magnitude is  $10^{-6}$  per year). This estimate includes consideration of the chemical and volume control system (CVCS) which contributes significantly to the estimate. CVCS lines greater than 5 inches are uncommon and exclusion of the CVCS for the refined estimate results in an initiating frequency for all LOCAs 5 inches and greater on the HL side of approximately  $3.6 \times 10^{-7}$  per year (i.e., the order of magnitude is  $10^{-7}$  per year).

The size of the break that could generate enough debris to challenge LTCC for a break on the CL side is much larger because smaller breaks do not generate enough debris to block flow to the core. Two cases for very high fiber plants are discussed in terms of generic applicability in Section 5.2.1.1. These demonstrate that only very large breaks, 12 inches and larger, generate significant debris for breaks on the CL side. The staff determined the order of magnitude for breaks in piping 12 inches and larger from Tables 7.7 and 7.2 of NUREG-1829. The resulting initiating frequency for all LOCAs 12 inches and greater in piping is approximately  $1 \times 10^{-6}$  per year. The corresponding value for the arithmetic mean is approximately  $6 \times 10^{-6}$  per year.

---

<sup>a</sup> The estimates in NUREG-1829 are on a per calendar year basis whereas initiating frequencies use a per reactor year basis. The difference between the two is the capacity factor (i.e. the portion of a calendar year that a reactor is at full power). Since the purpose is to determine an order of magnitude estimate, the staff used the calendar year values as if they were on a reactor year basis (i.e. did not account for the capacity factor) because the capacity factor (approximately 0.9 for the entire U.S. fleet) will not impact the order of magnitude estimate and the conclusions drawn therefrom.

Therefore, the order of magnitude of the initiating frequency of the relevant breaks is  $10^{-6}$  per year. These estimates are for all piping 12 inches or larger, regardless of its location in the RCS. Using the expert elicitation data from NUREG-1829 and the approach outlined in the previous paragraph, a refined estimate of the initiating frequency of breaks in piping 12 inches or larger on the CL side (i.e., the CL as well as piping connected to the CL) is  $1.4 \times 10^{-7}$  (i.e., the order of magnitude is  $10^{-7}$  per year).

In its comparison with the spectrum of risk thresholds in Section 5.5.1, the NRC staff assumed that an initiating event as defined in this section leads directly to core damage. That is, given a HLB greater than 5 inches or a CLB greater than 12 inches, core damage is assumed. The staff concludes that the margins not included in the assessment of core blockage reduce the risk significantly below that based solely on break frequency and that if core blockage occurs, there is DID available to provide LTCC.

In summary, the estimated order of magnitude of the frequencies of the initiating events (LOCAs) that can generate enough debris to challenge LTCC via IVDEs, along with the sequence of events necessary to result in a high-resistance debris bed at the core inlet discussed in Section 5.2 of this report, supports the staff's conclusions in this TER.

### 5.5.3 Safety Margins

Safety margins associated with the evaluation of IVDEs depend on plant-specific parameters. The margins associated with the analyses are discussed throughout this document and summarized here.

- This evaluation is performed assuming limiting conditions for debris generation. Many breaks will not generate the amounts of debris assumed.
- The transport assumptions in the evaluation are conservative. All fine fibrous debris that penetrates the strainer is assumed to be transported to the core. All fine particulate debris is assumed to reach the core. Some of this debris would settle or deposit on surfaces.
- The filtering characteristics of the strainer make larger breaks less problematic than would be assumed from their debris generation amounts. For the HLB, a 6-inch break is assumed. Larger breaks may generate significantly more debris, but the amount of debris that passes through the strainer decreases quickly with strainer load.
- The assumed time for switchover to recirculation is conservative. It is based on the smallest RWST water volume and highest ECCS and CSS flows for each plant. The assumed switchover time is 20 minutes for all AFP HLB analyses and all TRACE analyses (21). The fastest time for many plants is about 30 minutes. Times for less limiting but more likely breaks are much longer than 30 minutes. Longer switchover times result in lower decay heat levels which allow AFPs more time to respond to prevent any secondary heatup. Longer switchover times also allow more time for debris to settle.
- Unqualified coatings are assumed to fail as 100 percent fine particulate that is transported to the strainer and core. These coatings would actually fail in a range of sizes and some would not transport to the core.

- The evaluation of particulate debris concentration ignored liquid that would be present in the UP and used a limiting plant value for particulate debris mass. The concentration of particulate will be lower than that calculated for the CLB.
- A 50 percent void fraction is assumed for the core region for the particulate debris concentration calculation. The actual void fraction will be lower and will decrease with time. The concentration of particulate debris for the CLB will be lower than assumed.
- The AFP analysis assumed a uniform bed. This leads to a much lower fibrous debris amount than would actually be required to form a high-resistance bed at the core inlet. The fiber limits referred to in this analysis are based on a uniform bed. It is likely that a high resistance bed would not form even with significantly more fiber than represented by the limits.
- Chemical effects will probably not occur until after the plants have initiated HLSO. FA testing conducted for WCAP-16793 found that significantly larger amounts of fiber could be accommodated without causing excessive headloss if precipitates are not present. The staff identified plants that have the potential to incur precipitation before 24 hours. The PWROG chemical effects testing for WCAP-17788 identified that out of 44 groups, 37 would not incur precipitation before 24 hours. Two plants were identified that could have precipitation before HLSO. Of these, one is a low fiber plant that has already closed GL 2004-02 including IVDEs. The second plant is a single unit for which the staff was unable to confirm that precipitation would occur after HLSO and without more information, the staff considers this unit to be outside the key parameters of this TER.
- In the AFP analysis, the limiting fiber amounts were determined from testing using the limiting flow rate, limiting particulate to fiber ratio, and limiting particulate size distribution. Changing these parameters resulted in lower head loss values for the same amounts of fiber.
- The core inlet resistance value  $K_{max}$  was determined using a 60 second ramp rate for increasing the resistance at the time of SSO for Westinghouse and B&W designs. An alternate approach was used for CE designs. This results in a conservative  $K_{max}$  value, and therefore a conservative fiber limit, as described in Section 5.3.3.5.
- The design of RCS piping assures that it is robust. Implementation of code inspections for Class 1 piping provides some assurance that the piping does not have defects where LOCAs can initiate. Many plants have mitigated dissimilar metal welds to reduce the probability of primary water stress corrosion cracking. For unmitigated welds, the code requires augmented inspections for defects.
- The analysis does not credit leak before break. However, the most likely way for large piping to fail is for a crack to initiate and grow to a critical size, then rupture. All PWRs have systems designed to detect leakage at levels that would occur below the critical crack size. Technical specifications require that plants monitor for leakage and shut down when unidentified leakage indicates potential leakage in the RCS. The intention of the technical specification is to ensure the plant is shut down, leakage identified, and repairs implemented as required, before a LOCA occurs.

- The PCT limit of 800 °F used as an acceptance criterion in WCAP-17788 was based on long-term autoclave testing that showed no significant degradation in cladding properties would occur by spending 30 days at 800 °F. WCAP-16793-NP-A, Appendix A, discusses the basis for the temperature limit. A PCT up to this limit is not expected to challenge fuel integrity. The TH analyses from WCAP-17788 and TRACE show only short-term PCT increases.
- Decay heat in the AFP calculations was modeled similar to the requirements in 10 CFR Part 50, Appendix K (see Section 5.3.3.5).
- The limiting results for  $K_{max}/t_{block}$  in the AFP analyses were obtained from minimum recirculation flows, which is a conservative methodology.
- For the limiting AFP analyses,  $t_{block}$  was determined using a conservative ramp rate of 60 seconds for Westinghouse and B&W designs. This results in a conservative  $t_{block}$  value (see Section 5.3.3.5).
- B&W plants exhibited adequate LTCC when the core inlet was blocked in the AFP analysis. The B&W plant response to IVDEs was evaluated assuming a complete blockage at the core inlet beginning at the time of SSO.
- The AFP analyses assumed the limiting FA was operating with a top-peaked power shape, similar to that assumed in small-break LOCA analyses. This maximizes any secondary heatup if the core uncovers during a core inlet blockage.

## 6.0 CONCLUSION

The NRC staff determined that for the operating US PWR fleet, and within the range of assumed plant parameters, debris penetrating the sump strainer is very unlikely to prevent adequate LTCC following LOCAs via IVDEs. This TER considered a wide range of analytical and deterministic information from industry and NRC sources, supplemented by engineering judgement and risk insights.

Based on integrated decisionmaking supported by information from a variety of sources including risk insights, traditional engineering evaluations and insights, operational experience and historical plant performance, engineering judgment, and current regulatory requirements, the NRC staff concludes that the safety significance of the challenge to LTCC following LOCAs via IVDEs is low. The staff believes this analysis is conservative compared to typical operating US PWRs, but it is not an evaluation of any specific plant. It does not address methods for plants to demonstrate compliance with regulations or define licensing basis parameters for the IVDE issue.

The concept of safety significance, and the evaluation methods, findings, and conclusions discussed in this TER are limited in scope to the evaluation of IVDEs with respect to GSI-191 and GL 2004-02. NRC staff does not consider this concept to be applicable to additional issues or topics without further justification.

## **7.0 REFERENCES**

1. WCAP-16793-NP-A, Rev. 2, "Evaluation of Long-Term Cooling Considering Particulate, Fibrous and Chemical Debris in the Recirculating Fluid," July 2013 (ADAMS Package Accession No. ML13239A111).
2. PWR Owners Group, Submittal of WCAP-17788: "Comprehensive Analysis and Test Program for GSI-191 Closure (PA-SEE-1090)," July 17, 2016 (ADAMS Package Accession No. ML15210A667).
3. Title 10 of the Code of Federal Regulations Part 50 "Domestic Licensing of Production and Utilization Facilities".
4. Generic Letter 2004-02, "Potential Impact of Debris Blockage on Emergency Recirculation During Design Basis Accidents at Pressurized Water Reactors," September 13, 2004 (ADAMS Accession No. ML042360586).
5. WCAP-17360-P, Rev. 0, "Small Scale Unbuffered and Buffered Boric Acid Nucleate Boiling Heat Transfer Tests with Sump Debris in a Vertical 3x3 Rod Bundle," May 31, 2012 (ADAMS Accession Nos. ML12167A435 and ML12167A437) (non-public).
6. PWROG-15091-NP, Rev. 0, "Subscale Brine Test Program Report, Analysis committee, PA-ASC-1188," Parts 1 and 2, November 30, 2016 (ADAMS Accession Nos. ML15342A069 and ML15342A070).
7. Enclosure, "Revised Content Guide for Generic Letter 2004-02 Supplemental Responses," November 2007 (ADAMS Accession No. ML073110278).
8. Nuclear Energy Institute (NEI) 04-07, Vol. 1, "Pressurized Water Reactor Sump Performance Evaluation Methodology," December 2004 (ADAMS Accession No. ML050550138).
9. WCAP-16406-P-A, Rev. 1, "Evaluation of Downstream Sump Debris Effects in Support of GSI 191," March 2008 (not publicly available; proprietary Information).
10. SECY-12-0093 Closure Options For Generic Safety Issue-191, "Assessment Of Debris Accumulation On Pressurized-Water Reactor Sump Performance," July 12, 2012 (ADAMS Accession No. ML121310648).
11. Staff Requirements Memorandum SRM-SECY-12-0093, "Closure Options for Generic Safety Issue-191, Assessment of Debris Accumulation on Pressurized Water Reactor Sump Performance," December 14, 2012 (ADAMS Accession No. ML12349A378).
12. Final Safety Evaluation for Topical Report WCAP-16793-NP-A, Rev. 2, "Evaluation of Long-Term Cooling Considering Particulate Fibrous and Chemical Debris in the Recirculating Fluid," April 8, 2013 (ADAMS Package Accession No. ML13084A161).



13. "South Texas Project, Units 1 and 2, Issuance of Amendment Nos. 212 and 198 - Risk-Informed Approach to Resolving Generic Safety Issue 191," July 11, 2017 (ADAMS Package Accession No. ML17019A001).
14. WCAP-17788-P, Vol. 5, Rev. 0, "Comprehensive Analysis and Test Program for GSI-191 Closure (PA-SEE-1090) - Autoclave Chemical Effects Testing for GSI-191 Long-Term Cooling," July 2015 (ADAMS Accession Nos. ML15210A678, ML15210A680, ML15210A681). (non-public).
15. WCAP-17788-NP, Vol. 3, Rev. 0, "Comprehensive Analysis and Test Program for GSI-191 Closure (PA-SEE-1090) - Cold Leg Break (CLB) Evaluation Method for GSI-191 Long-Term Cooling," July 2015. (ADAMS Accession No. ML15210A671).
16. WCAP-17788-NP, Vol. 4, Rev. 0, "Comprehensive Analysis and Test Program for GSI-191 Closure (PA-SE-1090) - Thermal-Hydraulic Analysis of Large Hot Leg Break with Simulation of Core Inlet Blockage," July 2015. (ADAMS Accession Nos. ML15210A672 and ML15210A674).
17. "Staff Observations of Plant-Specific Testing for Generic Safety Issue 191 During February 26, 2006, Trip to the Alton Hydraulics Laboratory," April 17, 2006 (ADAMS Accession No. ML060750467).
18. "Staff Observations of Testing for Generic Safety Issue 191 During April 28, 2006, Trip to the Alton Hydraulics Laboratory," June 27, 2006 (ADAMS Accession No. ML061720514).
19. "Seabrook, Unit 1 - Updated Final Response to NRC Generic Letter 2004-02," January 31, 2018 (ADAMS Accession No. ML18031B248).
20. "Analysis Report - Post-LOCA PWR Core Inlet Blockage Assessment," February 26, 2007 (ADAMS Accession No. ML070860521).
21. "Assessment of Boric Acid Accumulation in a Reactor Core Blocked by Debris," NRC Office of Nuclear Regulatory Research, March 2019. (ADAMS Accession No. ML19086A270).
22. Transmittal of WCAP-17057-P/NP, Rev. 1, "GSI-191 Fuel Assembly Test Report for PWROG," PA-SEE-0312, September 2011 (ADAMS Package Accession No. ML112930439).
23. EPRI 1011753, "Design Basis Accident Testing of Pressurized Water Reactor Unqualified Original Equipment Manufacturer Coatings," Final Report, September 30, 2005 (ADAMS Accession No. ML071130075) (non-public).
24. "Keeler & Long PPG, "Design basis Accident Testing of Coating Samples from Unit 1 Containment, TXU Comanche Peak SES," April 13, 2006 (ADAMS Accession No. ML070230390).

25. Attachment 2: Revised Responses to NRC RAIs Related to WCAP-17788 Supporting the Closure of GSI-191 (PA-SEE-1090), September 28, 2018 (ADAMS Accession No. ML18285A019).
26. "Vogtle Electric Generating Plant Units 1 & 2, Supplemental Response to NRC Generic Letter 2004-02," April 21, 2017 (ADAMS Package Accession No. ML17116A096) (non-publicly available).
27. Draft Safety Evaluation Report by the Office of Nuclear Reactor Regulation Topical Report WCAP-17788-P, "Comprehensive Analysis and Test Program for GSI-191 Closure," Vol. 5, "Autoclave Chemical Effects Testing for GSI-191 Long Term Cooling," January 10, 2019 (ADAMS Accession No. ML19016A310) (non-public).
28. Trip Report for May 2013 NRC Staff Visit to the Westinghouse Churchill Laboratory to Observe Autoclave Testing, June 10, 2013 (ADAMS Accession No. ML13159A007).
29. Westinghouse Trip Report of November 19, 2013, December 24, 2013 (ADAMS Accession No. ML13337A479) (non-public).
30. NUREG/CR-6913, "Chemical Effects Head-Loss Research In Support of Generic Safety Issue 191," Argonne National Laboratory, December 2006 (ADAMS Accession No. ML070090553).
31. NUREG/CR-6914, Volume 2, "Integrated Chemical Effects Test Project: Test #1 Data Report," September 30, 2006 (ADAMS Accession No. ML062560111) (non-public).
32. WCAP-16530-NP-A, "Evaluation of Post-Accident Chemical Effects in Containment Sump Fluids to Support GSI-191," March 2008 (ADAMS Accession No. ML081150379).
33. "Staff Observations of Testing for Generic Safety Issue 191 During July 22 To July 24, 2009 Trip to the Allon Hydraulics Laboratory," September 24, 2009 (ADAMS Accession No. ML092670458).
34. "Aluminum Solubility in Boron Containing Solutions as a Function of pH and Temperature," Argonne National Laboratory, September 19, 2008 (ADAMS Accession No. ML091610696).
35. Attachment 1, "Responses to NRC RAIs Related to WCAP-17788, Volume 5 Supporting the Closure of GSI-191 (PA-SEE-1090) and Mark-ups to WCAP-17788 PROPRIETARY Attachment," May 23, 2017 (ADAMS Accession No. ML17293A220) (non-public).
36. WCAP-17788-NP, Vol. 1, Rev. 0, "Comprehensive Analysis and Test Program for GSI-191 Closure (PA-SEE-1090)," July 2015 (ADAMS Accession No. ML15210A669).
37. Response to RAIs on WCAP-17788 Vol. 4, B&W Plants Licensing Report, December 31, 2017 (ADAMS Accession No. ML18029A213) (non-public).

38. Attachment 1: "Westinghouse Responses to NRC RAIs Related to WCAP-17788, Volumes 1 and 4 Supporting the Closure of GSI-191 (PA-SEE-1090) and Mark-ups to WCAP-17788 Proprietary," December 19, 2017 (ADAMS Accession Nos. ML18029A210 and ML18029A211). (non-public).
39. ANP-3583P, Rev. 2, "Response to RAIs on WCAP-17788, Volume 4 - CE Plants: Licensing Report," July 31, 2018 (ADAMS Accession No. ML18285A021) (non-public).
40. WCAP-17788-P, Vol. 6, Rev. 0, "Comprehensive Analysis and Test Program for GSI-191 Closure (PA-SE-1090) - Subscale Head Loss Test Program Report," July 2016. (ADAMS Accession Nos. ML15210A681 and ML15210A682) (non-public).
41. WCAP-12945-P-A, "Code Qualification for Best Estimate LOCA Analysis," March 31, 1998 (ADAMS Package Accession No. ML093070051) (non-public).
42. Transmittal of WCAP-16009-P-A & WCAP-16009-NP-A, "Realistic Large Break LOCA Evaluation Methodology Using Automated Statistical Treatment of Uncertainty Method (ASTRUM)," January 31, 2005 (ADAMS Package Accession No. ML050910156) (non-public).
43. Safety Evaluation for Framatome ANP Topical Report EMF-2103(P) Rev. 1, Realistic Large Break LOCA Methodology for PWRs," Appendix H, "Containment Pressure" (TAC No. MC4259), January 19, 2016 (ADAMS Accession No. ML050190227) (non-public).
44. AREVA, Inc. Regarding Final Safety Evaluation for Topical Report EMF-2103(P), Rev. 3, Realistic Large Break LOCA Methodology for Pressurized Water Reactors,(TAC No. ME2904), June 2016 (ADAMS Package Accession No. ML16286A579).
45. Acceptance of Final Safety Evaluation for AREVA NP, Inc Topical Report BAW-10164(P), Rev. 6, RELAP5/MOD2-B&W - An Advanced Computer Program for Light Water Reactor LOCA and Non LOCA Transient Analysis, June 25, 2007. (ADAMS Accession No. ML091410456) (non-public).
46. Framatome Technologies, Inc., BAW-10192P-A, Rev. 0, "BWNT LOCA: BWNT Loss-of-Coolant Accident Evaluation Model for Once-Through Steam Generator Plants," BAW-10192P-A, Revision 0, June 1998, (ADAMS Accession No. ML093080467) (non-public; proprietary).
47. American Nuclear Society, ANS-5 Standards Subcommittee, Proposed ANS Standard, "Decay Energy Release Rates Following Shutdown of Uranium Fueled Thermal Reactors," October 1971.
48. American National Standards Institute/American Nuclear Society, ANSI/ANS-5.1-1979, "Decay Heat Power in Light Water Reactors," August 29, 1979.
49. "Assessment of Boric Acid Accumulation in a Reactor Core Blocked by Debris," March 2019 (ADAMS Accession No. ML19086A270) (non-public).

50. LIC-504, R. 4 "Integrated Risk-Informed Decision-Making Process for Emergent Issues," May 30, 2014 (ADAMS Accession No. ML14035A143).
51. NRC, "Regulatory Analysis Guidelines of the U.S. Nuclear Regulatory Commission," NUREG/BR-0068, Revision 5, draft for comment, April 30, 2017 (ADAMS Package No. ML17101A355).
52. Regulatory Guide 1.174, Rev. 3, "An Approach for Using Probabilistic Risk Assessment in Risk-Informed Decisions on Plant-Specific Changes to the Licensing Basis," January 2018 (ADAMS Accession No. ML17317A256).
53. IMC 0609, "Significance Determination Process," October 23, 2018 (ADAMS Accession No. ML18187A187).
54. SECY 97-077, "Draft Regulatory Guides, Standard Review Plans and NUREG Document in Support of Risk Informed Regulation for Power Reactors," April 8, 1997 (ADAMS Accession No. ML992920137).
55. NUREG-1829, "Estimating Loss-of-Coolant Accident (LOCA) Frequencies Through the Elicitation Process," Main Report, April 2008 (ADAMS Accession Nos. ML082250436 and ML081060300).
56. PWR Piping Raw Data for NUREG-1829, June 15, 2011 (ADAMS Accession No. ML080560011).
57. WCAP-16793-NP-A, Rev. 2, "Evaluation of Long-Term Cooling Considering Particulate, Fibrous and Chemical Debris in the Recirculating Fluid," July 2013 (ADAMS Package Accession No. ML13239A111). .
58. WCAP-16793-NP-A, Rev. 2, "Evaluation of Long-Term Cooling Considering Particulate, Fibrous and Chemical Debris in the Recirculating Fluid," July 2013 (ADAMS Package Accession No. ML13239A111). .

**WCAP-17788-NP**  
**Volume 1, Revision 1**

**Comprehensive Analysis and Test Program for GSI-191**  
**Closure (PA-SEE-1090)**

**December 2019**

Gordon J. Wissinger	Framatome
Adam M. Spontarelli	Framatome
James P. Spring	Westinghouse

Prepared by: Danial Utley\*  
LOCA and Containment Analysis

Reviewer: Timothy S. Andreychek\*  
Operating Plant Fluid Systems and Procedures

Approved: Timothy D. Croyle\*, Manager  
Operating Plant Fluid Systems and Procedures

Approved: Jay D. Boardman\*, Program Director  
PWR Owner's Group PMO

This work was performed under PWR Owners Group Project Authorization PA-SEE-1090

\*Electronically approved records are authenticated in the electronic document management system

---

Westinghouse Electric Company LLC  
1000 Westinghouse Drive  
Cranberry Township, PA 16066, USA

---

Framatome Inc.  
3315 Old Forest Road  
Lynchburg, VA 24501

© 2019 Westinghouse Electric Company LLC  
All Rights Reserved

## ACKNOWLEDGEMENTS

This report was developed and funded by the PWR Owners Group under the leadership of the participating utility representatives of the Systems & Equipment Engineering Committee. The authors thank the PWR Owners Group GSI-191 Technical Integration Group Engaged in Research (TIGER) Team for their support and contributions to this program; Mr. Jeffrey Brown, the late Mr. Phillip Grissom, Mr. Dana Knee, Mr. Ernie Kee, Mr. Kenneth Greenwood, Mr. Timothy Croyle, and associate members; Mr. Kurt Flaig and Mr. Paul Leonard. The authors also gratefully acknowledge and recognize Mr. Jay Boardman, PWR Owners Group Program Manager, and Mr. Paul Stevenson, Ms. Danielle Page Blair, Mr. Robert Schomaker, Mr. John Maruschak and Mr. David C. Kovacic, Project Managers, for their guidance and encouragement throughout the process of developing this report.

### LEGAL NOTICE

This report was prepared as an account of work performed by both Framatome Inc. and Westinghouse Electric Company LLC. Neither Framatome Inc., nor Westinghouse Electric Company LLC, nor any person acting on its behalf:

1. Makes any warranty or representation, express or implied including the warranties of fitness for a particular purpose or merchantability, with respect to the accuracy, completeness, or usefulness of the information contained in this report, or that the use of any information, apparatus, method, or process disclosed in this report may not infringe privately owned rights; or
2. Assumes any liabilities with respect to the use of, or for damages resulting from the use of, any information, apparatus, method, or process disclosed in this report.

### COPYRIGHT NOTICE

This report has been prepared by Framatome Inc. and bears a Framatome Inc. copyright notice. As a member of the PWR Owners Group, you are permitted to copy and redistribute all or portions of the report within your organization; however all copies made by you must include the copyright notice in all instances.

This report has been prepared by Westinghouse Electric Company LLC and bears a Westinghouse Electric Company copyright notice. As a member of the PWR Owners Group, you are permitted to copy and redistribute all or portions of the report within your organization; however all copies made by you must include the copyright notice in all instances.

### DISTRIBUTION NOTICE

This report was prepared for the PWR Owners Group. This Distribution Notice is intended to establish guidance for access to this information. This report (including proprietary and non-proprietary versions) is not to be provided to any individual or organization outside of the PWR Owners Group program participants without prior written approval of the PWR Owners Group Program Management Office. However, prior written approval is not required for program participants to provide copies of Class 3 Non-Proprietary reports to third parties that are supporting implementation at their plant, and for submittals to the NRC.

**PWR Owners Group**  
**United States Member Participation\* for WCAP-17788**

Utility Member	Plant Site(s)	Participant	
		Yes	No
Ameren Missouri	Callaway (W)	X	
American Electric Power	D.C. Cook 1 & 2 (W)	X	
Arizona Public Service	Palo Verde Unit 1, 2, & 3 (CE)	X	
Dominion Energy	Millstone 2 (CE)	X	
	Millstone 3 (W)	X	
	North Anna 1 & 2 (W)	X	
	Surry 1 & 2 (W)	X	
	V.C. Summer (W)	X	
Duke Energy Carolinas	Catawba 1 & 2 (W)	X	
	McGuire 1 & 2 (W)	X	
	Oconee 1, 2, & 3 (B&W)	X	
Duke Energy Progress	Robinson 2 (W)	X	
	Shearon Harris (W)	X	
Entergy Palisades	Palisades (CE)	X	
Entergy Nuclear Northeast	Indian Point 2 & 3 (W)	X	
Entergy Operations South	Arkansas 1 (B&W)	X	
	Arkansas 2 (CE)	X	
	Waterford 3 (CE)	X	
Exelon Generation Co. LLC	Braidwood 1 & 2 (W)	X	
	Byron 1 & 2 (W)	X	
	Calvert Cliffs 1 & 2 (CE)	X	
	Ginna (W)	X	
FirstEnergy Nuclear Operating Co.	Beaver Valley 1 & 2 (W)	X	
	Davis-Besse (B&W)	X	
Florida Power & Light \ NextEra	St. Lucie 1 & 2 (CE)	X	
	Turkey Point 3 & 4 (W)	X	
	Seabrook (W)	X	
	Pt. Beach 1 & 2 (W)	X	
Luminant Power	Comanche Peak 1 & 2 (W)	X	



**PWR Owners Group  
United States Member Participation\* for WCAP-17788**

Utility Member	Plant Site(s)	Participant	
		Yes	No
Pacific Gas & Electric	Diablo Canyon 1 & 2 (W)	X	
PSEG – Nuclear	Salem 1 & 2 (W)	X	
So. Texas Project Nuclear Operating Co.	South Texas Project 1 & 2 (W)	X	
Southern Nuclear Operating Co.	Farley 1 & 2 (W)	X	
	Vogtle 1 & 2 (W)	X	
Tennessee Valley Authority	Sequoyah 1 & 2 (W)	X	
	Watts Bar 1 & 2 (W)	X	
Wolf Creek Nuclear Operating Co.	Wolf Creek (W)	X	
Xcel Energy	Prairie Island 1 & 2 (W)	X	

\* Project participants as of the date the final deliverable was completed. On occasion, additional members will join a project. Please contact the PWR Owners Group Program Management Office to verify participation before sending this document to participants not listed above.

**PWR Owners Group**  
**International Member Participation\* for WCAP-17788**

Utility Member	Plant Site(s)	Participant	
		Yes	No
Asociación Nuclear Ascó-Vandellòs	Asco 1 & 2 (W)	X	
	Vandellos 2 (W)	X	
Centrales Nucleares Almaraz-Trillo	Almaraz 1 & 2 (W)	X	
EDF Energy	Sizewell B (W)	X	
Electrabel	Doel 1, 2 & 4 (W)	X	
	Tihange 1 & 3 (W)	X	
Electricite de France	58 Units	X	
Elektricitets Produktiemaatschappij Zuid-Nederland	Borssele 1 (Siemens)	X	
Eletronuclear-Elektrobras	Angra 1 (W)	X	
Emirates Nuclear Energy Corporation	Barakah 1 & 2	X	
Hokkaido	Tomari 1, 2 & 3 (MHI)	X	
Japan Atomic Power Company	Tsuruga 2 (MHI)	X	
Kansai Electric Co., LTD	Mihama 3 (W)	X	
	Ohi 1, 2, 3 & 4 (W & MHI)	X	
	Takahama 1, 2, 3 & 4 (W & MHI)	X	
Korea Hydro & Nuclear Power Corp.	Kori 1, 2, 3 & 4 (W)	X	
	Hanbit 1 & 2 (W)	X	
	Hanbit 3, 4, 5 & 6 (CE)	X	
	Hanul 3, 4, 5 & 6 (CE)	X	
Kyushu	Genkai 2, 3 & 4 (MHI)	X	
	Sendai 1 & 2 (MHI)	X	
Nuklearna Elektrarna KRSKO	Krsko (W)	X	
Ringhals AB	Ringhals 2, 3 & 4 (W)	X	
Shikoku	Ikata 2 & 3 (MHI)	X	
Taiwan Power Co.	Maanshan 1 & 2 (W)	X	

\* Project participants as of the date the final deliverable was completed. On occasion, additional members will join a project. Please contact the PWR Owners Group Program Management Office to verify participation before sending this document to participants not listed above.

**USE OF TECHNICAL REPORT WCAP-17788**  
**BY**  
**MEMBERS OF THE PRESSURIZED WATER REACTOR OWNERS GROUP**

This technical report is comprised of six volumes. All six volumes of Revision 0 of the technical report were submitted to the U.S. Nuclear Regulatory Commission (US NRC) with the objective of obtaining a Safety Evaluation (SE) on the complete report (all six volumes).

The US NRC initiated a review of the technical report and issued a number of Requests for Additional Information (RAIs). Responses to those RAIs were prepared and submitted to the US NRC to support their review. All RAIs and their responses are included in an appendix to the applicable volumes. It is noted that Volume 2 was not reviewed in detail by the US NRC, and as a result, no RAIs were provided for this volume of the technical report. It is also noted that sections of technical report PWROG-15091 Revision 0, "Subscale Brine Test Program Report" (Reference 1) were reviewed as supporting information to this technical report. The RAI and its response related to PWROG-15091 is included in the applicable Volume 1 appendix. Revision 1 of PWROG-15091 was also prepared and includes a modification committed to in the RAI response.

In the middle of 2019, the US NRC informed the PWROG that an SE would not be issued on this technical report. Rather, the US NRC would accept licensees referring to the technical report in their response submittals to Generic Letter (GL) 2004-02 (Reference 2), accompanied by a statement demonstrating the applicability of the referenced portion of the technical report to their specific PWR unit.

Additionally, the US NRC has used information contained in the technical report, along with other information, to prepare a Technical Evaluation Report (TER) that concludes in-vessel debris effects are of a low safety significance. The US NRC has used the TER to support closure of Generic Safety Issue (GSI) -191 (Reference 3). The TER is published in Volume 1 of this technical report revision.

To support the use of the technical report by PWROG members, Revision 1 of the technical report was prepared and includes all RAIs and their responses, as well as modifications committed to in the RAI responses. As noted previously, this technical report has not received an NRC SE. However, all six volumes of WCAP-17788 have been amended to Revision 1 and are made available to participating PWROG members for their use to respond to GL 2004-02 and close GSI-191 for the PWR units they operate.

This report may reference AREVA. Since revision 0 of this report was generated, AREVA has changed their name to Framatome Inc.

**REFERENCE**

1. PWROG-15091-NP, Revision 1, "Subscale Brine Test Program Report," November 2019. (Non-Proprietary)
2. NRC Generic Letter 2004-02, "Potential Impact of Debris Blockage on Emergency Recirculation during Design Basis Accidents at Pressurized-Water Reactors," ADAMS Accession Number ML042360586, September 13, 2004.
3. NRC Memorandum from R. V. Furstenau to H. K. Nieh, "Closure of Generic Issue GI-191, 'Assessment of Debris Accumulation on PWR Sump Performance,'" ADAMS Accession Number ML19203A303, July 23, 2019

## TABLE OF CONTENTS

LIST OF TABLES .....	xi
LIST OF FIGURES .....	xii
LIST OF ACRONYMS AND ABBREVIATIONS .....	xiv
1 EXECUTIVE SUMMARY .....	1-1
2 INTRODUCTION & BACKGROUND .....	2-1
2.1 PROGRAM INTRODUCTION AND PURPOSE .....	2-1
2.2 HISTORICAL BACKGROUND .....	2-2
2.3 REFERENCES .....	2-4
3 TECHNICAL BACKGROUND .....	3-1
3.1 PLANT TERMINOLOGY .....	3-1
3.2 DESCRIPTION OF REACTOR VESSEL AND FUEL COMPONENTS .....	3-1
3.3 DESCRIPTION OF PWR LOCA AND SAFEGUARDS OPERATIONS .....	3-13
3.3.1 General Sequence of Events Following a Large Break LOCA .....	3-13
3.3.2 ECCS Configuration and Performance during Sump Recirculation .....	3-14
3.3.3 Boric Acid Precipitation Control .....	3-16
3.4 DESCRIPTION OF IN-VESSEL DEBRIS CONCERNS .....	3-17
3.5 DEBRIS CONSTITUENTS .....	3-18
3.6 LIMITING SCENARIO .....	3-19
3.6.1 Debris Generation .....	3-20
3.6.2 Timing of Debris Arrival and ECCS Flow Rate .....	3-21
3.6.3 Debris Delivered to Reactor Coolant System .....	3-22
3.6.4 Conclusions .....	3-23
3.7 LONG-TERM CORE COOLING REQUIREMENTS AND ACCEPTANCE CRITERIA .....	3-24
3.8 CURRENT DEBRIS LIMITS .....	3-24
3.9 REFERENCES .....	3-28
4 METHOD FOR CALCULATING FIBER LIMIT .....	4-1
4.1 DEFINITION OF IN-VESSEL DEBRIS .....	4-3
4.2 LARGE HOT LEG BREAKS .....	4-4
4.2.1 Time of Sump Recirculation .....	4-7
4.2.2 Activation of Alternate Flow Path .....	4-7
4.2.3 Chemical Precipitate Formation .....	4-7
4.2.4 Implementation of Measures to Prevent Boric Acid Precipitation .....	4-8
4.2.5 Example Timelines .....	4-8
4.3 LARGE COLD LEG BREAKS .....	4-10
4.4 REFERENCES .....	4-11
5 MAJOR ASSUMPTIONS .....	5-1
5.1 HOT LEG BREAKS .....	5-1
5.2 COLD LEG BREAKS .....	5-2
5.3 UPPER PLENUM INJECTION PLANTS .....	5-3
5.4 REFERENCES .....	5-3
6 HOT LEG BREAKS .....	6-1

6.1	THERMAL-HYDRAULIC EVALUATION OF REACTOR COOLANT SYSTEM .....	6-1
6.1.1	Westinghouse Upflow Plant Category .....	6-2
6.1.2	Westinghouse Downflow Plant Category .....	6-2
6.1.3	Combustion Engineering Plant Category .....	6-3
6.1.4	Babcock and Wilcox Plant Category .....	6-3
6.2	CHEMICAL PRECIPITATE FORMATION .....	6-8
6.3	CORE INLET DEBRIS LIMIT .....	6-9
6.3.1	Analysis of Subscale Final Limits Data .....	6-9
6.3.2	Westinghouse Fuel .....	6-12
6.3.3	AREVA Fuel .....	6-15
6.4	IN-CORE DEBRIS LIMIT .....	6-18
6.4.1	Activation of Alternate Flow Path .....	6-18
6.4.2	Post Hot Leg Switchover .....	6-19
6.4.3	Justification for In-Core Debris Limit .....	6-19
6.4.4	Summary and Conclusion .....	6-23
6.5	METHOD FOR VERIFYING HOT LEG BREAK IN-VESSEL DEBRIS LIMITS ....	6-23
6.5.1	Overview .....	6-23
6.5.2	Inputs .....	6-25
6.5.3	Fiber Injection Rate .....	6-29
6.5.4	Potentially Limiting Cases .....	6-32
6.5.5	Methodology .....	6-32
6.5.6	Example Calculations .....	6-36
6.6	REFERENCES .....	6-42
7	COLD LEG BREAKS .....	7-1
7.1	COLD LEG BREAK IN-VESSEL DEBRIS LIMIT .....	7-1
7.1.1	Debris Collection at the Core Inlet .....	7-3
7.1.2	Suspended Debris in the Heated Core .....	7-17
7.1.3	Local Collection of Debris .....	7-21
7.1.4	Summary .....	7-21
7.2	METHOD FOR VERIFYING COLD LEG BREAK IN-VESSEL DEBRIS LIMIT ....	7-23
7.3	REFERENCES .....	7-25
8	UPPER PLENUM INJECTION PLANTS .....	8-1
8.1	COLLECTION OF DEBRIS IN THE REACTOR VESSEL .....	8-1
8.1.1	Large Cold Leg Break Scenario .....	8-2
8.1.2	Large Hot Leg Break Scenario .....	8-2
8.1.3	Method for Verifying In-Vessel Debris Limits .....	8-2
8.2	REFERENCES .....	8-3
9	DEBRIS LIMITS AND ACCEPTANCE CRITERIA .....	9-1
9.1	HOT LEG BREAK .....	9-1
9.1.1	Decay Heat Removal .....	9-1
9.1.2	Boric Acid Precipitation Control .....	9-2
9.2	COLD LEG BREAK .....	9-3
9.2.1	Decay Heat Removal .....	9-3
9.2.2	Boric Acid Precipitation Control .....	9-3
9.3	REFERENCES .....	9-4
10	MARGINS AND CONSERVATISMS .....	10-1

10.1	DEBRIS TRANSPORT AND ACCUMULATION .....	10-1
10.2	HOT LEG BREAKS .....	10-2
10.2.1	Uniform Buildup of Debris.....	10-2
10.2.2	Chemical Precipitates and Core Inlet Blockage .....	10-2
10.2.3	Cladding Temperature .....	10-2
10.2.4	Bounding Thermal-Hydraulic Analyses .....	10-3
10.2.5	Subscale Test Facility Design.....	10-3
10.2.6	Particulates Used in Testing.....	10-4
10.2.7	Flow Rates Used in Testing .....	10-4
10.2.8	Geometry Used in Testing .....	10-4
10.2.9	Reactor Vessel Fiber Limits.....	10-5
10.3	COLD LEG BREAKS .....	10-5
10.4	REFERENCES .....	10-5
11	SUMMARY AND CONCLUSION .....	11-1
APPENDIX A	– PHENOMENA IDENTIFICATION AND RANKING .....	A-1
APPENDIX B	- REQUESTS FOR ADDITIONAL INFORMATION AND RESPONSES.....	B-1

## LIST OF TABLES

Table 3-1	Comparison of System and Component Terminology by NSSS Vendor .....	3-3
Table 3-2	Example Debris Ratio Calculations .....	3-21
Table 6-1	Summary of Thermal-Hydraulic Output Parameters .....	6-3
Table 6-2	Equivalent Dimensionless Form-Loss Coefficient Linear Relations for Various NSSS designs with Westinghouse Fuel .....	6-14
Table 6-3	Acceptable Core Inlet Fiber Loads Prior to Reaching $t_{block}$ for Various NSSS designs with Westinghouse Fuel .....	6-15
Table 6-4	Equivalent Dimensionless Form-Loss Coefficient Linear Relations for Various NSSS designs with AREVA Fuel .....	6-17
Table 6-5	Acceptable Core Inlet Fiber Loads Prior to Reaching $t_{block}$ for Various NSSS designs with AREVA Fuel .....	6-17
Table 6-6	Input Biasing for Potentially Limiting Cases.....	6-32
Table 6-7	Test Case Inputs .....	6-39
Table 6-8	Hot Leg Break Example Case Results .....	6-42
Table 7-1	Double-Ended Cold Leg Break Thermal-Hydraulic Analysis .....	7-4
Table 7-2	SKBOR Core Inlet Blockage Sensitivity Study Case Matrix .....	7-12
Table A-1	PIRT Scenario Phases and Phase Duration .....	A-2

## LIST OF FIGURES

Figure 3-1 Typical Reactor Vessel Internals .....	3-4
Figure 3-2 Typical Core Barrel Hardware.....	3-5
Figure 3-3 Typical Fuel Assembly Components.....	3-6
Figure 3-4 Typical Fuel Rod and Spacer Grid Orientation .....	3-7
Figure 3-5 Westinghouse Upflow Barrel/Baffle Design (No Pressure Relief Holes) .....	3-8
Figure 3-6 CE Barrel/Baffle Design .....	3-9
Figure 3-7 B&W Barrel/Baffle Design .....	3-10
Figure 3-8 Westinghouse Downflow Barrel/Baffle Design .....	3-11
Figure 3-9 Westinghouse Upper Head Spray Nozzle Design .....	3-12
Figure 3-10 Strainer Bypass Fraction as a Function of Theoretical Debris Bed Thickness.....	3-23
Figure 4-1 Process Diagram for Determination of Plant-Specific In-Vessel Debris Limit.....	4-2
Figure 4-2 Overview of Hot Leg Break Methodology.....	4-6
Figure 4-3 Example Timing #1 .....	4-9
Figure 4-4 Example Timing #2 .....	4-10
Figure 6-1 $K_{split}$ as a Function of ECCS Recirculation Flow Rate from Westinghouse Upflow Analysis .....	6-4
Figure 6-2 Fraction of ECCS Recirculation Flow through the BB following $K_{split}$ from Westinghouse Upflow Analysis for Recirculation Flow Rates Greater than 18 gpm/FA.....	6-4
Figure 6-3 Fraction of ECCS Recirculation Flow through the BB following $K_{split}$ from Westinghouse Upflow Analysis for Recirculation Flow Rates Less than or Equal to 18 gpm/FA .....	6-5
Figure 6-4 $K_{split}$ as a Function of ECCS Recirculation Flow Rate from Westinghouse Downflow Analysis .....	6-5
Figure 6-5 Fraction of ECCS Recirculation Flow through the BB following $K_{split}$ from Westinghouse Downflow Analysis.....	6-6
Figure 6-6 $K_{split}$ as a Function of ECCS Recirculation Flow Rate from CE Analysis .....	6-6
Figure 6-7 Fraction of ECCS Recirculation Flow through the BB following $K_{split}$ from CE Analysis for Barrel/Baffle Resistance $K/A^2 = [ \quad ]^{a,c}$ .....	6-7
Figure 6-8 Fraction of ECCS Recirculation Flow through the BB following $K_{split}$ from CE Analysis for Baffle Resistance $K/A^2 = [ \quad ]^{a,c}$ .....	6-7
Figure 6-9 Limiting Conditions from Subscale Head Loss Testing Scaled to a Full-Area Fuel Assembly ...	6-10
Figure 6-10 Subscale Dimensionless Form-Loss Coefficient for Westinghouse Fuel .....	6-13



Figure 6-11 Subscale Equivalent Dimensionless Form-Loss Coefficients for Various NSSS Designs with Westinghouse Fuel .....	6-13
Figure 6-12 Subscale Dimensionless Form-Loss Coefficient for AREVA Fuel .....	6-15
Figure 6-13 Subscale Equivalent Dimensionless Form-Loss Coefficients for Various NSSS Designs with AREVA Fuel .....	6-16
Figure 6-14 Fiber Collection on Leading Edge of Spacer Grid .....	6-21
Figure 6-15 Fiber Collection on Internal Springs of Spacer Grid .....	6-22
Figure 6-16 System Schematic for Fiber Tracking .....	6-29
Figure 6-17 $K_{split}$ as a Function of ECCS Recirculation Flow Rate from B&W Analysis .....	6-38
Figure 6-18 Fraction of ECCS Recirculation Flow through the Barrel/Baffle Inlet following $K_{split}$ from B&W Analysis .....	6-38
Figure 7-1 Axial Liquid Velocity at the Inlet to the Hot Assembly (HA) .....	7-5
Figure 7-2 Axial Liquid Velocity at the Inlet to the Average Power (AV) Fuel Assemblies .....	7-6
Figure 7-3 Axial Liquid Velocity at the Inlet to the Average Power Fuel Assemblies below Guide Tubes (GT) .....	7-6
Figure 7-4 Axial Liquid Velocity at the Inlet to the Low Power (LP) Peripheral Fuel Assemblies .....	7-7
Figure 7-5 Reactor Vessel Outlet Steam Quality .....	7-7
Figure 7-6 Debris Collection Near Core Inlet in the 3x3 Heated Rod Bundle Test Facility .....	7-10
Figure 7-7 Temperature Measurements from Tests Conducted in the 3x3 Heater Rod Bundle Test Facility .....	7-11
Figure 7-8 Core Boric Acid Concentration .....	7-13
Figure 7-9 Lower Plenum Boric Acid Concentration .....	7-14
Figure 7-10 Core-to-Lower Plenum Exchange Mass Flow Rate .....	7-15
Figure 7-11 Core Boric Acid Concentration .....	7-16
Figure 7-12 3x3 Heated Rod Bundle Test Results Showing Fiber Accumulation on Outer Edge of Spacer Grid .....	7-19
Figure 7-13 Comparison of Bubble Characteristics from the 3x3 Heated Rod Bundle Tests with Unbuffered Boric Acid (BA) and Buffered Boric Acid with Debris .....	7-19
Figure 7-14 Comparison of Experimental Boiling Curves for Tests with Pure Water, Unbuffered Boric Acid, and Unbuffered Boric Acid with Debris .....	7-20
Figure 7-15 ECCS and CSS Flow Paths for a Cold Leg Break .....	7-24

**LIST OF ACRONYMS AND ABBREVIATIONS**

ACC	Accumulator(s)
ACRS	Advisory Committee on Reactor Safeguards
AFP	Alternate Flow Path
B&W	Babcock and Wilcox
BAMT	Boric Acid Mixing Tank
BAP	Boric Acid Precipitation
BAPC	Boric Acid Precipitation Control
BAST	Boric Acid Storage Tank(s)
BB	Barrel/Baffle
BN	Bottom Nozzle
BWST	Borated Water Storage Tank(s)
Cal-Sil	Calcium Silicate
CCI	Centrifugal Charging Injection
CE	Combustion Engineering
CFR	Code of Federal Regulations
CFT	Core Flood Tank(s)
CL	Cold Leg(s)
CLB	Cold Leg Break(s)
CS	Containment Spray
CSS	Containment Spray System
CVCS	Chemical and Volume Control System
DB	Design Basis
DEG	Double-Ended Guillotine
DH	Decay Heat
DHC	Decay Heat Cooler(s)
DHR	Decay Heat Removal
ECCS	Emergency Core Cooling System
EOP	Emergency Operating Procedure(s)
EPRI	Electric Power Research Institute
FA	Fuel Assembly(s)
GL	Generic Letter
GR	Guidance Report
GSI	Generic Safety Issue
HHSI	High Head Safety Injection
HL	Hot Leg(s)
HLB	Hot Leg Break(s)
HLSO	Hot Leg Switchover

**LIST OF ACRONYMS AND ABBREVIATIONS**

HPI	High Pressure Injection
HPSI	High Pressure Safety Injection
IHSI	Intermediate Head Safety Injection
LBLOCA	Large Break LOCA
LCP	Lower Core Plate
LEF	Lower End Fitting
LHSI	Low Head Safety Injection
LOCA	Loss-of-Coolant Accident
LOCADM	Loss-of-Coolant Accident Deposition Model
LP	Lower Plenum
LPI	Low Pressure Injection
LPSI	Low Pressure Safety Injection
LSP	Lower Support Plate
LTCC	Long-Term Core Cooling
MOV	Motor Operated Valve
NEI	Nuclear Energy Institute
NPSH	Net Positive Suction Head
NRC	Nuclear Regulatory Commission
NSSS	Nuclear Steam Supply System
p:f	Particulate-to-Fiber Ratio
PA	Project Authorization
PCT	Peak Cladding Temperature
PIRT	Phenomena Identification and Ranking Table(s)
PWR	Pressurized Water Reactor(s)
PWROG	Pressurized Water Reactor Owners Group
RAS	Recirculation Actuation Signal
RBS	Reactor Building Spray
RCS	Reactor Coolant System
RHR	Residual Heat Removal
RV	Reactor Vessel
RVVV	Reactor Vessel Vent Valve(s)
RWST	Refueling Water Storage Tank
RWT	Refueling Water Tank
SCS	Shutdown Cooling System
SCHX	Shutdown Cooling System Heat Exchanger(s)
SE	Safety Evaluation(s)
SEE	Systems & Equipment Engineering

**LIST OF ACRONYMS AND ABBREVIATIONS**

SG	Steam Generator(s)
SIT	Safety Injection Tank(s)
SIS	Safety Injection System
SoK	State of Knowledge
SSO	Sump Switchover
STP	South Texas Project
TH	Thermal-Hydraulic(s)
TN	Top Nozzle
U.S.	United States
UCP	Upper Core Plate
UHSN	Upper Head Spray Nozzle(s)
UP	Upper Plenum
UPI	Upper Plenum Injection
WCAP	Westinghouse Technical Report Number Preface (formerly Westinghouse Commercial Atomic Power)
ZOI	Zone of Influence

## 1 EXECUTIVE SUMMARY

The Pressurized Water Reactor Owners Group (PWROG) has undertaken a comprehensive test and analysis program as part of the resolution to generic safety issue (GSI) 191 to increase the fibrous debris limits per fuel assembly (FA). This report documents the methodology that member utilities can use to assess the time-dependent collection of fibrous debris in the reactor vessel (RV), which can then be used for final closure of Nuclear Regulatory Commission (NRC) Generic Letter (GL) 2004-02 and GSI-191. This work provides an alternative approach to the method detailed in WCAP-16793-NP-A, Rev. 2 for defining an in-vessel fibrous debris limit and provides a means for increasing the currently established in-vessel fibrous debris limit of 15 g/FA.

Title 10 Code of Federal Regulations (CFR) 50.46 requires that long-term core cooling (LTCC) be demonstrated for all break sizes and locations in the reactor coolant system (RCS). The technical development of this program is predicated on two fundamental criteria: (1) that decay heat removal (DHR) is assured such that the core temperature is maintained at an acceptably low level, and (2) that boric acid precipitation control (BAPC) is assured by maintaining the boron concentrations in the RV remain below the solubility limit.

This volume consolidates the results of five separate, but interrelated elements of the PWROG program. The individual program elements are described in detail in separate volumes, the collection of which, including the present volume (Volume 1), constitute WCAP-17788. The methodology for calculating the in-vessel debris limits are plant-specific and depend on inputs for each plant (or group of identical plants). This program is applicable to all Westinghouse, Combustion Engineering (CE), and Babcock and Wilcox (B&W) pressurized water reactor (PWR) Nuclear Steam Supply System (NSSS) plants.

Large, double-ended breaks are the focus of GSI-191 resolution since the effects of debris from these breaks bound all other break sizes. The break locations are divided into hot leg breaks (HLBs) and cold leg breaks (CLBs). Both break scenarios must be considered independently given the difference in system response, timing of debris introduction to the fuel, and the benefits of alternate flow paths (AFPs) for hot leg breaks.

This report further divides the plants into those that initially begin sump recirculation with ECCS recirculation flow to the cold legs and those that initially begin with ECCS recirculation flow to the upper plenum (UPI plants). Section 5 identifies the major assumptions used in the methodology for both types of plants. For plants that initially start with cold side recirculation, Section 4.2 outlines the methodology for HLB and Section 4.3 outlines the methodology for CLB. Sections 6 and 7 provide the details of the methods for calculating the amount of fiber delivered to the RCS for HLB and CLB, respectively. For UPI plants, Section 8 provides the methodology for both break locations. For the spectrum of large breaks, this methodology can be used to ascertain that the amount of debris generated in containment does not ultimately result in an excessive amount of debris (fiber and particulate) delivered to the RV such that LTCC is compromised.

The increased fiber limits may be applied for moderate to high fiber plants to justify the current debris source terms for deterministic closure of NRC GL 2004-02. High fiber plants may also apply this methodology to establish a basis for risk informed evaluation and closure of GL 2004-02. The remaining plants, and all plants, can exercise the methodology to ensure margin in response to possible plant design changes and/or operability assessments.

## 2 INTRODUCTION & BACKGROUND

### 2.1 PROGRAM INTRODUCTION AND PURPOSE

This report presents the final results of a program coordinated and funded by the PWROG to develop a deterministic approach and methodology for assessing the time-dependent collection of fibrous debris in the RV for member utilities. This assessment can then be used for final closure of NRC GL 2004-02 (Reference 2-1) and GSI-191. This work provides an alternative approach to the method detailed in WCAP-16793-NP-A, Rev. 2 (Reference 2-2) for defining an in-vessel fibrous debris limit and provides a means for increasing the currently established in-vessel fibrous debris limit of 15 g/FA.

The technical development of this program is predicated on two fundamental criteria which, if satisfied, ensure LTCC as defined in 10 CFR 50.46 (Reference 2-3) in the presence of entrained debris. These criteria are:

1. Decay Heat Removal - DHR requires that sufficient coolant be supplied to the core such that the core temperature is maintained at an acceptably low level. For previous GSI-191 evaluations, the maximum allowable post-quench peak cladding temperature (PCT) is 800°F (Reference 2-2). This conservative limit will be retained.
2. Boric Acid Precipitation Control - BAPC requires that boron concentrations in the RV remain below the solubility limit.

This volume consolidates the results of five separate, but interrelated elements of the PWROG program. The individual program elements are described in detail in separate volumes, the collection of which, including the present volume (Volume 1), constitute WCAP-17788. These respective program elements are:

- Volume 2 – Comprehensive Analysis and Test Program for GSI-191 Closure (PA-SEE-1090) – Phenomena Identification and Ranking Tables (PIRT) for GSI-191 Long-Term Cooling
- Volume 3 – Comprehensive Analysis and Test Program for GSI-191 Closure (PA-SEE-1090) – Cold Leg Break Evaluation Method for GSI-191 Long-Term Cooling
- Volume 4 – Comprehensive Analysis and Test Program for GSI-191 Closure (PA-SEE-1090) – Thermal-Hydraulic Analysis of Large Hot Leg Break with Simulation of Core Inlet Blockage
- Volume 5 – Comprehensive Analysis and Test Program for GSI-191 Closure (PA-SEE-1090) – Autoclave Chemical Effects Testing for GSI-191 Long-Term Cooling
- Volume 6 – Comprehensive Analysis and Test Program for GSI-191 Closure (PA-SEE-1090) – Subscale Head Loss Test Program Report

This program is applicable to Westinghouse, CE, and B&W PWR NSSS plants. The methodology for calculating the in-vessel debris limits described in this report is plant-specific and depends on inputs for each plant (or group of identical plants). The general approach for all plants is to separately assess the

debris limits for the CLB and HLB scenarios. Both break scenarios must be considered independently given the difference in system response, timing of debris introduction to the fuel, and the benefits of alternate flow paths (AFPs) for hot leg breaks.

The development of the PWROG program considers the results of a phenomena identification and ranking table (PIRT) (Volume 2). Information assembled by the PIRT determined, in part, the necessary testing and analysis. The development of the program was further informed by various oversight efforts including an independent third party review contracted to assess the results of previous in-vessel testing program efforts, and a challenge review board tasked with review of the proposed program described in this WCAP.

For the CLB scenario, a core inlet fiber limit is established such that a uniform debris bed does not form at the core inlet and exchange flow between the core and lower plenum (LP) is maintained. This exchange flow transports boron solute from the core region to the LP which slows the buildup rate of boron concentrations in the core region. Further, a methodology was developed (Volume 3) for plants to calculate a plant-specific in-vessel debris load to ensure that it remains below the established limit.

For the HLB scenario, the thermal-hydraulic (TH) analyses (Volume 4) establish the time-dependent blockage conditions and availability of the AFPs to ensure that cooling flow is available such that the cladding temperature limit is not exceeded. The correlation between the losses modeled in the TH analyses and the losses attributed to an actual debris bed is developed by physical (subscale) head loss testing (Volume 6). Critical inputs for the head loss testing (debris types and characterization) have been developed based on the range of prototypical conditions for plants. The chemical effects evaluation (Volume 5) establishes the minimum time for the formation of post loss-of-coolant accident (LOCA) sump fluid chemical effects (precipitates) for each plant or plant groups. The general approach is to confirm that the onset of precipitates for all plant groups is beyond the critical time defined by the TH analyses.

The collection of these analytic and testing programs establishes a methodology that may be applied on a plant-specific basis to establish allowable debris quantities (grams of fiber per FA) for those accident scenarios that generate debris and for which the Emergency Core Cooling System (ECCS) and Containment Spray System (CSS) is aligned to the containment sump for accident mitigation (i.e., LOCA). The results are predicated on deterministic methods (analysis and testing) and are applicable to those utilities attempting GL 2004-02 closure using a deterministic approach. The methods developed herein represent an alternative to the generic limit previously developed in WCAP-16793-NP-A, Rev. 2 (Reference 2-2). The plant-specific debris limits that result from the methods developed by this program may also be applied as the basis for a risk informed analysis as appropriate.

It should be noted that the discussions presented in this report apply to the effects of debris downstream of the sump strainer in the RV only. Any mention of “debris bed” is in reference to debris collecting at the core inlet.

## **2.2 HISTORICAL BACKGROUND**

On September 13, 2004, the NRC issued GL 2004-02, “Potential Impact of Debris Blockage on Emergency Recirculation During Design Basis Accidents at Pressurized-Water Reactors” (Reference 2-1)

as the primary vehicle for addressing and resolving concerns associated with GSI-191. The GL required that all PWR licensees use an NRC-approved method to:

1. Perform a mechanistic evaluation of the potential for post-accident debris blockage and operation with debris-laden fluids to impede or prevent the recirculation functions of the ECCS and CSS following all postulated accidents for which these recirculation functions are required.
2. Implement plant modifications or other corrective actions that the evaluation identifies as necessary to ensure system functionality.

Resolution of GSI-191 requires that every plant evaluate plant-specific debris generation and transport to their recirculation sump strainer(s) for a variety of breaks and break locations. Resolution of the generic issue also requires that the effects of debris that pass through (penetrate or bypass) the sump strainer are addressed. In particular, the PWROG completed an evaluation of the impact of debris accumulation at the core inlet and the consequential effect on core cooling. The results of this comprehensive analysis and testing program are documented in WCAP-16793-NP-A, Rev. 2 (Reference 2-2). The NRC issued a Safety Evaluation (SE) documenting approval of the method as modified by conditions and limitations identified in the SE.

The methodology presented in WCAP-16793-NP-A, Rev. 2 provides a single conservative value of 15 g/FA for all plants. The NRC SE for WCAP-16793-NP-A, Rev. 2 accepts 15 g/FA as a limit for the HLB scenario. A fraction of this value is also considered acceptable for the CLB scenario given that fiber and particulate will not provide a bed sufficiently dense to effectively filter the chemical precipitates. As a result, mixing between the core and LP is not precluded during the CLB scenario with the limited quantity of debris.

The WCAP-16793-NP-A, Rev. 2 methodology is based on non-prototypical assumptions regarding debris, timing, and the immediate onset of chemical effects that significantly increase the head loss across a fiber bed that forms at the core inlet. The associated limit is restrictive and does not support closure for a large fraction of the PWROG member plants.

To support utilities that could not otherwise close the in-vessel debris issues for final closure of GL 2004-02 (without substantial modifications to existing insulation systems), the PWROG Executive Committee directed the PWROG to develop and fund a revised in-vessel program to improve upon the WCAP-16793-NP-A, Rev. 2 results. In response, the PWROG sponsored a technical proposal to develop a testing and analysis program.

The NRC also identified that additional programs to increase the fiber limit beyond that approved by WCAP-16793-NP-A, Rev. 2 and the associated SE, would have to address the impact of debris on mixing with the concern that disruption of the communication between the core and LP by accumulated debris would increase the potential for boric acid precipitation (BAP) and would challenge core cooling.

The program that has been completed and documented herein provides a deterministic approach to establishing in-vessel debris limits. This approach is based on plant-specific (or plant group-specific) inputs and design characteristics. This alternate approach is consistent with guidance provided in NRC SECY-12-0093 "Closure Options for Generic Safety Issue – 191, Assessment of Debris



Accumulation on Pressurized-Water Reactor Sump Performance,” (Reference 2-4). The program provides for a refined evaluation methodology for determining in-vessel fiber limits and produces final limits that ultimately satisfy the evaluation of LTCC as defined in 10 CFR 50.46. The results may also be applied as the basis for a risk-informed approach to evaluating the in-vessel effects (ECCS performance will otherwise be evaluated from a risk informed perspective).

## 2.3 REFERENCES

- 2-1 GL 2004-02, “Potential Impact of Debris Blockage on Emergency Recirculation During Design Basis Accidents at Pressurized-Water Reactors,” ADAMS Accession Number ML042360586, September 2004.
- 2-2 WCAP-16793-NP-A, Rev. 2, “Evaluation of Long-Term Cooling Considering Particulate, Fibrous and Chemical Debris in the Recirculation Fluid,” July 2013.
- 2-3 10 CFR Part 50 §50.46, “Acceptance Criteria for Emergency Core Cooling Systems for Light Water Nuclear Reactors,” 72 Federal Register 49494, August 28, 2007.
- 2-4 SECY-12-0093, “Closure Options for Generic Safety Issue – 191, Assessment of Debris Accumulation on Pressurized-Water Reactor Sump Performance,” July 2012.

### 3 TECHNICAL BACKGROUND

#### 3.1 PLANT TERMINOLOGY

In the United States (U.S.) PWR fleet, there are three original equipment manufacturers and designers of the RCS. They are Westinghouse, CE, and B&W. While the different designs contain systems that perform similar functions, they typically have different names. To that end, it is useful to identify the equivalent systems and components involved in LTCC. This comparison is presented in Table 3-1. To avoid confusion, Westinghouse terminology will be used throughout this report when generic discussions are presented.

#### 3.2 DESCRIPTION OF REACTOR VESSEL AND FUEL COMPONENTS

The information in this section is general in nature and is presented for background purposes only. The system descriptions are intended to provide useful information about plant design and configuration but should not be used as input to licensing basis analyses.

The prototypical structure of the RV internals is shown in Figure 3-1 and Figure 3-2. Within the RV, the core barrel is suspended from a large flange above the cold leg connection, forming an annular region called the RV downcomer. The core barrel is equipped with a thermal shield (or neutron pad) which helps protect the RV from neutron fluence. At the bottom of the RV, the core barrel closes with the core support forging, which includes large flow passage holes. The core barrel also supports a diffuser plate and the lower support plate (LSP). The weight of the fuel rests on the lower core plate (LCP) which is supported by small vertical columns that connect the LCP to the LSP and diffuser plate, passing the load to the core support forging. A clearance exists between the core support forging and lower columns in the lower head of the RV. These supports only come into play when there is large down-ward displacement of the core barrel, to which the core support forging is welded. In-core instrumentation penetrates the RV from below.

The square FAs do not fit evenly into the round core barrel. To capture the outer perimeter of the FAs, baffle plates are mounted to the core barrel via horizontally running former plates. These former plates are equipped with holes or gaps to allow flow. Flow into the barrel/baffle (BB) region (the region between the core barrel and baffle plates) is NSSS dependent and described in more detail below. The baffle plates terminate at the top of the active core, just below the upper core plate (UCP). Flow holes or gaps provide for flow out of the BB region. The FAs are located between the LCP and UCP.

Holes in the UCP align the control rod guide tube assemblies. The control rod guide tube assemblies include slotted openings. The primary function of the guide tubes is to ensure that control rod deflection is minimized during insertion and that control rods remained aligned. The control rods themselves are supported at their top by a spider and at the bottom by the control rod guide thimbles in the FA. When the control rods are fully inserted, only the drive shaft occupies an appreciable fraction of the control rod guide tube cross section.

The FAs (Figure 3-3) consist of a bottom nozzle (BN), top nozzle (TN), spacer grids, fuel rods, and control rod thimble tubes (into which the control rods slide for shutdown). The fuel rods and thimble tubes are held in a square array by the spacer grids (Figure 3-4). The BN consists of small openings designed to capture foreign debris during normal operation. The thimble tubes are threaded at their end,

and bolts are used to connect the BN to the thimble tubes. The BN also has angled feet which contain alignment dimples that match corresponding bosses on the LCP. The TN is equipped with a hold-down spring that allows the FA to be held in place without resulting in appreciable stresses due to flow and thermal expansion. The TN has larger, oblong openings allowing the flow to move upward.

All U.S. PWRs have flow paths in the RV that may allow fluid to bypass the heated core during normal operations. Examples include flow through the BB region (for upflow BB plants) and/or flow through the upper head spray nozzles. The B&W, CE, and a portion of the Westinghouse fleet have upflow BB designs that provide a direct flow path between the lower support region and the upper plenum (UP) (Figure 3-5 through Figure 3-7). Westinghouse design upflow plants and B&W plants have pressure relief holes (LOCA holes) that allow direct communication between the BB and core periphery as well. Conversely, Westinghouse downflow plants have limited flow paths between the lower support region and the UP (Figure 3-8). Westinghouse plants also have upper head spray nozzles (UHSNs) that are a credited AFP. The spray nozzles provide a flow path between the top of the downcomer and upper head as shown in Figure 3-9. The size of the spray nozzles are indicated by the upper head temperature during normal operation. There are two categories: T-cold and T-hot plant types. The T-cold design has a fairly large available flow area and low flow resistance between the downcomer and upper head such that increased bypass flow can be expected, and the upper head temperature is consistent with the cold side (i.e., cold leg) temperature. The T-hot design has smaller nozzle openings and will not provide as much bypass flow as the T-cold design such that the upper head temperature is consistent with the hot side (i.e., hot leg) temperature.

Both the BB region (in upflow plants) and the UHSNs may provide a path for coolant to reach the core in the event that the core inlet becomes blocked with debris. In this context, these paths are termed AFPs as they provide an alternate path for coolant to reach the core other than the core inlet.

**Table 3-1 Comparison of System and Component Terminology by NSSS Vendor**

System Names	B&W	CE	Westinghouse
	Emergency Core Cooling System (ECCS)	Emergency Core Cooling System (ECCS)	Emergency Core Cooling System (ECCS)
	Reactor Building Spray (RBS) System	Containment Spray System (CSS)	Containment Spray System (CSS)
	Decay Heat Removal (DHR) System	Shutdown Cooling System (SCS)	Residual Heat Removal (RHR) System
	Low Pressure Injection (LPI)	Low Pressure Safety Injection (LPSI)	Low-Head Safety Injection (LHSI)
	High Pressure Injection (HPI)	High Pressure Safety Injection (HPSI)	High-Head Safety Injection (HHSI)
	Core Flood Tanks (CFTs)	Safety Injection Tanks (SITs)	Accumulators (ACCs)
	High head normal makeup and purification (HPI pumps for all but DB)	Centrifugal Charging Injection (CCI) Pumps	Centrifugal Charging Injection (CCI), Chemical and Volume Control System (CVCS)
Components by Function			
Tank that stores borated water for safety injection/refueling	Borated Water Storage Tank (BWST)	Refueling Water Tank (RWT)	Refueling Water Storage Tank (RWST)
Supplemental tanks with concentrated boric acid solution	Boric Acid Storage Tank (BAST)	Boric Acid Mixing Tank (BAMT)	Boric Acid Storage Tank (BAST)
Pump(s) used to supply low-head safety injection/recirculation flow	LPI Pump	LPSI Pump	LHSI Pump, Residual Heat Removal (RHR) Pump
Pump(s) used to supply high-pressure safety injection/recirculation flow	High Pressure Injection (HPI) Pump	High Pressure Safety Injection (HPSI) Pump	HHSI Pump, CCI Pump, or Intermediate-Head Safety Injection (IHSI) Pump
Heat exchangers that provide decay heat and residual heat removal	Decay Heat Coolers (DHCs)	Shutdown Cooling Heat Exchangers (SCHXs)	RHR Heat Exchangers
Pumps that supply containment spray flow	Reactor Building Spray (RBS) Pumps	Containment Spray (CS) Pumps	CS Pumps
Heat exchangers that cool containment spray	None	SCHXs	CS Heat Exchangers
Nozzles that deliver spray to containment building	Building Spray Nozzles	CS Nozzles	CS Nozzles

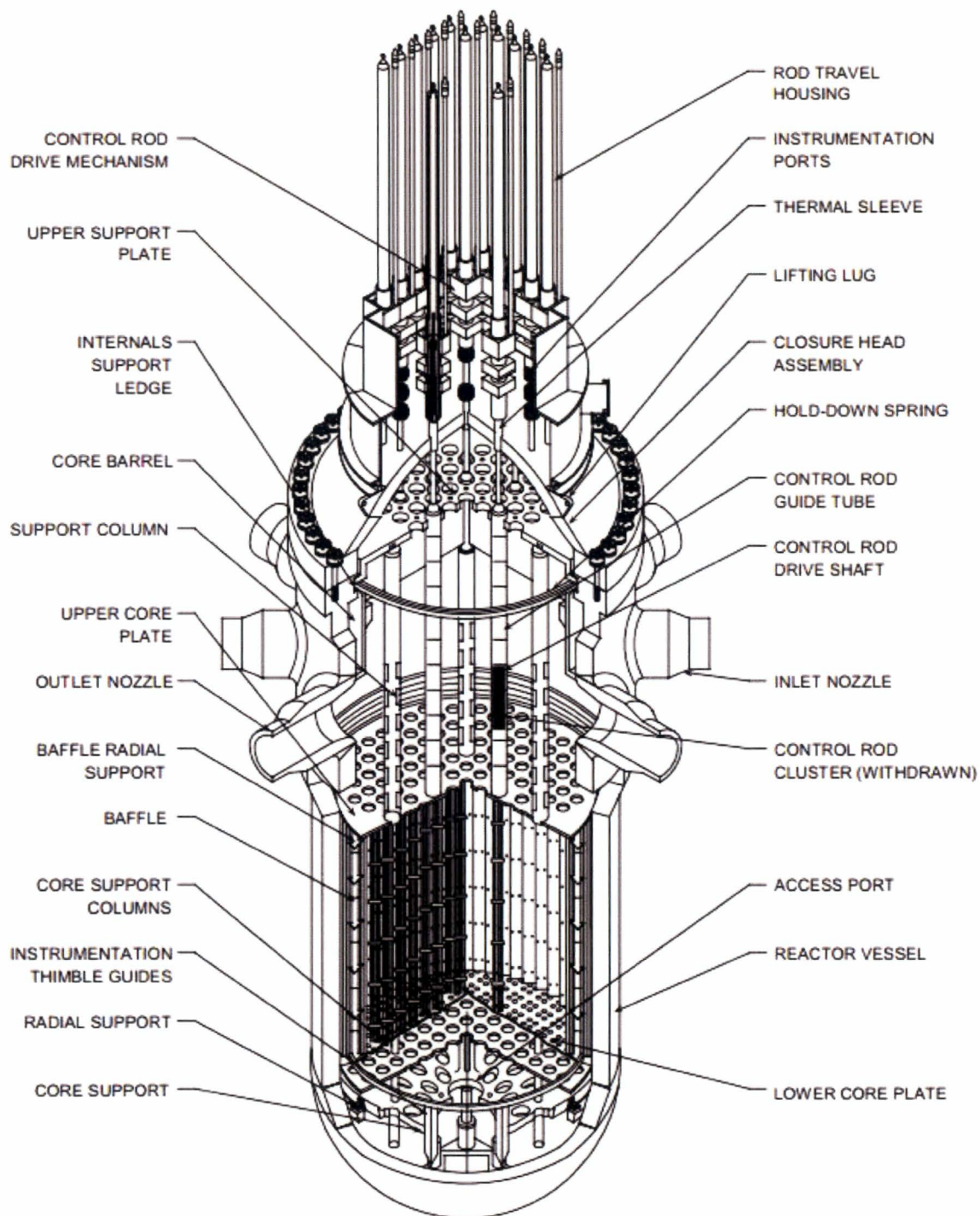


**Figure 3-1 Typical Reactor Vessel Internals**

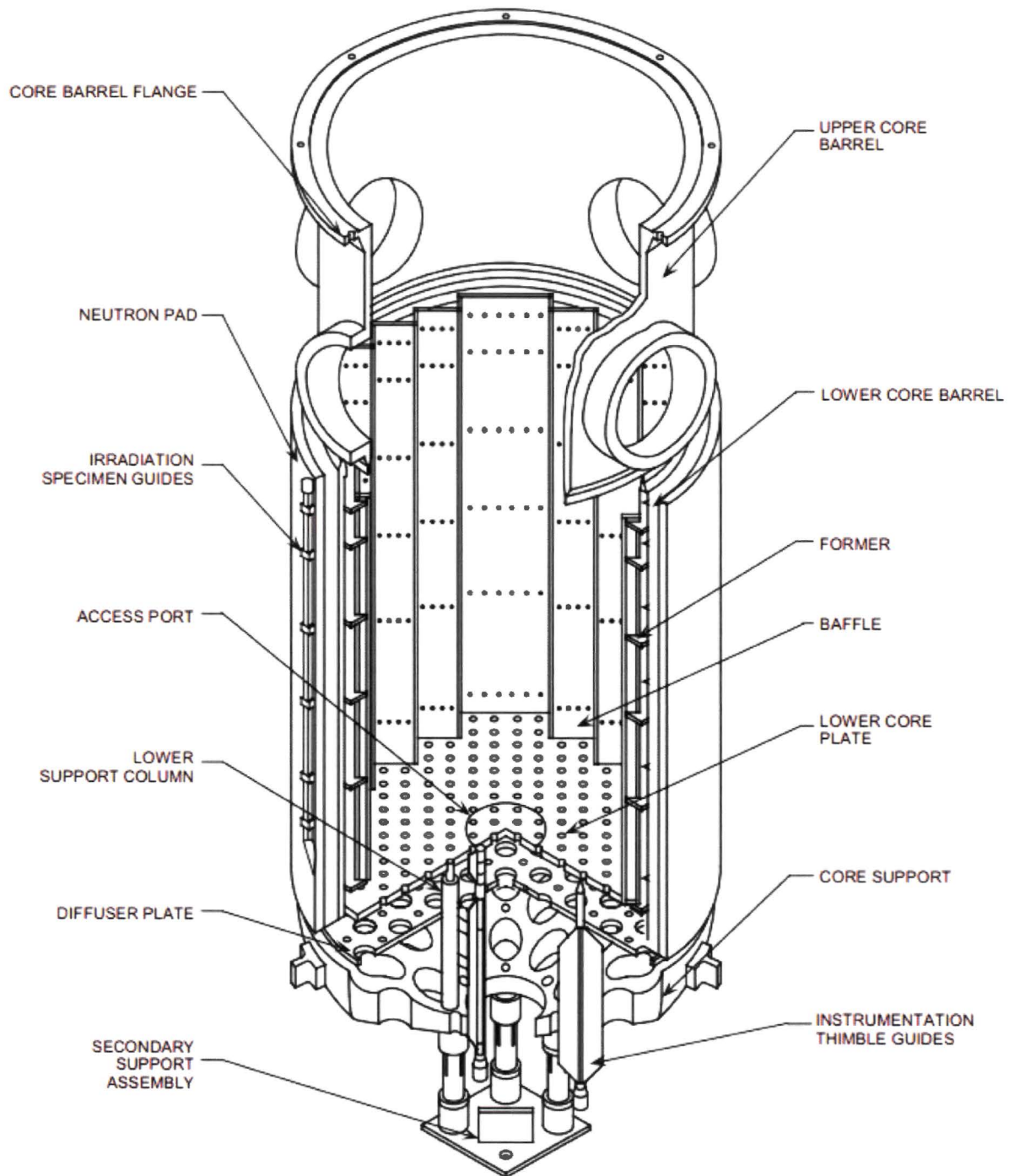


**Figure 3-2 Typical Core Barrel Hardware**



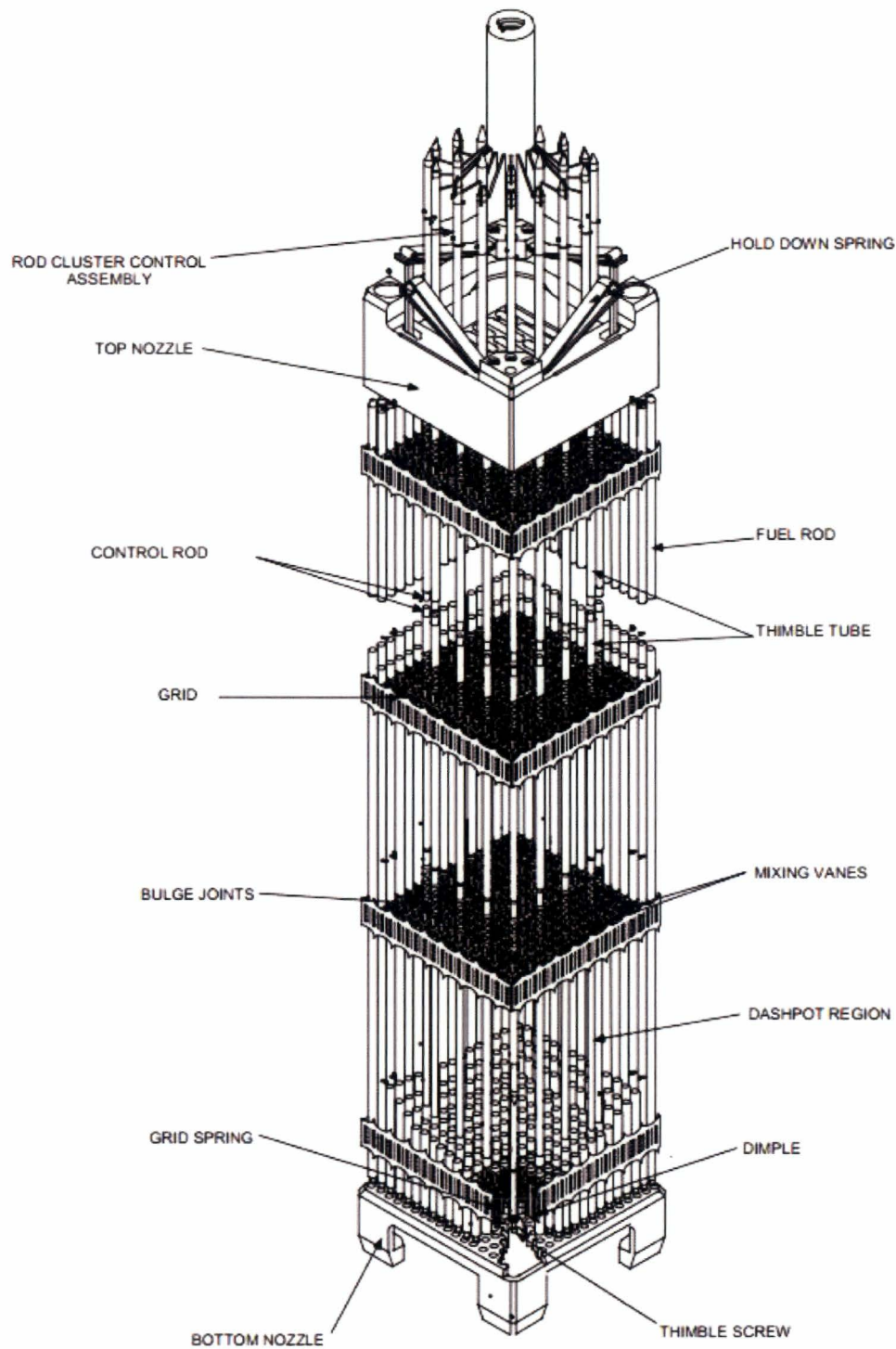


**Figure 3-3 Typical Fuel Assembly Components**

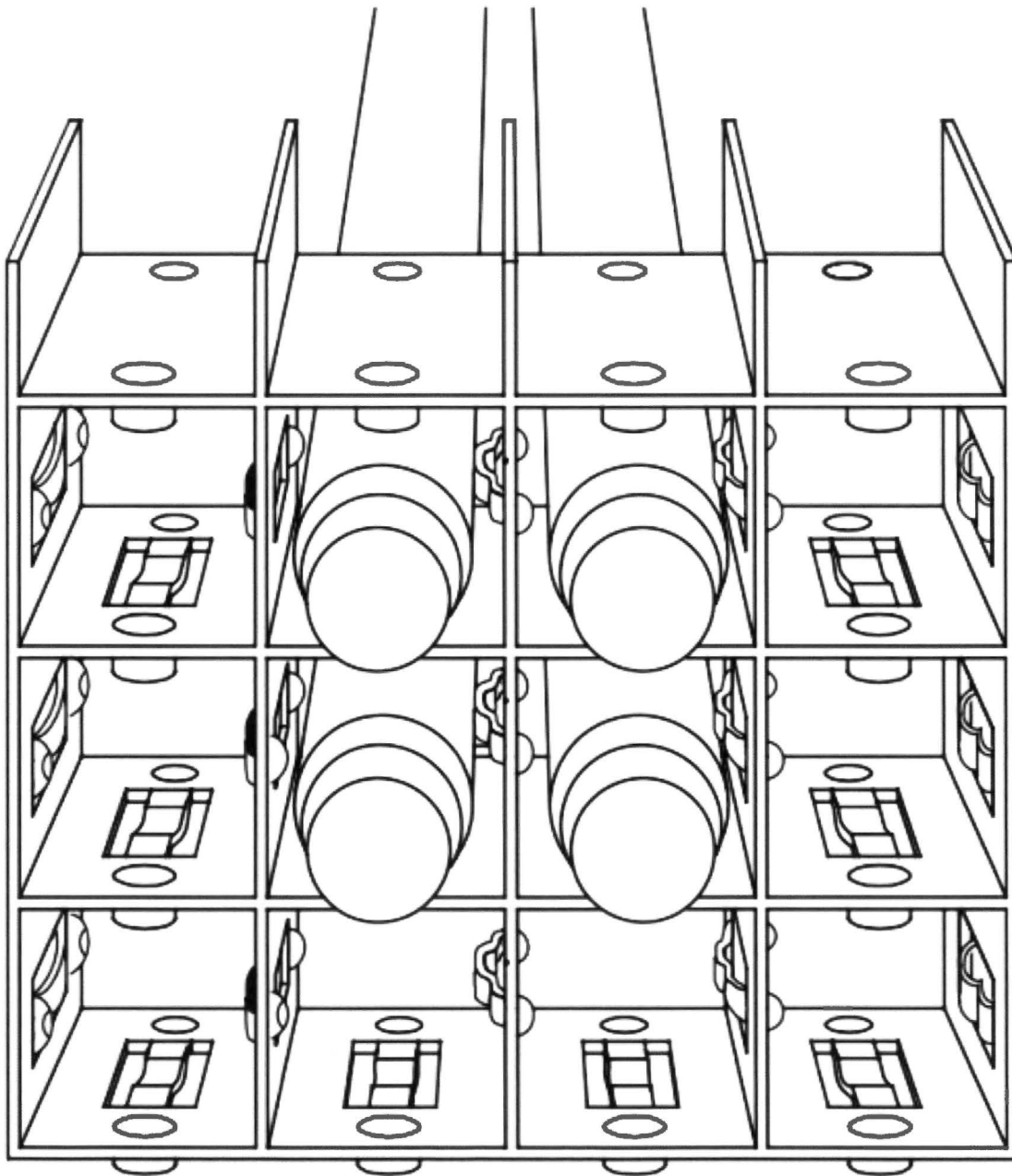


**Figure 3-4 Typical Fuel Rod and Spacer Grid Orientation**



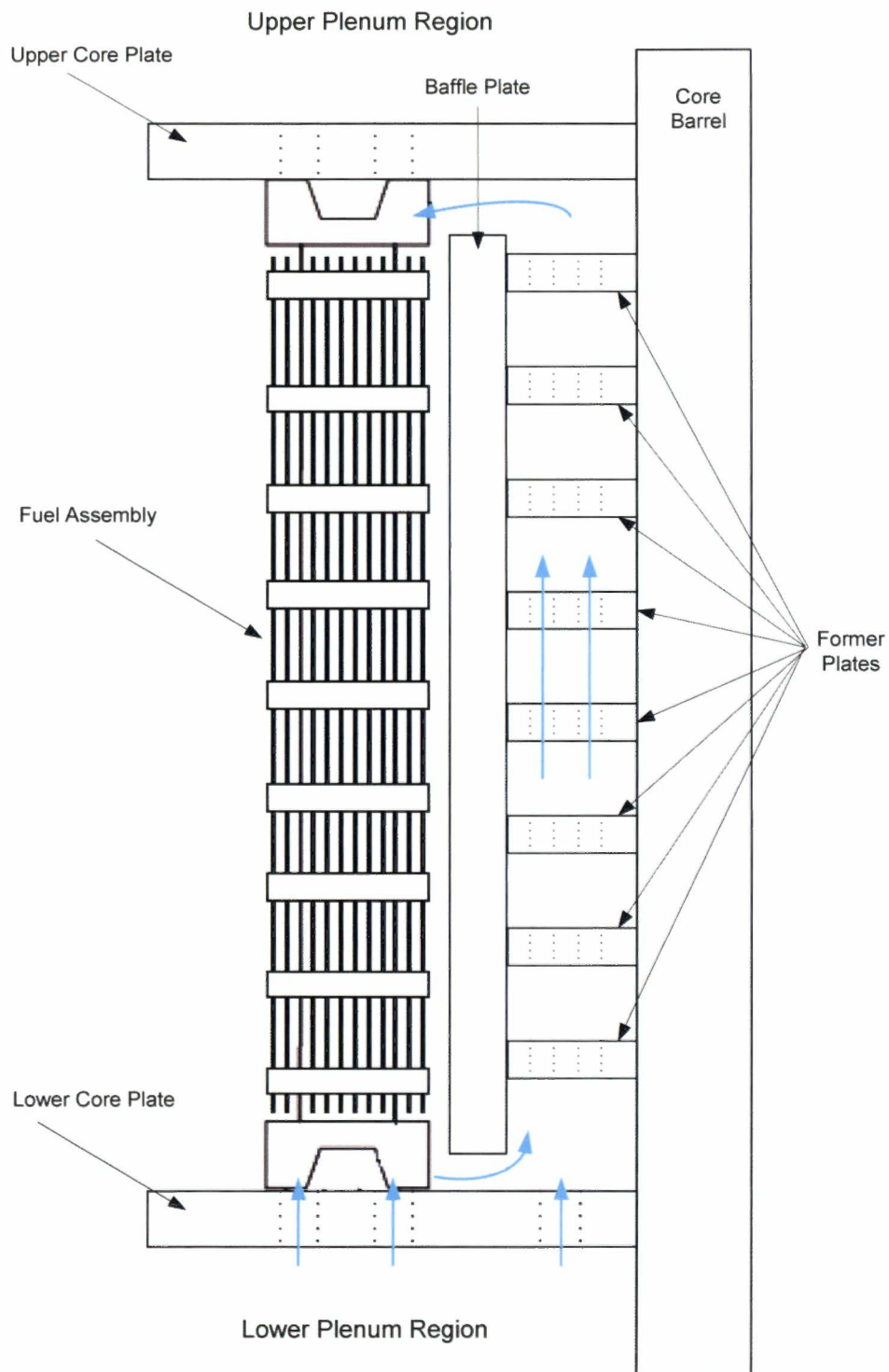


**Figure 3-5 Westinghouse Upflow Barrel/Baffle Design (No Pressure Relief Holes)**

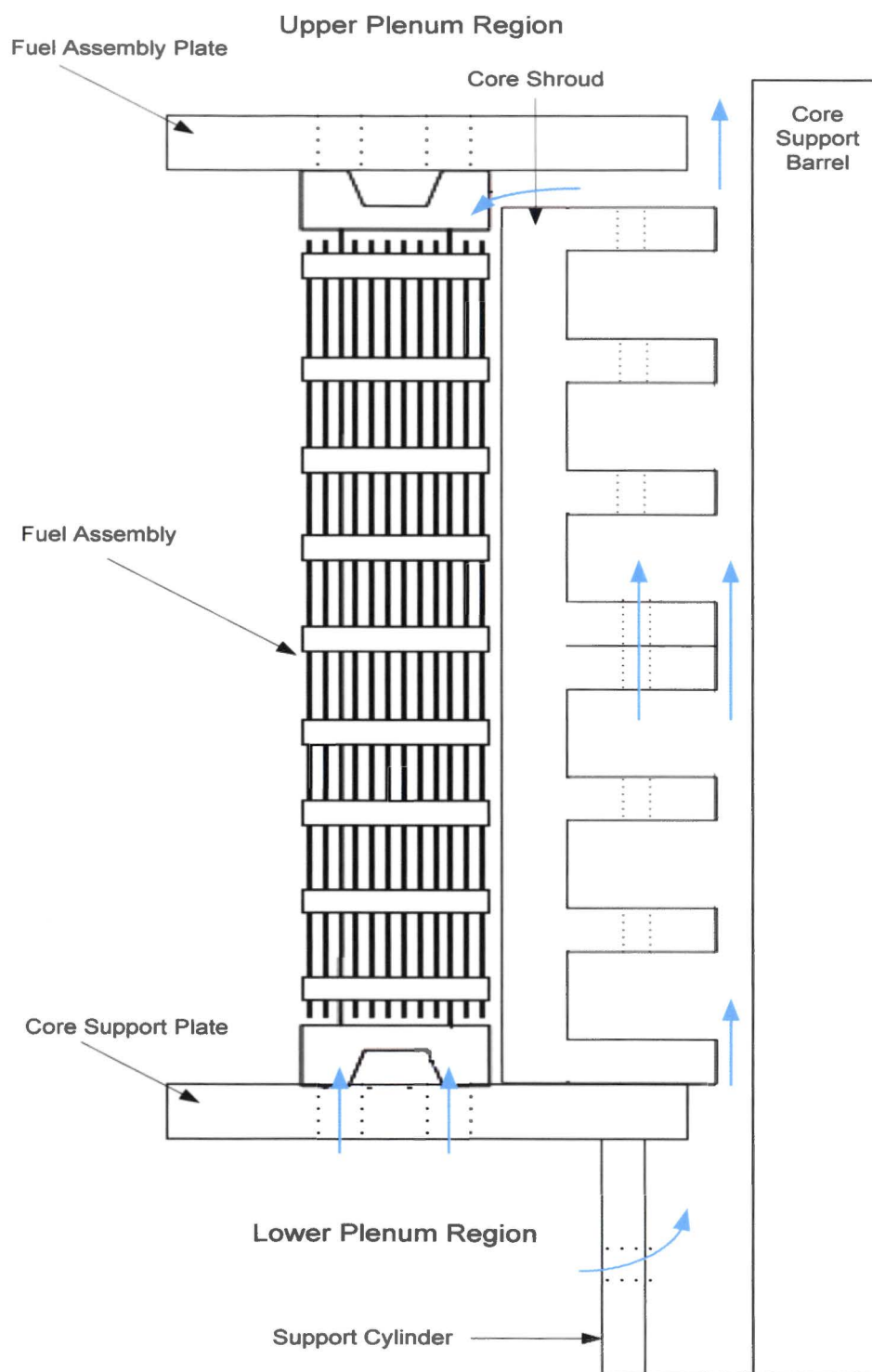


**Figure 3-6 CE Barrel/Baffle Design**

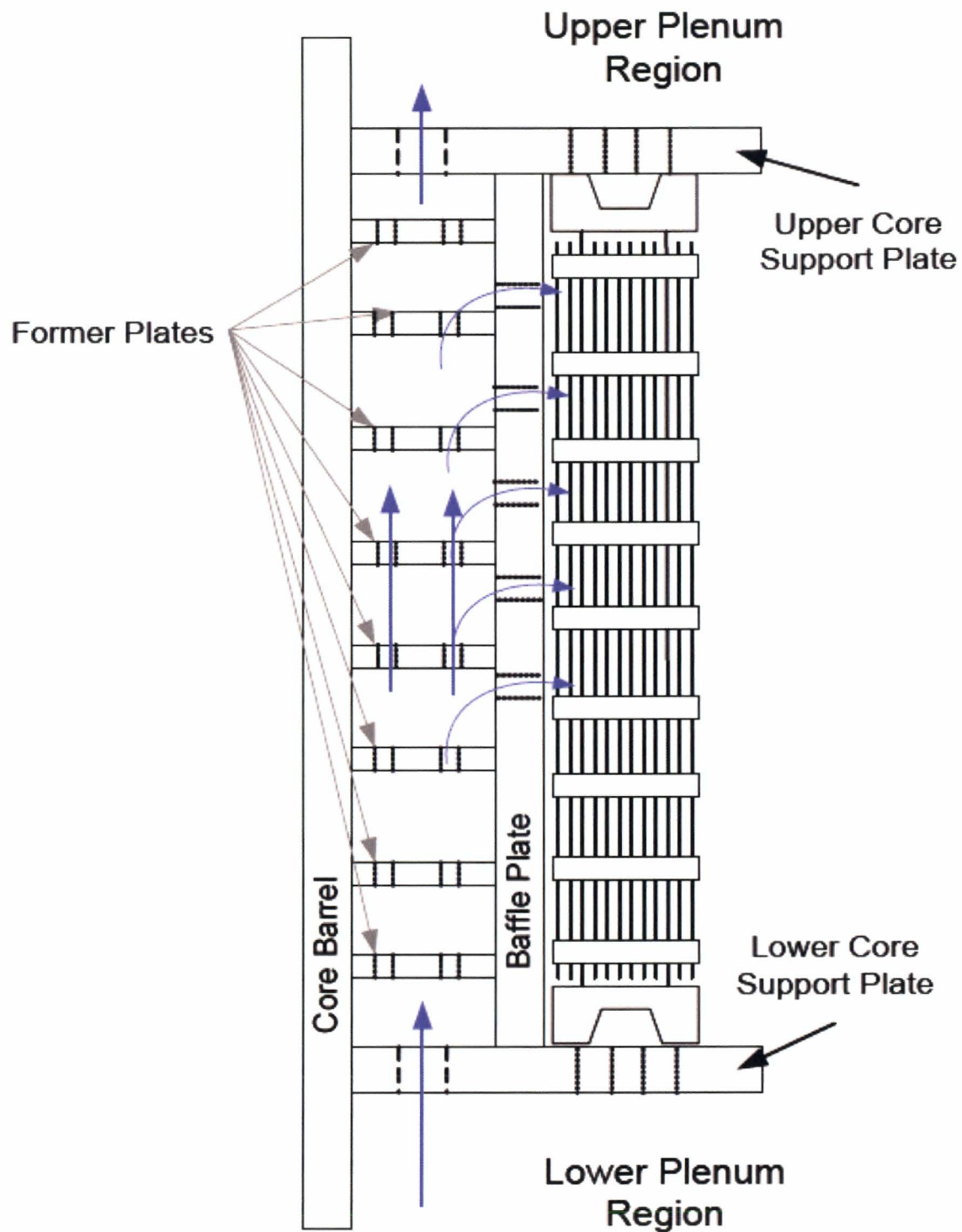
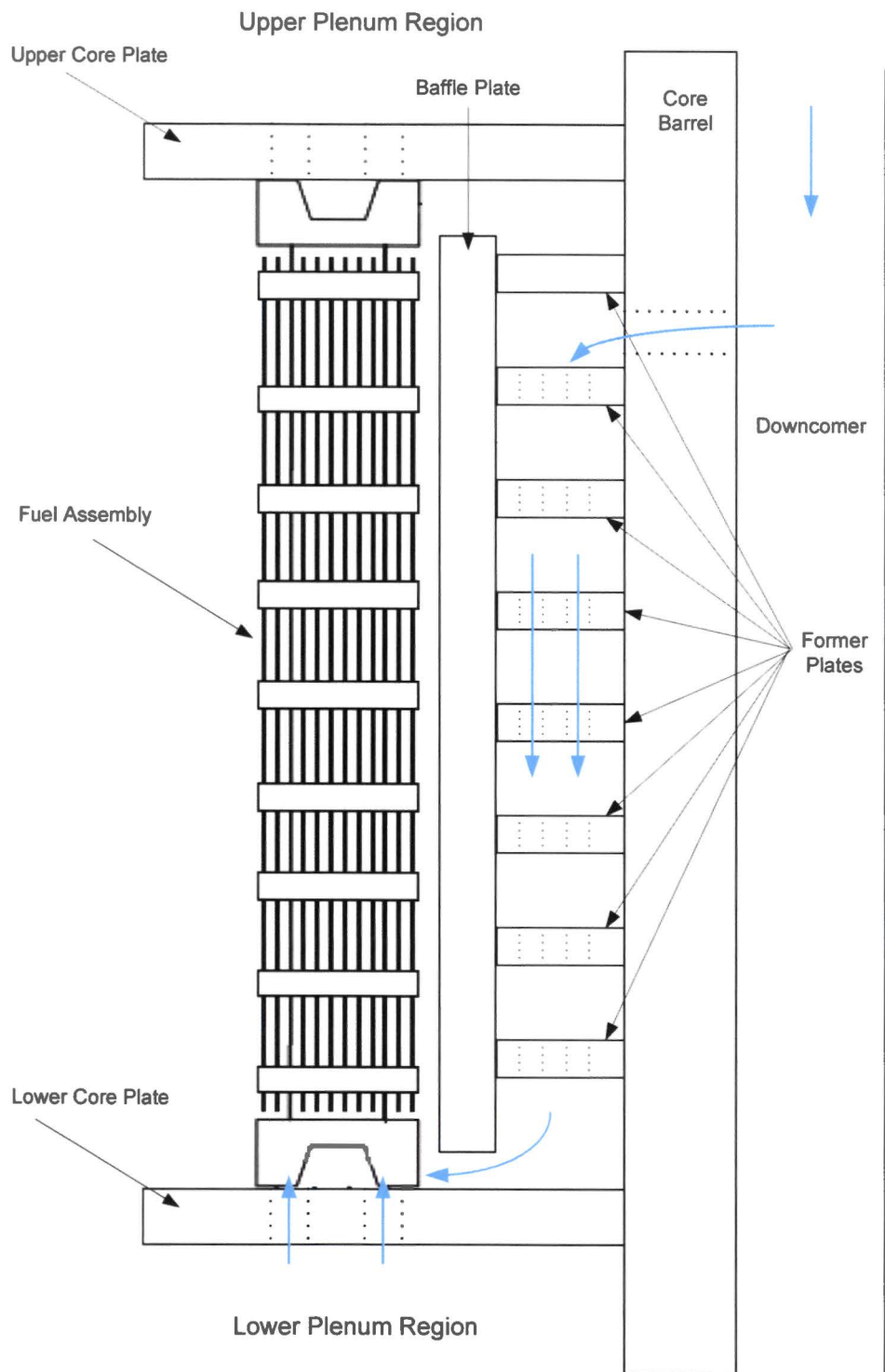
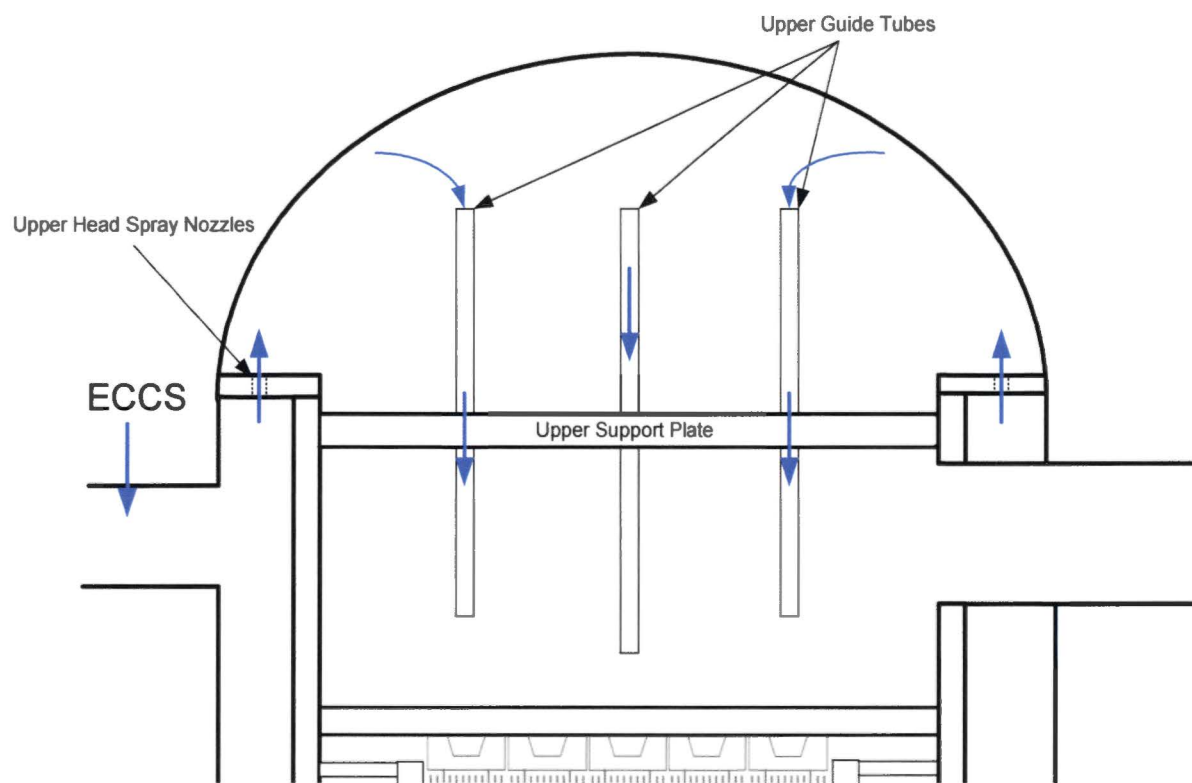


Figure 3-7 B&W Barrel/Baffle Design



**Figure 3-8 Westinghouse Downflow Barrel/Baffle Design**



**Figure 3-9 Westinghouse Upper Head Spray Nozzle Design**

### 3.3 DESCRIPTION OF PWR LOCA AND SAFEGUARDS OPERATIONS

The material in this section is general in nature and is presented for background purposes only. The system descriptions are intended to provide useful information about plant design and configuration but should not be used as input to licensing basis analyses.

Shortly after a LOCA, a number of safety systems automatically actuate to mitigate the event. In the longer term, operators take action to continue the mitigation and to ensure that the core remains cool. The specific systems that actuate are dependent on the plant design and the plant operating procedures. However, there are general similarities among the U.S. PWR fleet. This section provides an overview of the event in that context.

Note that the descriptions in the following sections relate to plants with cold side ECCS (i.e., plants that initially inject into the cold legs immediately following the LOCA) and are relevant to most of the operating PWR fleet in the U.S. However, there are a small number of plants that initially inject into both the RV UP and into the cold legs. These plants are referred to as upper plenum injection (UPI) plants and are Westinghouse 2-loop designs. While the sequence of events is similar, the flow path to the break during sump recirculation is typically opposite that of the cold leg recirculation plants. Additional discussion of the UPI plant is provided in Section 8.

#### 3.3.1 General Sequence of Events Following a Large Break LOCA

The following is a generic description of a large break LOCA progression in a PWR. Plant-specific designs and operations may result in plant-specific variations from the progression described below.

The large break LOCA (LBLOCA) is characterized by rapid depressurization of the RCS to a pressure in near equilibrium with the containment pressure and low enough to allow the operation of the low head safety injection (LHSI) pumps. Containment is isolated due to high containment pressure. In the short-term, all available ECCS inventory, including the accumulators, is necessary to refill the vessel and recover the core with allowance for a single active failure. The CSS could also be actuated. Supply for both the ECCS and CSS are initially drawn from the refueling water storage tank (RWST). The boric water from this tank helps to reflood the core with fluid containing an effective neutron absorber. Due to RWST injection, the core can be expected to be reflooded and quenched within a few minutes. Fuel cladding temperatures after reflood have decreased to within a few degrees of the liquid saturation temperature.

The RWST contains enough coolant for injection to last approximately 20 minutes at maximum ECCS and CSS flow (i.e., no single failures). Initial safety injection flow is into the cold legs (with the exception of UPI plants, where flow is injected into both the RV UP and cold legs). After the RWST has drained, an alternate source of coolant is required. At this point, the supply water source to the ECCS and CSS is switched from the RWST to the containment sump. Continued availability of this coolant assures LTCC.

At some point after sump switchover (SSO), the Emergency Operating Procedures (EOPs) require that the operators take some action to mitigate potential boric acid buildup in the core. This is primarily a consideration following a CLB where there is limited liquid throughput in the core; as the core continues to boil, boric acid may concentrate. For HLBs, this is generally not a concern, because there is

continuous liquid flow through the core to the break, which continually dilutes the boric acid. However, since the operators do not diagnose the break location, this action may be taken for all LOCAs. Westinghouse and CE designed PWRs require switching some or all safety injection to either hot leg recirculation (Westinghouse 3- & 4-loop and CE plants) or simultaneous hot and cold leg recirculation (Westinghouse 2-, 3-, 4-loop and CE plants). Some plants that do not maintain cold leg recirculation after the switch to hot leg recirculation require switching back and forth between hot leg and cold leg recirculation. B&W plants will only take action if core exit subcooling has not been reestablished. If an action is required, some B&W plants may open the decay heat drop line to address boron precipitation while others may actuate the pressurizer spray as a hot leg injection method. The timeline for operator action is plant-specific, but will generally occur between 2 and 12 hours following the LOCA.

### **3.3.2 ECCS Configuration and Performance during Sump Recirculation**

#### **3.3.2.1 Westinghouse Plants**

For the Westinghouse design, the ECCS components used during recirculation include the low head safety injection (LHSI) (also known as residual heat removal (RHR)) pumps and high head safety injection (HHSI) pumps, and various motor operated valves (MOVs), throttle valves, and check valves in the flow paths from the sump and the flow paths to the cold legs and to the hot legs.

To meet the single failure criteria, it is necessary that each active component be duplicated. All valves that need to be opened for proper safety injection system (SIS) function are duplicated in parallel; all valves that must be closed are duplicated in series. All pumps are duplicated in parallel and are designed so that only one pump in each group needs to operate to provide sufficient volume of water to cool the core or the containment atmosphere, as the case may be.

The recirculation phase following an accident is automatically or manually initiated either when the RWST low level alarm is actuated or when the operator is prepared to take positive action for a specific accident. Long-term recirculation will be required for any LOCA.

For large breaks, the RCS will be depressurized by the initial blowdown. The RHR pumps are aligned to inject directly to the RCS while also providing the suction source to the HHSI pumps. Component cooling water is supplied to the RHR heat exchangers for cooling the sump water. The recirculation phase can continue with one RHR pump operating for a considerable period of time. If one RHR pump should stop functioning or require maintenance, the second RHR pump can be brought into service.

The spray pump(s) will continue to inject RWST water into the containment through the spray headers until the RWST reaches a low-low level setpoint. In this case, it may be necessary to continue the spray to the containment using recirculation water. This duty can be performed by both the RHR pumps and the containment spray pumps.

The CSS functions to reduce the reactor containment building pressure and quantity of fission products in the containment atmosphere subsequent to a LOCA. Pressure reduction is accomplished by spraying water into the containment atmosphere. The system consists of two independent and identical subsystems. During recirculation, the failure of a single active or single passive component will not prevent the system from performing its safeguard function.



The CSS consists of two pumps, spray ring headers, a number of MOVs, and all necessary piping, instruments, and accessories to make the system operable. For the recirculation mode, manual operation of the system is performed remotely from the control room. When the RWST reaches the low-low level, spray pump suction is switched from the RWST to the containment sump. A separate containment sump suction line is provided to each spray pump. These lines each contain two MOVs in series, in order to provide containment isolation. Two identical spray pumps are installed in the system. Either pump provides sufficient capacity to perform the necessary containment spray function. Spray flow is delivered from the containment sump to the spray headers.

### **3.3.2.2 Combustion Engineering Plants**

For CE design plants, borated water for high pressure and low pressure core injection and containment spray is provided by the Refueling Water Tank (RWT). Upon depletion of the RWT volume, a Recirculation Actuation Signal (RAS) realigns the ECCS and CSS suction to the containment sump. The RAS opens the containment sump recirculation line isolation valves and operators close the RWT discharge isolation valves. Transfer to the recirculation mode can also be established manually.

In the recirculation mode, low pressure safety injection (LPSI) pumps are automatically secured and core flow is provided only by the high pressure safety injection (HPSI) pumps. However, operators may elect to restart LPSI flow during recirculation to provide additional core flow. Only one HPSI pump is required following recirculation since each train of HPSI is designed to provide sufficient flow to make up that inventory lost to boil off at the time of RAS.

Recirculation is required only for a LOCA; no other design bases accidents result in depletion of the RWT volume.

The decay heat and the latent system heat are removed post-accident to the ultimate heat sink by the shutdown cooling system heat exchangers (SCHXs) (through the CSS). In instances where there is sufficient net positive suction head (NPSH), the shutdown cooling system (SCS) can be aligned for LTCC.

### **3.3.2.3 Babcock and Wilcox Plants**

For B&W design plants, post-accident recirculation flow is provided by the low pressure injection (LPI) pumps. The recirculation alignment occurs when the borated water storage tank (BWST) has been drained and SIS inventory for recirculation comes from the containment sump, where the RCS discharged liquid and spilled ECCS inventory collects. Recirculation will be required only for a LOCA.

Only the LPI and RBS pumps are aligned to take suction from the sump during the recirculation mode. There are two separate pipes from the sump to the suction side of the LPI pumps and there is an MOV in each line. Depending on the plant, there are either two or three LPI pumps available. On the discharge side of the LPI pumps, there are check valves, MOVs, and the decay heat coolers.

There are two separate injection paths which inject only to the reactor vessel core flood tank nozzles. Each low pressure pump is aligned to one nozzle or two, depending on the plant design. The containment sump has two separate discharge lines. Opening MOVs in one line allows suction to one LPI or RBS.



The other line and separate MOVs align to the other set of redundant LPI or RBS pumps. One pump of each type is sufficient to provide LTCC, but both trains will be used if they are available and there is not adequate subcooling at the core exit.

The following component list is provided as a generic guideline for the type of equipment used for post-accident recirculation:

- Pumps: LPI, CS
- Heat exchangers: Decay heat coolers (DHR system)
- Valves: MOVs, checks, throttle
- Other: CS nozzles

B&W units have similar systems and capabilities that are described in more detail for the CE and Westinghouse plants. These systems include those for containment spray, containment atmosphere control and containment isolation. These systems are not described here as they are similar to and function in a like manner as those systems described for the CE and Westinghouse plants.

LTCC after a LBLOCA is well within the capability of a single decay heat removal pump operating at a containment pressure near atmospheric. Heat removal from the containment via containment spray and/or fan coolers will ensure that the containment pressure is near atmospheric pressure in the long-term post-LOCA environment. Therefore, indefinite operation of the high pressure injection (HPI) pumps is not required except under certain single failures for some plants during LTCC after a large break LOCA.

### 3.3.3 Boric Acid Precipitation Control

All three U.S. PWR designs (Westinghouse, CE, and B&W) use boron as a core reactivity control method and are subject to potential BAP in the core for scenarios that preclude ECCS flow through the core for extended periods following a LOCA. All three plant designs have ECCS features that include an active core dilution mechanism to prevent the core region boric acid concentration from reaching the precipitation point. These dilution mechanisms may or may not require operator action.

The common approach for demonstrating adequate boric acid dilution in a post-LOCA scenario includes the use of simplified methods with conservative boundary conditions and assumptions. These simplified methods are used with limiting scenarios in calculations that determine the time at which appropriate operator action must be taken to initiate an active boric acid dilution flow path or alternately, to show that BAP will not occur. The three U.S. PWR designs have different ECCS configurations, different methodologies, and procedures for BAPC. Nevertheless, there are common approaches, assumptions and simplifications that have been used in virtually all PWR calculations that address the potential for BAP.

For typical plant designs (Westinghouse 2-loop UPI plants excluded), the limiting scenario for BAP is a large cold leg (pump discharge) break where the downcomer is eventually filled, and the excess ECCS flow exits out of the break. The ECCS flow into the core region is largely limited to that quantity boiled-off in the core to remove the decay heat. The steam generated in the core travels around the intact hot

leg(s) (or through the internals reactor vessel vent valves (RVVVs) in the B&W designed plants) to exit the break. Boric acid left behind accumulates in the core region and the boric acid concentration in the core region increases.

The calculated rate of increase in boric acid concentration in the core region after a LOCA is directly affected by the calculated liquid volume. During this time, the core and UP are filled with a two-phase mixture for which the liquid content is dependent on the degree of voiding in the core and UP region. The degree of voiding is a function of the core decay heat and RCS pressure, and the pressure drop around the loop (or through the RVVVs) as it affects the hydrostatic balance between the downcomer head and the collapsed liquid level in the core. At low RCS pressures and high decay heat levels, the boiling in the core is vigorous, and the volume of liquid in the core region is smaller. As the decay heat drops off, the boiling becomes less vigorous and more liquid is retained in the core region.

Westinghouse 2-loop UPI plants differ from typical PWR designs in that they utilize low pressure UPI. For these plants, the limiting large break LOCA BAP scenario is a HLB where the cold leg high pressure safety injection may be terminated at or prior to sump recirculation. This scenario is relevant only with the very conservative assumption that all UPI flow in excess of core boil-off bypasses the core region and flows directly out the break (i.e., no mixing in the core and UP).

For Westinghouse design and CE design plants, BAP calculations are used to determine the appropriate time to switch some or all the ECCS sump recirculation flow to the hot leg or to otherwise show that BAP will not occur. For B&W-designed plants, BAP calculations are used to justify plant-specific active boric acid dilution methods or limitations on the dilution methods (e.g., plant-specific auxiliary pressurizer spray flows, protection of the sump strainer(s), prevention of potential water-hammer scenarios in the decay heat piping, challenges to NPSH limits for LPI pumps, hot and cold fluid mixing limits, prevention of BAP inside the decay heat cooler, etc.).

The influence of debris on BAPC and the evaluation completed by this program is discussed in Section 9.1.2 and Section 9.2.2 for the HLB and CLB scenarios, respectively.

### **3.4 DESCRIPTION OF IN-VESSEL DEBRIS CONCERNS**

Once the RWST has drained and the operators switch the ECCS suction source to the containment sump, debris laden coolant may begin to enter the RCS via the ECCS. The concentration of debris entering the RCS is a function of time and is dependent upon the sump condition, strainer filtering efficiency, and the ECCS configuration. For any break location, some portion of debris penetrating the sump strainer, traversing the ECCS, and reaching the RCS will enter the RV and some portion will go elsewhere.

For the fraction of debris that enters the RV, the path it takes is dependent upon the debris properties, specific vessel geometry, flow condition, break location, etc. During cold leg recirculation, flow transports debris through the downcomer, into the lower head where it encounters some form of lower internal configuration consisting of various plates and vertical columns. Some fraction of debris may collect or settle on these components, or it may remain suspended in the flow. Debris that continues with the flow, travels through the core support region and enters the core where it could accumulate, remain suspended in the flow, or exit the RCS through the break. Most likely, in-vessel debris transport results from some combination of the above and is distributed throughout the RV. For hot leg breaks, some

fraction of debris may flow out of the break since it is at the RV exit. For cold leg breaks, some of the debris will spill out of the break with the excess ECCS not needed to replace core boil-off. The remaining debris, which is a significantly smaller portion of the debris, enters the RV and can make it to the core due to the break location and the circulation patterns that are developed.

For ECCS recirculation to the hot legs or upper head, flow transports debris into the RV UP where it encounters some form of upper internal configuration consisting of various plates and vertical columns (e.g., control rod guide tube housings, instrument tube housings). Some fraction of debris may collect on these structures, or it may remain suspended in the flow. Debris that continues with the flow, travels through the upper core plate and enters the core where it could accumulate, remain suspended in the flow, or exit the RCS through the break. Most likely, the debris does some combination of the above and is distributed throughout the RV. For hot leg breaks, some fraction of debris may flow out of the break before it reaches the core since it is at the RV exit. For cold leg breaks, debris that is not captured in the core may settle in the RV LP or flow up the downcomer and out of the break.

Concerns have been raised about the potential for debris ingested into the ECCS to affect LTCC when recirculating coolant from the containment sump. The FA bottom nozzles are designed with flow passages that provide coolant flow from the RV LP into the region of the fuel rods. During operation of the ECCS to recirculate coolant from the containment sump, debris in the recirculating fluid that passes through the sump strainer(s) may collect on the bottom surface of the FA bottom nozzle, causing resistance to flow through this path. The collection of sufficient debris on the FA bottom nozzle is postulated to impede flow into the FA and core. Other concerns have been raised with respect to the collection of debris and post-accident chemical products within the core itself. Specifically, the debris has been postulated to either form blockages or adhere to the cladding, thereby reducing the ability of the coolant to remove decay heat from the core. Similarly, chemical precipitates have been postulated to plate out on fuel cladding, again resulting in a reduction of the ability of the coolant to remove decay heat from the core. Finally, debris may concentrate within the heated core region such that the fluid properties in the core change, and subsequently, the heat removal ability of the water/debris mixture is affected.

The potential for localized blockages within the core region, adherence of debris to the heated fuel rods, and plate-out of debris and chemical precipitates are evaluated in WCAP-16793-NP-A, Rev. 2 (Reference 3-1). These evaluations have been found acceptable to the NRC via the SE on Reference 3-1; therefore, no further work on these topics is presented in this report. This report instead focuses on the effects of the following concerns: (1) the effect of blockage by debris at the core inlet and (2) the accumulation and concentration of debris in the core region.

### 3.5 DEBRIS CONSTITUENTS

The Nuclear Energy Institute (NEI) Guidance Report (GR), NEI 04-07 (Reference 3-2), provides the guidelines for determining the type, size, and quantity of debris that is generated following a LOCA. The GR (Reference 3-2) adopts a two-size distribution for material inside the ZOI of a postulated break: small fines and large pieces. Small fines are defined as any material that could transport through gratings, trash racks, or radiological protection fences by blowdown, containment sprays, or post-accident pool flows. Furthermore, the small fines are assumed to be the basic constituent of the material for fibrous blankets (i.e., individual fibers) and pigments for coatings. The GR (Reference 3-2) assumes the largest openings of the gratings, trash racks, or radiological protection fences to be less than a nominal 4 inches by 4

inches (less than 20 square inches total open area). The remaining material that cannot pass through gratings, trash racks, and radiological protection fences is classified as large pieces.

For in-vessel effects, the debris of interest is small fines, which can be further characterized as either particulates or fibers. The debris characteristics for small fines are described in Section 3.4.3.6, Reference 3-2. The characteristic sizes listed are the most conservative values that can be associated with debris transport and head loss since they are the size that will have the highest transport factor and causes the highest head loss in a debris bed.

In addition to particulate and fibrous material, corrosion products may form due to chemical interactions among the material in containment and the sump fluid, which contains buffering agents and boric acid. Among the materials that are found inside containment and are susceptible to chemical reactions with the post-LOCA solution are aluminum, zinc, and non-metallic materials such as some coatings, thermal insulation (e.g., Cal-Sil, fiberglass), and concrete. The resulting chemical precipitates may include aluminum oxyhydroxide, sodium aluminum silicate, and calcium phosphate. These materials can combine with a debris bed resulting in an increased head loss across the bed. For in-vessel considerations, this can result in a reduced capability to maintain the necessary cooling flow through the core.

### 3.6 LIMITING SCENARIO

10 CFR 50.46 (Reference 3-3) requires that LTCC be demonstrated for all break sizes and locations in the RCS. To date, evaluations of in-vessel effects for GSI-191 have assumed that the double ended guillotine (DEG) break is limiting with respect to establishing debris. This assumption is based in part on the following points: (1) the largest break generates the largest amount of debris and will therefore deliver the most debris to the RCS; and (2) the largest break has the highest ECCS flow rates, which will minimize the potential for settling of particulate and fibrous debris in the containment and therefore maximize the transport of these types of debris to the RCS and deliver the debris to the RCS sooner than lower flow rates, which challenges core DHR since decay heat decreases with time.

This section outlines the basis for why a DEG break is limiting and can be considered as the only break for setting in-vessel debris limits. Assuming that the largest breaks will produce a limiting amount of debris, it is proposed that this condition will deliver the most debris to the RCS at the earliest time. Support for this conclusion is developed in the following steps:

1. Debris generation – A description and partial quantification of the debris in containment will be developed based on break size. It will be shown that larger breaks have the potential to generate more debris.
2. Timing of debris arrival to RCS – The effect of debris arrival time as it relates to the core debris limit will be discussed. It will be shown that for breaks that generate sufficient debris, the ECCS flow rates and timing of SSO are similar.
3. Debris delivered to RCS – An evaluation of the debris that can reach the RCS will be developed based on sump strainer coverage and filtration efficiency. It will be shown that the debris delivered to the RCS is proportional to the amount of debris that reaches the sump strainer.

### 3.6.1 Debris Generation

Debris in containment is either latent (i.e., dirt and dust that already exists in containment regardless of break size or location) or is generated by the effects of the break. All plants have latent debris that is independent of break size. Debris generated by the effects of the break fall into two categories: (1) insulation materials and qualified coatings within the ZOI of the break that fail due to jet impingement and (2) unqualified coatings that are assumed to fail as a result of the post-LOCA environment. All unqualified coatings are assumed to fail regardless of break size and ZOI and are further assumed to fail as particulates independent of break size (unless specific testing shows otherwise) and require no further discussion. Debris generated within the ZOI, however, is a function of break size and will vary accordingly.

The ZOI is defined as the volume about the break in which the fluid escaping from the break has sufficient energy to dislodge insulation, coatings, and other materials within the zone. For a DEG break, the boundary of the ZOI is assumed to be spherical, with the center of the sphere located at the break site. The use of a spherical ZOI is intended to encompass the effects of jet expansion resulting from impingement on and reflection from structures and components.

For single-sided breaks, cracks, or split/slot breaks, the ZOI is represented as a hemisphere. Since the radius of a ZOI for a DEG break is expressed as the ratio of distance from the break to the target ( $L$ ) to the break diameter ( $D_{\text{break}}$ ), or  $L/D_{\text{break}}$ , the radius of hemispherical ZOI for a break having an equivalent diameter as a DEG break is the same as the radius of the sphere for a DEG break. The volume of the ZOI for a single sided, split / fish-mouth break, however, is one-half ( $1/2$ ) that for the DEG break.

To determine the limiting amount of debris generated in containment, a survey of the RCS and attached piping is performed and the ZOI is moved along the pipe as appropriate. The amount of debris generated for a given ZOI in a given location is compared against all other ZOIs in all other locations. Typically, the maximum debris generation is for a DEG break in one of the large RCS pipe runs. Smaller breaks and single-sided breaks will not generate as much debris.

A volume ratio approach may be used to scale the amount of debris generated by full-area DEG break to a smaller break. This approach assumes that possible debris sources are uniformly distributed within the ZOI volume and that reducing the ZOI will not move the debris source outside of the ZOI. The break is evaluated based on the reduction in volume of the spherical ZOI. Since the volume,  $V$ , of a sphere is proportional to the radius to the third power, as the break becomes smaller, the volume of the ZOI decreases quickly. It should also be noted that for breaks on smaller pipes, the quantity of debris generated may be slightly larger than that assumed using the volume ratio approach due to the proximity of other insulated piping. This difference is negligible when comparing the quantity of debris generated for a large DEG to that of a small DEG or partial pipe break.

Table 3-2 shows an approximate reduction in debris with break size using this approach relative to a 36" DEG break for both the DEG break and single-sided breaks. It is clear that the amount of debris generated decreases quickly with a reduction in break size. Even for DEG breaks in attached piping (typically starting around  $0.5 \text{ ft}^2$ , or 4.8 inches in diameter for a DEG break), the amount of debris generated relative to a DEG break on the primary RCS piping will be small. As break size decreases, the amount of fiber approaching the sump strainer quickly approaches the latent fiber load only.

<b>Table 3-2 Example Debris Ratio Calculations</b>			
<b>Break Diameter</b>		<b>Debris Ratio</b>	
(in)	(ft)	DEG Break to 36 inch DEG Break	Single-Sided Break to 36 inch DEG Break
36	3	1	0.5
33	2.75	0.77	0.39
30	2.5	0.58	0.29
27	2.25	0.42	0.21
24	2	0.30	0.15
21	1.75	0.20	0.10
18	1.5	0.13	0.06
15	1.25	0.07	0.04
12	1	0.04	0.02
6	0.5	0.005	0.002

### 3.6.2 Timing of Debris Arrival and ECCS Flow Rate

Larger break sizes depressurize the RCS more quickly than smaller breaks. Since ECCS flow rate is a function of RCS pressure, two possible effects occur as a result: (1) smaller breaks may draw down the RWST slower and delay the time of SSO, which may affect the amount of debris that can be tolerated in the RCS; or (2) smaller breaks may result in lower ECCS flow rates that can affect the approach velocity to and capture efficiency of sump strainer(s) and the delivery rate of debris to the RCS.

LOCA analyses have shown that a 0.5-ft<sup>2</sup> break will depressurize the RCS in much the same fashion as a full-area DEG break. The depressurization rate is slightly slower, but the minimum pressure reached is well below the point at which the ECCS injection flow rate becomes constant (low head safety injection pumps have constant flow rates below approximately 50-80 psid). The difference in timing of reaching the low head injection set point will be delayed by a few minutes at most. Consequently, the variation in time of SSO will not be significantly different among break sizes between approximately 0.5 ft<sup>2</sup> and a DEG break of the RCS piping. Further, the minimum RCS pressure will be similar between the two break sizes such that the total low head ECCS flow rate will be the same. However, the debris generated by the 0.5 ft<sup>2</sup> break (break diameter of 9.6 inches for a single sided break or 4.8 inches for a DEG break) will be less than two percent of that generated for the full area DEG break (Table 3-2), a value far less than necessary to meet or exceed the in-core fiber limit.

### 3.6.3 Debris Delivered to Reactor Coolant System

The debris that is generated within the ZOI, along with any latent debris and unqualified coatings, is transported to the containment sump. While the ECCS and CSS are drawing from the clean RWST, the break effluent is accumulating in the sump where the velocities in the sump are low and the debris is essentially suspended in the liquid. Once the transition of the ECCS and CSS pump suction from the RWST to the sump is complete, this debris will be drawn towards the sump strainers. As fiber arrives at the sump strainer, it will begin to collect in localized areas on the sump strainer. These areas will increase the local pressure drop such that flow and fiber will be diverted to adjacent locations. In this manner, the debris bed will spread across the sump strainer and develop a bed over the entire strainer surface as it spreads.

In their proposed GSI-191 Resolution Criteria for “Low Fiber” Plants<sup>1</sup> (Reference 3-4 and Reference 3-5), NEI suggested that a “Low/No Fiber plant” has a sump strainer capture efficiency of 55 percent (i.e., 45 percent of the debris passes through the strainer). A “Low/No Fiber plant” is defined as a plant with essentially only latent fiber (i.e., no fibrous insulation within a ZOI). Therefore, a capture efficiency of 55 percent or more can be assumed for latent fiber loads (i.e., fiber masses).

As additional fiber is considered in the system and continues to build, the capture efficiency of the sump strainer will increase up to the point that the sump strainer is completely covered. Once the entire strainer is covered, then the filtration efficiency will plateau at approximately 100 percent. This behavior was noted during testing performed for South Texas Project (STP) (Reference 3-7). The following is noted from Reference 3-7:

1. Under clean strainer conditions, the minimum observed capture efficiency was evaluated to be about 65 percent.
2. Over several tests, the filtration efficiency was observed to increase in an approximately linear manner from the clean strainer value to about 100 percent.
3. Once 100 percent filtration efficiency was observed, it remained constant.
4. Limited shedding of fibrous debris from the bed formed on the strainer was observed.

The filtration efficiency for the STP tests suggests that the sump strainer capture efficiency increases as the fiber load (i.e., fiber mass) on the strainer increases. After complete coverage, the shedding observed in the STP sump strainer tests demonstrates that a limited amount of fibrous debris will continue to penetrate the sump strainer.

---

<sup>1</sup> Reference 3-6 documents the NRC’s review of the criteria proposed by NEI. In their review of the proposed NEI GSI-191 Resolution Criteria, the NRC noted that the guidance was, “. . . high level guidance and there are a number of details that individual licensees will need to document to clearly establish the new licensing basis for their plant.” The enclosure to the NRC’s letter offered additional considerations for plants to use when developing the plant-specific licensing basis.

This result has also been demonstrated for other plant designs and is illustrated in Figure 3-10. While the fraction of fiber penetrating the sump strainer and reaching the RCS continually decreases as the fiber load on the strainer increases, the total amount of fiber passing through the strainer continues to increase with the fiber load reaching the sump strainer (as evidenced by the integral of the curve).

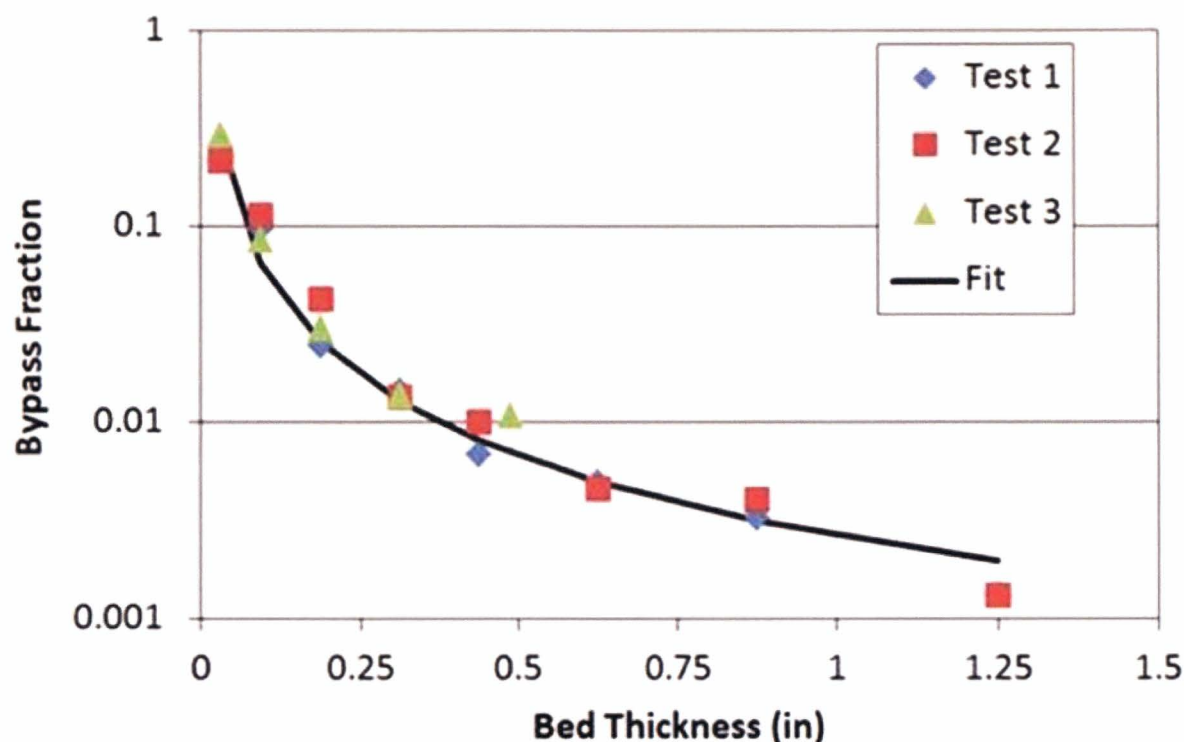


Figure 3-10 Strainer Bypass Fraction as a Function of Theoretical Debris Bed Thickness

### 3.6.4 Conclusions

As described above, a description and partial quantification of the debris in containment demonstrates that larger breaks generate significantly more debris than smaller breaks. In fact, debris generated within the ZOI quickly decreases with break size such that negligible debris relative to a DEG break in the RCS piping is noted for breaks below 0.5 ft<sup>2</sup>.

The effect of debris arrival time and ECCS flow rate as it relates to the core debris limit was also discussed. Breaks above approximately 0.5 ft<sup>2</sup> will not significantly change the time of SSO or the ECCS flow rate.

Finally, an evaluation of the debris that can reach the RCS was developed based on sump strainer coverage, which is related to the amount of debris that reaches the sump strainer. For the smallest amounts of fiber (i.e., latent fiber only), sump capture efficiency was shown to be approximately 55 to 65 percent. As fiber amounts increase, the strainer capture efficiency will increase as well until the strainer is completely covered, at which point the capture efficiency approaches a maximum. After the sump strainer is completely covered, some debris will continue to penetrate the sump strainer due to



shedding. Therefore, the amount of fiber penetrating the sump strainer and reaching the RCS is proportional to the amount of debris reaching the sump strainer. Since larger breaks will generate sufficient debris to completely cover the sump strainer, larger breaks will deliver more debris to the RCS.

It is concluded that the largest breaks will produce the largest amount of debris, which will deliver the most debris to the RCS at the earliest time. Therefore, DEG breaks are evaluated for establishing in-vessel debris limits.

### **3.7 LONG-TERM CORE COOLING REQUIREMENTS AND ACCEPTANCE CRITERIA**

The acceptance criteria are established to adequately maintain LTCC after a postulated LOCA event. The two aspects of LTCC that pertain to the 10 CFR 50.46 (Reference 3-3) are:

1. Decay Heat Removal - DHR requires that sufficient coolant be supplied to the core such that the core temperature is maintained at an acceptably low level.
2. Boric Acid Precipitation Control - BAPC requires that boron concentrations in the RV remain below the solubility limit.

For previous GSI-191 evaluations, DHR was assured if the maximum core PCT remains below 800°F (Reference 3-1). This conservative value is retained for this evaluation. Further, in the event that debris deposits on the fuel rods, the thickness of the buildup can be no more than 0.050 inch<sup>(2)</sup>.

For the DEG HLB scenario with core inlet blockage, BAPC requires demonstrating adequate break quality to flush boron from the RV and demonstrating adequate core mixing such that the entire core volume can be assumed to be a near homogeneous boron concentration.

For the DEG CLB scenario, BAPC requires demonstrating that the core inlet debris load does not create a uniform blockage such that communication between the core and LP remains and that BAPC measures remain effective at flushing boron from the RV.

### **3.8 CURRENT DEBRIS LIMITS**

The PWROG sponsored a previous program to provide analyses and information on the effects of debris and chemical products on core cooling for PWRs when the ECCS is realigned to circulate coolant from the containment sump. The intent was to demonstrate adequate heat removal capability for all plant scenarios. This program is documented in WCAP-16793-NP, Rev. 0.

After working through responses to NRC RAIs on the topical report (which included further testing to address NRC staff questions), WCAP-16793-NP-A, Rev. 2 (Reference 3-1) was submitted to the NRC for formal review. This report included the results of a significant experimental test program that

---

<sup>2</sup> Debris deposition on the fuel rods is addressed using the LOCADM methodology described and approved in WCAP-16793-NP-A, Rev. 2 (Reference 3-1). This process is still a part of the methodology to address the in-vessel effects of GSI-191. However, no changes to this methodology are presented herein and the use of the LOCADM as described in Reference 3-1 continues to be applicable.

investigated blockages formed on approximately one-third height test assemblies. The debris composition tested included particulate and fiber debris, as well as post-accident chemical products. The program was performed such that the results of this program apply to the fleet of PWRs, regardless of the design (Westinghouse, CE, or B&W).

The evaluation considered the design of the PWR, the design of the open-lattice fuel, the design and tested performance of replacement containment sump strainer(s), the tested performance of materials inside containment, and the tested performance of fuel assemblies in the presence of debris. Specific areas addressed in this evaluation included:

- Blockage at the Core Inlet
- Collection of Debris on Fuel Grids
- Collection of Fibrous Material on Fuel Cladding
- Protective Coating Debris Deposited on Fuel Clad Surfaces
- Production and Deposition of Chemical Precipitates
- Coolant Delivered from the Top of the Core

The following acceptance bases were established for the evaluation of the topical areas identified above:

1. The maximum clad temperature shall not exceed 800°F.
2. The thickness of the cladding oxide and the fuel deposits shall not exceed 0.050 inch in any fuel region.
3. The maximum fibrous debris that reaches the core after a LOCA is less than or equal to 15 g/FA.

These acceptance bases were applied after the initial quench of the core and are consistent with the LTCC requirements stated in 10 CFR 50.46 (Reference 3-3). They do not represent, nor are they intended to be, new or additional LTCC requirements. These acceptance bases demonstrate that local temperatures in the core are stable or continuously decreasing and that debris entrained in the cooling water supply will not affect decay heat removal. The 800°F cladding temperature was selected based on autoclave data that demonstrated oxidation and hydrogen pick-up was minimal at and below the 800°F temperature.

Therefore, there would be minimal reduction in post-LOCA load carrying capability. A discussion of the technical basis for the 800°F temperature is given in Appendix A, Reference 3-1. The 0.050 inch limit for oxide plus deposits was selected so as to preclude the formation of deposits that would bridge the space between adjacent rods and block flow between fuel channels. Finally, FA testing has demonstrated that the most severe combinations of fibrous, particulate, and chemical precipitant debris loads with less than or equal to 15 g/FA of fiber will not impede core cooling.

In order to demonstrate reasonable assurance of LTCC, all plants must evaluate the areas identified above and demonstrate they are bounded by the debris load acceptance criteria, maximum fuel cladding temperature and maximum deposit thickness requirements. Specifically:

- Adequate flow to remove decay heat will continue to reach the core even with debris from the sump reaching the RCS and core. Plants that operate at (or below) 15 grams of fiber per FA can state that debris that bypasses the sump strainer will not build an impenetrable blockage at the core inlet.
- Decay heat will continue to be removed even with debris collection at the FA spacer grids. Plants that operate at (or below) 15 grams of fiber per FA can state that debris that bypasses the sump strainer will not build an impenetrable blockage at the fuel spacer grids. This assertion is bolstered by numerical and first principle analyses.
- Fibrous debris, should it enter the core region, will not tightly adhere to the surface of fuel cladding. Thus, fibrous debris will not form a “blanket” on clad surfaces to restrict heat transfer and cause an increase in clad temperature. Therefore, adherence of fibrous debris to the cladding is not plausible and will not adversely affect core cooling.
- Protective coating debris, should it enter the core region, will not restrict heat transfer and cause an increase in clad temperature. Therefore, adherence of protective coating debris to the cladding is not plausible and will not adversely affect core cooling.
- The chemical effects method developed in WCAP-16530-NP-A (Reference 3-8) was extended to develop a method to predict chemical deposition on fuel cladding. The calculational tool, LOCADM, can be used by each utility to perform a plant-specific evaluation. It is expected that each plant will be able to use this tool to show that decay heat would be removed and acceptable fuel clad temperatures would be maintained.
- PWRs use boron as a core reactivity control method and are subject to concerns regarding potential post-LOCA BAP in the core. In light of NRC staff and Advisory Committee on Reactor Safeguards (ACRS) challenges to the simplified methods commonly used, it has recently become clear that additional insights and new methodologies are needed to answer fundamental questions about boric acid mixing and transport in the RCS and potential precipitation mechanisms that may occur both during the ECCS injection phase and the sump recirculation phase after a LOCA.
- The PWROG FA test results demonstrated that sufficient flow will reach the core to remove core decay heat. The debris load acceptance criteria developed is bounding and applicable to all PWR plants, including UPI plants.

In conclusion, WCAP-16793-NP-A, Rev. 2 (Reference 3-1) stated that a very conservative, bounding, and generic limit of 15 grams of fiber per FA could be established. This limit is independent of particulate and chemical precipitate quantity. The report also concluded that higher limits could be possible depending on plant-specific conditions.

The NRC concurred with the acceptance criteria and stated conclusions when issuing the SE on Reference 3-1. However, there are 15 conditions and limitations associated with the limits approved in WCAP-16793-NP-A, Rev. 2 (Reference 3-1). While many of these conditions provided guidance to utilities on what information is needed in a GL 2004-02 submittal and how to properly use the information in the report, some of them also provided guidance on what should be considered for increasing the debris limits if that path was chosen. Of relevance are the following limitations (*italics added to identify actions*):

1. Licensees should confirm that their plants are covered by the PWROG sponsored fuel assembly tests by confirming that the plant available hot-leg break driving head is equal to or greater than that determined as limiting in the proprietary fuel assembly tests and that flow rate is bounded by the testing. Licensees should validate that the fuel types and inlet filters in use at the plant are covered by the test program (with the exception of LTAs). Licensees should limit the amount of fibrous debris reaching the fuel inlet to that stated in Section 10 of the WCAP (15 grams per fuel assembly for a hot-leg break scenario).

*Alternately, licensees may perform plant-specific testing and/or evaluations to increase the debris limits on a site-specific basis. The available driving head should be calculated based on the core exit void fraction and loop flow resistance values contained in their plant design basis calculations, considering clean loop flow resistance and a range of break locations. Calculations of available driving head should account for the potential for voiding in the steam generator tubes. These tests shall evaluate the effects of increased fiber on flow to the core, and precipitation of boron during a postulated cold leg break, and the effect of p/f ratios below 1:1. The NRC staff will review plant-specific evaluations, including hot- and cold-leg break scenarios, to ensure that acceptable justification for higher debris limits is provided.*

3. Section 3.1.4.3 of the WCAP states that alternate flow paths in the RV were not credited. The section also states that plants may be able to credit alternate flow paths for demonstrating adequate LTCC.

*If a licensee chooses to take credit for alternate flow paths, such as core baffle plate holes, to justify greater than 15 grams of bypassed fiber per fuel assembly, the licensee should demonstrate, by testing or analysis, that the flow paths would be effective, that the flow holes will not become blocked with debris during a LOCA, that boron precipitation is considered, and that debris will not deposit in other locations after passing through the alternate flow path such that LTCC would be jeopardized.*

5. In RAI Response number 18 in Reference 13, the PWROG states that numerical analyses demonstrated that, even if a large blockage occurs, decay heat removal will continue. The NRC staff's position is that a plant must maintain its debris load within the limits defined by the testing (e.g., 15 grams per assembly).

*Any debris amounts greater than those justified by generic testing in this WCAP must be justified on a plant-specific basis.*

12. Section 3.1 of the WCAP discusses a prototypical test program designed to establish limits on the amount of debris that could bypass the ECCS sump strainer, enter the core, and still allow adequate flow to enter the core to ensure adequate LTCC. The WCAP states that a test protocol and test procedures were developed to include investigation of possible thin bed effects and that the debris used in testing represented debris that could be present in the RCS following a LOCA.

*Plants that can qualify a higher fiber load based on the absence of chemical deposits should ensure that tests for their conditions determine limiting head losses using particulate and fiber loads that maximize the head loss with no chemical precipitates included in the tests. Note that in this case, licensees must also evaluate the other considerations discussed in Item 1 above.*

This work provides an alternative approach to the method detailed in WCAP-16793-NP-A, Rev. 2 (Reference 3-1) for defining an in-vessel fibrous debris limit and provides a means for increasing the currently established in-vessel fibrous debris limit of 15 g/FA by addressing the above concerns.

### 3.9 REFERENCES

- 3-1 WCAP-16793-NP-A, Rev. 2, "Evaluation of Long-Term Cooling Considering Particulate, Fibrous and Chemical Debris in the Recirculation Fluid," July 2013.
- 3-2 NEI 04-07, Rev. 0, "Pressurized Water Reactor Sump Performance Evaluation Methodology," December 2004.
- 3-3 10 CFR Part 50 §50.46, "Acceptance Criteria for Emergency Core Cooling Systems for Light Water Nuclear Reactors," 72 Federal Register 49494, August 2007.
- 3-4 Letter from John C. Butler (NEI) to Stewart N. Bailey (U.S. NRC), "Transmittal of GSI-191 Resolution Criteria for "Low Fiber" Plants," ADAMS Accession Number ML113570219, December 2011.
- 3-5 Attachment to ML113570219, "GSI-191 Resolution Criteria Low/No Fiber Plants," ADAMS Accession Number ML113570226, 2 pages, December 2011.
- 3-6 Letter from William H. Ruland (U.S. NRC) to John C. Butler (NEI) "NRC Review of Nuclear Energy Institute Clean Plant Acceptance Criteria for Emergency Core Cooling Systems," ADAMS Accession Number ML120730181, May 2012.
- 3-7 STP-RIGSI191-V03.06, Rev. 5, "South Texas Project Risk-Informed GSI-191 Evaluation, Filtration as a Function of Debris Mass on the Strainer: Fitting a Parametric Physics-Based Model," June 2013.
- 3-8 WCAP-16530-NP-A, Rev. 0, "Evaluation of Post-Accident Chemical Effects in Containment Sump Fluids to Support GSI-191," March 2008.

## 4 METHOD FOR CALCULATING FIBER LIMIT

The method for calculating the in-vessel debris limits described in this report is plant-specific and depends on inputs for each plant (or group of identical plants). The remainder of this report details a method that utilities can use to assess plant-specific debris limits for closure of NRC GL 2004-02.

As discussed in Section 3.6, large breaks are the focus of GSI-191 resolution. Further, the break locations are divided into HLBs and CLBs. Both break scenarios must be considered independently given the difference in system response, timing of debris introduction to the fuel, and the benefits of alternate flow paths (AFPs) for hot leg breaks. Section 5 identifies the major assumptions used in the methodology. For plants that initially start with cold side recirculation, Section 4.2 outlines the methodology for HLB, and Section 4.3 outlines the methodology for CLB. Sections 6 and 7 provide the details of the methods for calculating the amount of fiber delivered to the RCS for HLB and CLB, respectively. For UPI plants, Section 8 provides the methodology for both break locations. For the spectrum of large breaks, this methodology can be used to ascertain that the amount of debris generated in containment does not ultimately result in an excessive amount of debris (fiber and particulate) delivered to the RV such that LTCC is compromised. The evaluation process is illustrated in Figure 4-1.

The methodology is predicated, in part, on plant-specific ECCS strainer design and the efficiency of that strainer to collect debris. Containment recirculation sump strainers are designed to act as filters to collect post-accident debris, thus preventing a wide range of debris from entering the ECCS and CSS. However, a portion of the debris may be sufficiently small or deformable to actually “pass through” the recirculation sump strainer(s) and enter the ECCS and CSS. This “pass through” (also sometimes called “bypass” or “penetration”) debris in the ECCS may then enter the RCS. For either a HLB or a CLB, the CSS flow is returned to the containment where it eventually returns to the sump and is again filtered by the recirculation sump strainer(s) before the coolant enters either the ECCS or the CSS.

Where available, quantification of that fraction of debris that penetrates the sump strainer(s) should be used. Otherwise, conservative assumptions must be applied to ultimately determine allowable fiber quantities in containment. Plants that have performed strainer testing have quantified the total penetration considering several time-dependent mechanisms. These may include initial penetration of debris as it builds on the sump strainer, continued penetration of debris if the sump strainer is not fully covered, and debris shedding if the strainer is fully covered. Flow (and the corresponding debris) to the CSS suction can also be considered if it is in operation.

Formation of chemical precipitates must also be considered. As described previously, the in-vessel fiber evaluations documented in WCAP 16793-NP-A Rev. 2 (Reference 4-1) demonstrated significant head loss in the presence of the chemical precipitate surrogate used during testing, thereby limiting the fiber quantities. In the present effort, the method assumes that all chemical precipitates are sufficiently delayed and do not form until after a critical point where sufficient cooling occurs as a result of flow directed through the AFPs. Based on autoclave testing described in Volume 5, the earliest time that total core blockage due to chemical effects is expected to occur is 4 hours. In all cases, this method assumes that chemical precipitates form at 24 hours if they don't form earlier.

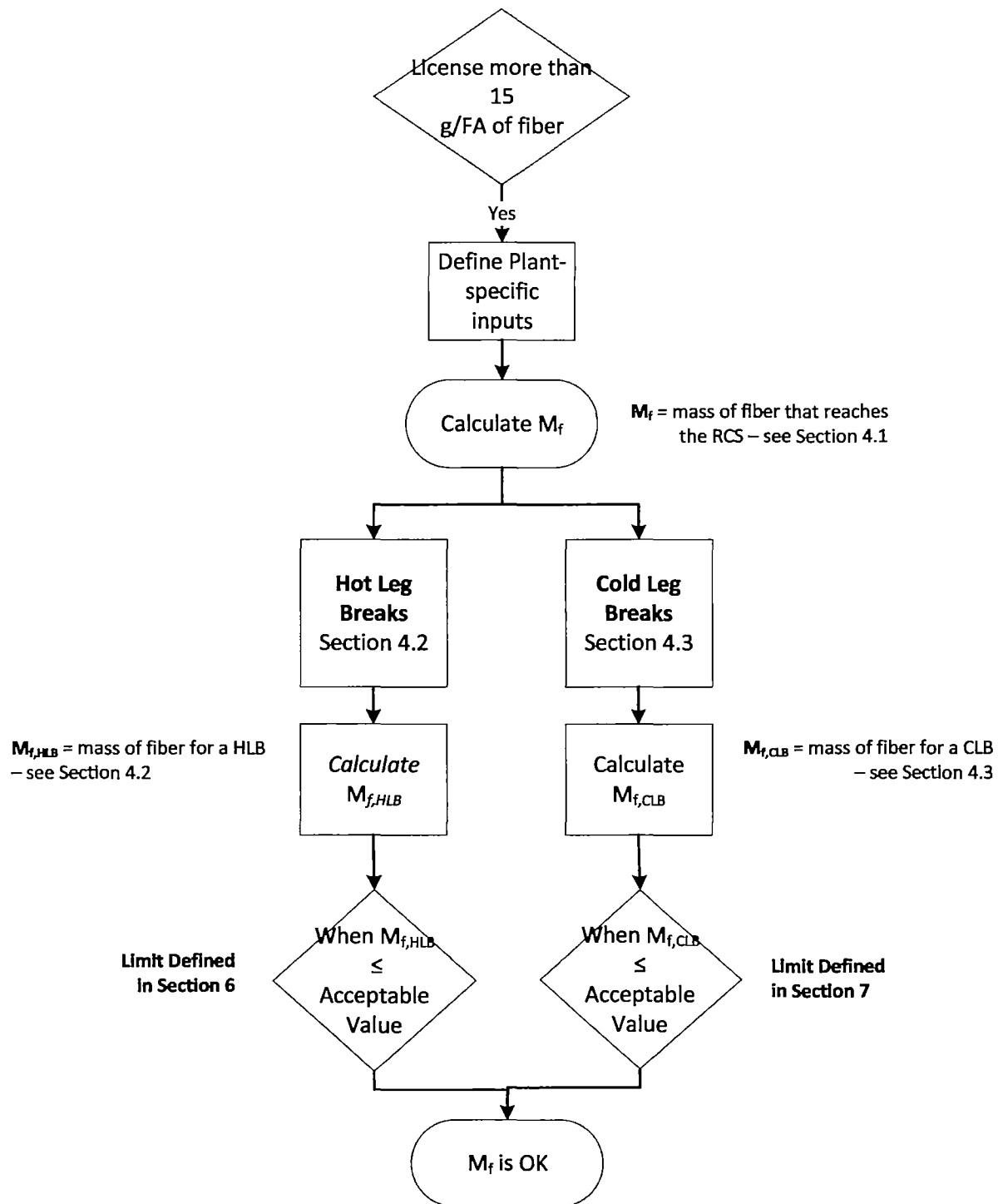


**Figure 4-1 Process Diagram for Determination of Plant-Specific In-Vessel Debris Limit**

The debris limits defined using this method applies to all fuel designs that are in production by Westinghouse and AREVA as of January 2015 with one notable exception. AREVA fuel with the **TRAPPER™** fine mesh filter showed markedly different results from the **FUELGUARD™** filter design in the WCAP-16793-NP-A, Rev. 2 (Reference 4-1) testing. However, the **TRAPPER** fine mesh filter design is no longer in production, and was therefore not tested in this program. If it is used, it would only be used in a limited quantity in the core periphery or center core location. The use of the **TRAPPER** fine mesh filter fuel design in limited quantities would not alter the limits defined by this methodology. The method presented here may be used for fuel designs developed after January 2015 provided the applicability of this method to those designs is evaluated.

The discussion in this section pertains directly to the Westinghouse, CE, and B&W plants that initiate cold side injection immediately following the break. Discussions pertaining to UPI plants are provided in Section 8.

#### 4.1 DEFINITION OF IN-VESSEL DEBRIS

For the purposes of defining in-vessel debris, it is useful to explicitly define what is meant by “in-vessel.” The initial concern of GSI-191 is that, following a LOCA, debris generated within containment from the break could collect on the sump strainer(s) and create sufficient resistance to the recirculating flow such that LTCC might be challenged. The effect of the debris that may pass through the sump strainer(s) and enter the ECCS where it may accumulate at the core inlet and on components or the fuel must be also considered.

The sump strainer “bypass fraction” is the portion of debris transported to the sump strainer that is not collected on the sump strainer, and instead passes through the sump strainer and is transported into either the CSS or RV. Fluid that goes to the CSS is returned to containment without reaching the fuel. Only debris that reaches the RV and enters the core region has the potential to block the cooling water flow to the fuel within the RV. Therefore, the methods for calculating in-vessel debris described in this document define the amount of debris that can reach the RV itself and enter the core region and is not necessarily the amount of debris that bypasses the sump strainer.

Once in the RV, debris can travel to and possibly accumulate in multiple locations. For CLBs with cold side recirculation or HLBs with hot side recirculation, some debris may exit the break and return to containment while the rest of the debris will continue into the RV. For HLBs with cold side recirculation or CLBs with hot side recirculation, essentially all of the debris will enter the RV. In the RV, debris that is held up on large components (e.g., neutron pads or LP internals) will not compromise core cooling, because the flow areas around these obstructions are large and cannot be completely blocked by debris. Settling in the RV LP will occur where the fluid velocities are low, facilitating “dead zones” for accumulation of significant quantities of debris. This precludes blockage of the flow paths in lower region of the LP. Debris collecting in these locations is, however, conservatively neglected.

---

TRAPPER and FUELGUARD are trademarks or registered trademarks of their respective owners. Other names may be trademarks of their respective owners.



Debris transported to the core inlet may accumulate at the inlet (below the heated core) and/or some portion of that debris may transport upward within the heated core. Accumulation of debris in these locations is addressed in the remainder of this report.

The amount of debris that ultimately reaches the RCS is comprised of the above components. That is:

$$M_f = M_{f,CI} + M_{f,in-core} + M_{f,break} \quad \text{Equation 4-1}$$

where,

$M_f$  = the total fiber mass that reaches the RCS for either break location

$M_{f,CI}$  = the mass of fiber at the core inlet

$M_{f,in-core}$  = the mass of fiber in the heated core

$M_{f,break}$  = the mass of fiber returned to containment via the break (for CLBs with cold side recirculation, this may be a significant fraction of the debris and is credited. For CLBs with hot side recirculation and HLBs this is conservatively assumed to be zero)

As a point of clarification, the discussions that follow focus on fiber only, referring to the final solution as a fiber limit rather than that of combined fibrous and particulate debris. This is done primarily as a means of simplification. Rather than solving the problem for various particulate to fiber ratios, experimental testing described in Volume 6 has determined the most limiting ratio, and that ratio is embedded in the correlations developed in other sections of this volume. The impact of particulate is therefore implicit in the equations used throughout this calculation.

## 4.2 LARGE HOT LEG BREAKS

Immediately prior to SSO, no debris has entered the system. The clean ECCS liquid flows from the injection location, through the core to the break. Upon transfer of the suction flow to the sump, debris in the sump will be transported to the sump strainer and a portion will pass (bypass) through the sump strainers and eventually enter the RV.

The amount of debris that reaches the RCS for this hot leg break scenario is a function of the accumulation of debris in two locations: (1) at the core inlet and (2) within the core itself. While debris may reach the break (i.e., not be captured in the core during cold side recirculation or go directly to the break during hot side recirculation), it is conservatively assumed not to. How and when the debris arrives at the core inlet or in the heated core is dependent on plant inputs and the occurrence of key events.

The amount of debris that can accumulate at the core inlet and not impede LTCC is defined by a number of supporting analyses. The TH analyses described in Volume 4 determine the earliest time at which complete core inlet blockage can occur and still maintain the cladding temperature below 800°F. This time is defined as  $t_{block}$ . These analyses show that before  $t_{block}$ , flow through the AFPs alone is not sufficient to keep the cladding temperature below 800°F. After  $t_{block}$ , however, the analyses demonstrate that the AFPs are effective for ensuring LTCC.

The autoclave testing described in Volume 5 determined the time at which chemical precipitates form. This time is defined as  $t_{chem}$ . Once chemical precipitates form (i.e.,  $t_{chem}$  is exceeded) the resistance through the debris bed at the core inlet will be greatly increased, and as the fiber load is increased above 15 g/FA, flow through this path may be stopped completely (Reference 4-1). While it is true that flow through the bed will exist for fiber loads less than 15 g/FA, the effect of chemical precipitates on the head loss through these lesser debris beds has not been rigorously studied. It is therefore conservative to assume that no matter the existing fiber load at the core inlet, complete blockage will occur coincident with  $t_{chem}$ . That said, if  $t_{chem} < t_{block}$ , then the method described in this document cannot be used to address GSI-191 concerns related to in-vessel effects until a method is devised or plant changes are made to make  $t_{chem} > t_{block}$ .

The TH analyses were also used to determine the maximum resistance at the core inlet that would maintain the cladding temperature below 800°F prior to reaching complete core inlet blockage. This parameter is defined as  $K_{max}$ . The FA testing with debris described in Volume 6 correlates the head loss at the core inlet due to debris to the actual quantity of debris. In this manner, debris accumulation at the core inlet can be compared to  $K_{max}$ . The TH analyses demonstrate that as long as the resistance due to debris is less than  $K_{max}$  prior to reaching  $t_{block}$ , the cladding temperature remains below 800°F.

At some point in the transient, sufficient debris may accumulate at the core inlet such that flow and debris are diverted to the AFPs. The TH analyses described in Volume 4 provide the conditions at which this occurs and the flow splits between the core inlet and AFPs as well. These parameters are defined as  $K_{split}$  and  $m_{split}$ , respectively. Debris that travels through these paths may reach the heated core. Further, after hot leg switchover (HLSO) occurs, debris may reach the heated core from the hot legs. The amount of debris that can accumulate in the heated core without affecting LTCC is defined in Section 6.4.

Since the timing of the event is plant dependent, the final debris limits must be established by plant-specific analyses, which are described in Section 6.5. An overview of the process for calculating the amount of debris that reaches the RCS following a HLB is provided in Figure 4-2. The plant-specific inputs are used to calculate  $M_{f, HLB}$  which is the mass of fiber entering the RV for the HLB scenario. The parameter  $M_{f, HLB}$  is then compared to the acceptance criteria as described in Section 6.5 to determine if the RV fiber load is acceptable.

To help in understanding the process for defining where debris accumulates for a HLB, it is useful to identify various, key events. Specifically, the following events are significant: time of sump recirculation, activation of AFP, formation of chemical precipitates, and implementation of measures to prevent BAP. These events are expanded upon in the following subsections. As part of the program, a substantial investigation was performed to further understand these various events and the phenomena associated with them. The following subsections also provide an overview of how these times are defined as part of the overall solution for improving the debris limits. Finally, some example timelines are presented to illustrate how the timing affects the location of debris deposited within the RV.

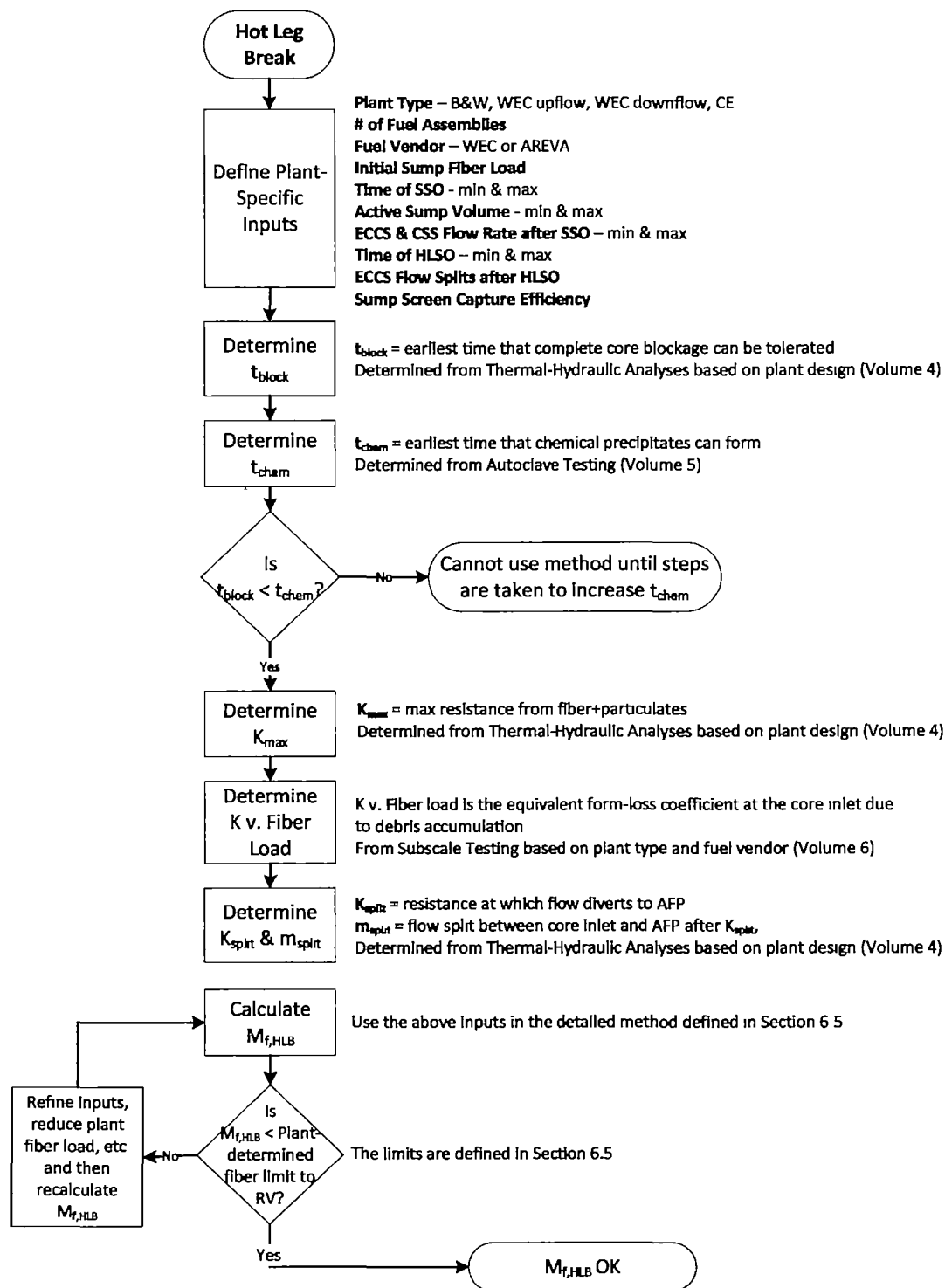


Figure 4-2 Overview of Hot Leg Break Methodology

#### 4.2.1 Time of Sump Recirculation

The time of sump recirculation (or SSO) defines the earliest point at which debris can reach the RCS and is plant dependent. The timing depends on the volume of water sources supplying the ECCS and CSS, ECCS flow rate, and CSS flow rate among other parameters. This time is usually available in plant documentation. Guidance on important considerations for calculating this parameter is provided in Section 6.5.2.6.

#### 4.2.2 Activation of Alternate Flow Path

The AFPs are described in detail in Section 3.2. During post-LOCA scenarios in which debris accumulates at the core inlet, these AFPs may provide flow to the core to remove decay heat at some point after the LOCA. Consequently, these paths can assist in providing adequate flow to maintain LTCC.

Shortly after sump recirculation, any debris that reaches the core LP is conservatively assumed to accumulate at the core inlet and/or lowermost spacer grid. At this point, the in-vessel AFPs do not provide a path for debris to reach the core. As debris accumulates at or near the core inlet, resistance to flow increases and leads to conditions that “activate” the AFP such that flow is diverted through the AFPs and entrained debris is transported to other regions of the core. For a period of time, debris will continue to accumulate at the core inlet but will also pass into the AFP.

A number of items need to be defined for this scenario. First, the resistance that debris imposes to flow as it accumulates at the core inlet needs to be defined. Correlation of the head loss as a function of accumulated debris is determined by the FA testing described in Volume 6. The end result is a core inlet resistance as a function of debris load, which is provided in Section 6.3.

Second, the conditions at which the AFP becomes active need to be defined. These are essentially the conditions under which the flow from the LP begins to split between the core inlet and the AFP. Once the AFP becomes active (i.e., flows up from the LP in the BB or begins to pass fluid through the UHSN), the flow split between the core inlet and AFP needs to be defined so that debris can be appropriately tracked. These details are provided by TH analyses as described in Section 6.1.

Finally, it must be shown that the debris that enters the AFP will not accumulate locally, resulting in subsequent blockage of the limiting flow paths within the AFPs. Verification that the flow paths are not blocked due to accumulation of debris is provided in Volume 6.

#### 4.2.3 Chemical Precipitate Formation

Chemical reactions begin to occur as soon as coolant released from the break comes into contact with debris and other materials inside the containment. Then, as the sump begins cool, continued chemical reactions and the products of those chemical reactions can result in the formation of precipitates. If sufficient debris is present at the core inlet, formation of chemical precipitates can block flow through this path (Reference 4-1). Therefore, the time at which these precipitates form can have a significant effect on the in-vessel debris limit.

The time that chemical precipitates form is plant dependent. However, to better understand the conditions that lead to precipitate formation, significant testing has been completed as part of this program. These efforts are summarized in Section 6.2 and described in detail in Volume 5. The results documented in Volume 5 establish the time to onset of chemical precipitates for all plants,  $t_{chem}$ .

Before  $t_{chem}$ , the debris in the RV will be comprised of fiber and particulate only. The FA testing described in Volume 6 defines the pressure drop for debris beds made of particulate and fiber only. At the time of  $t_{chem}$ , it will be assumed that the core inlet is completely blocked in accordance with the conclusions and SE from WCAP-16793-NP-A, Rev. 2 (Reference 4-1). After this time, the AFPs may be able to provide adequate core cooling. This evaluation is provided by TH analyses as described in Section 6.1.

#### 4.2.4 Implementation of Measures to Prevent Boric Acid Precipitation

As described in Section 3.3.3, each plant will take actions to mitigate the buildup of boric acid in the RV and core. Depending on the plant design, some or all of the ECCS flow may be diverted to the hot legs. By this point in the transient, the amount of debris passing through the sump strainer has substantially decreased. However, some debris can be introduced to the core exit. The evaluation of debris reaching the core from the top is provided in Section 6.4.

#### 4.2.5 Example Timelines

The sequence of events for any given scenario is plant dependent. After SSO, the timing of mitigation actions depend on the available equipment, sump volume, sump chemistry, etc. Further, the timing of activation of the AFP or formation of chemical precipitates depends on the amount of debris in the system, ECCS flow rates, and/or materials in containment. The actual timing of these various events will change where and how debris builds in the RV. For illustration purposes, two cases will be examined. These examples should be used for information purposes only.

In the first case, the sequence of events is: SSO, followed by AFP activation, followed by formation of chemical precipitates, and finally followed by operator action to initiate HLSO. The location of debris accumulation is illustrated by Figure 4-3. In this case, SSO occurs and cold side recirculation continues. Debris begins to build at the core inlet until enough debris has built up such that the AFP becomes active, in which case debris continues to accumulate at the core inlet but is also diverted to the core via the AFP. Once chemical precipitates form, the core inlet is assumed to block completely such that no further fiber or particulate is added to this location; instead all debris then travels through the AFP to the core. Sometime after that, the operators take action to initiate HLSO by switching most of the ECCS flow to the hot legs. Thereafter, debris may be introduced to the core via the AFP (by the small, remaining cold leg recirculation) and the hot leg recirculation.

In the second case, the sequence of events is: SSO, followed by AFP activation, followed by HLSO, and finally followed by formation of chemical precipitates. The location of debris accumulation is illustrated by Figure 4-4. In this case, SSO occurs and cold side recirculation continues. Debris begins to build at the core inlet until enough debris has built up such that the AFP becomes active, in which case debris continues to accumulate at the core inlet but is also diverted to the core via the AFP. Once the operators take action to initiate HLSO by switching most of the ECCS flow to the hot legs, debris may be

introduced to the core via the AFP or core inlet (by the small, remaining cold leg recirculation) and the hot leg recirculation. Once chemical precipitates form, the core inlet is assumed to block completely such that no further fiber or particulate is added to this location; instead all debris from the cold leg recirculation travels through the AFP to the core.

The above examples are only a couple of instances of a sequence of timing that may occur. For example, HLSO may occur before the AFP becomes active and before chemical precipitates form. In this case, debris will continue to accumulate at the core inlet only until HLSO occurs. The process detailed in Section 6.5 includes plant-specific inputs that define how this timeline will evolve for a specific set of conditions.

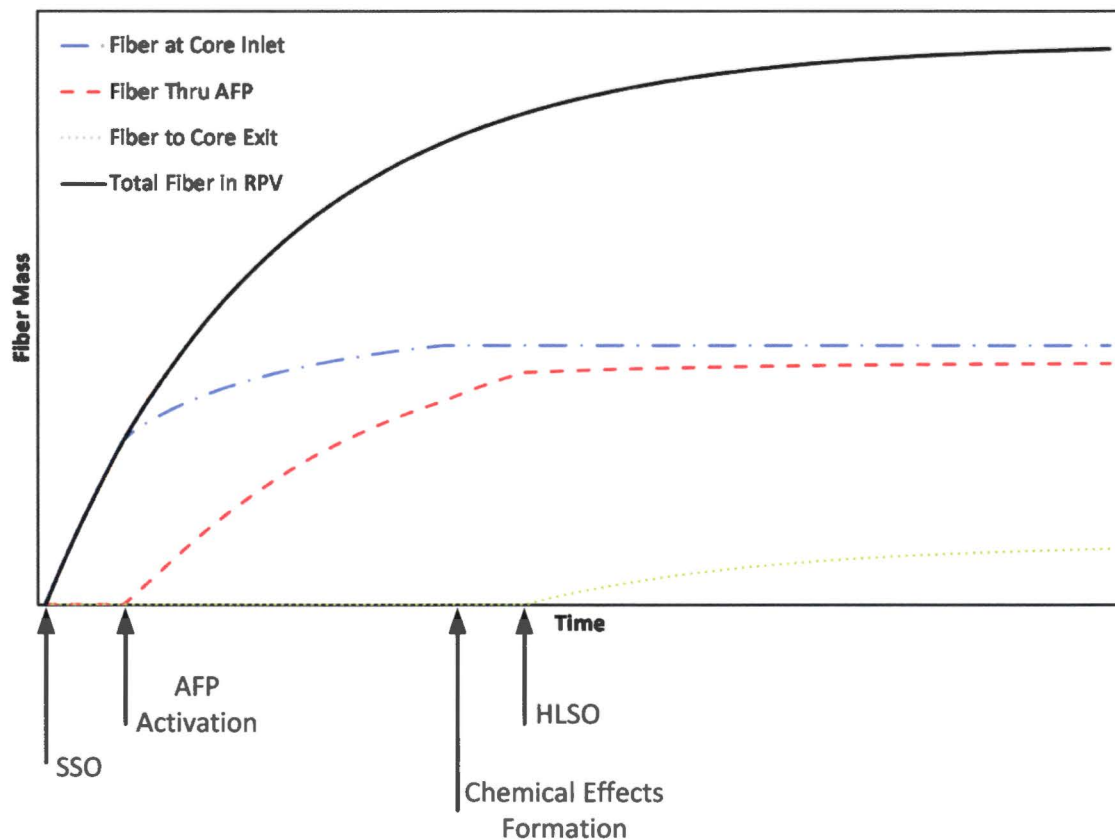


**Figure 4-3 Example Timing #1**



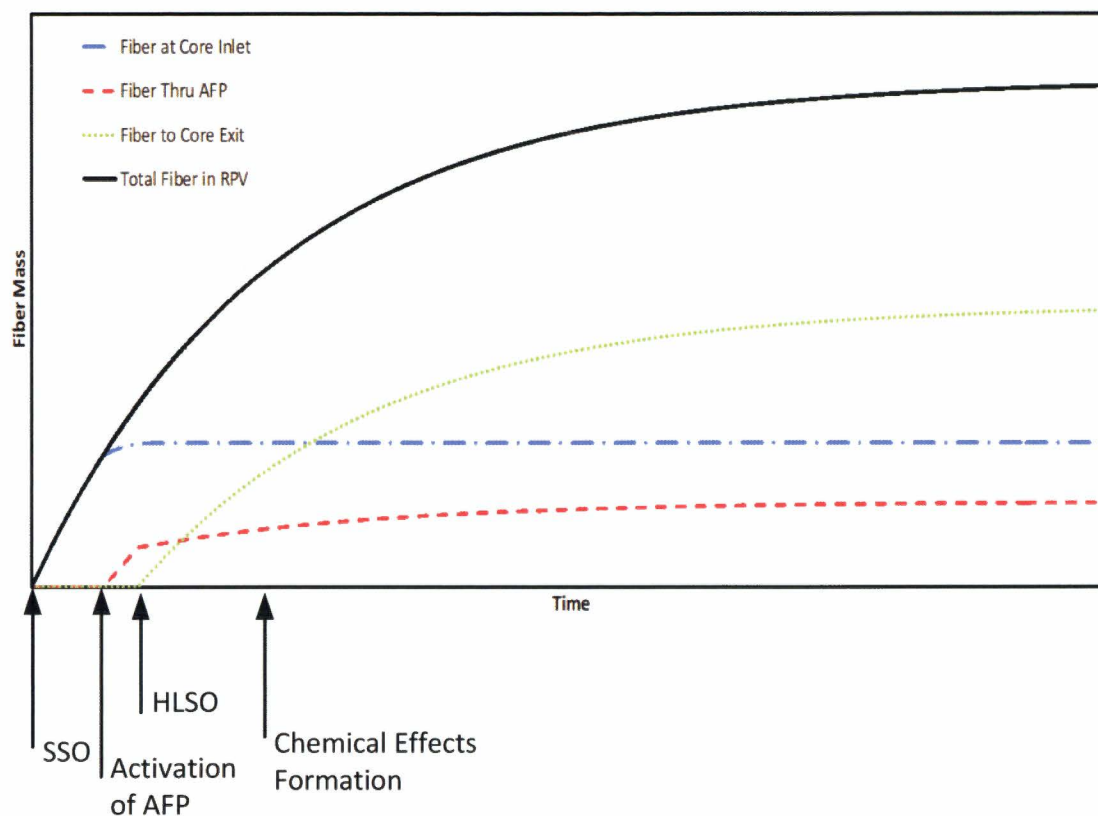


**Figure 4-4 Example Timing #2**

### 4.3 LARGE COLD LEG BREAKS

Immediately prior to SSO, similar to the HLB scenario, no debris has entered the system. The clean ECCS liquid flows from the injection location and makes up for the core boil-off. The excess ECCS liquid exits that break and returns to the sump. Upon transfer of the suction flow to the sump, debris in the sump will be transported to the sump strainer and a portion will pass (bypass) through the sump strainer(s) and eventually enter the RV.

After SSO, debris begins to enter the RCS where it may exit the break or continue to the downcomer as described above. Once in the RV LP, it will first approach the core and accumulate near the core inlet (below the heated region of the core).

The spilled coolant from the break and coolant from containment sprays is collected in the sump pool. Chemical reactions begin to occur as soon as coolant released from the break comes into contact with debris and other materials inside the containment. Then, as the sump begins cool, continued chemical reactions and the products of those chemical reactions can result in the formation of precipitates. If sufficient debris is present at the core inlet, formation of chemical precipitates can be collected by the debris at the core entrance, blocking flow through this path (Reference 4-1). Consequently, the time at

which these precipitates form may have a significant effect on the in-vessel debris limit. For the CLB scenario, a maximum fiber limit of [ ]<sup>a,c</sup> at the core inlet is defined in Section 7.1. This limit is predicated on the fact that: (1) fiber loads at or below the limit will not form a contiguous bed at the core inlet, (2) the pressure drop through the regions of the core inlet with a fiber and particulate bed is negligible, and (3) the addition of chemical precipitates will not further impede flow into the core. Therefore, chemical effects formation need not be considered in the CLB methodology.

As described in Section 3.3.3, each plant will take actions to mitigate the buildup of boric acid in the RV and core. One of these actions is commonly called HLSO. After this point, many plants divert some or all ECCS flow to the hot legs, which can introduce debris at the core exit. Typically following a CLB, the majority of debris that will reach the core has already done so by the time of HLSO. Consequently, any debris that is transported to the RV through the hot leg flow path will be well below the in-vessel debris limit defined in Section 6.4. To that end, the CLB calculation described in Section 7.2 may be stopped at the time of HLSO to define the CLB debris limit. For plants that don't initiate HLSO, debris will continue to build up at the core inlet. The CLB calculation described in Section 7.2 should continue until all debris has been collected on the containment building sump strainer(s) and at the core inlet.

The amount of debris that can collect at the core inlet and not impede LTCC is defined in Section 7.1 to be [ ]<sup>a,c</sup>. The amount of debris that actually reaches the RCS (i.e., the CLB in-vessel debris limit, termed  $M_{f, CLB}$ ) and core inlet is determined using the method described in Section 7.2.

#### 4.4 REFERENCES

- 4-1 WCAP-16793-NP-A, Rev. 2, "Evaluation of Long-Term Cooling Considering Particulate, Fibrous and Chemical Debris in the Recirculation Fluid," July 2013.



## 5 MAJOR ASSUMPTIONS

In all scenarios, the following assumptions are made:

1. The fiber and particulate are well mixed in the sump fluid such that a homogeneous mixture is present at the time of sump recirculation. Therefore, the debris transport is proportional to the ECCS flow rate.
2. No debris is held up in any location other than the sump strainer(s), core inlet or within the core. Further, no settling of debris is credited in any location of the RCS. Therefore, the maximum amount of debris reaches the core.
3. Chemical precipitates are assumed to form at 24 hours if the chemical analysis of plant-specific sump chemistry does not indicate that they will form earlier.
4. The fiber is in its constituent form, i.e., individual fibers. This is consistent with maximum transport assumptions.

### 5.1 HOT LEG BREAKS

The following assumptions are made specifically for evaluating HLBs for plants with initial ECCS to the cold legs only:

5. After transfer to sump recirculation, all debris that enters the RV is assumed to collect at the core inlet until the AFP is activated. No debris enters the in-core region (i.e., no debris penetration through the core inlet). This maximizes the calculated debris load at the core inlet.
6. When chemical precipitates form, the core inlet is assumed to be completely blocked. This initiates flow to the AFP at an earlier time, which reduces the amount of fiber buildup at the core inlet and minimizes the overall fiber limit.
7. It is assumed that debris that travels through the AFP continues to the heated core and does not accumulate in the BB or upper head. Testing of the AFP in Volume 6 indicated that some debris may be held up in this region (although it will not block any of the flow passages). Neglecting this holdup maximizes the debris that is transported to the core.
8. It is assumed that no debris exits the break (i.e., once it is in the RCS, it stays in the RCS). Therefore, the maximum amount of debris reaches the core.
9. The code simulations assume that sump debris will build-up across the core inlet in a uniform manner, and blockage is only considered at the core inlet. This is a simplifying, conservative assumption. In reality, it is expected that the build-up of debris at the core inlet will follow the flow distribution at the core inlet. Some regions of the core with higher power will have a higher flow at the core inlet, while other regions of the core with lower power will have lower flow, or even downflow, at the core inlet. From a DHR standpoint, applying a uniform build-up at the core

inlet is more challenging as was demonstrated in the TH analysis contained in WCAP-16793-NP-A, Rev. 2 (Reference 5-1).

10. The code simulations assume fluid properties of pure water. During the LTCC phase of the post-LOCA transient, the build-up of solute concentrations in the inner regions of the RV can be a concern. If the concentrations reach high enough levels, the effect on fluid properties may need to be considered. Since these analyses will simulate a large HLB scenario, it is expected that the liquid carryover out of the break will be sufficient to limit the concentration build-up of solutes in the RV and thus limit the influence on fluid properties. This assumption is justified by the simulation results discussed in Volume 4, Section 7.
11. In the code simulations, some cases consider an “instantaneous” ramp of core inlet resistance. The instantaneous ramp will occur over a one minute period to aid in code stability. The modeling of debris build-up over one minute is a non-realistic condition since debris transport from the sump to the core inlet occurs over a longer period of time. In other cases, a longer ramp period will be considered. For these cases it will be assumed that the resistance due to the build-up of debris occurs over a more realistic, yet still conservative time period.
12. In the code simulations, a top-skewed power shape is assumed to be most limiting for core uncover. The uncover process is governed by boil-off and subsequent dry out that begins at the top of the core and propagates downward. Using a top-skewed power shape will maximize cladding heatup in the event of core uncover and provides the most challenge for meeting the 800°F acceptance criterion.
13. In the code simulations, it is assumed that the flow path through the thimble tubes is blocked and no bypass flow through the tubes will be credited. This assumption removes an additional path for fluid to reach the core, limiting the paths to either the core inlet or the AFPs discussed above.
14. The code simulations assume that the secondary side is isolated and not depressurized consistent with the short-term LOCA analysis approach. This results in a high secondary side temperature that helps to inhibit flooding of the steam generator (SG) on the primary side such that SG spillover, if predicted, is delayed.

## 5.2 COLD LEG BREAKS

The following assumptions are made specifically for evaluating CLBs for plants with initial ECCS to the cold legs only.

15. Any debris that reaches the core LP is conservatively assumed to accumulate at the core inlet and/or lowermost spacer grid.
16. To allow for uncertainties, the fluid volume entering the fuel is assumed to be 1.2 times the boil-off flow rate requirement based on the decay heat at any given time in the transient starting at recirculation initiation. A 20 percent increase in the flow required to satisfy boil-off requirements increases the amount of fiber laden fluid reaching the core.

### 5.3 UPPER PLENUM INJECTION PLANTS

The following assumptions are made specifically for evaluating UPI plants:

17. It is assumed that all debris that enters the RV through UPI enters the core region for the CLB scenario. Given the complex structures within the UP, it is expected that some fraction of debris will be held-up within the UP.
18. For CLBs with cold leg recirculation, it is assumed that all debris enters the RV and is transported to the core inlet.

### 5.4 REFERENCES

- 5-1 WCAP-16793-NP-A, Rev. 2, "Evaluation of Long-Term Cooling Considering Particulate, Fibrous and Chemical Debris in the Recirculation Fluid," July 2013.

## 6 HOT LEG BREAKS

Debris that enters the RV following a HLB will initially approach the core inlet. The program has performed substantial investigation to understand where this debris might accumulate and the effect that it might have on LTCC. The following subsections provide the details of this work.

The discussion in this section pertains directly to plants that initiate cold side injection immediately following the break. Discussions pertaining to UPI plants are provided in Section 8.

### 6.1 THERMAL-HYDRAULIC EVALUATION OF REACTOR COOLANT SYSTEM

During operation of the ECCS to recirculate coolant from the containment sump, debris in the recirculating fluid that passes through the sump strainer(s) may collect on the bottom surface of the FA bottom nozzle or FA spacer grids, causing resistance to flow through this path. The collection of sufficient debris on the fuel is postulated to impede flow into the fuel assemblies and core.

As described in Section 3.1, all U.S. PWRs have flow paths in the RV that may allow fluid to bypass the heated core during normal operations. Examples include flow through the BB region (for upflow BB plants) and/or flow through the UHSNs. During post-LOCA scenarios in which the core inlet becomes blocked by debris, these AFPs may provide sufficient flow to the core to remove decay heat at some point after the postulated LOCA. Consequently, it is postulated that these paths can assist in providing adequate flow to maintain LTCC. Additional PWROG work was initiated to examine the effectiveness of AFPs to provide cooling flow to the core that may support an increase in the fibrous debris limit compared to Reference 6-1. These TH analyses are described in detail in Volume 4. The relevant results are summarized here.

For this evaluation, four sets of analyses were performed to evaluate the AFPs for the U.S. PWR fleet:

1. Westinghouse design with upflow BB
2. Westinghouse design with downflow BB
3. CE design
4. B&W design

The plant models and inputs were selected to bound the plants in each class.

The overall goal of this analysis was to evaluate the adequacy of RV AFPs for maintaining LTCC following switchover to recirculation and the postulated formation of a highly resistive debris bed at the core inlet for a large hot leg break LOCA scenario for U.S. PWR plant designs. The objectives for this analysis were met. Specifically, each analysis simulated the evolution of debris bed formation over a range of conditions and determined the following four parameters:

1. The minimum time that complete core inlet blockage can occur and meet the acceptance criteria defined in Section 3.7. This time is defined as  $t_{block}$  and represents the earliest possible time for

which chemical precipitates can be tolerated on a completely formed fiber and particulate debris bed at the core inlet, which is assumed to lead to complete core inlet blockage. This value is compared to results from chemical effects testing contained in Volume 5.

2. The maximum resistance at the core inlet that can occur prior to reaching  $t_{block}$  and meet the acceptance criteria defined in Section 3.7. This parameter is defined as  $K_{max}$  and represents the resistance of a fiber and particulate only bed that can be tolerated from the time of SSO to  $t_{block}$ , the earliest allowable time of complete core inlet blockage. This value is compared to the results from subscale head loss testing contained in Volume 6 to establish an upper bound on the amount of particulate and fibrous debris that can be tolerated at the core inlet.
3. The resistance at the core inlet that begins to divert flow into the AFP. This parameter is defined as  $K_{split}$ . The subscale head loss testing has defined a correlation between the amount of fiber and an equivalent form-loss coefficient as discussed in Volume 6.  $K_{split}$  can then be used to define how much fiber accumulates at the core inlet before flow is diverted to the AFP.
4. The flow split between the core inlet and the AFP after  $K_{split}$ . This parameter is defined as  $m_{split}$ . Combined with  $K_{split}$  and the subscale head loss test results contained in Volume 6,  $m_{split}$  will be used to track where the debris accumulates after flow is diverted to the AFP.

The values that were determined for each plant category are discussed separately below. A summary of the results for  $K_{max}$  and  $t_{block}$  is provided on Table 6-1. These values and curves are used in Section 6.4 to track the fiber accumulation in the RV and to check to ensure acceptable results. Given that these analyses are conservative representations of a number of plants, margin may be available to individual plants by performing plant-specific analyses to calculate the parameters above using the same methods described in Volume 4.

### 6.1.1 Westinghouse Upflow Plant Category

1. The minimum time that complete core inlet blockage can be tolerated ( $t_{block}$ ) was found to be 143 minutes (2.38 hours).
2. The maximum resistance at the core inlet that can be tolerated prior to reaching complete core inlet blockage ( $K_{max}$ ) was found to be  $5 \times 10^5$ .
3. The resistance at the core inlet that begins to divert flow into the AFP ( $K_{split}$ ) was found for a range of ECCS flow rates. These results are shown in Figure 6-1.
4. The flow split between the core inlet and the AFP after  $K_{split}$  ( $m_{split}$ ) was found for a range of ECCS flow rates. A curve that bounds the results was also developed. These results are shown in Figures 6-2 and 6-3.

### 6.1.2 Westinghouse Downflow Plant Category

1. The minimum time that complete core inlet blockage can be tolerated ( $t_{block}$ ) was found to be 260 minutes (4.33 hours).

2. The maximum resistance at the core inlet that can be tolerated prior to reaching complete core inlet blockage ( $K_{max}$ ) was found to be  $4.75 \times 10^5$ .
3. The resistance at the core inlet that begins to divert flow into the AFP ( $K_{split}$ ) was found for a range of ECCS flow rates. These results are shown in Figure 6-4.
4. The flow split between the core inlet and the AFP after  $K_{split}$  ( $m_{split}$ ) was found for a range of ECCS flow rates. A curve that bounds the results was also developed. These results are shown in Figure 6-5.

### 6.1.3 Combustion Engineering Plant Category

1. The minimum time that complete core inlet blockage can be tolerated ( $t_{block}$ ) was found to be 333 minutes (5.6 hours).
2. The maximum resistance at the core inlet that can be tolerated prior to reaching complete core inlet blockage ( $K_{max}$ ) was found to be  $6.5 \times 10^6$ .
3. The resistance at the core inlet that begins to divert flow into the AFP ( $K_{split}$ ) was found for a range of ECCS flow rates. These results are shown in Figure 6-5.
4. The flow split between the core inlet and the AFP after  $K_{split}$  ( $m_{split}$ ) was found for a range of ECCS flow rates. A curve that bounds the results was also developed. These results are shown in Figures 6-7 and 6-8.

### 6.1.4 Babcock and Wilcox Plant Category

1. The minimum time that complete core inlet blockage can be tolerated ( $t_{block}$ ) was found to be 20 minutes (0.33 hours).
2. The maximum resistance at the core inlet that can be tolerated prior to reaching complete core inlet blockage ( $K_{max}$ ) was found to be  $1 \times 10^8$ .
3. The resistance at the core inlet that begins to divert flow into the AFP ( $K_{split}$ ) can be assumed to be exceeded at 20 minutes (or the time of sump switchover).
4. The flow split between the core inlet and the AFP after  $K_{split}$  ( $m_{split}$ ) can be assumed to be 1.0 for all times after  $K_{split}$  is exceeded.

Table 6-1 Summary of Thermal-Hydraulic Output Parameters		
Plant Type	$K_{max}$ (-)	$t_{block}$ (min)
Westinghouse Upflow	$5.0 \times 10^5$	143
Westinghouse Downflow	$4.75 \times 10^5$	260
CE	$6.5 \times 10^6$	333
B&W	$1.0 \times 10^8$	20



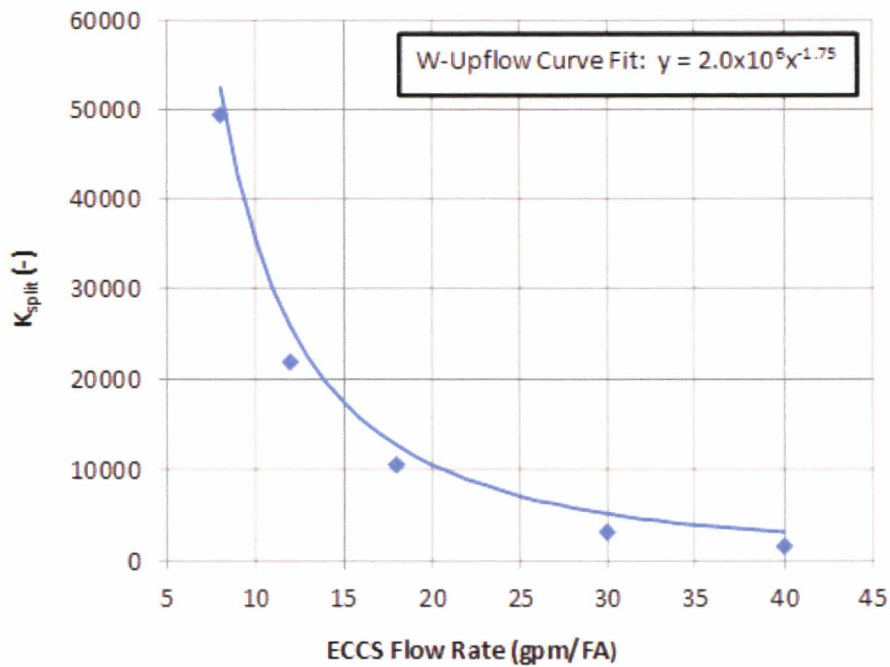


Figure 6-1  $K_{split}$  as a Function of ECCS Recirculation Flow Rate from Westinghouse Upflow Analysis

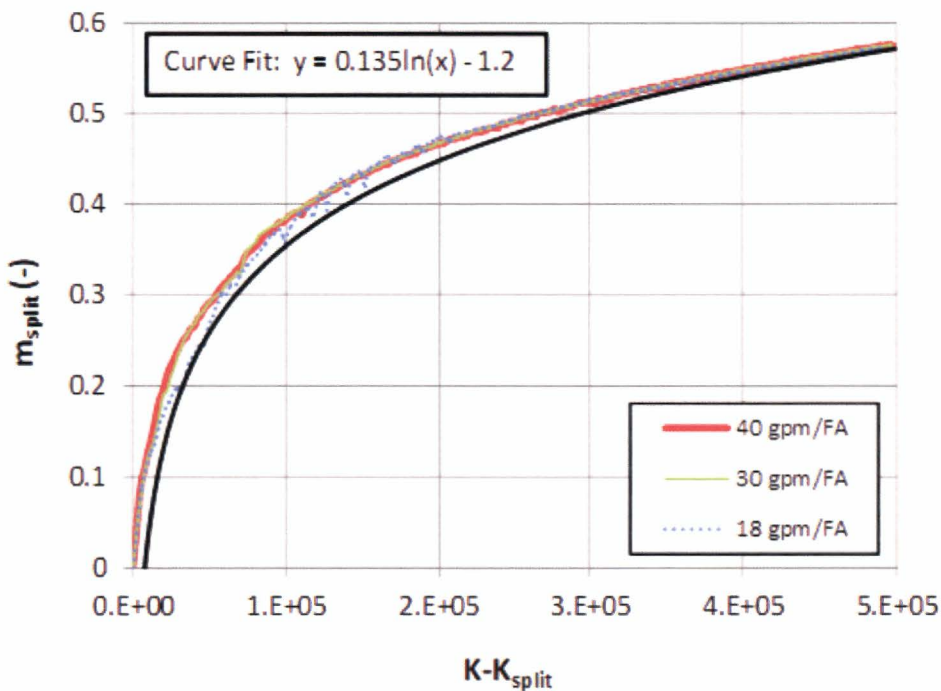
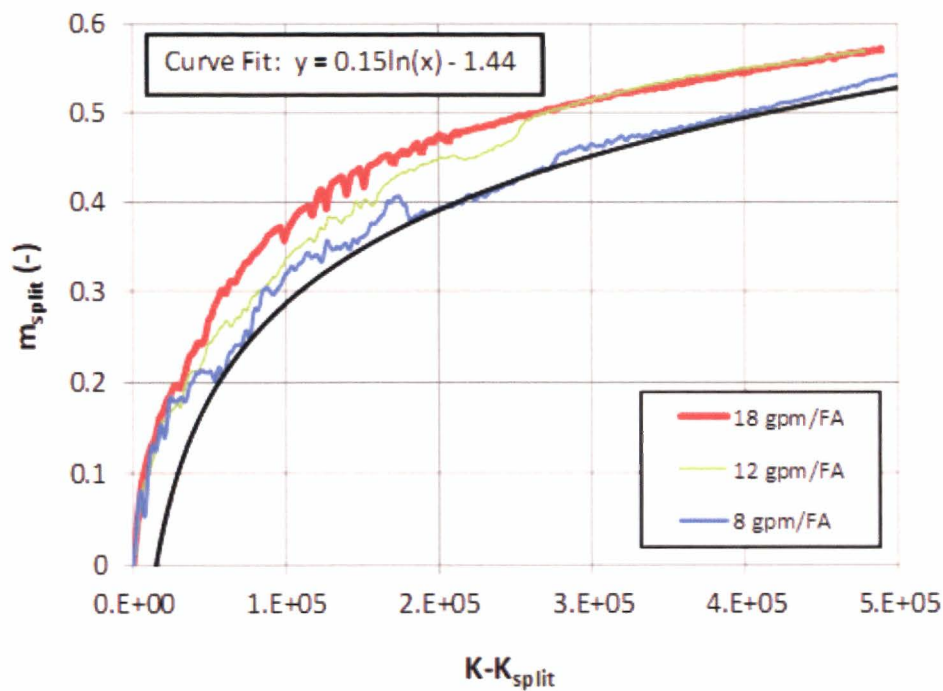
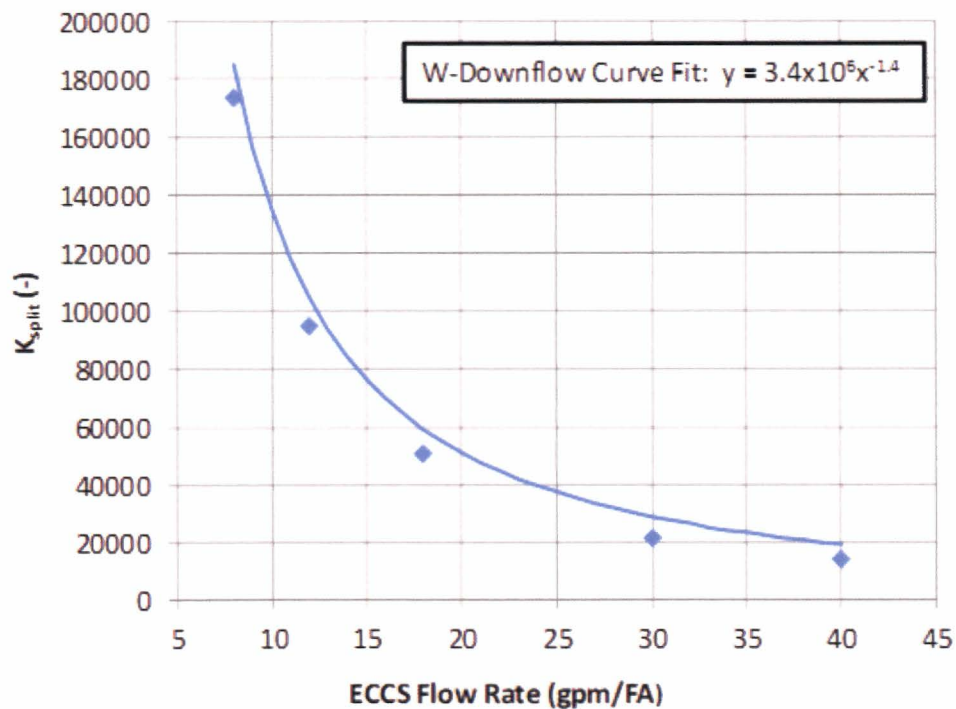


Figure 6-2 Fraction of ECCS Recirculation Flow through the BB following  $K_{split}$  from Westinghouse Upflow Analysis for Recirculation Flow Rates Greater than 18 gpm/FA



**Figure 6-3 Fraction of ECCS Recirculation Flow through the BB following  $K_{split}$  from Westinghouse Upflow Analysis for Recirculation Flow Rates Less than or Equal to 18 gpm/FA**



**Figure 6-4  $K_{split}$  as a Function of ECCS Recirculation Flow Rate from Westinghouse Downflow Analysis**



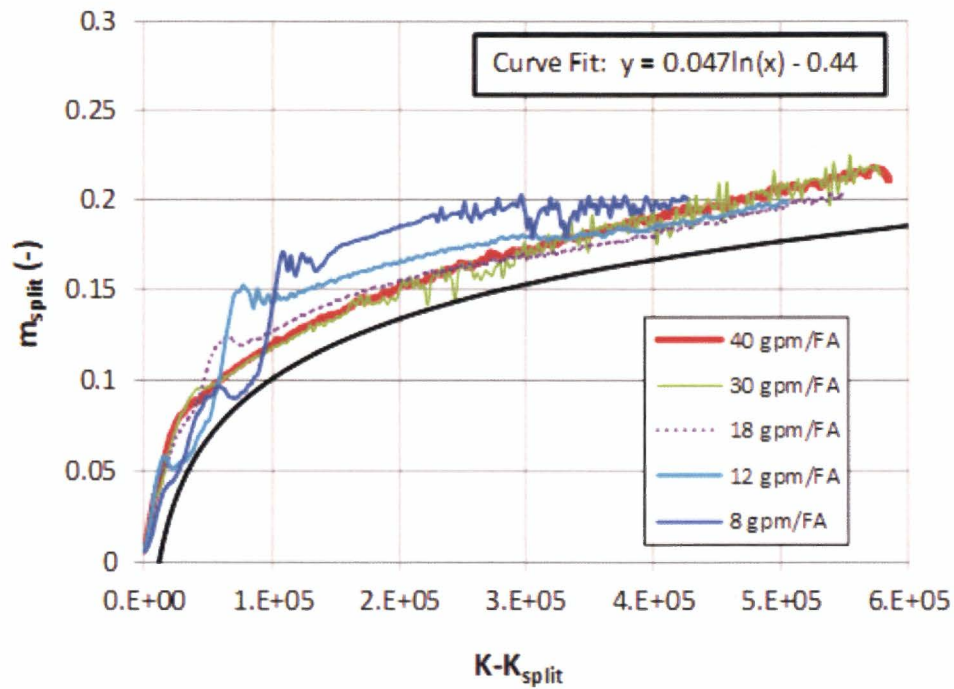


Figure 6-5 Fraction of ECCS Recirculation Flow through the BB following  $K_{split}$  from Westinghouse Downflow Analysis

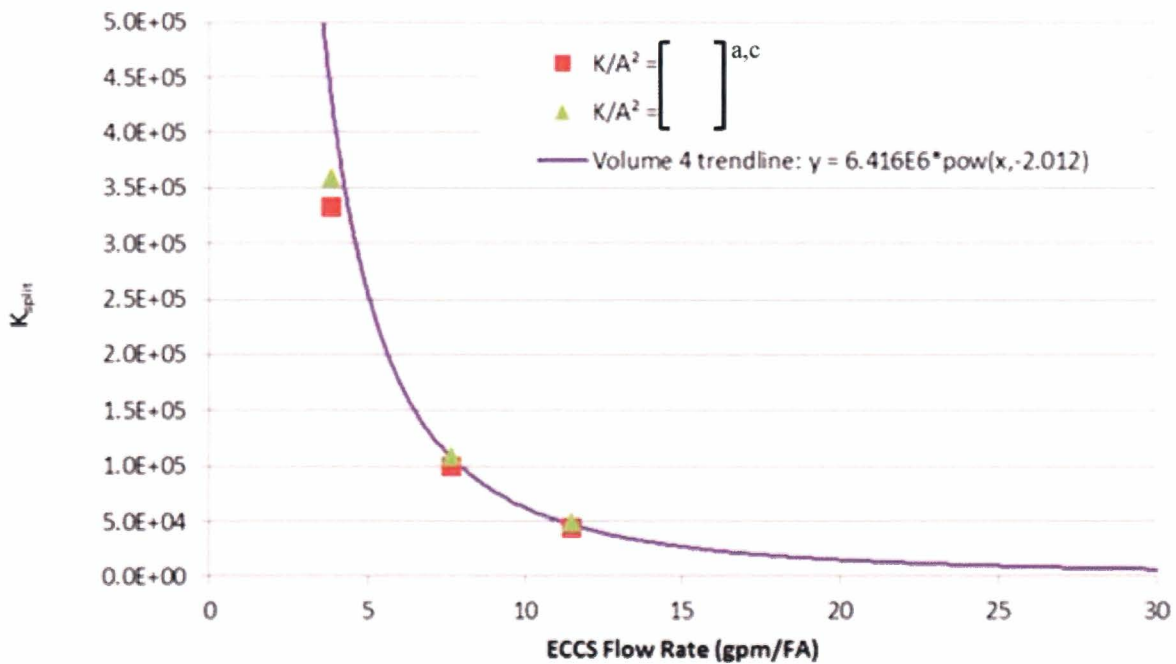


Figure 6-6  $K_{split}$  as a Function of ECCS Recirculation Flow Rate from CE Analysis

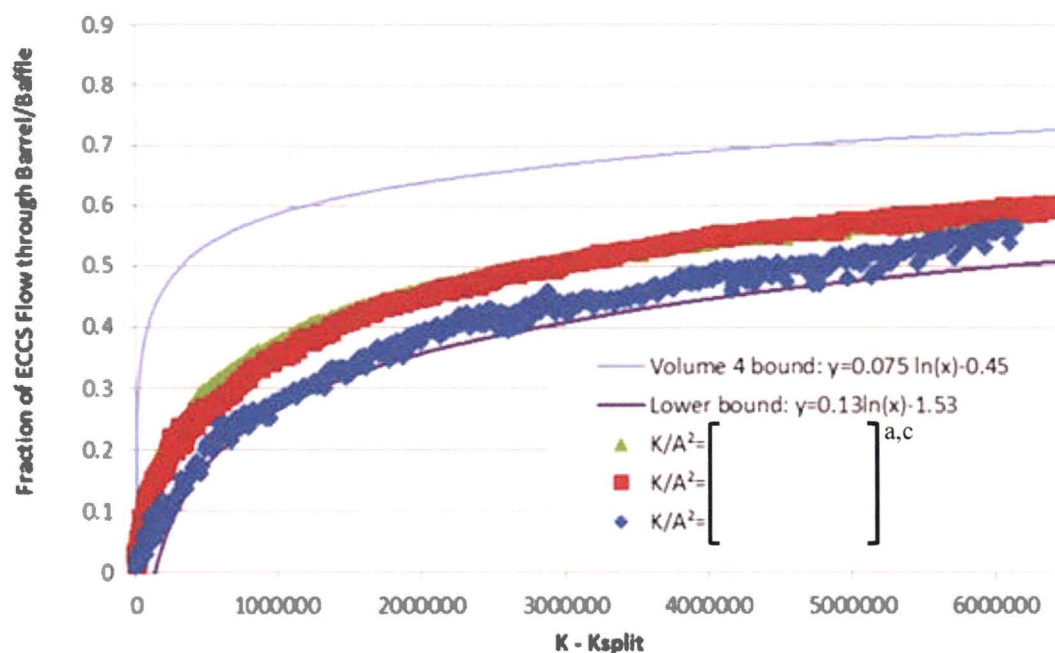


Figure 6-7 Fraction of ECCS Recirculation Flow through the BB following  $K_{split}$  from CE Analysis for Barrel/Baffle Resistance  $K/A^2 = [ ]^{a,c}$

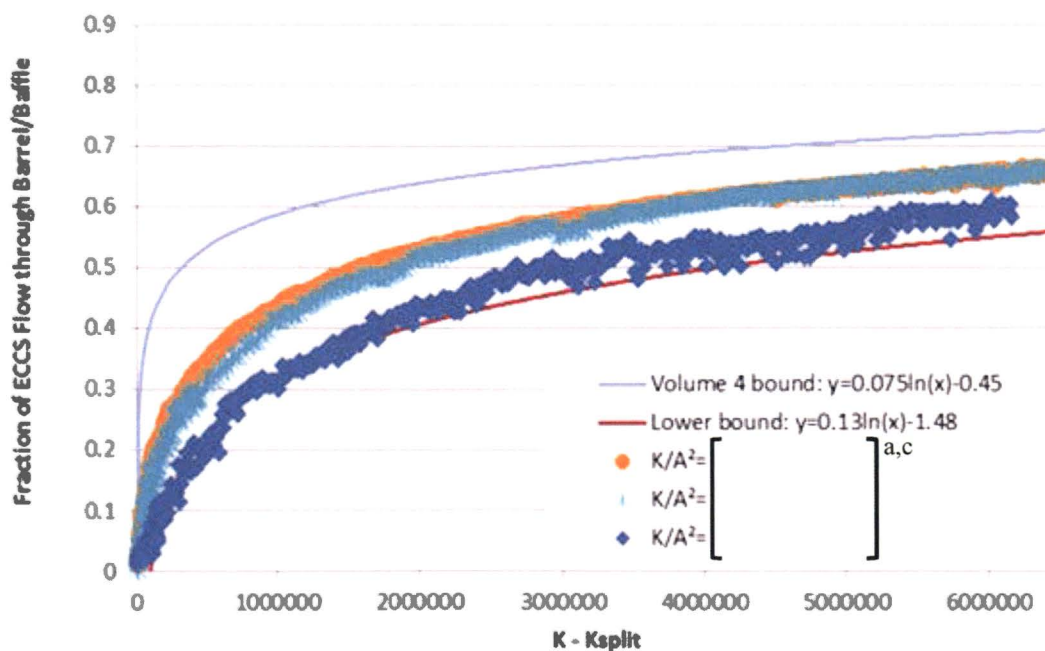


Figure 6-8 Fraction of ECCS Recirculation Flow through the BB following  $K_{split}$  from CE Analysis for Baffle Resistance  $K/A^2 = [ ]^{a,c}$

## 6.2 CHEMICAL PRECIPITATE FORMATION

As part of this comprehensive program, the experimental study of the chemical products that may form as certain containment materials are exposed to the recirculating coolant in the containment sump under accident conditions was undertaken. The details of this study are provided in Volume 5. The relevant results are summarized here.

The ability of chemical products to clog a fibrous debris bed was demonstrated in WCAP-16793-NP-A Rev. 2 (Reference 6-1). To improve on the fibrous debris limits set in WCAP-16793-NP-A, Rev. 2, the creation of chemical products that would reach the core becomes a critical phenomenon. Determination of the timing of chemical production in the post-LOCA environment is complicated by the large number of possible debris mixtures that could be generated, in combination with variations in coolant chemistries and coolant temperature profiles. For this reason, a large number of autoclave tests were designed to span the range of possible conditions in the industry (based on responses from two industry surveys). There were 45 test groups that represented conditions either at a single plant or a group of 2 to 4 plants. Additional tests were performed to explore how variations in different test parameters affected the generation of chemical products. Variations in pH, debris dispersion, and material quantities were explored.

The purpose of the testing was to investigate post-accident corrosion, dissolution, and precipitation reactions by running autoclave experiments that simulated post-LOCA plant conditions. The timing of any precipitation reactions ( $t_{chem}$ ) was of primary importance, since the early generation of chemical products in conjunction with a core inlet debris bed could block the core flow when high flow must be maintained ( $t_{chem} < t_{block}$  – see Section 6.1 for definition of  $t_{block}$ ), whereas later precipitation and core blockage could be tolerated because adequate coolant flow could be achieved through AFPs ( $t_{chem} > t_{block}$ ).

Tested materials were exposed to representative containment sump conditions as determined by the industry survey responses mentioned above. Both the containment sump chemistries and temperatures were representative of the post-LOCA scenario being simulated. Water samples were taken for chemical analysis, turbidity measurements, and timed filtration tests. The results were used to screen plants for the onset of chemical product generation.

The chemical effects tests demonstrated that for most plants the generation of chemical products was delayed beyond 6 hours (360 minutes). This conservatively exceeds all values of  $t_{block}$  (Table 6-1), the time when sufficient core cooling will be provided by flow through AFPs available within the RV to cool the core, per Section 6.1.

A method was also provided for plants to demonstrate that chemical effects are delayed beyond the time when AFPs can provide sufficient core cooling (i.e.,  $t_{chem} > t_{block}$ ). Plants have two options to demonstrate delayed chemical effects:

1. Showing that bounding plant conditions match test conditions producing an acceptable delay of chemical effects.

2. Establishing that aluminum release and plant pH and temperature conditions preclude aluminum precipitation until after the time when the core can be cooled by AFPs. This can be accomplished by reference to a precipitation map provided in Volume 5.

Option 2 is possible because the testing demonstrated that under a wide range of representative plant conditions, the precipitation of aluminum was the only chemical process that produced significant chemical effects. Option 2 may be useful if a plant makes a modification in their projected post-LOCA conditions such that the plant no longer matches any of the conditions tested in this research.

### 6.3 CORE INLET DEBRIS LIMIT

Core inlet debris limits are determined using experimental data from the subscale test facility. The details of the test facility and experiments are provided in Volume 6. The relevant results are summarized here.

The subscale facility is a well-scaled test apparatus that represents approximately one-quarter of a full-area FA. The facility is designed to conduct systematic separate effects tests under well-controlled laboratory conditions in order to generate fundamental debris bed resistance data. The facility is capable of operating over a wide range of conditions representative of those expected in a PWR during the post-LOCA phase of a postulated LBLOCA.

When defining the core inlet debris limits for a large HLB, it is assumed that debris laden coolant entering the RV through the ECCS during sump recirculation will be transported to the core inlet region where it has the potential to collect on fuel components. The core inlet region is defined as the region extending downstream of the lower core plate to the first spacer grid. This region includes the FA lower end fitting and any additional filtering grids that the specific fuel design may have (e.g., Westinghouse P-grid) before reaching the first spacer grid. This region is assumed to be part of the non-boiling region of the core and consists of single phase liquid. A detailed description of the core inlet geometries tested in the subscale facility to define the final debris limits are provided in Sections 3.5.3 and 3.5.4, Volume 6 for Westinghouse and AREVA fuel products, respectively.

The core inlet debris limit, defined by the subscale facility testing, considers only fibrous and particulate debris constituents and it is assumed that the arrival of significant chemical precipitates results in complete core inlet blockage. Although this test program did not confirm this assumption experimentally, previous testing (Reference 6-1) has demonstrated that the collection of chemical precipitates on a fibrous debris bed > 15 g/FA results in high resistances such that flow through the core inlet is significantly reduced. Since the overall methodology described in this report assumes complete core inlet blockage with the arrival of chemical precipitates, there was no need to perform tests that included chemical precipitates in the subscale facility.

#### 6.3.1 Analysis of Subscale Final Limits Data

The scaling analysis presented in Volume 6 demonstrates that the subscale facility is comparable to a full-area FA in terms of distortions related to pressure drop across a debris bed. It has been shown that the geometric scale of the subscale facility has negligible distortion when compared to a full-area FA. It has also been shown that the dominant physical phenomena expected to drive debris bed head loss are reasonably preserved. Using the flow area ratio between the subscale and a full-area FA it is possible to

relate the subscale debris loading to that of a full-area FA. It is also possible to relate the subscale flow condition to that of the full-area FA using the same flow area ratio. It is noted that the debris loads presented in this section, in terms of g/FA, were scaled assuming a FA pitch of [                      ] If the FA pitch is different, than the debris load needs to be scaled to account for this difference. See Section 6.5.5, Step 8 of the method for verifying hot leg break debris limits.

Subscale testing determined that a low-flow condition was limiting because fiber penetration through the lower end fittings tested was minimized. Minimizing the quantity of fiber penetration resulted in a single debris bed on the upstream edge of the lower end fitting. Experimental results confirmed that, for the debris loadings tested, a single debris bed formed at the lower end fitting resulted in a higher overall pressure drop compared to tests performed at higher flow rates that created multiple beds within the test section. For this reason, the low flow tests are used to conservatively define the final core inlet debris limits.

Subscale testing also determined that capture geometry has a strong influence on the pressure drop across a debris bed. As a result, the subscale data sets used to define the final core inlet debris limits are different for each fuel vendor since their respective core inlet geometries are significantly different. Figure 6-9 shows the debris bed pressure drop as a function of fiber load (i.e., fiber mass), scaled to a full-area FA from the final limits data sets for Westinghouse and AREVA fuel. This is Figure 6-1 in Volume 6.



**Figure 6-9 Limiting Conditions from Subscale Head Loss Testing Scaled to a Full-Area Fuel Assembly**

Using the pressure drop data shown in Figure 6-9, a dimensionless form-loss coefficient can be calculated for the limiting subscale datasets. This parameter is defined as  $K_{test}$  and is different for the two core inlet geometries tested.

Recall that the TH analyses described in Section 6.1 calculated a value for  $K_{max}$  for each plant category. This parameter is the maximum resistance that can be tolerated at the core inlet due to fiber and particulate debris alone. Since the flow area at which the debris bed was built in the subscale facility is different than the flow area that the debris bed was modeled in the TH analysis,  $K_{test}$  cannot be compared directly to  $K_{max}$ .

First, an equivalent form-loss coefficient needs to be derived from the subscale form-loss coefficient ( $K_{test}$ ) for each of the four plant categories from the TH analysis. The equivalent form-loss coefficients are defined as  $K_{eq}$  and can be compared directly to  $K_{max}$  from the TH analyses. They are also used in conjunction with  $K_{split}$  and  $m_{split}$  to determine when the AFP is active and what the fraction of debris through the AFP is following  $K_{split}$ .

Using the core inlet pressure drop data shown in Figure 6-9, a dimensionless form-loss coefficient is calculated using:

$$K_{test} = \frac{2g_c dP}{\rho v^2} \quad \text{Equation 6-1}$$

where:

$dP$  = measured debris bed pressure drop

$\rho$  = liquid density

$v$  = average superficial velocity through the debris bed

Subscale testing was completed at low pressures using liquid at 130°F. At atmospheric pressure, the liquid density at the tested temperature is 61.55 lbm/ft<sup>3</sup>.

The average superficial velocity through the debris bed is calculated using:

$$v = \frac{\left( \frac{Q}{A_{column}} + \frac{Q}{A_{BN}} \right)}{2} \quad \text{Equation 6-2}$$

where:

$Q$  = volumetric flow rate prescribed during the test

$A_{column}$  = subscale column flow area

$A_{BN}$  = bottom nozzle flow area used in the subscale facility

Next, since the flow area of the subscale column is different from the flow area at which the resistance due to debris accumulation was simulated in the T/H analyses, an equivalent form-loss coefficient needs to be calculated by taking the ratio of the flow areas squared:

$$K_{eq} = K_{test} \frac{A_{TH}^2}{A_{column}^2} \quad \text{Equation 6-3}$$

where:

$A_{TH}$  = flow area used in the TH analysis to simulate resistance due to a debris bed

The equivalent form-loss coefficient calculated using Equation 6-3 can be compared directly to the TH results.

### 6.3.2 Westinghouse Fuel

Using Equations 6-1, 6-2, and 6-3, an equivalent form-loss coefficient can be calculated for each plant category considered in the TH analyses for Westinghouse fuel.

First, Equation 6-2 is used to calculate the average superficial velocity through the debris bed. The Westinghouse final dataset used the Final-Low flow reduction curve shown in Figure 3-8, Volume 6. From Section 3.4, Volume 6, the subscale column flow area is 16 in<sup>2</sup>. From Table 3-7, Volume 6, the Westinghouse tested bottom nozzle flow area is [ ]<sup>a,c</sup>

With the average superficial velocity calculated, the pressure drop data from Figure 6-9, along with the liquid density, is used to calculate the dimensionless form loss coefficient,  $K_{test}$ . Figure 6-10 shows  $K_{test}$  plotted as a function of cumulative fiber load for Westinghouse fuel.

Next, an equivalent form-loss coefficient is calculated for each plant category using Equation 6-3. Since the TH analyses for Westinghouse upflow and downflow BB plants used the same flow area, only three equivalent form-loss calculations are required; Westinghouse NSSS, CE NSSS, and B&W NSSS. From Section 6, Volume 4, the flow areas used in the TH analyses for the three NSSS designs are; [ ]<sup>a,c</sup> respectively.

Figure 6-11 shows the equivalent dimensionless form-loss coefficients,  $K_{eq}$ , for each NSSS design that is applicable to plants with Westinghouse fuel. Also shown in the figure are linear curve fits derived to fit the equivalent form loss-coefficient data. These curve fits are described in detail below and are used in the method for verifying the hot leg break in-vessel fiber limits, as described in Section 6.5, to calculate resistance at the core inlet. This is necessary to determine when the AFP activates and to determine the fraction of debris that travels through the AFP once it activates.



**Figure 6-10 Subscale Dimensionless Form-Loss Coefficient for Westinghouse Fuel**



**Figure 6-11 Subscale Equivalent Dimensionless Form-Loss Coefficients for Various NSSS Designs with Westinghouse Fuel**



The equivalent form-loss coefficient curve fits are broken into three discrete regions that are related to the physical particulate capture mechanisms present in a fibrous debris bed as observed in the subscale testing. For the Westinghouse core inlet fuel geometry, at fiber loads less than [ ]<sup>a,c</sup> the fiber bed formed at the core inlet is not an efficient particulate filter. Since only a small fraction of the total injected particulate load captures in the fiber bed, the pressure drop, and thus, the dimensionless resistance remain relatively low. As the fiber load increases beyond [ ]<sup>a,c</sup> the filtration efficiency improves, because of the additional fiber and particulate, and the resistance rate increases. As the fiber load continues to increase beyond [ ]<sup>a,c</sup> the debris bed is capturing particulates at nearly 100 percent efficiency and the rate of resistance increase is at its highest.

A simple linear relation between debris bed resistance and fiber load is used for each of the three regimes:

$$K_{eq} = m M_f + b \quad \text{Equation 6-4}$$

where:

$m$  = slope of linear relation

$M_f$  = cumulative fiber load (g/FA)

$b$  = y-intercept of linear relation

Table 6-2 provides the slope and y-intercept for the three regimes applicable to Westinghouse fuel for each of the three NSSS designs.

Table 6-2 Equivalent Dimensionless Form-Loss Coefficient Linear Relations for Various NSSS designs with Westinghouse Fuel						
NSSS Design	slope (m)			y-intercept (b)		
Westinghouse						
CE						
B&W						

With the equivalent form-loss from the subscale data defined, it can now be compared directly to the T/H analysis results to determine the limiting fiber load for debris bed formation at the core inlet. This is done by using the linear relation for regime 3, rearranging to solve for the mass of fiber and setting  $K_{eq}$  equal to  $K_{max}$ . Table 6-3 provides the results of this calculation for the four plant categories considered in the TH analysis. The Westinghouse upflow and downflow BB categories use the same relation for equivalent form-loss. Since  $K_{max}$  from the CE and B&W plant categories results in an equivalent resistance that is greater than the maximum debris load tested, the maximum debris load is chosen as the acceptable fiber load for these plant categories. It is noted that these are the acceptable core inlet fiber loads prior to reaching  $t_{block}$ . For times after  $t_{block}$ , the core inlet fiber load can exceed the values shown in Table 6-3 since complete core inlet blockage can be tolerated at times after  $t_{block}$ . This is described further in Section 6.5.

Table 6-3     Acceptable Core Inlet Fiber Loads Prior to Reaching $t_{block}$ for Various NSSS designs with Westinghouse Fuel		
Plant Category	$K_{max}$	Acceptable Core Inlet Fiber Load (g/FA)
Westinghouse Upflow Barrel/Baffle	[	]
Westinghouse Downflow Barrel/Baffle		
CE		
B&W		
<b>Note:</b> <sup>1</sup> [                      ] <sup>a,c</sup> is the maximum debris load tested. $K_{max}$ is greater than the resistance due to this debris load.		

### 6.3.3 AREVA Fuel

The same approach is taken for determining equivalent form-loss coefficients for AREVA fuel.

The AREVA final dataset also used the Final-Low flow reduction curve shown in Figure 3-8, Volume 6. From Section 3.4, Volume 6, the subscale column flow area is 16 in<sup>2</sup>. From [                      ] <sup>a,c</sup> the AREVA tested bottom nozzle flow area is [                      ] <sup>a,c</sup>

With the average superficial velocity calculated, the pressure drop data from Figure 6-9, along with the liquid density, is used to calculate the dimensionless form loss coefficient,  $K_{test}$ . Figure 6-12 shows  $K_{test}$  plotted as a function of cumulative fiber load for AREVA fuel.

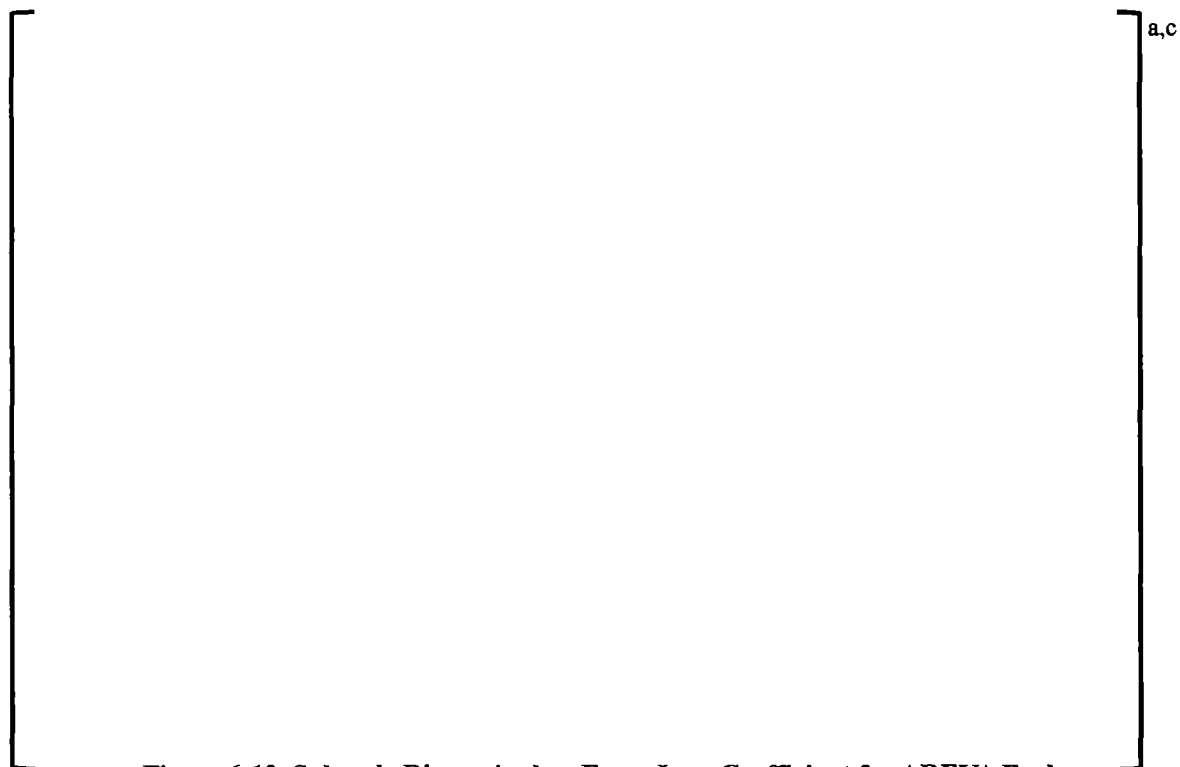


**Figure 6-12 Subscale Dimensionless Form-Loss Coefficient for AREVA Fuel**

Next, an equivalent form-loss coefficient is calculated for each plant category using Equation 6-3. Since the TH analyses for Westinghouse upflow and downflow BBs used the same flow area, only three equivalent form-loss calculations are required; Westinghouse NSSS, CE NSSS, and B&W NSSS. From Section 6, Volume 4, the flow areas used in the TH analyses for the three NSSS designs are; [ ]<sup>a,c</sup> respectively.

Figure 6-13 shows the equivalent dimensionless form-loss coefficients,  $K_{eq}$ , for each NSSS design that is applicable to plants with AREVA fuel. Also shown in the figure are linear curve fits derived to fit the equivalent form loss-coefficient data. These curve fits are described in detail below and are used in the method for verifying the hot leg break in-vessel fiber limits, as described in Section 6.5, to track the resistance at the core inlet. This is necessary to determine when the AFP activates and to determine the fraction of debris that travels through the AFP once it activates.



**Figure 6-13 Subscale Equivalent Dimensionless Form-Loss Coefficients for Various NSSS Designs with AREVA Fuel**

The equivalent form-loss coefficient curve fits are broken into three discrete regions that are related to the physical particulate capture mechanisms present in a fibrous debris bed observed in the subscale testing. For the AREVA core inlet fuel geometry, at fiber loads less than [ ]<sup>a,c</sup> the fiber bed formed at the core inlet is not an efficient particulate filter. Since only a small fraction of the total injected particulate load captures in the fiber bed, the pressure drop, and thus, the dimensionless resistance remain relatively low. As the fiber load increases beyond [ ]<sup>a,c</sup> the filtration efficiency improves because of the additional fiber and particulate, and the resistance rate increases. As the fiber load

continues to increase beyond [ ]<sup>a,c</sup> the debris bed is capturing particulates at nearly 100 percent efficiency and the rate of resistance increase is at its highest.

Table 6-4 provides the slope and y-intercept used in Equation 6-4 for the three regimes applicable to AREVA fuel for each of the three NSSS designs.

<b>Table 6-4      Equivalent Dimensionless Form-Loss Coefficient Linear Relations for Various NSSS designs with AREVA Fuel</b>						
NSSS Design	slope (m)			y-intercept (b)		
Westinghouse						
CE						
B&W						

a,c

With the equivalent form-loss from the subscale data defined, it can now be compared directly to the TH analysis results to determine the limiting fiber load for debris bed formation at the core inlet. This is done by using the linear relation from regime 2 for the Westinghouse categories and regime 3 for the CE and B&W plant categories, rearranging to solve for the mass of fiber and setting  $K_{eq}$  equal to  $K_{max}$ . Regime 2 is used to determine the acceptable fiber load for the Westinghouse plant categories in this case because  $K_{max}$  for the Westinghouse plant categories falls within regime 2. Table 6-5 provides the results of this calculation for the four plant categories considered in the TH analysis. The Westinghouse upflow and downflow BB categories use the same relation for equivalent form-loss. Since  $K_{max}$  from the B&W plant category results in an equivalent resistance that is greater than the maximum debris load tested, the maximum debris load is chosen as the acceptable fiber load for this plant category. It is noted that these are the acceptable core inlet fiber loads prior to reaching  $t_{block}$ . For times after  $t_{block}$ , the core inlet fiber load can exceed the values shown in Table 6-5 since complete core inlet blockage can be tolerated at times after  $t_{block}$ . This is described further in Section 6.5.

<b>Table 6-5      Acceptable Core Inlet Fiber Loads Prior to Reaching <math>t_{block}</math> for Various NSSS designs with AREVA Fuel</b>		
Plant Category	$K_{max}$	Acceptable Core Inlet Fiber Load (g/FA)
Westinghouse Upflow Barrel/Baffle		
Westinghouse Downflow Barrel/Baffle		
CE		
B&W		
Note: <sup>1</sup> [ ] <sup>a,c</sup> is the maximum debris load tested. $K_{max}$ is greater than the resistance due to this debris load.		

a,c

## 6.4 IN-CORE DEBRIS LIMIT

As has been described previously, debris may enter the RCS as early as the time that the plant is placed in sump recirculation. Because the debris is well mixed within the sump and the Stokes number is significantly less than one, it travels in proportion to the ECCS flow rate.

Once in the RCS, where the debris is transported depends on the break location, plant design, and operator actions. Most plants in the U.S. (Westinghouse UPI plants excluded) initially direct ECCS injection to the cold legs. For these plants, debris will initially approach the core inlet where testing has shown that it may capture below the heated core near the core inlet, either at the bottom nozzle or at the first mechanical spacer grid. If debris does not capture at this location, it will continue to the heated region of the core. As the transient progresses, debris may begin to enter the heated core through two possible mechanisms. First, the resistance to debris at the core inlet may build to the point that the AFP becomes active, directing flow and debris through the AFP to the core region. The TH analyses described in Section 6.1 identify the conditions under which the AFP becomes active. Second, the operator may take action to initiate HLSO in which all or a fraction of the ECCS flow is transferred to the hot leg to mitigate the buildup of boric acid in the core. The exact ECCS configuration after HLSO is plant-specific. However, after HLSO, some or all of the ECCS reaches the core from the top. If there is debris in this coolant, it may be introduced to the heated core. Therefore, the total amount of debris to reach the core must include the contribution from both the AFP and the hot leg.

The discussion in the following subsections provides the basis for a fiber limit of [ ]<sup>5c</sup> in the heated core region (i.e., in-core), which is in addition to the fiber limit established at the core inlet. This amount of fiber (and associated particulate) will not compromise core cooling or established BAPC actions.

### 6.4.1 Activation of Alternate Flow Path

The specific geometry of the AFP and how fluid from that region reaches the core is dependent on the plant design. TH analyses have shown that, in general, the flow patterns in the core are up through the hot fuel assemblies and down in the core peripheral and lower power assemblies regardless of plant design or the amount of blockage at the core inlet (see Section 6.1 for a detailed discussion and basis). For Westinghouse and CE plants with upflow BB designs and no pressure relief holes in the core barrel, debris will flow up through the BB region and join the core downflow on the periphery of the core near the top of the fuel assemblies. B&W plant designs and some Westinghouse upflow BB plant designs have pressure relief holes in the core barrel from near the core mid-plane to the top of the core. These are the locations that debris will pass into the core region, enter the peripheral fuel assemblies and join the core downflow.

For Westinghouse plants with downflow BBs, the BB region does not communicate with the top of the core and the AFP credited is the path through the upper head spray nozzles. As resistance due to the collection of debris at the core inlet builds, the downcomer level increases and eventually reaches the UHSN elevation. At this point, debris laden coolant will flow through the UHSN, drain through the upper guide tubes and reach the core exit where it will tend toward the core periphery and join with the pre-established core flow patterns described above.

Testing in the subscale loop demonstrated that debris entering the AFP will not block the flow paths in that region (Volume 6). The testing demonstrated that some debris will accumulate in the AFP without blocking the flow passages. However, it is conservative to neglect this accumulation to maximize debris transport to the core. Therefore, any debris that reaches the AFP will be assumed to travel on to the core.

#### 6.4.2 Post Hot Leg Switchover

For plants that initiate HLSO, coolant will enter the RCS in one or more hot legs. Depending on the time in the event that HLSO is initiated, it is likely that the sump strainer has filtered out most or all of the debris. However, there may be some debris remaining in the sump that introduces debris later in the event. In any case, the coolant and debris will either exit the break or reach the top of the core.

It is expected that some or all of the hot leg recirculation flow will exit the broken loop, taking debris with it back to containment, where it will be re-filtered before returning to the ECCS. However, it is conservative to neglect this break carryover of debris with respect to debris accumulation in the core. Therefore, any debris that enters the RV through the hot leg will be assumed to reach the core region.

#### 6.4.3 Justification for In-Core Debris Limit

In all scenarios, a number of pieces of information can be used to justify that [ ]<sup>sc</sup> of fiber can be tolerated in the heated core (in addition to what can be tolerated at the core inlet). This section provides the details of this information for any plant type that initially starts cold leg ECCS recirculation (including times after HLSO). UPI plants are discussed in Section 8.

##### 6.4.3.1 Debris Accumulation

Shortly after the time of SSO, the core is boiling, and the average void fraction can be as much as 50 percent or greater. Even after 6-12 hours, the decay heat is high enough to generate boiling in the core, and the void fraction is greater than 20 percent. Given that all or most of the debris reaches the core region within the first few hours, debris will be entering a highly voided core region.

The boiling process, in and of itself, precludes significant debris accumulation. While the general flow patterns in the core are well established by the TH analyses (Section 6.1), the local flow patterns are quite complex due to the nature of the boiling process. Boiling at any given location in the core is quite erratic. The instabilities of the boiling process introduce energy to the fluid that varies with time and location. In the event of debris beginning to accumulate at the leading edge of a spacer grid (similar to what is seen at the core inlet – see Figure 6-14), the perturbations of the local conditions due to this small debris buildup will lead to boiling that will dislodge the debris before a large, contiguous bed can be established that significantly interrupts the core flow patterns. Therefore, debris beds like those seen at the core inlet will not establish in the presence of boiling. Rather, local blockages around spacer grid dimples, springs and other areas with small clearances are expected that do not significantly impact decay heat removal or create conditions that could lead to premature BAP (see Figure 6-15).

The discussion above is supported by testing sponsored by the PWROG as described in WCAP-17360 (Reference 6-3). This testing was performed to investigate the heat transfer behavior of buffered and unbuffered boric acid solutions with and without debris under conditions simulating that expected during

the LTCC phase following a post-LOCA transient. The testing considered a 3x3 heated rod bundle with a heated length of 22 inches. The loop was open to the atmosphere at the top and fluid was provided to the bottom of the bundle to replace the fluid lost to boiling. Debris was introduced with the fluid and continually concentrates in the test section since no fluid was drawn from the top. The testing included an equivalent fiber load of [ ]<sup>a,c</sup> with a p:f ratio of [ ]<sup>a,c</sup> for a total debris loading of [ ]<sup>a,c</sup> of fiber and particulate. ALOOH was included as a chemical precipitate surrogate.

The results of the testing program documented in Reference 6-3 indicate, in part, that for the test rig design and debris loadings used, [ ]<sup>a,c</sup>

These test results represent a cold leg break scenario. [ ]<sup>a,c</sup>

The same response can be expected for a hot leg break scenario when debris begins to reach the core through the AFP or after HLSO. The TH analyses described in Section 6.1 show that the flow through the AFPs are in excess of the boil-off rate of the core. To that end, a significant amount of liquid is reaching and exiting the break. Since the debris is traveling with the liquid, it is expected that a significant portion of the debris will exit the break and return to containment and be re-filtered on the sump strainer before returning to the RCS. The amount of debris that exits the break (or remains in the core) is dependent on plant conditions. While a plant-specific analysis may try to quantify this effect, the general solution proposed by the PWROG is to neglect any debris exiting the break and assume that any debris reaching the core remains in the core. To that end, the 3x3 testing indicates that up to [ ]<sup>a,c</sup> of fiber per FA can be tolerated in the core region in the presence of boiling.

As the transient progresses, the core decay heat will decrease, which decreases boiling in the core. In particular, lower power regions of the core (i.e., the core periphery) may stop boiling while the higher power assemblies continue to boil. In these liquid only regions of the core, it may be possible that debris may begin to accumulate on the leading edge of the spacer grid. Subscale testing has demonstrated that flow through a debris bed made of fiber and particulate only will continue for fairly high amounts of fiber (on the order of [ ]<sup>a,c</sup>). The addition of chemical precipitates may preclude flow through established debris beds of more than 15 g/FA. However, any debris bed that forms in the liquid only region of the core will not extend across the entire core, because boiling continues in the higher power assemblies. The open lattice fuel design will allow flow around any of these types of blockages. Should any region near a blockage become starved for flow, the fluid will heat up and eventually boil. The boiling will either dislodge a debris bed (if it formed on the top side of the spacer grid), or the decreased density of the boiling region will draw fluid in to replace the boiled off fluid (if the debris beds have formed on the bottom side of the grids and are not dislodged by boiling). In either case, the open lattice design of the fuel will ensure that the core is cooled and that localized regions with increased boron concentration will not develop even for blockages across small portions of the core.

While boiling precludes buildup at the leading edge of a spacer grid, the energy from the boiling process may force debris into internal grid locations such as the springs or dimples (see Figure 6-15). The limited size of these geometric features limits the expanse of the debris collection such that the effects would be localized. However, the boiling process will continue to force liquid either through the debris collection or very near it such that cooling will continue. In the extreme case that some volume in the spacer grid around a single rod is starved of flow, axial conduction through the cladding to the region just upstream or downstream of the blockage is sufficient to keep the cladding cool as demonstrated in WCAP-16793-NP-A, Rev. 2 (Reference 6-1). The open lattice design of the fuel assemblies ensures that fluid is free to flow just upstream and downstream of these localized blockages.

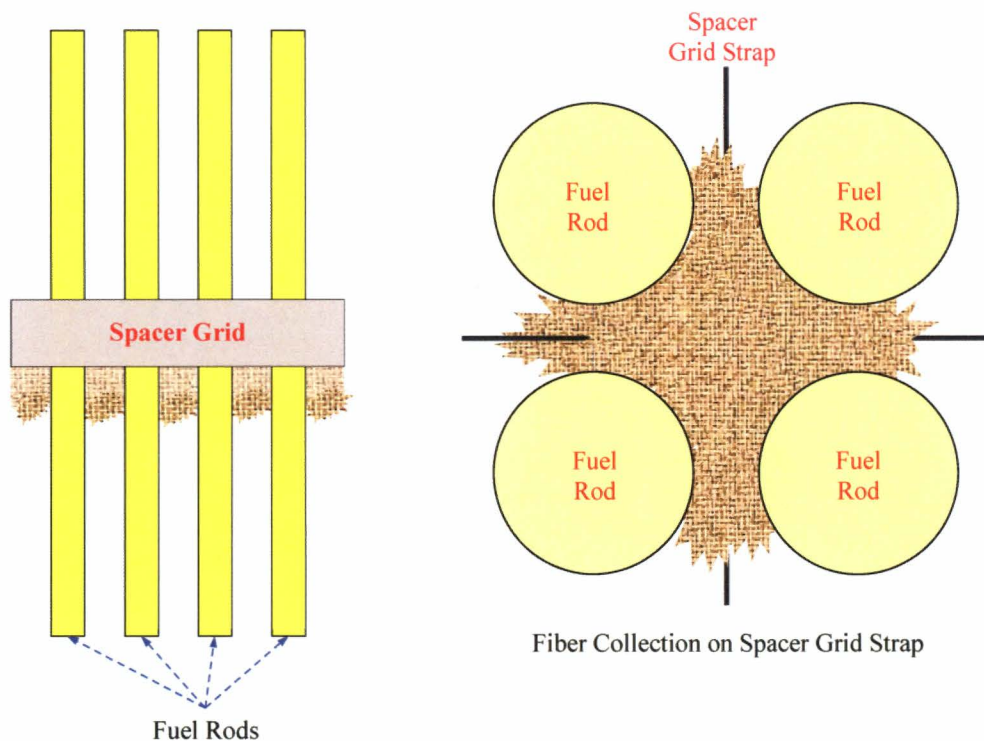


**Figure 6-14 Fiber Collection on Leading Edge of Spacer Grid**



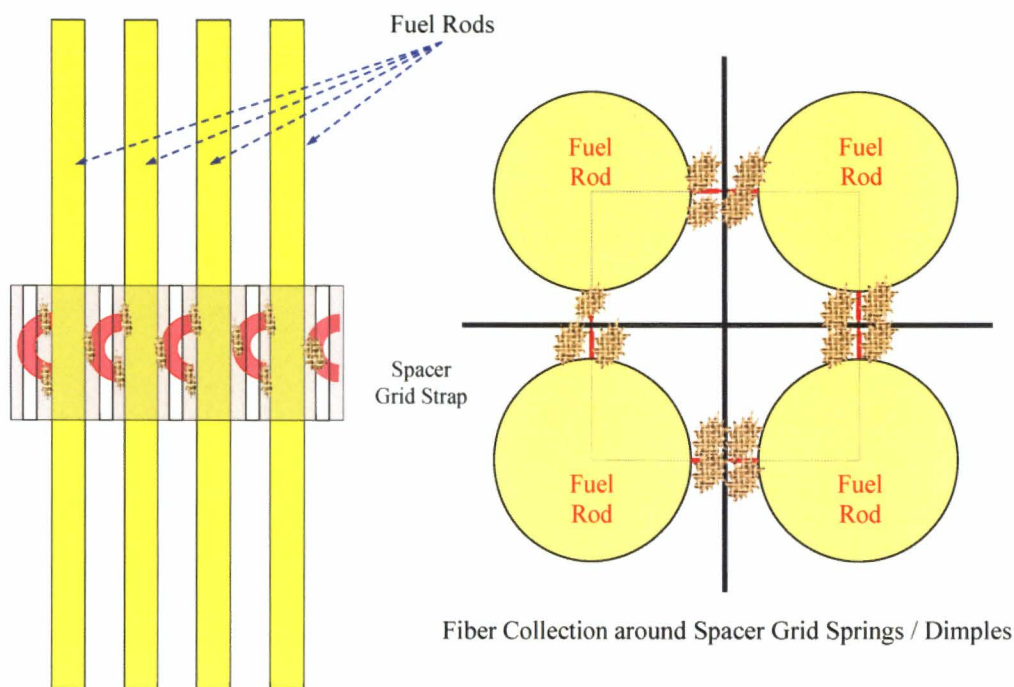


**Figure 6-15 Fiber Collection on Internal Springs of Spacer Grid**

#### 6.4.3.2 Effect of Debris on Cladding Heat Removal

Under large HLB conditions, break flow is approximately equal to the flow supplied by the emergency core cooling system (ECCS) less boil-off and the liquid needed to account for the slow inventory increase in the reactor vessel due to the diminishing decay heat. Under this condition, the mechanisms for particulate retention in the reactor vessel are limited. Some fraction of particulate entering the reactor vessel may settle out of the flow in the lower plenum, and some fraction of particulate is expected to be captured within any fibrous debris beds that may have formed at or near the core inlet. There are no mechanisms for particulates to concentrate in the suspended fluid since there is a continuous throughput of liquid from the ECCS injection points to the break. Particulates that do not settle out, penetrate, or bypass any fibrous debris beds will continue to transport with the liquid through the reactor vessel and out the break. As such, the concentration of particulates in the reactor vessel liquid will be less than or equal to the particulate concentration within the sump pool.

When unrealistic assumptions are made regarding the arrival time and accumulation rate of debris at the core inlet, it is possible to retard the throughput of liquid from the ECCS injection points to the break. Under this condition, particulate could concentrate in the reactor vessel liquid inventory. However, the WCAP-17788, Volume 4 thermal-hydraulic analyses, which applied these unrealistic assumptions, demonstrated that any reduction in liquid throughput due to debris accumulation at the core inlet would be temporary. As such, the resulting concentration buildup of particulate would also be temporary and would not result in significant increases in the reactor vessel particulate load.

Given that there is no mechanism for debris concentration in the core following a HLB, the effect of particulates on the core TH response following a HLB will be bounded by the effects of a CLB where, much a like a boric acid precipitation scenario, debris can concentrate (see Section 7 for details).

#### 6.4.4 Summary and Conclusion

The discussion in the preceding subsections provides the basis for a conservative in-core fiber limit of [ ]<sup>a,c</sup>. This limit is in addition to the amount of fiber that can be tolerated at the core inlet. This amount of fiber (and associated particulate) will not compromise core cooling or established BAPC actions. This value is used in Section 6.5 to ensure acceptable results.

### 6.5 METHOD FOR VERIFYING HOT LEG BREAK IN-VESSEL DEBRIS LIMITS

Using the information from the previous sections, a method for calculating plant-specific fiber limits for large HLBs for cold leg recirculation plants was developed. (While this Section 6 pertains mainly to cold side recirculation plants, the method presented here is flexible enough to also analyze UPI plants. Guidance on how to do this is provided as needed below.) The details of this method are described here in enough detail that plant engineers can determine a plant-specific fiber limit using the calculation method of their choosing. Demonstration cases using the described method are also provided for use by utilities as an additional way of validating their calculations. The sections below are intended to provide the information necessary for a utility engineer to implement the method and replicate the results.

The following process can be explicitly followed for all plant categories. However, as discussed in Volume 4, Section 11.2.3, the application of this method and the results of the thermal-hydraulic analyses demonstrate that the operating B&W plants will have an in-vessel fiber limit that corresponds to the in-core fiber limit. Therefore, the calculations described need not be implemented for the operating B&W plants, and they can declare an in-vessel fiber limit of [ ]<sup>a,c</sup>. The sump fiber load can then be determined using Equation 6-27 from Section 6.5.3 with  $M_{f,RV}(t_{end}) = [ ]^{\text{a,c}}$  and plant specific values for strainer efficiency and ECCS flow rates.

#### 6.5.1 Overview

Following a large HLB, debris can accumulate in the RV in a number of locations depending on the time in the event and plant-specific parameters. For the purposes of tracking the fiber, there are several key times that should be noted:

1. Beginning of Sump Recirculation
2. Activation of AFP
3. Complete Core Inlet Blockage
4. BAPC Action

Fiber injection begins at the time of SSO. Thereafter, the rate of fiber injection to the RV is a function of ECCS flow rate, sump strainer bypass, containment spray flow rate, and total system liquid mass, as

described in greater detail below. Knowing the rate of injection and an estimate of the initial fiber load, a mass of fiber injected into the system as a function of time can be calculated.

With the exception of UPI plants, all of the ECCS recirculation flow to the RCS is initially through the cold legs. Consequently, the net ECCS flow rate reaching the RV LP is equal to the total ECCS flow rate, since the only path to the break at this point in the transient is through the RV. Neglecting hold-up and settling between the ECCS strainer and the RV, it is assumed that all debris that reaches the ECCS system will reach the RV LP.

The TH analyses described in Section 6.1 show that, for some period of time immediately after SSO, the flow into the core is only through the core inlet. That is, the AFP is not active in transporting debris to the core and debris buildup is only at the core inlet. As debris accumulates at the core inlet, the resistance through this flow path increases. Eventually, the BB channel or UHSNs will offer less resistance than the core inlet, and flow will begin to divert through this AFP as a result. Because of the relatively low mass of particulate and fibrous debris, the motion of the debris is tightly coupled to the fluid motion and is therefore assumed to be uniformly distributed throughout the fluid. As a result, flow through the AFP will take with it a fiber mass ratio equal to the mass flow ratio. During this period, debris continues to accumulate at the core inlet while also transporting a fraction to the core region by way of the AFP. If either  $K_{max}$  is reached (the maximum resistance due to debris that can be tolerated at the core inlet from fuel testing) or  $t_{chem}$  is reached (the time that chemical precipitates are calculated to form), the core inlet is assumed to become completely blocked, after which time debris will be delivered to the core via the AFP only. Finally, the operators will take some action to mitigate boric acid buildup in the core region. For most plants, this means that debris can potentially be introduced directly to the core exit. The timing of this action may occur at any point such that the AFP may or may not be active or the core inlet may or may not be blocked. Clearly, the events that occur during this time period are plant dependent (see Section 4.2). While not strictly rigorous, the above discussion is useful in tracking and discussing debris accumulation.

For every plant, there is a limit to the amount of fiber that can be tolerated within the RV. This limit is a combination of debris in the core itself as described in Section 6.4 and the debris at the core inlet as defined by subscale testing in Section 6.2. When a plant aligns ECCS to sump recirculation, some or all of the fiber that penetrates the sump strainers is transported through the ECCS to the RV. An understanding of the post-LOCA system response can be used to track where the fiber might end up in the RV such that a fiber limit can be calculated. The criteria are that: (1) the fiber accumulation in the heated region of the core does not exceed the in-core limit defined in Section 6.4 or (2) the fiber accumulation at the core inlet does not exceed the core inlet limit defined in Section 6.3. For all HLB and ECCS configurations, no credit is taken for debris that might exit the break. (For UPI plants, this means that after simultaneous recirculation is initiated, credit is not taken for debris lost out the cold leg break.) Therefore, the HLB debris limit is defined as the sum of the fiber that is captured at the core inlet and the heated core region (in-core):

$$M_{f,HLB} = M_{f,CI} + M_{f,in-core} \quad \text{Equation 6-11}$$

where,

$$M_{f,HLB} = \text{the total fiber mass limit for hot leg breaks}$$

$M_{f,CI}$  = the mass of fiber at the core inlet

$M_{f,in-core}$  = the mass of fiber in the heated core

The mass of fiber that reaches the heated core can travel through two paths, either the AFP or from hot leg recirculation (either UPI or after HLSO):

$$M_{f,in-core} = M_{f,AFP} + M_{f,CE} \quad \text{Equation 6-12}$$

where,

$M_{f,AFP}$  = the mass of fiber that reaches the heated core through the AFP

$M_{f,CE}$  = the mass of fiber that reaches the heated core through the core exit

### 6.5.2 Inputs

Several inputs are needed to perform this evaluation. Details of how to define these inputs are provided in the following sub-sections. The following fixed inputs are required:

- Time Step
- Plant Type
- Fuel Vendor
- Number of FAs
- Initial Sump Fiber Load

In addition to these fixed inputs, there are inputs that can vary within a range of values. Because it's not known whether the plant will be limited by the core inlet fiber load or the in-core fiber load; two separate cases will need to be analyzed. The first case biases the inputs in order to maximize the core inlet fiber load, and the other case biases the inputs to maximize the in-core fiber load. Recommendations for each of these inputs are discussed in detail in the subsections below, with guidance on how to calculate the inputs (i.e., where to obtain min/max volumes, what conditions to determine min/max flow rates, whether to include containment sprays, etc.). Table 6-6 presents the combination of inputs that should be used to calculate the two limiting cases.

- Time of SSO
- Active Sump Volume
- Time of Chemical Effects,  $t_{chem}$
- Sump Strainer Bypass Fraction

- CSS Flow Rate
- ECCS Flow Rate after SSO
- Time of HLSO and Resulting Flow Splits

#### 6.5.2.1 Time Step

Because this problem contains time varying boundary conditions, specifically the core inlet resistance and ECCS configuration, an iterative solution with respect to time is necessary.

Time step sensitivity should be performed in order to demonstrate stable results calculated by the chosen time step. The time step should be small enough such that the important processes, namely the injection of fiber, do not change by more than 1% as a result of a change in time step. A starting value of 100 seconds is recommended.

#### 6.5.2.2 Plant Type

The values for  $t_{block}$  as well as the correlations used to calculate  $K_{split}$  and  $m_{split}$  are dependent on plant type, as described in Section 6.1. Therefore, the plant design must be identified. The plant types of interest for this analysis are:

1. B&W Design
2. Westinghouse Upflow BB Design
3. Westinghouse Downflow BB Design
4. CE Design

#### 6.5.2.3 Fuel Vendor

The core inlet head loss with debris is dependent on fuel vendor, as described in Section 6.3. Therefore, the fuel vendor must be identified. The fuel vendors of interest for this analysis are:

1. AREVA
2. Westinghouse

#### 6.5.2.4 Number of Fuel Assemblies

The total number of fuel assemblies is used to calculate the value of  $K_{split}$ , as described in Step 6 of Section 6.5.3. This value is fixed for each plant and therefore does not need to be parameterized.

#### 6.5.2.5 Initial Sump Fiber Load

The initial sump fiber load is plant dependent and should bound the largest total sump fiber load 30 days after event initiation. This fiber load consists only of the fiber fines in the sump, not the total of all fiber, as described in Section 3.5.

#### 6.5.2.6 Time of Sump Switchover

The time of SSO,  $t_{SSO}$ , also known as sump recirculation or recirculation activation, defines the start of the analysis, as it marks the beginning of fiber injection into the RV. An early SSO will result in more fiber being injected through the initial flow path prior to operator action to mitigate boric acid buildup (e.g., HLSO, etc.), which will be more likely to challenge the  $K_{max}$  criterion. A late SSO will have the opposite effect, decreasing the fiber accumulated at the core inlet and posing a greater challenge to the in-core fiber limit.

The analyzed range of  $t_{SSO}$  should therefore bound all possible times for a large hot leg break. This means that a calculation of minimum  $t_{SSO}$  should consider the possibility for maximum ECCS and containment sprays depleting the RWST as well as minimal delays for the necessary actions. Meanwhile the maximum  $t_{SSO}$  should consider all conditions that would delay the re-alignment to sump suction, such as the minimum rate of RWST depletion and maximum delays for action during a large HLB.

#### 6.5.2.7 Active Sump Volume

The active sump volume is the volume of liquid in the containment sump that actively participates in the recirculation process. Hold-up volumes and “dead” volumes within the sump should be excluded. This volume acts as the system inventory when calculating the concentration of debris to be injected into the RCS. A maximum value will therefore dilute the debris concentration and decrease the rate of injection, while a minimum value will concentrate the debris and increase the rate of injection. Both minimum and maximum sump volume should be examined.

A higher rate of fiber injection will challenge the core inlet criterion, while a lower rate of injection will challenge the in-core criterion.

#### 6.5.2.8 Time of Chemical Effects

The time at which chemical precipitates affect the debris bed,  $t_{chem}$ , is governed by the chemical testing described in Section 6.2 and is plant-dependent. The times reported in that section provide the earliest time of chemical precipitates that will cause an earlier diversion of fiber into the core region. The earlier  $t_{chem}$  occurs, the more likely it will occur before  $t_{block}$ . The plant-specific value calculated should be used as the minimum value for this input. A maximum time of 24 hours should also be analyzed, allowing for more fiber accumulation at the core inlet.

#### 6.5.2.9 Sump Strainer Bypass Fraction

The sump strainer bypass fraction determines the fraction of total available fiber that bypasses the sump strainer, making itself available for transport through the CSS or into the RV. Utilities may perform sump

strainer bypass testing to determine the amount of debris that reaches the RCS, and at the same time, determine the capture efficiency of the sump strainer. The suggested protocol for determining debris bypass is described in Reference 6-9. The testing protocol indicates that debris should be introduced in batches with data collected for debris bypass for each batch. These data are then used to estimate the quantity of fiber transported to the RCS. This testing process is conservative as the batch addition considers bypass for small amounts of fibers reaching the sump strainer. This effectively provides data for smaller break sizes where smaller amounts of debris would be generated.

If test data is not available, Reference 6-10 provides for the use of a 45 percent bypass fraction, stating that, “a plant may use the 45 percent bypass assumption if it can be shown to be valid for their plant conditions.”

#### **6.5.2.10 CSS Flow Rate**

The containment spray system helps reduce the total mass of debris delivered to the RV by diverting a fraction of debris that bypasses the sump strainer back into the sump. Higher CSS flow rates result in less fiber delivered to the RCS. Therefore, a minimum CSS flow rate should be used if sprays are credited. Additionally, the CSS pump configuration that results in the lowest CSS flow should also be used (e.g., single pump operation in a plant with two trains of CSS).

#### **6.5.2.11 ECCS Flow Rate after Sump Switchover**

The ECCS flow rate after the time of SSO is used to calculate the rate of fiber injection into the RV and therefore should reflect the total ECCS flow rate that reaches the RV. It is also used to calculate the value of  $K_{split}$ , which is a function of ECCS flow reaching the core inlet. A minimum ECCS flow after SSO will deposit the least amount of fiber at the core inlet and be less capable of diverting flow through the AFP. A maximum value will deposit the most fiber at the core inlet, but will also be more likely to divert flow through the AFP. Since the ECCS flow rate is only used to deliver fiber to the core in this calculation, it should only specify the flow to the RCS and not include the containment spray flow rate regardless of whether CS is actuated.

Both a minimum and maximum ECCS flow rate should be analyzed.

#### **6.5.2.12 Time of HLSO and Resulting Flow Splits**

HLSO actions can vary significantly from plant-to-plant. The timing of HLSO can vary (if it occurs at all), a fraction of flow can be recirculated to the HLs simultaneously with recirculation to the CLs, or a complete HL recirculation can be activated. There can also be time varying transition between hot side and cold side recirculation. All of the post-SSO ECCS configurations relevant to the plant being analyzed must be captured or bounded. This can be done effectively by using a time dependent table of flow fractions to the hot side and cold side. For plants that continually switch between hot and cold side recirculation, only a few switches may need to be simulated based on the termination criteria defined in Section 6.5.5. As with the ECCS flow rate, minimum and maximum values should also be examined.

The BAPC licensing basis requires that the actions be performed within a specified time window, typically a target value plus or minus 30 minutes. Therefore, minimum and maximum times should be

examined in the analyses. That is, the minimum value would be the initiation time minus the uncertainty; similarly, the maximum time would be the initiation time plus the uncertainty. For those plants that continually switch between hot side and cold side recirculation, it is reasonable to bias every switch in the same direction.

### 6.5.3 Fiber Injection Rate

In order to determine whether the RV fiber limits are exceeded given an initial sump fiber load, the rate of fiber injection into the system must be known. This can be done by starting with an initial sump fiber load, calculating the rate at which fiber bypasses the sump strainers, and subtracting the mass of fiber diverted through the containment spray system, thus providing a time varying mass of fiber entering the RV. This approach is similar to that developed for the CLB methodology (Volume 3).

The system consists of four major components: the sump, the sump strainer, the containment spray, and the RV. Figure 6-16 presents a schematic of the variables important to the injection and tracking of fiber.

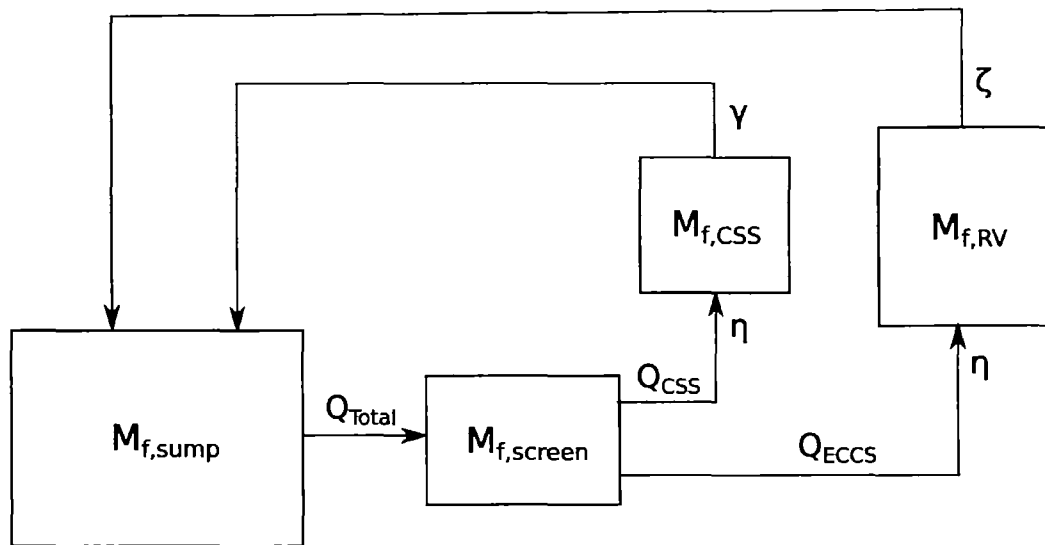


**Figure 6-16 System Schematic for Fiber Tracking**

The variables in this schematic are defined as follows:

$M_{f,sump}$  = the mass of fiber in the sump

$M_{f,screen}$  = the mass of fiber in the sump strainer

$M_{f,CSS}$  = the mass of fiber in the containment spray system

$M_{f,RV}$  = the mass of fiber in the RV

$Q_{total}$  = the total volumetric flow rate passing through the sump strainer



$Q_{CSS}$  = the volumetric flow rate to the containment spray system

$Q_{ECCS}$  = the total volumetric flow rate entering the RV

$\eta$  = the bypass fraction of fiber through the sump strainer

$\gamma$  = the bypass fraction of fiber that transfers from the CSS to the sump

$\zeta$  = the bypass fraction through the RV to the break

The rate at which fiber mass changes in each of these components without any simplifications is presented below, beginning with the sump:

$$M'_{f, \text{sump}} = \frac{dM_f}{dt}_{in} - \frac{dM_f}{dt}_{out} \quad \text{Equation 6-13}$$

By the time of SSO, there are two sources of fiber injecting into the sump: (1) the fiber being recirculated through the containment sprays, and (2) the fiber being dumped out of the break:

$$\frac{dM_{f, \text{sump}}}{dt}_{in} = \gamma \eta Q_{CSS} \frac{M_{f, \text{sump}}(t)}{V} + \zeta \eta Q_{ECCS} \frac{M_{f, \text{sump}}(t)}{V} \quad \text{Equation 6-14}$$

The outgoing fiber from the sump consists of the fiber delivered to the sump strainer, which is the sump fiber concentration times the total volumetric flow rate through the strainer:

$$\frac{dM_{f, \text{sump}}}{dt}_{out} = Q_{total} \frac{M_{f, \text{sump}}(t)}{V} \quad \text{Equation 6-15}$$

The rate of change of fiber load in the sump is therefore equal to:

$$M'_{f, \text{sump}} = \gamma \eta Q_{CSS} \frac{M_{f, \text{sump}}(t)}{V} + \zeta \eta Q_{ECCS} \frac{M_{f, \text{sump}}(t)}{V} - Q_{total} \frac{M_{f, \text{sump}}(t)}{V} \quad \text{Equation 6-16}$$

The sump strainer fiber load increases due to the total flow rate across it (ECCS plus CSS flow) and is a function of the strainer bypass fraction,  $\eta$ . Note that this also means that the bypass fraction is inversely proportional to sump strainer fiber load. For utilities that have information on the time dependent behavior of the sump strainers,  $\eta$  can be modified accordingly; whereas, for those utilities that only have the average bypass fraction,  $\eta$  should be treated as a constant.

$$M'_{f, \text{screen}} = Q_{total} \frac{M_{f, \text{sump}}(t)}{V} - \eta Q_{CSS} \frac{M_{f, \text{sump}}(t)}{V} - \eta Q_{ECCS} \frac{M_{f, \text{sump}}(t)}{V} \quad \text{Equation 6-17}$$

The fiber mass in the containment spray system is equal to the fiber mass concentration through the sump strainer times the volumetric flow rate entering the containment spray, the same concentration times the fraction of fiber that exits the CSS and ultimately returns to the sump,  $\gamma$ .

$$M'_{f,CSS} = \eta Q_{CSS} \frac{M_{f,ump}(t)}{V} - \eta \gamma Q_{CSS} \frac{M_{f,ump}(t)}{V} \quad \text{Equation 6-18}$$

The RV fiber load increases as a function of the ECCS flow rate and fiber load past the sump strainer. It can also decrease due to fiber transported out of the break.

$$M'_{f,RV} = \eta Q_{ECCS} \frac{M_{f,ump}(t)}{V} - \eta \zeta Q_{ECCS} \frac{M_{f,ump}(t)}{V} \quad \text{Equation 6-19}$$

Equations 6-16 through 6-19 provide a description of the system in the most general sense. However, in deriving the equations used to track fiber for the HLB methodology, two major conservative assumptions are made. First, all fiber that enters the RV remains in the RV, meaning that no credit taken for fiber removal by the break. This is implemented by setting  $\zeta$  equal to zero. The second major assumption is that any fiber that is diverted to the CSS will return to the sump, meaning that no credit is taken for fiber capture throughout the containment building. This is implemented by setting  $\gamma$  to 1.0. While these assumptions serve as conservative simplifications, they do not preclude a utility with information about these parameters from implementing them accordingly.

With the assumption of  $\zeta$  equal to zero,  $\gamma$  equal to 1.0, constant ECCS flow rate after sump switchover and constant strainer efficiency, the general equations used to govern fiber transport are simplified into equations 6-20 through 6-23.

$$M'_{f,ump} = Q_{total} \frac{M_{f,ump}(t)}{V} \quad \text{Equation 6-20}$$

$$M'_{f,screen} = Q_{total} \frac{M_{f,ump}(t)}{V} - \eta Q_{CSS} \frac{M_{f,ump}(t)}{V} - \eta Q_{ECCS} \frac{M_{f,ump}(t)}{V} \quad \text{Equation 6-21}$$

$$M'_{f,CSS} = 0 \quad \text{Equation 6-22}$$

$$M'_{f,RV} = \eta Q_{ECCS} \frac{M_{f,ump}(t)}{V} \quad \text{Equation 6-23}$$

Solving for this system of differential equations with an initial sump fiber load of  $M_{f,ump}(0)$  and zero fiber in all other locations produces the equations used to track the fiber load versus time in the sump, sump strainer, and RV, respectively:

$$M_{f,ump}(t) = M_{f,ump}(0) \times e^{-\frac{t}{V}(\eta Q_{ECCS} - Q_{total}(\eta - 1))} \quad \text{Equation 6-24}$$

$$M_{f,screen}(t) = \frac{(\eta - 1)M_{f,ump}(0) \times Q_{total} \left( e^{-\left(\frac{t}{V}(\eta Q_{ECCS} - Q_{total}(\eta - 1))\right)} - 1 \right)}{\eta Q_{ECCS} - Q_{total}(\eta - 1)} \quad \text{Equation 6-25}$$

$$M_{f,CSS}(t) = 0 \quad \text{Equation 6-26}$$

$$M_{f,RV}(t) = \frac{\eta Q_{ECCS} M_{f,ump}(0)}{\eta Q_{ECCS} - Q_{total}(\eta - 1)} \left( 1 - e^{-\left( \frac{t}{V} (\eta Q_{ECCS} - \eta Q_{total} + Q_{total}) \right)} \right) \quad \text{Equation 6-27}$$

#### 6.5.4 Potentially Limiting Cases

Given the range of possible values for each of the preceding inputs, two potentially limiting scenarios should be considered. The first is a scenario that most challenges the  $K_{max}$  criterion at the core inlet, and the second is one that most challenges the maximum fiber load criterion in the core (i.e., [ ]<sup>a,c</sup>).

Based on the discussion provided for each of the inputs in Section 6.5.2, Table 6-6 presents the combinations of inputs needed in order to calculate the two potentially limiting cases.

<b>Table 6-6 Input Biasing for Potentially Limiting Cases</b>		
<b>Parameter</b>	<b>Core Inlet Limiting Conditions</b>	<b>In-Core Limiting Conditions</b>
Time of SSO	min	max
Active sump volume	min	max
Time of chemical precipitates	max	min
Sump strainer bypass fraction	max	max
CSS flow rate	min	min
ECCS flow rate	max	min
Time of HLSO	max	min

#### 6.5.5 Methodology

Once the inputs are defined, the following steps can be used to determine whether or not the RV fiber load criteria are met for a hot leg break for a given sump fiber load. Two separate cases should be run; one that challenges the core inlet fiber limit, and one that challenges the in-core fiber limit. This is done to ensure that the bounding scenario is captured. The combination of inputs necessary for these two cases is provided in Table 6-6.

The existing fiber load at the start of each time step is used to calculate the flow splits. The fiber is then deposited using these splits, and the resistances at each location are calculated based upon the fiber loads at the end of the time step.

1. Obtain the minimum acceptable time of complete core inlet blockage,  $t_{block}$ , and the maximum core inlet resistance prior to complete core inlet blockage,  $K_{max}$ . These values are developed in Section 6.1 and are shown on Table 6-1. These values will be used as termination criteria in Step 10.

2. Begin the time iteration by starting at the time of SSO. Further, no debris is injected to the system until SSO, so no calculations are needed prior to this time.
3. Calculate the fiber load in the sump, sump strainer, and RV at the current time using the equations derived in Section 6.5.3
4. Calculate the mass of fiber injected into the RV since the previous time step:

$$M_{f,inj}(t) = M_{f,RV}(t) - M_{f,RV}(t - \Delta t) \quad \text{Equation 6-28}$$

5. Obtain the volumetric ECCS flow rate,  $Q_{ECCS}$ , and split between CL ( $\theta_{CL}$ ) and HL ( $\theta_{HL}$ ) for the current time. The ECCS flow split between the cold side and hot side is governed by the plant-specific EOPs and is a function of time. Any time-varying transition between injection locations should be captured as well. The flow splits will be used to calculate the core inlet resistance,  $K_{split}$ , volumetric flow rates, and fiber loads in Steps 8, 9, 6 and 3, respectively.
6. Using the calculated flow split between the AFP and core inlet from Step 9 of the previous time step, as well as the split between cold side and hot side recirculation from Step 5, calculate the liquid volumetric flow rates approaching the core inlet, AFP, and core exit. These flow rates reflect the flows in the presence of the existing debris bed (i.e., prior to the addition of the debris associated with the current time step).

$$Q_{CI} = (1 - m_{split}) \times \theta_{CL} \times Q_{ECCS} \quad \text{Equation 6-29}$$

$$Q_{AFP} = m_{split} \times \theta_{CL} \times Q_{ECCS} \quad \text{Equation 6-30}$$

$$Q_{CE} = \theta_{HL} \times Q_{ECCS} \quad \text{Equation 6-31}$$

where,

$Q_{CI}$  = the volumetric flow rate in gpm approaching the core inlet

$Q_{AFP}$  = the volumetric flow rate in gpm approaching the AFP

$Q_{CE}$  = the volumetric flow rate in gpm approaching the core exit

$Q_{ECCS}$  = the volumetric flow rate in gpm entering the RV after the time of SSO

$m_{split}$  = the fraction of total cold side flow diverted into the AFP

$\theta_{CL}$  = the fraction of total flow diverted into the cold leg

$\theta_{HL}$  = the fraction of total flow diverted into the hot leg

7. Using the mass of fiber injected into the RV in Step 3 and the flow splits calculated in Step 6, calculate the fiber load at the core inlet, AFP, core exit, and total. Knowing the total mass of fiber injected into the system in a given time interval and the flow rates at each core location, the mass of fiber at each location can be calculated by assuming that the fluid and debris are well mixed.

$$M_{f,CI}(t) = \frac{Q_{CI}}{Q_{ECCS}} \times M_{f,Inj} \quad \text{Equation 6-32}$$

$$M_{f,AFP}(t) = \frac{Q_{AFP}}{Q_{ECCS}} \times M_{f,Inj} \quad \text{Equation 6-33}$$

$$M_{f,CE}(t) = \frac{Q_{CE}}{Q_{ECCS}} \times M_{f,Inj} \quad \text{Equation 6-34}$$

$$M_{f,RV}(t) = M_{f,CI} + M_{f,AFP} + M_{f,CE} \quad \text{Equation 6-35}$$

where,

$M_{f,Inj}$  = the mass of fiber injected into the system over the current time step, as calculated in Step 4.

8. Calculate the core inlet K factor using the mass of fiber at the core inlet calculated in Step 7. This calculation is made by first checking to see if complete core inlet blockage has occurred. If not, then the K factor is calculated based on the results of the subscale testing.

Note that the debris loads used in the subscale testing were scaled to units of g/FA assuming a FA pitch of [            ]. If the FAs in the plant being analyzed have a different pitch, then the K factor must be calculated using an adjusted core inlet fiber mass to account for this difference. While the actual fiber mass calculated in Step 7 does not change, it must be adjusted as follows to calculate the proper core inlet K factor.

The first step is to determine the appropriate scaling factor,  $R_m$ :

$$R_m = \frac{R}{A_s} (P_{FA})^2 = \left[ \quad \quad \quad \right]^{a,c} \quad \text{Equation 6-36}$$

Where,

$R$  = the subscale-to-full-area FA scaling ratio applied in WCAP-17788, Volume 6.

$A_s$  = the subscale test column flow area.

$P_{FA}$  = the pitch of the FA being analyzed.

Using the scaling factor,  $R_m$ , it is possible to relate the core inlet debris load calculated in Step 7 to an equivalent core inlet debris load based on a FA pitch of [            ]<sup>a,c</sup>

$$M_{ef,CI} = \frac{M_{f,CI}}{R_m} \left[ \frac{g}{FA} \right] \quad \text{Equation 6-37}$$

Where,

$M_{ef,CI}$  = the equivalent core inlet debris load (g/FA) based on a FA pitch of [ ]<sup>a,c</sup>

$M_{f,CI}$  = the core inlet debris load (g/FA) calculated in Step 7.

$R_m$  = the scaling factor determined from Equation 6-36.

Note that if the FA pitch is [ ]<sup>a,c</sup> then  $M_{ef,CI} = M_{f,CI}$ . The equivalent core inlet debris load calculated by Equation 6-37 is then used to determine the core inlet K factor using Equation 6-4 in Section 6.3.

- a. Check for an infinite core inlet K factor (i.e., complete blockage of the core inlet). If the core inlet is completely blocked then all fluid and debris is transported to the AFP. There are two potential conditions which can force the core inlet resistance to infinity: chemical effects in the presence of a sufficient debris bed or exceeding the maximum fiber load tested.

Once chemical precipitates form (i.e.,  $t_{chem}$  is exceeded) the resistance through the debris bed will be greatly increased, and as the fiber load is increased above 15 g/FA, flow through this path will be stopped completely. While it is true that flow through the bed will exist for fiber loads less than 15 g/FA, the effect of chemical precipitates on the head loss through these lesser debris beds has not been rigorously studied. It is therefore conservative to assume that, so long as there exists a fiber load at the core inlet, complete blockage will occur coincident with  $t_{chem}$ . This is accomplished by setting the K factor to a value large enough ( $1 \times 10^{20}$ ) to prevent all flow through the inlet, thus diverting all flow through the AFP. The subscale testing was performed up to a maximum fiber load. Due to a lack of data, once the fiber load at the core inlet exceeds the maximum tested value, it must be conservatively assumed that the core inlet becomes completely blocked.

- b. If the core inlet K factor is not infinite, then it can be calculated as a function of the existing core inlet fiber bed, governed by the fuel-specific correlation developed during subscale testing, which is based on fuel vendor and plant design. Details of these correlations are presented in Section 6.3.
9. Compare the core inlet K calculated in Step 8 to  $K_{split}$ . If K is less than or equal to  $K_{split}$ , then  $m_{split}$  is zero, and flow continues to pass through the core inlet only, with all fiber depositing at the inlet. If the core inlet K factor is greater than  $K_{split}$ , then calculate the flow split between the core inlet and AFP. Flow is diverted through the AFP according the value of  $m_{split}$ , with a fraction of fiber captured at the core inlet and the remaining fiber passing through the AFP into the core region. This fiber split is directly proportional to  $m_{split}$ , as the fluid and debris are assumed to be well mixed. For core inlet K-factors of  $1 \times 10^{20}$  (i.e., complete core inlet blockage)  $m_{split}$  is set to 1.0. The  $K_{split}$  and  $m_{split}$  correlations are plant-type dependent and described in Section 6.1 and shown in Figure 6-1 through Figure 6-8. If two curve fits are provided, the

minimum fit should be used to maximize the debris buildup at the core inlet. The calculated  $m_{split}$  values should be given an upper bound of 1.0.

10. Now that the core inlet fiber load is known, the following stopping criteria can be tested:
  - a. If the core inlet K factor is greater than  $K_{max}$  before the time of  $t_{block}$ , then the calculation does not meet the acceptance criteria defined by the TH analyses (Section 6.1). In this case, steps should be taken to reduce the sump fiber load or minimize the delivery of debris to the RCS (e.g., credit CSS or decrease the strainer bypass fraction).
  - b. If the in-core ( $M_{f,AFP} + M_{f,CE}$ ) fiber load is greater than the maximum allowable in-core fiber limit (Section 6.4 for non-UI plants and Section 8 for UPI plants), then adequate core cooling cannot be guaranteed.
  - c. If the total RV fiber load (core inlet plus in-core) exceeds the in-core limit of [ ]<sup>a,c</sup> then the calculation should be terminated. This is done because fiber capture at the core inlet cannot be guaranteed. This criterion ensures that in the event that debris penetrates the core inlet, the in-core limit is not exceeded due to that penetration.
  - d. If using this method to analyze a CLB for a UPI plant, an additional stopping criterion is needed at the core inlet. As discussed in Section 8, after simultaneous recirculation is re-established, the core inlet fiber load,  $M_{f,CI}$ , cannot exceed [ ]<sup>a,c</sup>

If the case fails on any criterion, steps should be taken to reduce the sump fiber load or minimize the delivery of debris to the RCS (e.g., credit CSS or decrease the strainer bypass fraction).

11. Iterate in time until the sump fiber load is depleted. This is determined as the time at which the sump fiber load is less than 1 percent of the initial sump fiber load. At this point, it is reasonable to terminate the calculation:

$$\frac{M_{f,ump}(t)}{M_{f,ump}(0)} \leq 0.01, \text{ terminate calculation} \quad \text{Equation 6-38}$$

If the calculation is terminated based upon this criteria, then all of the acceptance criteria have been met and the plant conditions analyzed have been shown not to challenge core cooling for a HLB scenario.

### 6.5.6 Example Calculations

This section provides example calculations that can be used to verify an implementation of this methodology. Two cases are discussed below; the time dependent results are available to the utilities upon request. Note that the inputs for these cases are not intended to reflect realistic plant conditions; rather, they are intended to test implementation of the methodology. Also note, the time values for inputs are relative to the initiation of the LOCA event, whereas time values in the methodology are relative to the time of sump recirculation.

The first case has a time of chemical precipitation,  $t_{chem}$ , coincident with the time of SSO. Because chemical effects will cause complete core inlet blockage at the initiation of the transient, all fiber injected into the RV will accumulate in the core. Given an initial sump fiber load, the final fiber load in the RV can be calculated. The inputs for Case 1 are provided in the Table 6-7.

The second case is a time-dependent calculation with more representative inputs, which are described on Table 6-7. This analysis considers a B&W plant with Westinghouse fuel. As noted in Volume 4, the B&W plants do not need to perform this analysis and can instead set the in-vessel fiber limit to 100 g/FA. However, Case 2 is still useful for WEC and CE plants in validating the implementation of the fiber tracking method described herein. In order to perform Case 2, the information on Figures 6-17 and 6-18 will be needed. Note that these figures are provided ONLY for the sample case and are not to be used for plant applications.



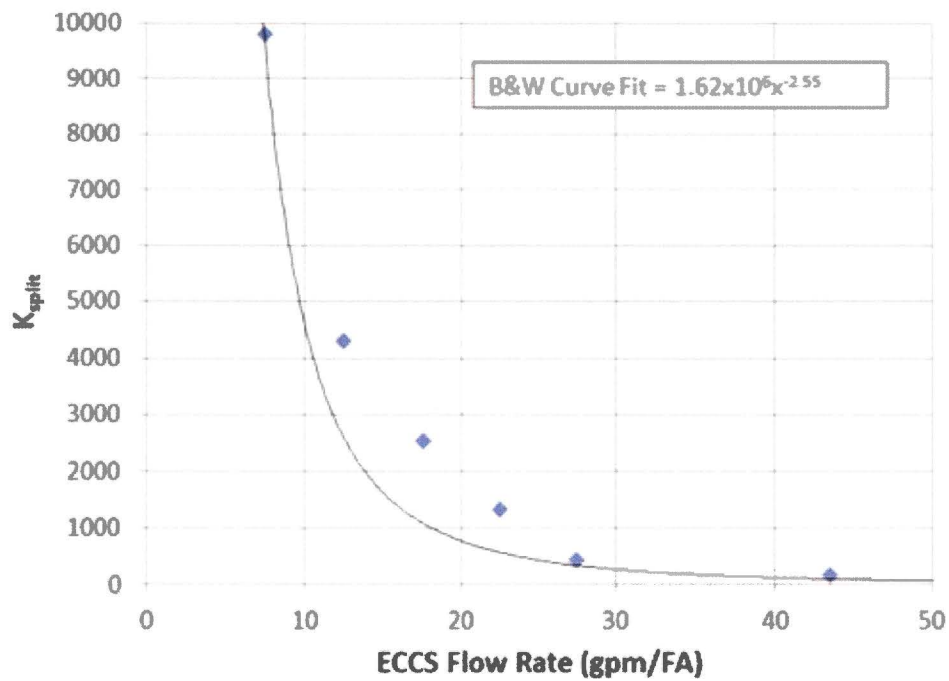


Figure 6-17  $K_{split}$  as a Function of ECCS Recirculation Flow Rate from B&W Analysis

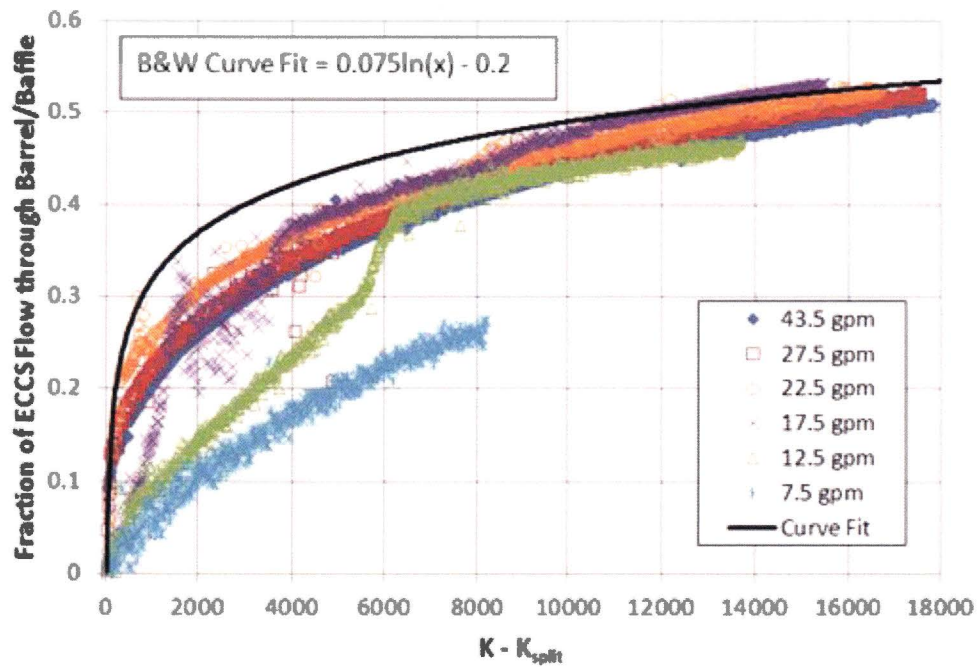


Figure 6-18 Fraction of ECCS Recirculation Flow through the Barrel/Baffle Inlet following  $K_{split}$  from B&W Analysis

Table 6-7 Test Case Inputs		
Input Parameter	Case 1	Case 2
Plant Type	CE	B&W
Number FA	225	177
Fuel Type	AREVA	Westinghouse
Time Step (sec)	100	100
Sump Volume (gal)	350000	350000
Sump Strainer Bypass Fraction	0.45	0.1
Initial Sump Fiber Load (g/FA)	100	1000
$t_{SSO}$ (hr)	4.3	0.5
$t_{chem}$ (hr)	4.3	6
ECCS Flow after SSO (gpm)	1000	5000
CSS Flow (gpm)	0	1000
HL ECCS Flow Split (time (hr), fraction)	0, 0.0, 1.49, 0.0, 1.5, 0.5, 1E6, 0.5	0, 0.0, 1.49, 0.0, 1.5, 0.5, 1E6, 0.5
CL ECCS Flow Split (time (hr), fraction)	0, 1.0, 1.49, 1.0, 1.5, 0.5, 1E6, 0.5	0, 1.0, 1.49, 1.0, 1.5, 0.5, 1E6, 0.5

Given the inputs for Case 1, the final fiber load in the core can be predicted using Equation 6-27 from Section 6.5.3. Since only the RV fiber load at the end of the event is needed, the equation can be simplified, as the exponential term approaches zero as time approaches infinity:

$$M_{f,RV}(t_{end}) = \frac{\eta Q_{ECCS} M_{f, sump}(0)}{\eta Q_{ECCS} - Q_{total}(\eta - 1)} \quad \text{Equation 6-39}$$

$$M_{f,RV}(t_{end}) = -\frac{0.45 \times 1000 \times 100}{0.45 \times 1000 - 1000(0.45 - 1)} = 45 \text{ g/FA}$$

The methodology should therefore calculate a RV fiber load of 45 g/FA, with all of that fiber located in the core.

If the utility would like to know the margin between their analyzed sump fiber load and their acceptable sump fiber load, this can be accomplished through iteration. The calculation would be performed again with a higher sump fiber load until finding the highest load that does not violate the criteria established in Step 10 of Section 6.5.6. For Case 1, the maximum allowable initial sump fiber load is [ ]<sup>a,c</sup> since any more fiber would result in an in-core fiber load greater than the maximum allowable value of [ ]<sup>a,c</sup>

Case 2 exercises more of the method: fiber injection, diversion through the AFP, HL switchover, and chemical effects. The complexity of this case prevents any hand calculation of the result, as was done for

Case 1. Instead, a single time iteration through Case 2 is provided using the input in Table 6-7, along with key results of the calculation in order to clarify the methodology.

First obtain the values of  $t_{block}$  and  $K_{max}$  from Table 6-1, as these will be used throughout the calculation. Since Case 2 is a B&W plant,  $K_{max}$  should equal  $1 \times 10^8$ , and  $t_{block}$  should equal 20 minutes. Next set the initial problem time equal to  $t_{SSO}$ , as this marks the beginning of fiber injection. Begin the iterative loop over time by incrementing the time by the time step. The first iteration should therefore be calculating values at 100 seconds, the amount of time that has passed since SSO.

Calculate the fiber load at the sump, sump strainer, and RV at 1900 seconds (100 seconds after SSO) using Equations 6-24, 6-25, and 6-27, respectively, from Section 6.5.3:

$$M_{f, \text{sump}}(100) = 1000e^{-\left(\frac{100}{350000 \times 60}(0.1 \times 5000 - 0.1 \times 6000 + 6000)\right)} = 972.3 \text{ g/FA}$$

$$M_{f, \text{screen}}(100) = \frac{6000 \times 1000 \times (0.1 - 1)}{0.1 \times 5000 - 6000(0.1 - 1)} \left( e^{-\left(\frac{100}{350000 \times 60}(0.1 \times 5000 - 0.1 \times 6000 + 6000)\right)} - 1 \right)$$

$$= 25.37 \text{ g/FA}$$

$$M_{f, \text{RV}}(100) = \frac{0.1 \times 5000 \times 1000}{0.1 \times 5000 - 6000(0.1 - 1)} \left( 1 - e^{-\left(\frac{100}{350000 \times 60}(0.1 \times 5000 - 0.1 \times 6000 + 6000)\right)} \right) = 2.35 \text{ g/FA}$$

A check is made on this calculation by ensuring that the sum of the fiber loads in the sump, strainer, and RV equal the initial sump fiber load at all times:

$$M_{f, \text{sump}}(0) = M_{f, \text{sump}}(t) + M_{f, \text{screen}}(t) + M_{f, \text{RV}}(t) \quad \text{Equation 6-40}$$

At 100 seconds, the calculation passes this check.

$$1000 = 972.3 + 25.37 + 2.35$$

Next calculate the mass of fiber injected into the RV over the previous time step.

$$M_{f, \text{inj}}(100) = M_{f, \text{RV}}(100) - M_{f, \text{RV}}(100 - 100) = 2.35 \text{ g/FA}$$

Since there was no fiber in the system previously, the amount injected is equal to the total fiber load in the RV.

Obtain the volumetric ECCS flow split between the cold and hot legs. According to the inputs, 100 percent of the ECCS flow is directed to the cold legs until 1.5 hours after LOCA initiation. Since SSO occurs at 1800 seconds for this case and the first iteration is at 1900 seconds after LOCA, all ECCS flow is still directed to the cold legs.

Calculate the volumetric flow to the core inlet, AFP, and core exit. Use the  $m_{split}$  value of the previous time step.

$$Q_{CI} = (1 - 0) \times 1.0 \times 5000 = 5000 \text{ gpm}$$

$$Q_{AFP} = 0 \times 1.0 \times 5000 = 0$$

$$Q_{CE} = 0.0 \times 5000 = 0$$

Using the mass of fiber injected into the RV calculated previously and the flow splits from above, calculate the fiber load at the core inlet, AFP, core exit, and total.

$$M_{f,CI}(t) = \frac{5000}{5000} \times 2.35 = 2.35 \text{ g/FA}$$

$$M_{f,AFP}(t) = \frac{0}{5000} \times 0$$

$$M_{f,CE}(t) = \frac{0}{5000} \times 0$$

$$M_{f,RV}(t) = 2.35 + 0 + 0 = 2.35 \text{ g/FA}$$

The core inlet K factor can now be calculated according to Step 8. First, determine if the inlet resistance should be infinite. Because  $t_{SSO}$  is less than  $t_{chem}$ , the chemical precipitates have not yet arrived. Similarly, because there is not yet any fiber in the system, the core inlet fiber limit has not yet been exceeded. Therefore, the K factor will not be set to infinity, but will instead be calculated according to Step 8b. For a B&W plant with Westinghouse fuel, Table 6-2 provides the core inlet K factor as a function of fiber load at the core inlet:

$$[ \quad ]^{a,c}$$

Calculate the values of  $K_{split}$  and  $m_{split}$ . Since Case 2 is a B&W plant type, the calculation is as follows:

$$K_{split} = 1.62 \times 10^6 \times \left( \frac{5000}{177} \right)^{-2.55} = 323.2$$

$$\Delta K = K - K_{split} = 4209$$

$$m_{split} = 0.075 \ln(4209) - 0.2 = 0.4259$$

Test the stopping criteria:

1.  $K(100)$  is less than  $K_{max}$ .
2. The in-core fiber load is 0 grams at 100 seconds; therefore, the in-core limit is not exceeded.

3. The total RV fiber load is less than the in-core limit.
4. Since this is not a UPI plant, this criterion can be ignored.

None of the criteria are violated; therefore, the calculation may continue.

Check whether 99 percent of the sump fiber has been depleted.

$$\frac{972.3}{1000} = 0.972$$

Since 97 percent of the sump fiber load still remains to be injected, the time should be iterated and the loop repeated.

The Table 6-8 presents the primary results of interest for both cases, which can be used as a form of validation.

<b>Table 6-8 Hot Leg Break Example Case Results</b>		
<b>Result</b>	<b>Case 1</b>	<b>Case 2</b>
$M_{f,screen} \left( \frac{g}{FA} \right)$	54.45	906.12
$M_{f,RV} \left( \frac{g}{FA} \right)$	44.55	83.9

## 6.6 REFERENCES

- 6-1 WCAP-16793-NP-A, Rev. 2, "Evaluation of Long-Term Cooling Considering Particulate, Fibrous and Chemical Debris in the Recirculation Fluid," July 2013.
- 6-2 [ ]<sup>a,c</sup>
- 6-3 WCAP-17360-P (Proprietary) and WCAP-17360-NP (Non-Proprietary), "Small Scale Unbuffered and Buffered Boric Acid Nucleate Boiling Heat Transfer Tests with Sump Debris in a Vertical 3x3 Rod Bundle," May 2012.
- 6-4 Sannervik, Bolmstedt, and Tragardh, "Heat Transfer in Tubular Heat Exchangers for Particulate Containing Liquid Foods," Journal of Food Engineering, 1996.
- 6-5 Kainjah and Dhir, "Experimental and Analytical Investigation of Dispersed Flow Heat Transfer," Experimental Thermal and Fluid Science, 1989.
- 6-6 Drucker and Dhir, "Studies of Single- and Two-Phase Heat Transfer in a Blocked Four-Rod Bundle," EPRI NP-3485, Project 1118-1, Final Report, June 1984.
- 6-7 Hewitt, Delhay, and Zuber, "Multiphase Science and Technology: Volume 8 – Two-Phase Flow Fundamentals," 1994.

- 6-8 NEI 04-07, Rev. 0, "Pressurized Water Reactor Sump Performance Evaluation Methodology," December 2004.
- 6-9 NEI Publication, "Revised Draft Generic Guideline, Strainer Filter Bypass Test Protocol," December 7, 2011.
- 6-10 Letter from John C. Butler (NEI) to Stewart N. Bailey (U.S. NRC), "Transmittal of GSI-191 Resolution Criteria for "Low Fiber" Plants," ADAMS *Accession Number* ML113570219, December 22, 2011.

## 7 COLD LEG BREAKS

During the recirculation phase for a CLB LOCA, the ECCS draws suction from the sump. Containment recirculation sump strainers are designed to act as filters to collect post-accident debris, thus preventing a wide range of debris from entering the ECCS and CSS. However, a portion of the debris may be sufficiently small or deformable to actually “pass through” the recirculation sump strainer and enter the ECCS and CSS. This “pass through” (also sometimes called “bypass”) debris in the ECCS may then enter the CSS (if they are operating) or the RV. Once in the RV, the portion of coolant flow into the RV LP region is driven by a balance between the available driving head of the water height in the downcomer and the rate of boil-off of liquid inventory due to removal of decay heat from the core. Any excess coolant flow exits the break and returns to containment. The excess flow returned to containment via the break or CSS flow is ducted to the sump and again filtered by the recirculation sump strainer before the coolant enters either the ECCS or the CSS.

Unlike hot leg breaks, flow through the AFP is not considered for cold leg breaks. The resistance to flow of the BB region is much higher than the resistance to flow through the core inlet, even with debris accumulation. Further, the upper head spray nozzles are above the liquid level due to the break location. Therefore, all flow and debris will approach the core through the core inlet.

The discussion in this section pertains directly to plants that initiate cold side injection immediately following the break. Discussions pertaining to UPI plants are provided in Section 8.

### 7.1 COLD LEG BREAK IN-VESSEL DEBRIS LIMIT

Determination of the total allowable in-vessel fiber quantity following a CLB is dependent upon establishing a fiber limit that does not adversely impact LTCC. This section establishes the basis for an in-vessel fiber limit of [ ]<sup>ac</sup> for the CLB scenario. This limit is compared to a plant-specific CLB debris load calculated using the method described in Section 7.2.

Following a large CLB, the RCS is essentially an open loop natural circulation system. Liquid from the ECCS is injected into the cold legs, flows down the downcomer, turns into the lower regions of the inner RV, and enters the core region. To remove decay heat, liquid in the core boils, creating a two-phase region in the core and upper plenum. Steam flows from the RV, through the broken loop or RLVs, and out of the break to containment where it is condensed and returned to the sump. The two-phase mixture level in the core and upper plenum is governed by a manometric pressure balance between the downcomer liquid level and pressure losses through the inner RV and broken loop piping, or RLVs, to the break location. The downcomer liquid level is limited to the break elevation, as ECCS flow in excess of core makeup will spill from the break. Pressure losses through the inner RV are dependent on the core collapsed liquid level and two-phase losses in the core and upper plenum region, which are governed by the decay heat level. Losses through the loop piping, or RLVs, to the break are due to the flow of a single-phase vapor or a two-phase mixture, depending on the time of the transient and location in the system.

At the time of transfer to sump recirculation, decay heat is still relatively high and boiling in the core is vigorous. The two-phase mixture level in the RV extends into the upper plenum region, and there is sufficient liquid carryover into the hot-side loop piping to limit the build-up rate of boron solute

concentrations in the RV. As decay heat decreases, so does the two-phase mixture level, which in-turn, reduces the amount of liquid carryover into the hot-side loop piping. As a result of this reduced liquid carryover, boron solute concentrations in the RV begin to build.

Initially, the build-up of boron concentration is limited to the boiling region of the core and the two-phase region of the upper plenum. Turbulent dispersion due to the boiling process keeps the boron distribution in the core and upper plenum fairly homogenous. Transport of boron solutes to regions of the RV below the boiling region of the core is expected to be limited at this point in the transient; however, flow patterns can develop due to more vigorous boiling in the central region of the core that leads to downward flow in the periphery of the core that can penetrate into the lower regions of the RV. This is referred to as the chimney effect. This flow pattern will serve to transport boron solute from the core into the LP during the early phase of the boron build-up transient.

As the transient progresses, the build-up of boron solutes in the core region creates a density gradient between liquid in the core and liquid in the LP. Eventually, this density gradient becomes large enough to overcome the upward flow through the core inlet, and any opposing density gradient due to a temperature difference, such that buoyancy-driven convection develops and higher concentration boron solution in the core is exchanged with the lower concentration solution in the LP. As boiling in the core decreases, due to the reduction of decay heat, this convective process becomes the primary mechanism for the transport of boron solutes from the core to the LP.

The arrival of debris to the RV begins shortly after the transfer to sump recirculation, and the majority of debris will arrive to the RV in the first few hours of the sump recirculation phase. Debris that enters the RV can have several effects on LTCC. First, debris may increase the pressure losses through the inner RV (i.e., regions of the RV inside the core barrel) such that the two-phase mixture level is reduced and decay heat removal is challenged. As was seen in the HLB scenario, debris accumulation at the core inlet will impose a hydraulic resistance. If the hydraulic resistance becomes large enough, the two-phase mixture level will decrease below that required to keep the core covered, and a cladding heatup will occur. Debris that penetrates through the core inlet, or bypasses the core inlet via another flow path, can also impart additional pressure losses through the inner RV. Debris that remains suspended in the liquid-phase can affect fluid properties, which in turn, affects the gravity head and two-phase pressure losses. Suspended debris can also alter two-phase pressure losses by changing flow regimes, flow regime transition points, bubble structure, and heat transfer processes. Local collection of debris on spacer grids within the core region can also increase frictional resistance through the core region or influence heat transfer. Similar to debris collection at the core inlet, increasing pressure losses through the inner RV will decrease the two-phase mixture level and could result in a cladding heatup.

The presence of debris in the RV may also accelerate the build-up rate of boron solutes by affecting the mixing and transport mechanisms that govern the boron concentration distribution in the RV. Accumulation of debris at the core inlet has the potential to reduce the transport of higher concentration boron solution from the core to the LP by influencing the flow patterns that exist at the core inlet or by creating additional resistance to buoyancy-driven convection. The presence of suspended debris in the RV may alter the two-phase mixture level, thus reducing liquid carryover into the hot-side loop piping and accelerating the time that boron solutes begin to accumulate in the RV. Suspended debris may also impact the boron precipitation mode, thus changing the timing or location in which precipitation is expected to occur.



In order to adequately address these potential consequences related to in-vessel debris, an in-vessel fiber limit of [ ]<sup>ac</sup> for the CLB scenario is established. In establishing this limit, the following aspects are considered in demonstrating that the established CLB scenario debris limit will not adversely impact LTCC:

- Debris collection at the core inlet resulting in increased pressure losses through the inner RV such that the two-phase mixture level is reduced below that required to keep the core covered.
- Debris collection at the core inlet such that the transport of high concentration boron solution from the core to the LP is reduced below that required to maintain adequate BAPC.
- Suspended debris in the liquid-phase within the RV resulting in increased pressure losses through the inner RV due to changes in apparent fluid properties, two-phase flow characteristics, and heat transfer processes.
- Suspended debris in the liquid-phase within the RV resulting in premature BAP due to a reduction in the two-phase mixture level or liquid inventory, a reduction in liquid carryover, or changes to the precipitation mode or precipitation location.
- Local collection of debris on spacer grids within the core region resulting in increased frictional resistance through the core region or reduced heat transfer.

Below, each of the above aspects is addressed to demonstrate that the established CLB fiber limit meets the LTCC acceptance criteria defined in Section 3.7.

#### **7.1.1 Debris Collection at the Core Inlet**

Debris collection at the core inlet is governed by the resulting flow distribution that develops upstream of the core inlet. To better understand the expected flow distribution and fluid behavior at the core inlet following a large CLB, a thermal-hydraulic analysis completed with WCOBRA/TRAC is examined. Table 7-1 provides a summary of the thermal-hydraulic analysis which considered a double-ended guillotine break on one of the cold legs. The simulation considers the first hour of the post-LOCA transient and the ECCS performance is also provided in Table 7-1. As shown in the table, the transfer to sump recirculation begins at 45 minutes which is the earliest time that debris will begin to arrive in the RV for the simulation.

<b>Table 7-1 Double-Ended Cold Leg Break Thermal-Hydraulic Analysis</b>					
<b>Plant Type</b>	<b>Barrel/Baffle Design</b>	<b>Decay Heat Model</b>	<b>Initial Core Power (MW<sub>i</sub>)</b>	<b>Number of Core Channels</b>	<b>Notes</b>
Westinghouse 3-Loop	Downflow	10 CFR 50 Appendix K	2652	4	Interfacial drag multiplier of 0.8xnominal used consistent with Westinghouse NSSS analyses in WCAP-17788, Volume 4.
<b>ECCS Performance</b>					
0 – 15 min after break: 1 RHR pump, 2 HHSI pumps, typical injection phase modeling with single active failure.					
15 – 45 min after break: 2 HHSI pumps, typical safety injection phase modeling for this plant.					
45 – 47 min after break: No flow, interruption at cold leg recirculation.					
47 min – termination: 2 HHSI pumps.					

The axial liquid velocities predicted at the core inlet for the hot assembly core channel, average core channel, average core channel below guide tubes, and low power peripheral channel are shown in Figure 7-1 through Figure 7-4, respectively. These figures provide a representation of what the flow distribution at the core inlet is expected to look like at the time debris begins to arrive at the core inlet. At the inlet to the hot assembly channel (HA), the velocity is generally positive (i.e., upward flow from the LP into the channel). At the inlet to the average core channels (AV & GT), the velocity tends to be predominately positive with intermittent periods of negative flow. The velocity at the inlet to the low power peripheral channel (LP) is predominantly negative, meaning that the flow is downward from the core into the LP.

While this simulation is completed for a Westinghouse 3-loop PWR, the predicted trends in core inlet velocity are expected to be similar for other NSSS designs in that the axial core inlet flow is expected to be distributed radially across the core inlet, with higher upward flows entering the hotter regions of the core, lower upward flows with intermittent periods of downflow at the inlet to the average power regions of the core, and predominately downward flow around the core periphery. This predicted flow pattern is representative of the chimney effect described previously, which is not dependent on any specific PWR plant design. Following the assumption that debris entering the RCS will transport in proportion to the liquid flow, debris collection at the core inlet will be distributed consistent with the flow distribution. That is, for regions where the flow is upward, debris will flow upward and may collect at the core inlet. For regions where the flow is downward, debris will not be able to collect at the core inlet.

Since WCOBRA/TRAC does not contain models for simulating buoyancy-driven flow due to density gradients between the core and the LP, the axial liquid velocities shown below are only applicable to the time period of sump recirculation when liquid carryover into the hot legs is sufficient to limit the build-up of boron solutes in the core region. Once decay heat decreases to the point where liquid carryover in the hot legs is reduced, and boron concentrations in the core region begin to increase, the core inlet flow distribution predicted by WCOBRA/TRAC becomes unreliable. The onset of buoyancy-driven countercurrent exchange flow between the core and LP is expected to increase the flow oscillations and downward flow compared to the WCOBRA/TRAC simulation results. Figure 7-5 below shows the steam quality leaving the RV. As shown in the figure, the steam quality remains below 0.8 prior to the transfer to sump recirculation. This result demonstrates that liquid carryover prior to sump recirculation is

sufficient to limit the build-up of boron solutes in the core region such that the predicted core inlet flow distribution at the time of debris arrival is valid. As the transient progresses, the onset of buoyancy-driven exchange flow will generate additional secondary flow patterns between the core and LP such that the non-uniformity in the core inlet flow distribution is expected to increase compared to the WCOBRA/TRAC simulation results.

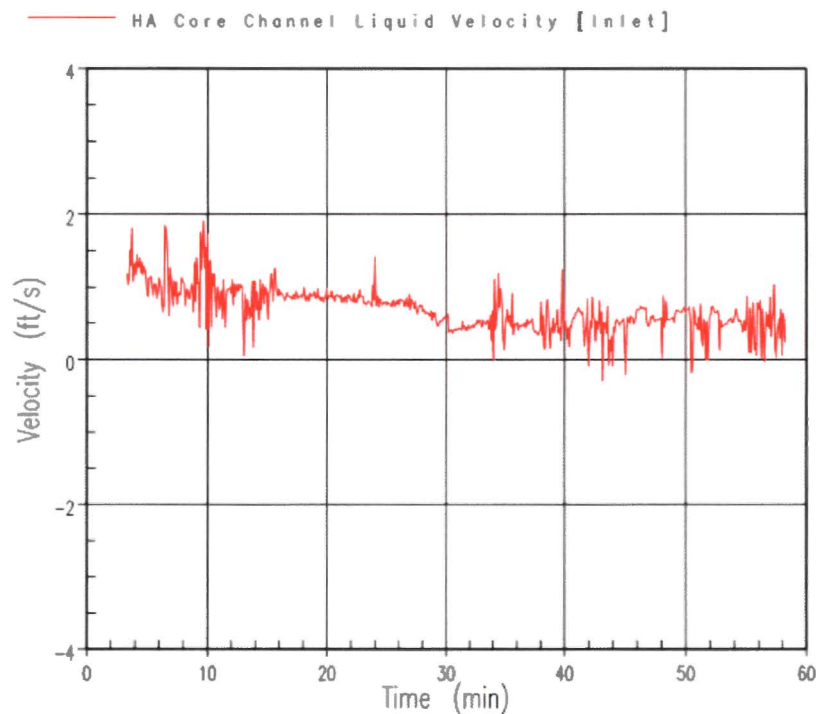


**Figure 7-1 Axial Liquid Velocity at the Inlet to the Hot Assembly (HA)**

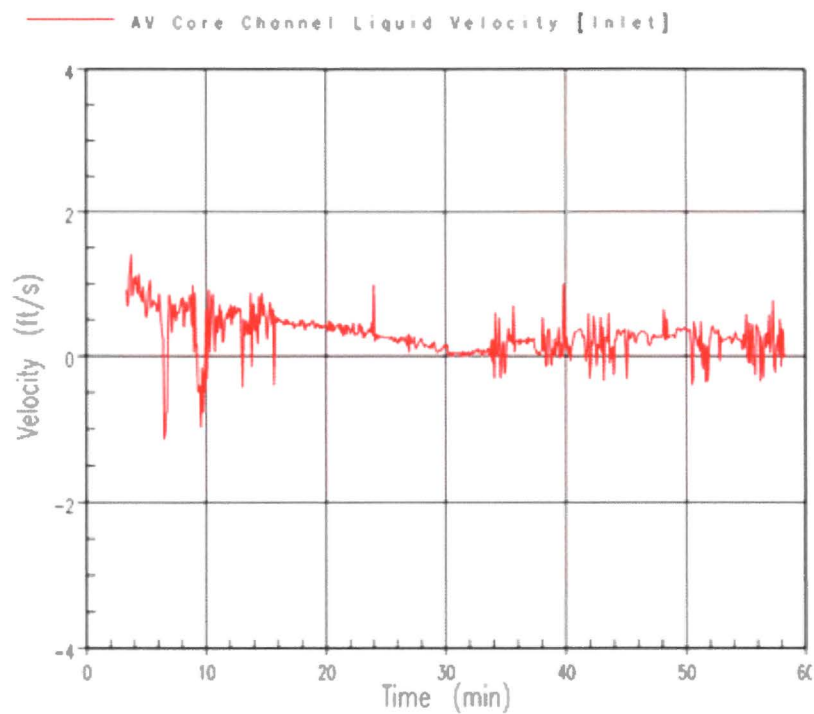


**Figure 7-2 Axial Liquid Velocity at the Inlet to the Average Power (AV) Fuel Assemblies**

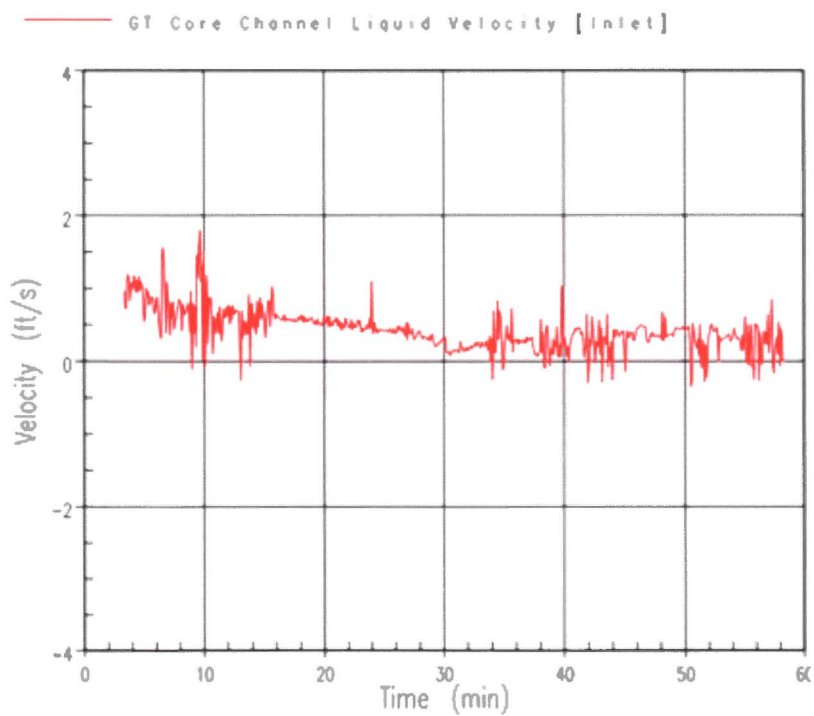


**Figure 7-3 Axial Liquid Velocity at the Inlet to the Average Power Fuel Assemblies below Guide Tubes (GT)**

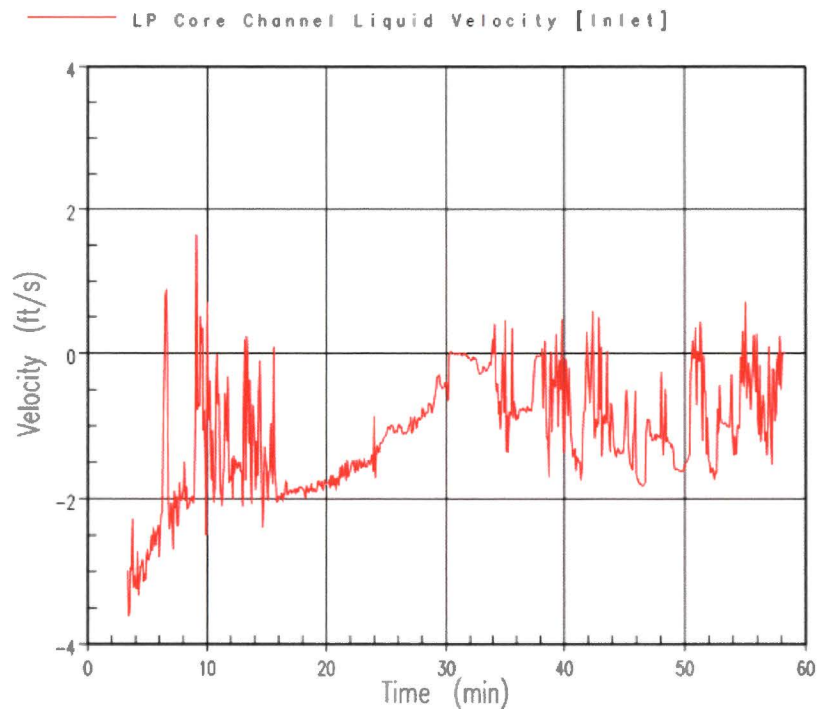


**Figure 7-4 Axial Liquid Velocity at the Inlet to the Low Power (LP) Peripheral Fuel Assemblies**

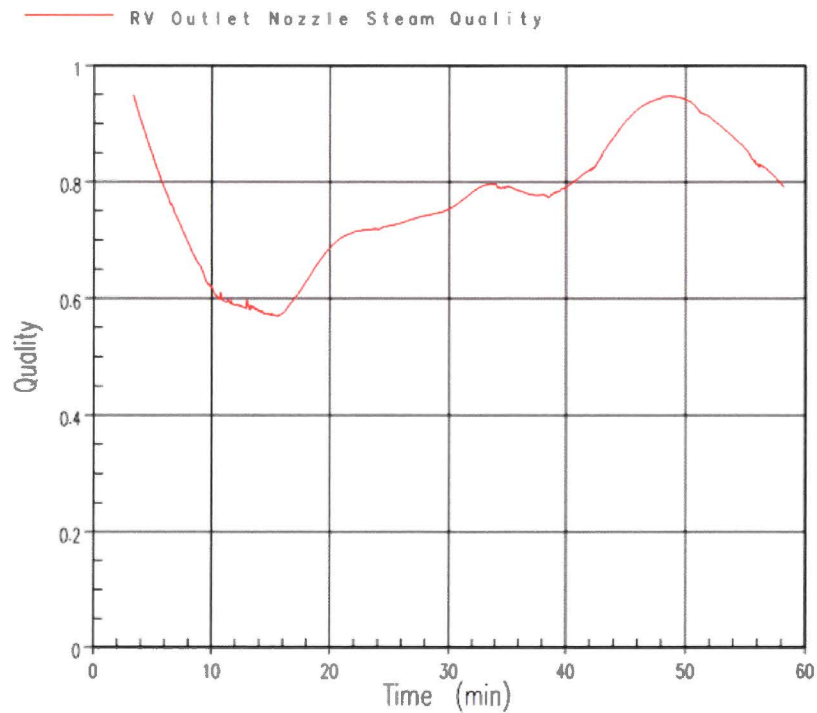


**Figure 7-5 Reactor Vessel Outlet Steam Quality**

### 7.1.1.1 Subscale Brine Test Program

As the above discussion and analysis shows, some debris may initially accumulate at the core inlet below the higher power regions of the core, but due to the radial distribution of core inlet velocity, debris will not collect uniformly across the entire core inlet. As the post-LOCA transient progresses, density gradients between the core and the LP develop and buoyancy-driven countercurrent exchange flow will begin to occur across the core inlet. It has been postulated that this buoyancy-driven exchange flow will continue to preclude debris buildup or provide a mechanism to break-up any debris beds that may have formed at the core inlet.

The subscale brine test program documented in PWROG-15091 (Reference 7-1) was conducted to improve the state of knowledge of density driven mass transport between the core and LP in the presence of in-vessel debris and has determined that this mechanism is capable of disrupting debris beds that have formed at the core inlet. The test program has also collected pressure drop data across debris beds formed under large CLB conditions which show that highly resistive debris beds cannot be formed at the established CLB in-vessel fibrous debris limit.

The testing considered a broad range of conditions prototypic of those expected to occur following a postulated large CLB LOCA and considered both Westinghouse and AREVA core inlet geometries by using prototypic fuel components. In the testing, the density gradient that develops between the core and the LP due to the build-up of boron solutes in the core was simulated using a potassium bromide (i.e., brine) solution. Flow through the test column was scaled based on the boil-off rate calculated for prototypic post-LOCA conditions. For tests that had brine injection, the flow rate was reduced during each test consistent with the decay heat curve. For tests conducted with debris only (no brine injection) to collect pressure drop data, the flow rate was held constant at a value consistent with decay heat boil-off calculated at 20 minutes post-LOCA using the 10 CFR 50 Appendix K decay heat model.

Fibrous debris loadings of 2.5 – 22.5 g/FA arriving at the core inlet were considered in the testing. A limited number of tests were completed with fibrous and particulate debris to understand the impact that particulate debris has on the resulting debris bed and the core-to-LP buoyancy-driven exchange process.

For the range of debris loads tested, it was shown that debris beds formed under low-flow conditions prototypic of a large CLB scenario resulted in minimal head loss. Section 8 of Reference 7-1 presents pressure drop results from tests completed without brine injection and show that the maximum pressure drop achieved across the debris bed was less than [ ]<sup>a,c</sup> when experimental uncertainty was considered. The maximum pressure drop was achieved during test T033, which was conducted with a fibrous debris load of 22.5 g/FA and no particulate. The second highest pressure drop from the debris only tests was achieved in test T034, which was also conducted with a fibrous debris load of 22.5 g/FA, but included a particulate load with a p:f ratio of 12:1. By comparing pressure drop measurements from these two tests, it was determined that [ ]

[ ]<sup>a,c</sup> This observation is consistent with that seen in the subscale head loss testing documented in Volume 6, which showed that [ ]<sup>a,c</sup>

For tests conducted with concurrent brine and debris injection, it was shown in Section 10 of Reference 7-1 that [

] <sup>a,c</sup> Densimetric Froude number provides the relative importance of inertia to buoyancy forces and provides a means to predict the conditions under which the buoyancy-driven exchange process will be impeded by a debris bed. As Froude number decreases, buoyancy forces become more dominant. In this situation, a reduction in upward liquid velocity or an increase in density difference results in a reduction in Froude number. Using data from these tests, critical Froude numbers for given debris bed fiber masses have been determined. At any point in time, if the Froude number [

] <sup>a,c</sup>

The brine test results demonstrate that [

] <sup>a,c</sup>

#### 7.1.1.2 Experimental Results from Rod Bundle Boiling Tests

Testing documented in WCAP-17360 (Reference 7-2) was completed using a vertical 3x3 rod bundle with dimensions and materials prototypic of PWR fuel components. The rods used in the test facility were heated such that boiling conditions representative of those expected following a large CLB could be simulated.

This testing showed that a debris bed could not be formed at the core inlet. Instead, as seen in Figure 7-6, debris passed through the bottom nozzle, settled on top of the nozzle, or continued into the heated core region. This location for debris accumulation is not unexpected given that a low-flow, recirculation zone will occur downstream of the bottom nozzle. The boiling condition downstream of the inlet produced instabilities that lead to flow oscillations in this region. These instabilities precluded a debris bed from forming at the core inlet.



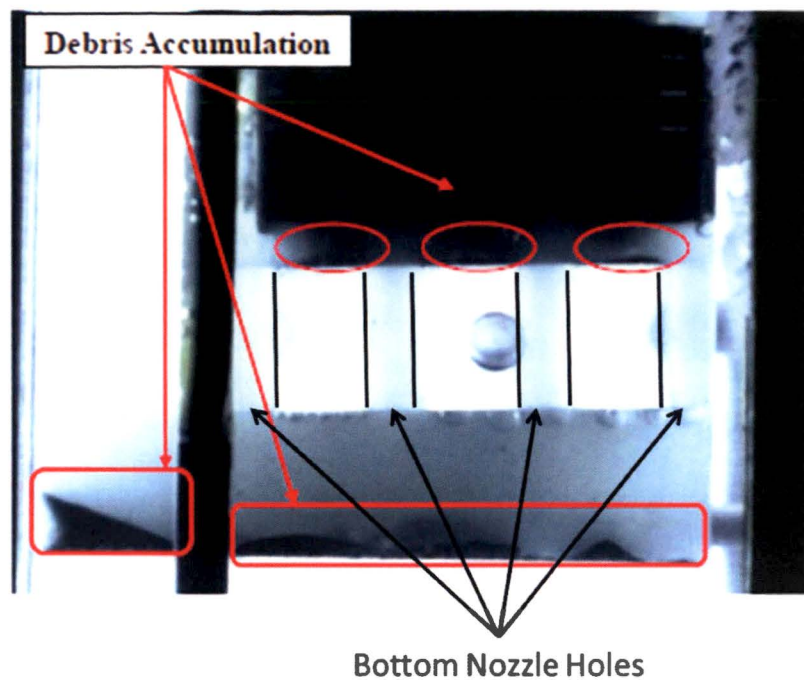
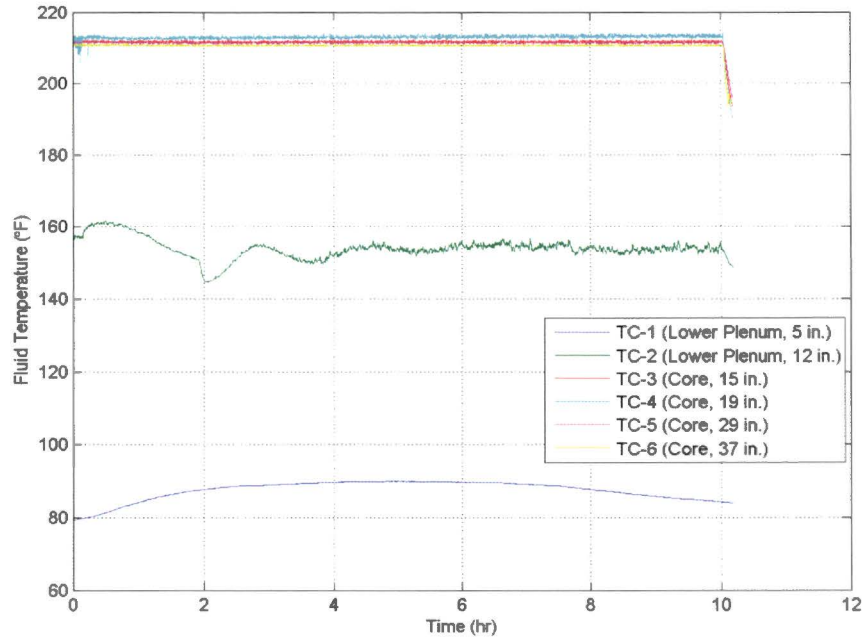


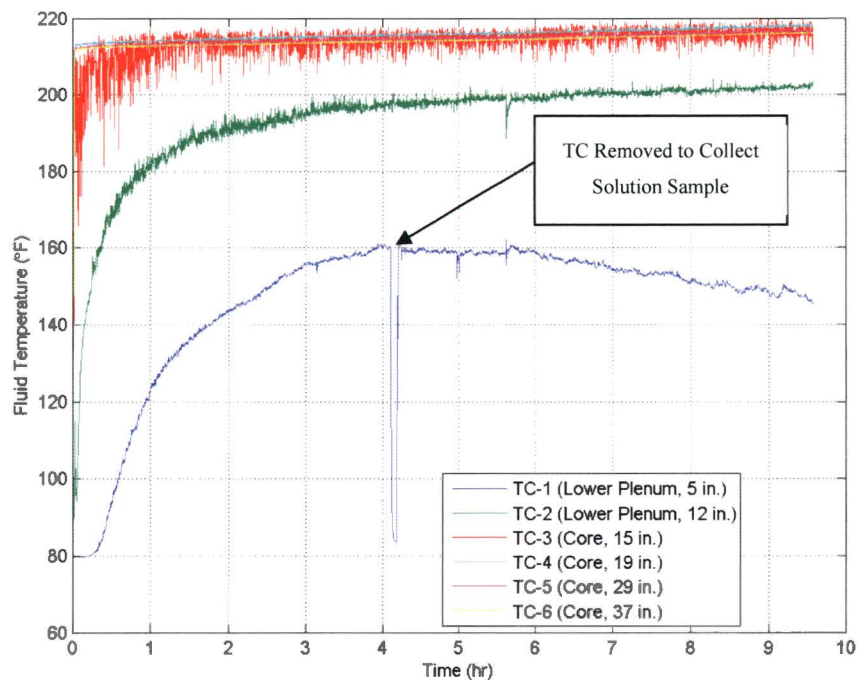
**Figure 7-6 Debris Collection Near Core Inlet in the 3x3 Heated Rod Bundle Test Facility**

Although online solute concentrations measurements were not made in the 3x3 heated rod bundle tests, temperature measurements from the core and LP can be used to show that buoyancy-driven exchange flow also occurred in this experiment. Figure 7-7(a) shows temperature measurements from the core, the top of the LP, and the bottom of the LP from a test conducted using pure water. As the figure shows, there is clear temperature stratification between the core and the LP. Conversely, Figure 7-7(b) shows temperature measurements from a test conducted with buffered boric acid and debris. As the figure shows, the temperatures in the LP from this test increase as the test progresses. This result indicates that there is an exchange process (transfer of heat) happening between the core and LP which is analogous to mass transfer. This was verified by taking a physical sample of the solution within the LP at approximately four hours. Analysis of the physical sample confirmed that the boron concentration in the LP at four hours was well-above the source concentration being injected into the test facility downcomer. This experimental observation provides additional confirmation that core-to-LP mass transport occurs in the presence of in-vessel debris





(a) Test Conducted with Pure Water



(b) Test Conducted with Buffered Boric Acid and Debris

**Figure 7-7 Temperature Measurements from Tests Conducted in the 3x3 Heater Rod Bundle Test Facility**

### 7.1.1.3 SKBOR Simulation

The above WCOBRA/TRAC simulation and test results from the subscale brine testing (Reference 7-1) and the 3x3 heated rod bundle testing (Reference 7-2) demonstrate that a continuous debris bed will not form across the entire core inlet. However, it cannot be ruled out that a debris bed could form across some portions of the core inlet, and the subscale brine testing has shown that the presence of a debris bed at the core inlet will reduce the exchange process. In order to show that a partial debris bed, formed across some fraction of the core inlet, still allows for adequate core-to-LP exchange flow, a sensitivity study is performed using the calculation tool SKBOR (Reference 7-3). The simulations were completed using a high-power density PWR plant model, the 10 CFR 50 Appendix K decay heat model, and a make-up coolant boron concentration of 2500 ppm. Core voiding is modeled in these simulations, and it is assumed that the two-phase mixture level in the upper plenum extends to the bottom of the hot leg. This assumption leads to a conservative effective mixing volume and results in faster boron solute accumulation rates.

Table 7-2 provides the case matrix used to examine the impact of core inlet blockage (CIB). As shown in the table, seven simulation cases were completed. The simulation identified as *Licensing* assumed that the effective mixing volume included 50 percent of the LP volume from the start of the simulation, which is consistent with typical Westinghouse licensing basis analyses. Simulations identified as *Exchange Flow* applied the two-region boron transport model described in Section 3.3 of PWROG-15091 (Reference 7-1). For these cases, 100 percent of the LP is credited after the onset of buoyancy-driven convection is reached. The simulation identified as *No Lower Plenum* does not credit any LP volume as part of the effective mixing volume used for calculating the build-up rate of boron solutes.

To simulate partial core inlet blockage, the number of lower core plate holes input into the boron transport model was reduced. Case No. 1 serves as the baseline condition and represents a typical licensing basis calculation. Case No. 2 is completed using the boron transport model and assumes that exchange flow occurs across the entire core inlet. This represents a case in which a debris bed is not present anywhere across the core inlet. Case No. 3 blocks 25 percent of the lower core plate holes which is equivalent to a condition in which 25 percent of the core inlet is blocked by debris. Here it is assumed that no exchange flow occurs across this fraction of the core inlet. Similarly, Case No. 4 assumes that 50 percent of the core inlet is blocked by debris and Case No. 5 assumes that 75 percent of the core inlet is blocked by debris.

<b>Case No.</b>	<b>Case Description</b>	<b>LP Credit</b>	<b>Core Inlet Blockage (CIB) Fraction</b>	<b>Accumulation Start Time</b>
1	Licensing	50%	0%	100 seconds
2	Exchange Flow	100%	0%	100 seconds
3	Exchange Flow	100%	25%	100 seconds
4	Exchange Flow	100%	50%	100 seconds
5	Exchange Flow	100%	75%	100 seconds
6	Exchange Flow	100%	75%	40 minutes
7	No Lower Plenum	0%	100%	2 hours 30 minutes

In Case Nos. 1 – 5, it is assumed that the accumulation of boron solutes begins 100 seconds after the LOCA. As was described previously, the accumulation of boron in the RV is not expected to occur until much later in the transient, because liquid carryover to the hot-side piping is sufficient to limit the build-up rate of boron in the inner RV. To quantify the influence of delayed boron accumulation, Case Nos. 6 and 7 were completed. Case No. 6 applies the boron transport model, assumes 75 percent core inlet blockage and delays the start of boron accumulation 40 minutes after the LOCA. Case No. 7 does not credit any LP volume and delays the start of accumulation 2 hours and 30 minutes.

Figure 7-8 compares the core region boric acid concentration from Case Nos. 1 – 5. As seen in the figure, Case No. 1 (50 percent LP volume), which represents a typical Westinghouse licensing basis calculation, shows that the boric acid solubility limit is reached after approximately 6 hours. In comparison, Case No. 2 (0 percent CIB), which applies the boron transport model, shows that the boric acid solubility limit is reached at approximately 8 hours. As partial core inlet blockage is applied, the figure shows that Case No. 3 (25 percent CIB) and Case No. 4 (50 percent CIB) reach the boric acid solubility limit after the time predicted by Case No. 1. The figure also shows that Case No. 5 (75 percent CIB) reaches the solubility limit before Case No. 1.

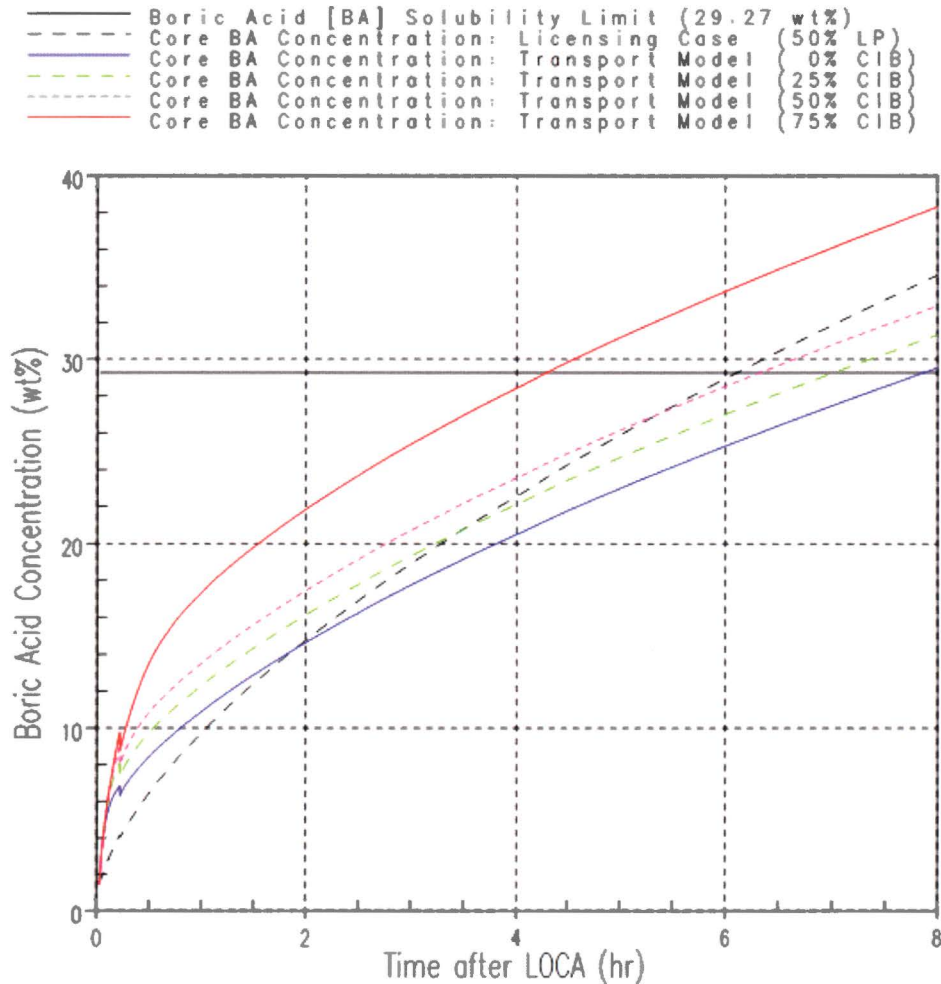


**Figure 7-8 Core Boric Acid Concentration**

The results shown in Figure 7-8 demonstrate that up to 50 percent of the core inlet can be completely blocked with debris before the exchange flow is reduced to a point that crediting 50 percent of the LP volume becomes questionable. These simulations also made the highly conservative assumption that the accumulation of boron solutes in the core region begins 100 seconds after the LOCA. If the build-up of boron solutes in the RV is delayed, a larger fraction of the core inlet can be blocked.

For Case Nos. 2 – 4, the boron transport model was used. Figure 7-9 shows the LP boric acid concentrations from these simulations. As shown in the figure, simulating core inlet blockage by reducing the number of active holes in the lower core plate results in a longer delay until the onset of buoyancy-driven convection is reached. This result is consistent with trends seen in the subscale brine testing (Reference 7-1) which showed that the addition of debris created additional resistance to the buoyancy-driven exchange process that delayed the onset. This consistency in trends between the testing and simulation provides indication that the modeling of core inlet blockage by reducing the number of active holes is appropriate.

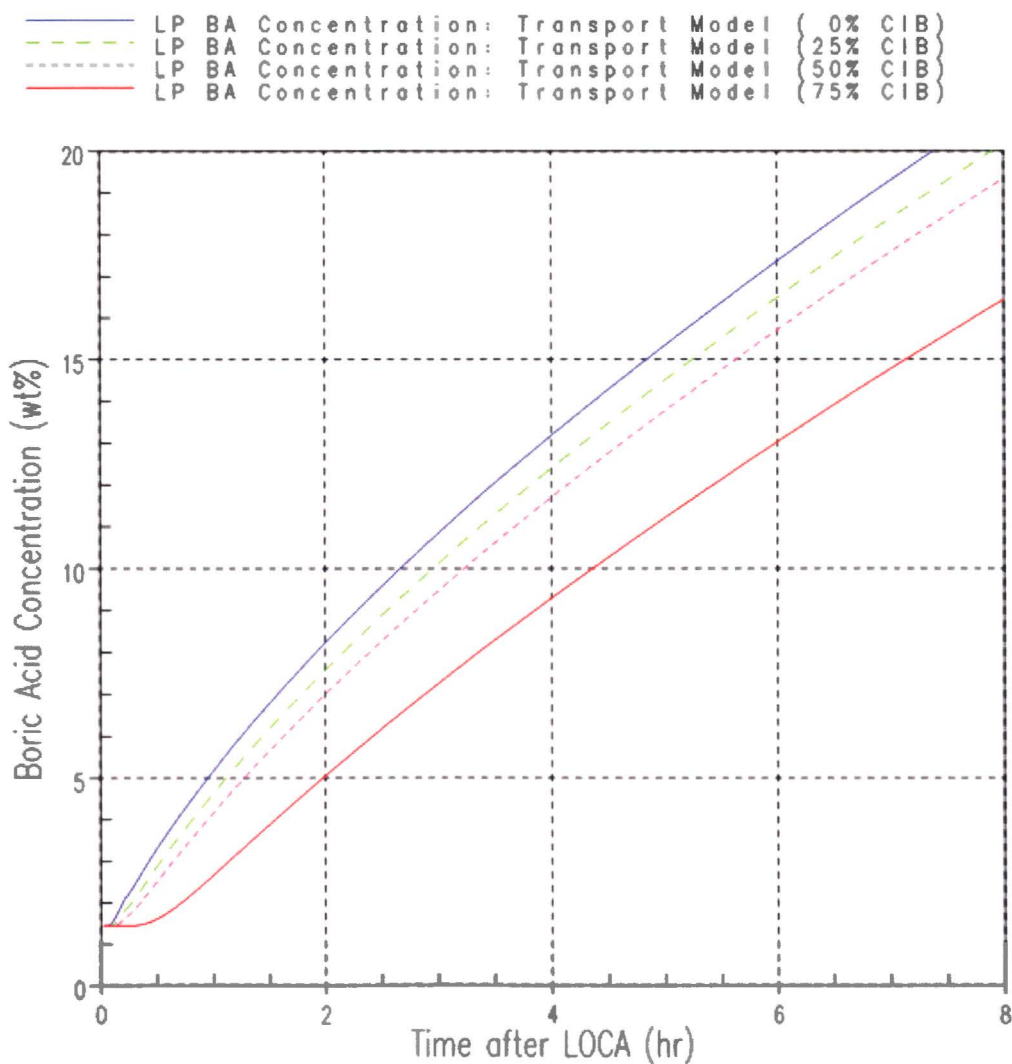


**Figure 7-9 Lower Plenum Boric Acid Concentration**



It is also relevant to compare the exchange mass flow rate predicted by the boron transport model. This comparison is provided in Figure 7-10. The figure also provides the boil-off rate calculated by SKBOR. As the figure shows, increasing the fraction of core inlet blockage results in a reduction in the exchange flow rate. This is expected and is also consistent with results from the subscale brine testing (Reference 7-1), which showed that increasing the debris load resulted in a decrease in the exchange flow rate.

It is also interesting to compare the predicted exchange flow rates to the boil-off rate. As seen in Figure 7-10, increasing the fraction of the core inlet blocked by debris increases the time required for the exchange flow rate to exceed to boil-off rate. Once the boil-off rate is exceeded by the exchange flow rate, the build-up of boric acid in the core region is significantly reduced, because more boron solute is being transported to the LP than is accumulating in the core due to boil-off. Results show that more than 50 percent of the core inlet must be blocked before the exchange flow rate, at the time the solubility limit is reached, does not exceed boil-off.

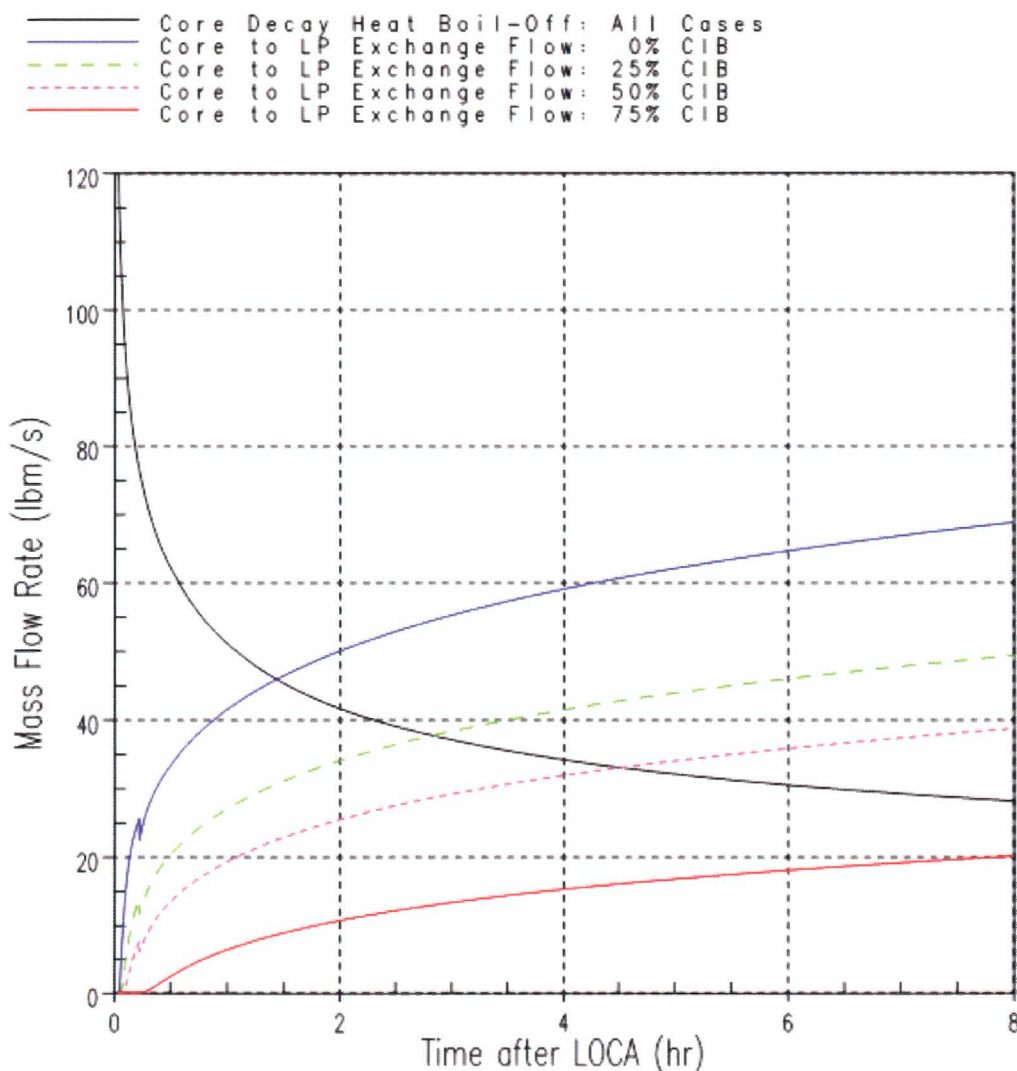


**Figure 7-10 Core-to-Lower Plenum Exchange Mass Flow Rate**

As was noted previously, Case Nos. 1 – 5 apply the highly conservative assumption that the accumulation of boron solutes in the inner RV begin 100 seconds after the LOCA. In reality, it is not unreasonable to expect that liquid carryover into the hot-side loop piping will delay the start of accumulation until later in the post-LOCA transient. The WCOBRA/TRAC results presented above show that the RV exit steam quality remains less than 80 percent until approximately 40 minutes after the LOCA. This steam exit quality is sufficient to limit the build-up rate of boron solutes in the RV.

As seen in Figure 7-11, delaying the start of accumulation until 40 minutes after the LOCA extends the time required for the core region boric acid concentration to reach the solubility limit. For Case No. 6 (75 percent CIB), it is shown in Figure 7-11 that a 40 minute delay to the start of accumulation results in a time of 6 hours after the LOCA to reach the boric acid solubility limit. Even for Case No. 7, which applies the very conservative assumption of 100 percent core inlet blockage (0 percent LP volume), it is shown that a 2 hour 30 minute delay to the start of boron solute accumulation results in a post-LOCA time of 6 hours to reach the solubility limit.

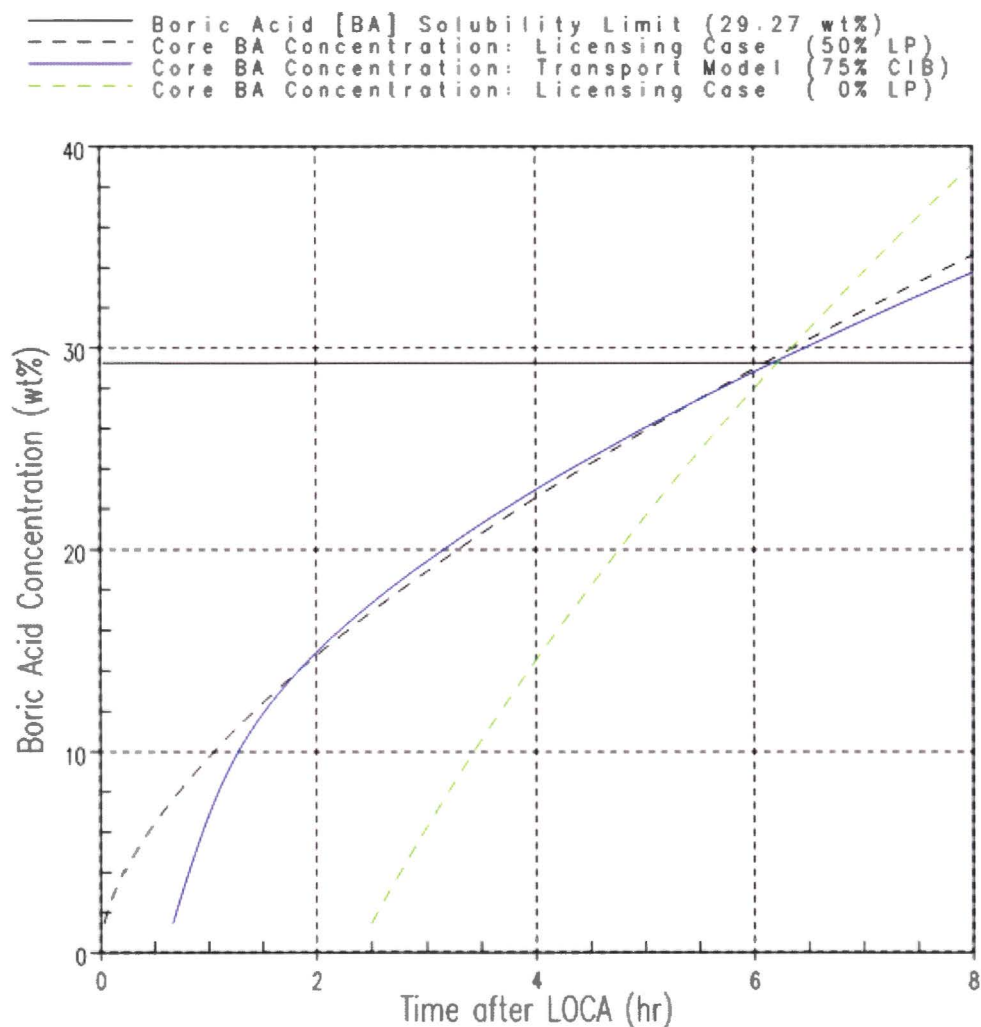


**Figure 7-11 Core Boric Acid Concentration**



### 7.1.2 Suspended Debris in the Heated Core

Debris that penetrates the core inlet or bypasses the core inlet through an alternate path will reach the heated region of the core and upper plenum. Given that all or most of the debris reaches the RV within the first few hours of the sump recirculation phase, debris will be entering a two-phase mixture with significant vapor generation and void (i.e., vapor) motion. Void motion in the two-phase region of the RV is a phenomenon that causes turbulent agitation and mixing (i.e., dispersion) of the liquid inventory. The chaotic motion of the voids pushes and drags liquid as the voids circulate through the two-phase mixture. The two-phase flow regime is considered to have a very important impact on the void motion phenomenon. For example, the churn-turbulent two-phase flow regime would be expected to provide more effective vigorous void motion and therefore turbulent mixing of debris in the liquid inventory relative to the bubbly flow regime which is less turbulent. Even though the two-phase flow pattern or veracity of boiling-induced void motion may change with decay heat level or safety system design or alignment, boiling and associated turbulent transport/mixing will always be present in the core region. As a result, debris that reaches the two-phase region of the RV is expected to be reasonably dispersed and will remain suspended in the liquid-phase.

The ability of turbulent transport and mixing due to boiling and void motion to disperse debris and keep it suspended in the liquid-phase was observed in the 3x3 heated rod bundle tests documented in Reference 7-2. For the test rig design and debris loadings used, [

]<sup>a,c</sup> When a large lower plenum design was utilized, debris did accumulate in the bottom of the lower plenum thus reducing the effective mixing volume and reducing the debris concentration in the core region. When the facility was modified to reduce the volume of the lower plenum, it was observed that only a small amount of debris settled in the lower plenum thus increasing the debris concentration in the core region. Figure 7-12 shows images of the rod bundle and a spacer grid taken from the end of a test that utilized the smaller volume lower plenum. As seen in the figure, only a small amount of debris had collected on the outer edge of the spacer grid where it mated with the acrylic test section.

Based on the understanding of the void motion phenomenon that causes turbulent agitation and mixing of the liquid inventory, which is supported by observations from the 3x3 heated rod bundle tests (Reference 7-2), the majority of debris that enters the two-phase region within the reactor vessel is expected to remain suspended in the liquid-phase. The addition of suspended debris in the liquid-phase may have an effect on the heat transfer and hydrodynamic characteristics of the flow. The following assessment is made to demonstrate that the maximum expected in-vessel debris loads will not significantly impact the flow characteristics such that it can be concluded that adequate decay heat removal will continue even if suspended debris is present in the core region.

Given the relatively small in-vessel fibrous debris limit for the CLB scenario, particulates will be the primary debris source that can remain suspended in the core region. For the purposes of in-vessel debris evaluations, the particulate debris load, defined as the amount of particulate debris that can transport to the reactor vessel and remain suspended in the liquid volume is set to a mass fraction of [ ]<sup>a,c</sup> This value bounds the maximum expected in-vessel particulate load for the US PWR fleet. If all the particulate suspended in the core liquid volume are assumed to have a density of 94 lbm/ft<sup>3</sup>, the equivalent volume fraction is [ ]<sup>a,c</sup> As particulate density increases, the equivalent volume

fraction reduces. For example, applying a particulate density of 169 lbm/ft<sup>3</sup> to the [ ]<sup>a,c</sup> mass fraction results in a volume fraction of approximately [ ]<sup>a,c</sup>

Suspended particle flows at, and below, a [ ]<sup>a,c</sup> particulate mass load are commonly referred to as dilute particle flows and these types of flows have been studied extensively for industrial applications such as pneumatic conveying of dry powders, transport of liquid-solid slurry flows, and fluidized beds used in the chemical industry. The introduction of solid particulates into a fluid stream has a direct effect on the heat transfer and hydrodynamic characteristics of the multiphase flow. Under dilute particulate loads; the available experimental and analytical research concludes that the addition of solid particles into a fluid stream causes additional mixing and turbulence. As a result, the friction factors and heat transfer coefficients of particulate flows become greater than those of single-phase flows. Further, it is commonly accepted that a fluid-particle flow with a Stokes number approaching zero, which is the case for the suspended particulate flow in the core during a large cold leg break scenario, is characterized by velocity equilibrium and can be regarded as a single-phase flow with modified properties (Reference 7-5). Therefore, showing that the effect of a [ ]<sup>a,c</sup> particulate loading has only a minimal effect on the bulk fluid properties of the flow is sufficient to conclude that the hydrodynamic characteristics will not change significantly.

For a given fixed volume, the bulk density of a suspended particulate flow is approximately proportional to the particulate loading of the flow. Therefore, the bulk density of a liquid with a [ ]<sup>a,c</sup> particulate loading is approximately [ ]<sup>a,c</sup> greater than the density of pure water. A density increase of [ ]<sup>a,c</sup> is small and will not significantly affect the hydrodynamic characteristics of the flow. Given this small increase, the increase in gravitational head loss in the RV will also be small. Bulk liquid density will have a similar magnitude effect on the two-phase pressure losses through the core. Overall, the presence of suspended debris in the RV will result in only a small increase to the overall pressure drop across the RV such that adequate available driving head in the downcomer remains and the core will remain covered with a two-phase mixture.

Given that the bulk density calculation performed in RAI-1.3 (see pages B-28 and B-29) shows that the increase due to suspended debris in the core region is small, the impact to other fluid properties is also expected to be minimal. Fluid viscosity and surface tension are important properties that influence the characteristics of two-phase flow. Flow visualizations from the 3x3 heated rod bundle tests show no significant changes to the two-phase flow characteristics or bubble structure as demonstrated by the photographs shown in Figure 7-13. As seen in the figure, the addition of buffer and debris resulted in only minor changes to the structure of the bubbly flow regime when compared to the bubbly flow regime for unbuffered boric acid solution. Further, the changes to the two-phase flow structure seen in the figure are most likely due to the presence of concentrated boron and buffer solutes as opposed to suspended debris.



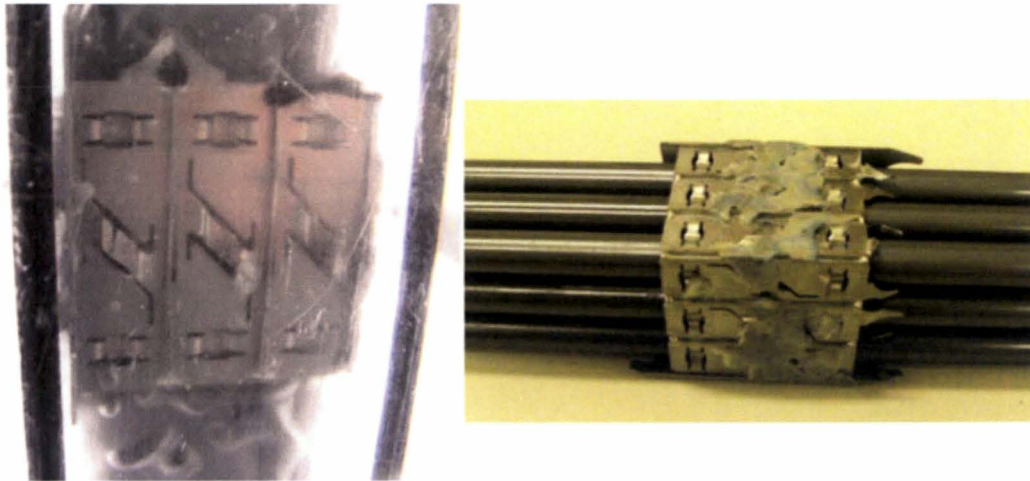


**Figure 7-12 3x3 Heated Rod Bundle Test Results Showing Fiber Accumulation on Outer Edge of Spacer Grid**

Run NRL02

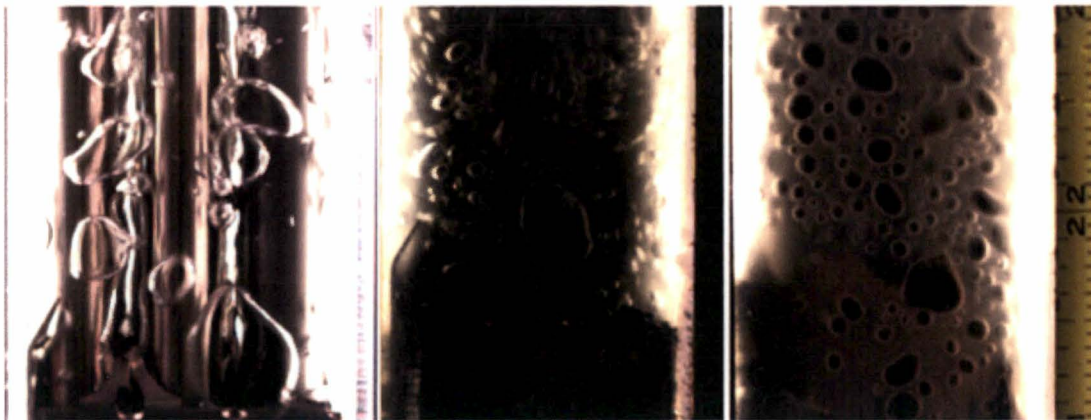
Run NRL06

Run NRL08

BA

BA + TSP + Debris

BA + NAOH + Debris



Bundle Power: 1700 – 1800 W

**Figure 7-13 Comparison of Bubble Characteristics from the 3x3 Heated Rod Bundle Tests with Unbuffered Boric Acid (BA) and Buffered Boric Acid with Debris**

In addition to the effect of suspended debris on fluid properties and the characteristics of two-phase flow, changes to the heat transfer processes should also be considered. Results from the 3x3 heated rod bundle tests (Reference 7-2) confirms that no major degradation in heat transfer occurred across the entire range of achievable core debris concentrations considered. Figure 7-14 shows the experimental boiling curve from tests conducted with pure water, unbuffered boric acid, and unbuffered boric acid with debris. As seen in the figure, the boiling curves are similar for all test conditions. This indicates that the addition of debris will not have an effect on the subsequent heat removal ability of the water/debris mixture. This conclusion is supported by work in the open literature that indicates that the addition of suspended particulates in a fluid will actually improve heat transfer.

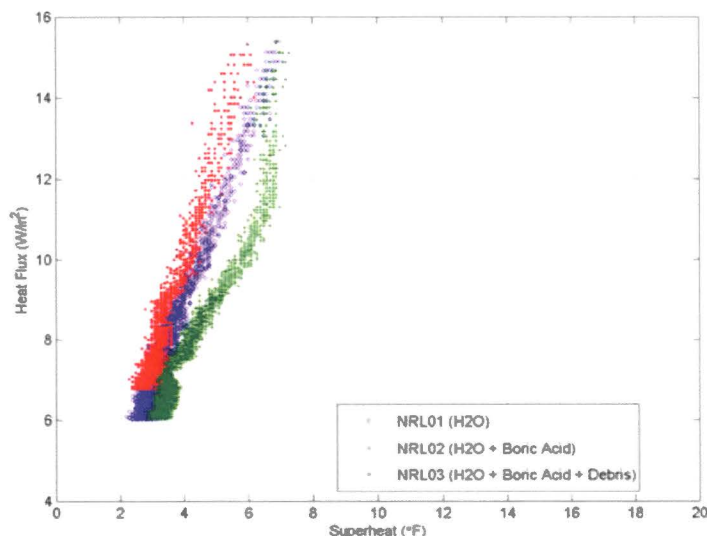


**Figure 7-14 Comparison of Experimental Boiling Curves for Tests with Pure Water, Unbuffered Boric Acid, and Unbuffered Boric Acid with Debris**

The effects of suspended debris in the RV also need to be considered from the standpoint of BAP. The addition of suspended debris in the liquid-phase can reduce liquid inventory, thus reducing the effective mixing volume that boron solutes concentrate in. As was shown in the calculation of apparent fluid density, the addition of suspended debris in the core region liquid-phase displaces only a small amount of liquid volume. As a result, any increase in the build-up rate of boron solutes in the RV will be negligible. It is also expected that, due to the relatively small fibrous debris limit established for the CLB scenario, that any reduction in liquid carryover into the hot-side piping of the RCS will be minimal and that the location and timing of BAP in the RV would be similar when debris quantities on the order of the CLB limit are present. The assertion that debris quantities on the order of the CLB scenario limit will not result in premature BAP is supported by the 3x3 heated rod bundle tests (Reference 7-2) which concluded that precipitation modes and transport/mixing phenomena were not adversely affected by the addition of debris to the core region.

### 7.1.3 Local Collection of Debris

While boiling precludes buildup at the leading edge of a spacer grid and tends to keep debris suspended in the two-phase mixture, the energy from the boiling process may force debris into internal grid locations such as the springs or dimples (see Figure 6-15 and Figure 7-12). The limited size of these geometric features limits the expanse of the debris collection such that the effects would be localized. However, the boiling process will continue to force liquid either through the debris collection or very near it such that cooling will continue. Should some volume in the spacer grid around a single rod be starved of flow, axial conduction through the cladding to the region immediately upstream or downstream of the blockage is sufficient to keep the cladding cool as demonstrated in WCAP-16793-NP-A, Rev. 2 (Reference 7-4). The open lattice design of the FAs ensures that fluid is free to flow just upstream and downstream of these localized blockages.

As the sump recirculation phase of the transient progresses, core decay heat continues to decrease, which decreases boiling in the core. In particular, lower power regions of the core (i.e., the core periphery) may stop boiling while the higher power assemblies continue to boil. In these liquid-only regions of the core, it may be possible that debris begins to accumulate on the leading edge of the spacer grid. Any debris bed that forms in the liquid-only region of the core will not extend across the entire core, because boiling continues in the higher power assemblies. The nature of the fiber and particulate bed will continue to allow flow through these blockages and the resulting pressure drop will be on the order of those measured across debris beds formed at the core inlet during the subscale brine testing (Reference 7-1). As a result, any increased pressure losses through the core region due to this type of debris bed will not become greater than the available driving head in the downcomer and the core region will remain covered with a two-phase mixture. Should any region near a blockage become starved of flow, the fluid will heatup and eventually boil. The vapor generation will either dislodge a debris bed, or the decreased density within the reestablished boiling region will draw fluid in to replace the generated vapor. In either case, the open lattice design of the fuel will ensure that the core is cooled and that localized regions with increased boron concentration will not develop even for blockages across small portions of the core.

### 7.1.4 Summary

Determination of the total allowable in-vessel fiber quantity following a CLB is dependent upon establishing a fiber limit that meets the LTCC acceptance criteria defined in Section 3.7. In determining an acceptable CLB in-vessel fiber limit, the following aspects have been addressed:

- Debris collection at the core inlet resulting in increased pressure losses through the inner RV such that the two-phase mixture level is reduced below that required to keep the core covered.
- Debris collection at the core inlet such that the transport of high concentration boron solution from the core to the LP is reduced below that required to maintain adequate BAPC.
- Suspended debris in the liquid-phase within the RV resulting in increased pressure losses through the inner RV due to changes in apparent fluid properties, two-phase flow characteristics, and heat transfer processes.

- Suspended debris in the liquid phase within the RV resulting in premature BAP due to a reduction in the two-phase mixture level or liquid inventory, a reduction in liquid carryover, or changes to the precipitation mode or precipitation location.
- Local collection of debris on spacer grids within the core region resulting in increased frictional resistance through the core region or reduced heat transfer.

With regard to debris collection at the core inlet, it has been shown through analysis and experimentation that a uniform debris bed will not form across the entire core inlet such that the core will remain covered with a two-phase mixture and adequate BAPC is maintained.

For regions of the core inlet where a debris bed may form, head loss testing under large CLB conditions completed as part of the subscale brine test program (Reference 7-1) has determined that the pressure drop across a debris bed of up to 22.5 g/FA results in negligible head loss such that the available driving head produced by the downcomer liquid level is sufficient to maintain a two-phase mixture level in the core region that covers the fuel and precludes any post-quench secondary heatup. Testing completed by the subscale brine test program (Reference 7-1) and the 3x3 heated rod bundle program (Reference 7-2) has demonstrated that the transport of high concentration boric acid from the core to the LP will continue in the presence of in-vessel debris.

Sensitivity studies performed using SKBOR have demonstrated that sufficient exchange flow from the core to the LP exists when up to 50 percent of the core inlet is blocked. This was shown to be the case when applying the highly conservative assumption that the accumulation of boron solutes in the inner RV starts 100 seconds after the LOCA. In reality, the accumulation of boron solutes in the RV is expected to start later in the post-LOCA transient. A thermal-hydraulic analysis of the large CLB scenario has demonstrated that the RV exit steam quality is sufficient to limit the build-up of boron solutes in the RV until at least 40 minutes after the LOCA. If the accumulation of boron solutes in the RV is delayed until 40 minutes after the LOCA, the SKBOR study shows that up to 75 percent of the core inlet can be blocked and adequate exchange flow exists such that BAPC is maintained.

It has also been shown that if the entire CLB in-vessel debris limit quantity penetrates, or bypasses, the core inlet and reaches the core that it will not adversely impact LTCC by remaining suspended in the liquid-phase or collecting locally around spacer grids of other regions in the core with small clearances. The 3x3 heated rod bundle tests (Reference 7-2) show that [

]<sup>a,c</sup> The testing also shows that the presence of suspended debris does not change apparent fluid properties, two-phase flow characteristics, nor heat transfer processes such that a post-quench heatup will not occur. The testing has also shown that the presence of suspended debris does not result in premature BAP.

The presence of local blockages around spacer grids is not sufficient to create a core uncover and cladding heatup. Considering the lower pressure drops obtained from the head loss testing completed under the subscale test program, local blockages will not create head loss sufficient to increase the frictional losses through the core beyond the available driving head created by the downcomer liquid level. Further, should some volume in the spacer grid around a single rod be starved of flow, axial conduction through the cladding to the region immediately upstream or downstream of the blockage is sufficient to keep the cladding cool as demonstrated in WCAP-16793-NP-A, Rev. 2 (Reference 7-4).

## 7.2 METHOD FOR VERIFYING COLD LEG BREAK IN-VESSEL DEBRIS LIMIT

As part of the current program, a method has been developed to conservatively predict and assess the time-dependent delivery of fibrous debris to the RV and core for a CLB once the ECCS has been realigned to take suction from and recirculate the coolant in the containment recirculation sump. The method assumes that any fibrous debris delivered to the RV and core is captured near the core inlet. The discussion in this section pertains directly to the Westinghouse, CE, and B&W plants that initiate cold side injection immediately following the break. Discussions pertaining to UPI plants are provided in Section 8.

The method is an extension of the approach described in Section 5.0 of WCAP-16406-P-A (Reference 7-6). The method applied to the CLB scenario tracks the depletion of fibrous debris concentration in the recirculating coolant due to capture of that debris on both recirculation sump strainers and near the core inlet. The method uses plant-specific values in the calculation method to track fibrous debris through the sump strainer and through the ECCS, the CSS, and to the RV and core to make a determination of the amount of fibrous debris that is delivered to the bottom entrance of the core for a CLB LOCA. This mass of fiber is termed  $M_{f, CLB}$ . A description of the method and the inputs required for the method to operate on a specific plant is detailed in Volume 3. A summary is provided here.

To evaluate the potential for accumulation of fiber at the core entrance, this evaluation method considers the complete system requirement for a cold leg break LOCA, including containment spray, cold leg safety injection, and core boil-off requirements. Figure 7-15 provides a general schematic of the flow paths for coolant when the ECCS and the CSS are realigned from drawing suction from the RWST to recirculating coolant from the reactor containment building recirculation sump. For a CLB scenario:

- The ECCS draws coolant from the sump through the recirculation sump strainer and pumps it into the RCS. Coolant in excess of that needed to match boil-off spills from RV out the broken loop and back into the sump. Only the coolant that is needed to make up boil-off carries debris into the core.
- The CSS also draws coolant from the sump through the recirculation sump strainer, pumps it to the CSS spray headers, where the coolant is released to the containment and is returned to the sump.

These two flow paths drawing from a common source suggest a simple model may be used to evaluate the total amount of fibrous debris delivered to the core while accounting for the depletion of fibrous debris in the sump coolant due to capture by the recirculation sump strainer(s) and the fibrous debris that is delivered to the RV and core. Plant-specific applications should confirm the applicability of these flow paths and model them as appropriate.

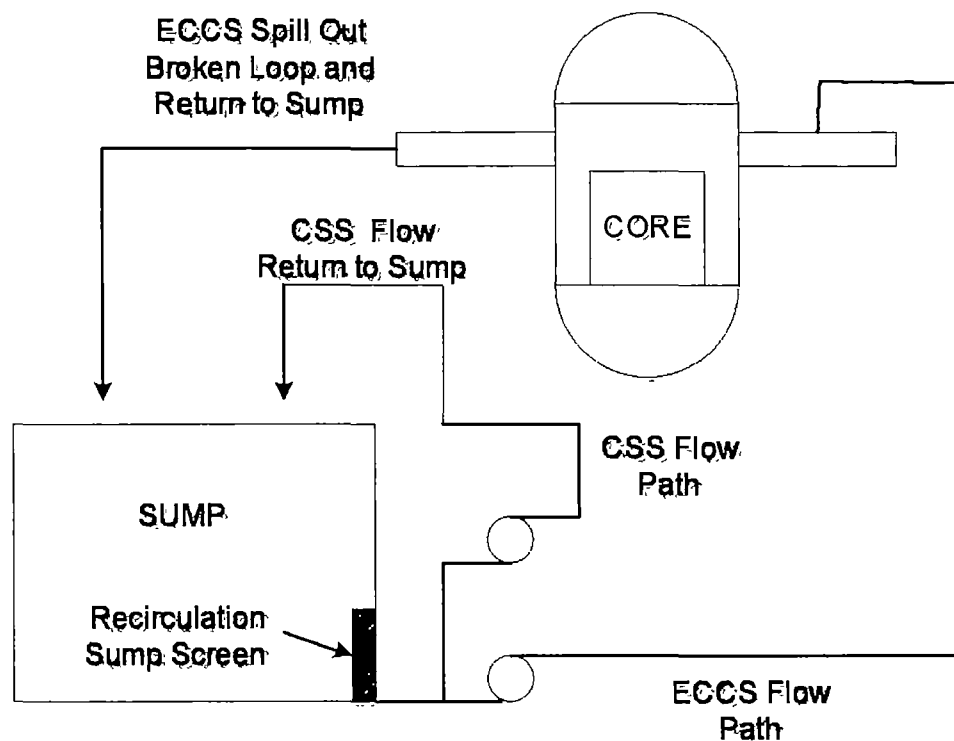


**Figure 7-15 ECCS and CSS Flow Paths for a Cold Leg Break**

The constituent equations for the method are presented in Volume 3, Section 3 and are consistent with those used in prior debris depletion evaluations (Reference 7-7). Along with the method itself, assumptions and input parameters for the calculations have been identified. An example calculation is presented in Volume 3, Section 4.

As an alternative to the CLB method described in Section 10.2, a simplified method is presented in Volume 3, Section 5.

These methods were developed for use by utilities to evaluate plant-specific PWR CLB performance in the presence of post-LOCA debris.

1. These methods provide a means for plants to calculate the plant-specific amount of fiber actually reaching the core in a large CLB scenario, which can then be compared to the core inlet CLB fiber limit (established in Section 7.1). A value lower than this defined fiber limit is interpreted as an acceptable condition to provide for LTCC of the core.
2. Alternatively, a utility can use these methodologies to develop a plant-specific limit on the amount of fiber that can bypass the recirculation sump strainers in a CLB scenario and still stay beneath the core inlet limit defined in Section 7.1. This limit can then be used in conjunction with HLB limits using the method described in Section 6.5 to determine the overall plant-specific limit on fiber bypassing the sump strainer.

### 7.3 REFERENCES

- 7-1 PWROG-15091-P (Proprietary) and PWROG-15091-NP (Non-Proprietary), "Subscale Brine Test Program Report," November 2015.
- 7-2 WCAP-17360-P (Proprietary) and WCAP-17360-NP (Non-Proprietary), "Small Scale Unbuffered and Buffered Boric Acid Nucleate Boiling Heat Transfer Tests with Sump Debris in a Vertical 3x3 Rod Bundle," May 2012.
- 7-3 WCAP-16793-NP-A, Rev. 2, "Evaluation of Long-Term Cooling Considering Particulate, Fibrous and Chemical Debris in the Recirculating Fluid," July 2013 (pages E-17, E-18, H-46, H47 & H-48).
- 7-4 WCAP-16793-NP-A, Rev. 2, "Evaluation of Long-Term Cooling Considering Particulate, Fibrous and Chemical Debris in the Recirculating Fluid," July 2013.
- 7-5 Crowe, C., Sommerfeld, M., Tsuji, Y., "Multiphase Flows with Droplets and Particles," CRC Press LLC, 1998.
- 7-6 WCAP-16406-P-A, Rev. 1, "Evaluation of Downstream Sump Debris Effects in Support of GSI-191," March 2008.
- 7-7 WCAP-16530-NP-A, Rev. 0, "Evaluation of Post-Accident Chemical Effects in Containment Sump Fluids to Support GSI-191," March 2008.



## 8 UPPER PLENUM INJECTION PLANTS

For Westinghouse 2-loop UPI plants, initial ECCS flow to the RV from the RWST is through the cold legs and injection nozzles located in the UP. At transfer to sump recirculation, ECCS flow to the cold legs is secured, and flow to the UP is maintained. Therefore, during the sump recirculation phase of the transient, the direction of liquid flow through the core is the reverse of plants with typical cold leg ECCS alignments.

For a large hot leg break scenario, the bulk of flow into the RV UP during sump recirculation flows out the break, carrying the bulk of suspended debris with it. The two-phase mixture level is maintained at or above the break elevation. Flow into the core region is by gravitational force and is only that needed to replenish the coolant boiled away. Excess ECCS flow is discharged through the break. Therefore, the LTCC phase for a large hot leg break scenario represents the minimum core flow condition for a UPI plant. It also represents the condition with the minimum debris load reaching the core since a significant fraction of debris entering the UP will be carried out the break with the excess ECCS flow and re-filtered by the containment sump strainers.

For a large cold leg break scenario, ECCS flow delivered to the UP flows through the core and out the break. Since core flow is in excess of that required to replenish the coolant boiled away, boiling in the core will be suppressed. In addition, since all ECCS flow delivered to the UP has the potential to travel through the core, all debris entering the UP also has the potential to enter the core region. Therefore, a large cold leg break represents the limiting scenario for UPI plants since it results in the greatest debris load expected to reach the core region.

Some UPI plants utilize cold leg recirculation to control boric acid concentration within the core. Cold leg recirculation would be established several hours after transfer to sump recirculation to aid in flushing boric acid from the core in the event of a hot leg break. Plants other than the UPI design use hot leg recirculation to flush boric acid from the core in the event of a cold leg break. Since cold leg recirculation is initiated several hours after sump recirculation begins, the quantity of debris in the containment sump available for transport to the cold leg (bottom of the core) will be depleted due to collection on the sump strainer, collection in the RV, and collection in containment due to entrapment or settling in the containment sump liquid.

### 8.1 COLLECTION OF DEBRIS IN THE REACTOR VESSEL

Considering the above, debris begins to enter the RV in an UPI plant within the UP. Regardless of break location, boiling in the core is vigorous at transfer to sump recirculation and dispersed flow exists at the top of the core and UP. Given the high void fraction within the UP, ECCS flow exiting the UPI nozzles is in the form of a jet. The jets impact structures within the UP which help to disperse the flow and increase turbulence. Liquid that reaches the top of the core from the UP may be in the form of large droplets or liquid films falling from the structures within the UP. Liquid in the two-phase mixture above the hot leg elevation may drain into the hot legs and smaller droplets generated in the UP will be entrained by steam and can exit the RV or be deposited on the UP structures. Since debris is expected to be uniformly distributed within the ECCS flow, debris will follow a similar flow path; a fraction of debris will enter the top of the core, a fraction will exit the RV, and a fraction may collect and remain within the UP structures.



The flow split and, thus, debris split is dependent on the break location and will be discussed separately for the cold leg and hot leg break scenarios, respectively.

### 8.1.1 Large Cold Leg Break Scenario

For the large cold leg break scenario, the majority of ECCS flow entering the UP through the UPI nozzles will enter the top of the core. Only a small fraction is expected to bypass the core region and make its way to the break. Flow that enters the top of the core carries debris with it, and the turbulent mixing due to the boiling process will tend to keep the debris suspended in the liquid phase. Debris that does deposit on fuel components is expected to be localized to regions where the boiling is less vigorous (i.e., core periphery). The debris deposits are expected within the spacer grids where the grid springs and dimples create “pinch points” for which debris can readily capture. Section 6.4.3 provides the justification for an in-core fibrous debris limit of [ ]<sup>a,c</sup> which also applies to UPI plants. While the ECCS alignments and limiting break location for UPI plants may differ from other PWR designs, the debris transport and capture mechanisms within the core region remain the same.

### 8.1.2 Large Hot Leg Break Scenario

For the large hot leg break scenario, only the fraction of ECCS flow required to make-up for boil-off is expected to enter the core region. The same is true for debris since it is reasonably dispersed within the ECCS flow. For this reason, the in-core debris load for the large hot leg break scenario is bounded by the in-core debris limit expected for the large cold leg break scenario described in Section 8.1.1. However, the large hot leg break scenario is the limiting scenario for BAP since it leads to a pool boiling condition in which boron concentrations can build within the core.

For UPI plants that control boron concentrations in the core by switching a fraction of the ECCS flow back to the cold leg(s), it must be ensured that the flushing flow through the core is not impeded by debris induced resistance at the core inlet. Therefore, for the large hot leg break scenario, if the debris source is not depleted by the time cold leg recirculation is established, the quantity of debris entering the cold leg must be tracked and is assumed to collect at the core inlet. The core inlet fibrous debris limit for this scenario is [ ]<sup>a,c</sup> because it was shown in Reference 8-1 that the arrival of chemical products does not lead to complete core inlet blockage, at this debris load, which ensures that adequate flushing flow through the core will continue.

### 8.1.3 Method for Verifying In-Vessel Debris Limits

The method for verifying the in-vessel debris limit for UPI plants is similar to that described in Section 6.5. Following switchover to sump recirculation, debris is tracked within the RV and the quantity of debris calculated to enter the core region is compared to the in-core limit. The in-core limit for UPI plants is [ ]<sup>a,c</sup> which is the same in-core limit for typical cold leg recirculation plants. While the ECCS alignments and limiting break location for UPI plants may differ from other PWR designs, the debris transport mechanisms to the core region can be treated similarly.

For plants that transfer some ECCS flow back to the cold leg(s) to mitigate the potential for BAP, an additional check is required. If the debris source has not depleted at the time cold leg recirculation is established, the quantity of debris entering the cold side of the RCS must be calculated. The calculated

debris quantity is compared to a core inlet fibrous debris limit of [ ]<sup>a,c</sup> This debris limit is used because the arrival of chemical products to a fiber bed of this quantity does not lead to complete core inlet blockage such that flushing flow through the core is ensured.

## 8.2 REFERENCES

- 8-1 WCAP-16793-NP-A, Rev. 2, "Evaluation of Long-Term Cooling Considering Particulate, Fibrous and Chemical Debris in the Recirculation Fluid," July 2013.

## 9 DEBRIS LIMITS AND ACCEPTANCE CRITERIA

The two acceptance criteria for this analysis are identified in Section 3.7. First, DHR requires that sufficient coolant be supplied to the core such that the core temperature is maintained at an acceptably low level. For previous GSI-191 evaluations, the maximum allowable core PCT is 800°F. Second, BAPC requires that boron concentrations in the core region remain below the solubility limit. How these acceptance criteria are met is described in this section.

### 9.1 HOT LEG BREAK

#### 9.1.1 Decay Heat Removal

Following a HLB, DHR is assured by calculating a fiber load that does not challenge the limits as described in Section 6.5. This method uses the results from a number of interrelated analyses and tests. Implicit in the HLB method are the following three criteria that ensure adequate DHR.

First,  $t_{block}$  may not be violated. This means that the core may not become completely blocked for any reason before the time of  $t_{block}$ . Two primary mechanisms are assumed to exist that cause complete core inlet blockage, the first of which is the formation of chemical precipitates which occur at  $t_{chem}$ . At the time of  $t_{chem}$ , it is assumed that the core inlet is completely blocked due to the arrival of chemical precipitates such that no flow can enter the core through the normal flow path. Instead, flow must traverse the AFP.  $t_{block}$  was determined by the TH analyses (Volume 4) as the time at which complete core inlet blockage could occur and the AFPs would allow sufficient fluid into the core to keep the peak cladding temperature below 800°F. Therefore, if  $t_{chem}$  occurs after  $t_{block}$ , DHR is assured.

Similarly, prior to  $t_{block}$ , the resistance at the core inlet due to debris must be less than  $K_{max}$ . The TH analyses (Volume 4) demonstrated that the cladding temperature remains below 800°F when a resistance equal to  $K_{max}$  is applied to the core inlet. Beyond  $K_{max}$ , it is assumed that the core inlet is blocked such that the only flow available for DHR is through the AFP.  $t_{block}$  was determined by the TH analyses (Volume 4) as the time at which complete core inlet blockage could occur and the AFPs would allow sufficient fluid into the core to keep the peak cladding temperature below 800°F. The subscale testing (Volume 6) defined the resistance at the core inlet as a function of debris load. Therefore, if  $K_{max}$  is exceeded after  $t_{block}$ , DHR is assured.

The second criterion is that the amount of debris reaching the heated core is less than [ ]<sup>a,c</sup> This amount of fiber (and associated particulate) will not compromise core cooling, as described in Section 6.4.

Finally, the amount of debris reaching the RV (core inlet plus in-core) is less than [ ]<sup>a,c</sup> This limit is imposed because fiber capture at the core inlet cannot be guaranteed. This criterion ensures that, in the event that debris penetrates the core inlet, the in-core limit is not exceeded due to that penetration.

Since the method described in Section 6.5 accounts for all of these items, the cladding temperature will remain below 800°F and DHR is assured.

### 9.1.2 Boric Acid Precipitation Control

Following a large HLB, BAPC is a passive process. The path from the cold side, through the core to the break ensures a continuous flushing flow and boric acid concentrations in the RV remain close to the source concentration.

As debris accumulates at the core inlet, the resistance to flow through the core inlet increases and flow begins to bypass the core inlet through the AFP. Before complete core inlet blockage, flow above the boil-off rate continues to enter the core either through the core inlet alone or through a combination of the core inlet and AFP. The core is well mixed and the break quality is low enough that flushing of boric acid continues. After complete core inlet blockage, flow above the boil-off rate will enter the core through the AFP. The majority of flow that exits the AFP flows into the peripheral core channel and the flow direction is predominately downward. Once in the core periphery, cross flow provides liquid to the central core channels and hot assembly, ensuring that the core is well mixed. Because the amount of liquid entering the core has reduced due to the loss of the core inlet flow path, boiling in the core becomes more vigorous. This leads to more chaotic void motion that tends to increase the overall mixing in the core by enhancing the cross flow radially across the core. Further, the excess flow (above boil-off rate) will carry liquid to the break such that the break exit quality is low enough to ensure that the core is continually flushed even after complete core inlet blockage.

In Reference 9-1, a simple evaluation of BAPC following a large HLB was performed that considered complete core inlet blockage. The purpose of the evaluation was to quantify the amount of liquid carryover out the HLB necessary to preclude BAP before currently established control measures could be implemented.

The major assumptions used in the Reference 9-1 analysis are as follows:

- The transient begins 100 seconds after the LOCA event and assumes that a highly resistive debris bed is present at that time such that the lower plenum volume is not credited as part of the boron mixing volume.
- The initial core boron concentration is equal to the sump mixed mean concentration. The mixed mean concentration is determined by taking all the possible sources of liquid in containment (i.e., RWST, accumulators, RCS, and BIT) and assuming that they are homogenously mixed within the associated control volumes (RV and sump).
- The effective mixing volume used to track the boric acid concentration build-up considers core voiding and a two-phase mixture to the bottom of the hot legs.
- Flow into the core is in excess of boil-off. Flow into the core is assumed to occur through the highly resistive debris bed, or through flow that bypasses the core inlet via AFPs or through some combination of both. Regardless of the flow path, liquid in excess of boil-off is reaching the core.
- Liquid in the effective mixing volume is assumed to be well mixed such that the boric acid concentration is uniform in the mixing volume.

Results from the analysis described above indicate that as little as 5 percent liquid carryover out of the HLB is sufficient to preclude BAP well past any currently established BAPC action times. Assuming 5 percent liquid carryover indicates that flow into the core must be, at minimum, 5 percent in excess of boil-off for this result to hold, because any reduction in core flow would result in a reduction in two-phase mixture level which would reduce the liquid carryover out of the RV and result in a faster build-up of boric acid in the reactor vessel.

With regard to the analysis assumptions, assuming that a debris bed is present at the core inlet 100 seconds after the LOCA event is conservative. Early SSO times occur on the order of 20 min (1200 seconds) and this is the earliest possible time that debris can enter the RV. Further, it will take some finite period of time for a debris bed to form at the core inlet. Prior to the formation of a debris bed at the core inlet, the flushing flow is high such that boron concentrations in the core will be close to the source concentration. Delaying the formation of the debris bed at the core inlet will delay the build-up of boric acid in the core.

The TH analyses also confirm that flow into the core region is in excess of boil-off even after the application of complete core inlet blockage. The analyses also confirm that the core can be considered well mixed due to the boiling process and chaotic void motion.

Finally, due to the large amount of liquid carryover out of the break before and after complete core inlet blockage, BAP is controlled and boron concentrations in the RV will remain well below the solubility limit for the duration of the transient.

Although the Reference 9-1 evaluation was only completed for one PWR plant type, the quantity of liquid carryover predicted in the TH analyses is so high, a rigorous plant- or type- specific analysis is not required to ensure that currently established BAPC measures are appropriate when in-vessel debris is considered.

## **9.2 COLD LEG BREAK**

### **9.2.1 Decay Heat Removal**

Following a CLB, DHR is assured by limiting the fiber build up at the core inlet to [ ]<sup>°C</sup> or less as described in Section 7. This limit is predicated on the fact that: (1) fiber loads at or below the limit will not form a contiguous bed at the core inlet, (2) the pressure drop through the regions of the core inlet with a fiber and particulate bed is negligible, and (3) the addition of chemical precipitates will not further impede flow into the core. Therefore, the flow into the core will not reduce below that required to make up for the liquid lost to boil-off and the cladding temperature will remain below 800°F.

### **9.2.2 Boric Acid Precipitation Control**

Similarly, following a CLB, BAPC is assured by limiting the fiber build up at the core inlet to less than [ ]<sup>°C</sup> as described in Section 7. Fiber loads at or below this limit will not form a contiguous bed at the core inlet. Consequently, open areas will remain in the debris bed that will allow communication between the core and LP such that mixing will occur between these regions. Therefore, the presence of debris will not change the current licensing basis calculations for defining the action time to preclude

BAP and the current actions to prescribe BAPC measures for a CLB will continue to keep the boron concentrations in the core region remain below the solubility limit even in the presence of debris.

### 9.3 REFERENCES

1. OG-13-205, "PWR Owners Group, NRC Technical Concerns Regarding Boric Acid Precipitation in the Presence of In-vessel Fibrous Debris and the Consequential Effects on Long-Term Core Cooling (PWROG PA-SEE-1090 and PA-SEE-1072)," ADAMS Accession Number ML14161A043, May 2013.

## 10 MARGINS AND CONSERVATISMS

The testing and calculations presented in this report were designed to ensure a conservative fiber load is calculated to address GSI-191 concerns. To that end, the various conservatisms (and where possible, margins) are identified to help define the conservative nature of the calculations. These conservatisms and margins are identified with the intent that individual plants can recover some of these margins on a plant-specific basis.

### 10.1 DEBRIS TRANSPORT AND ACCUMULATION

Various assumptions in Section 5 relate to debris transport and accumulation throughout the system. Most of these assumptions were made to ensure that debris transports to and accumulates in the most restrictive region of the RCS:

1. Debris is assumed to be in its constituent form (Assumption 4).
2. Debris does not accumulate in any location other than the sump strainer, core inlet, or within the core (Assumptions 2, 7, 17).
3. Debris does not exit the break under the following conditions (Assumptions 7 and 18):
  - a. Hot leg recirculation during a CLB
  - b. Hot or cold leg recirculation during a HLB
  - c. Cold leg recirculation during a CLB in a UPI plant

Further, assumptions are made to ensure that debris generated in containment reaches the sump strainer such that the maximum amount of debris has the opportunity to penetrate the sump strainer. These assumptions are inherent in the testing done by utilities to determine the strainer bypass fraction (i.e., the amount of debris that penetrates the strainer and reaches the RCS). These steps and assumptions represent a significant conservatism in establishing an in-vessel debris limit. In reality, the liquid velocities in much of containment are too low to transport much of the debris to the sump strainer. This is shown by the steps taken in strainer testing to introduce debris immediately upstream of the strainers such that it was able to reach the strainer.

Once debris passes through the sump strainers and reaches the RCS, there are numerous locations where velocities are low and debris may settle out of the flow stream. During cold side recirculation, the velocities in the RV LP are low for the limiting scenarios. Following a CLB, the core inlet flow rate is defined by the core boil-off rate. Following a HLB, the core inlet flow rate may be higher than that of a CLB, yet the limiting scenario was for low flow rates. At these velocities, some of the debris of the size expected to reach the RV will settle in the LP, as was observed during subscale testing (Volume 6). Again, some of the debris of the size expected to reach the RV will settle out of the flow stream before it reaches the core inlet.

For debris that is diverted to the BB region, any accumulation in that region is neglected even though the subscale testing of this region discussed in Volume 6 noted that debris accumulated below the former plates. While the amount was not quantified, the buildup was visible and not insignificant.

For plants that initiate simultaneous hot and cold side recirculation following a HLB, the coolant from the cold legs is used to replace boil-off and cool the core. Consequently, a fraction of the coolant injected into the hot legs is likely to exit the break directly, carrying debris along with it. However, this analysis assumes that if debris enters the RV in a HLB scenario, it remains there.

## **10.2 HOT LEG BREAKS**

### **10.2.1 Uniform Buildup of Debris**

The analyses and method provided in this report assume that debris builds up at the core inlet in a uniform manner (Assumption 9). In reality, the flow patterns approaching the core inlet will not be uniform. Before the ECCS reaches the core inlet, it must travel down the downcomer and turn 180 degrees along the lower hemisphere of the RV to begin the upward progression towards the core inlet. In this region, there are a number of internal structures that impede and direct the flow. Consequently, debris will likely be delivered to the core in a non-uniform manner, leading to a non-uniform distribution of debris at the core inlet. As has been discussed elsewhere in this report, if the debris does not build a uniform bed at the core inlet, then the effects of the resulting debris bed will be less than predicted by the method herein.

### **10.2.2 Chemical Precipitates and Core Inlet Blockage**

The analyses and method provided in this report assume that formation of chemical precipitates and any amount of debris at the core inlet will result in complete blockage (Assumption 6). This assumption is based in part on the results of the testing done for WCAP-16793-NP, Rev. 2 (Reference 10-1) in which the chemical precipitate surrogate Aluminum Oxyhydroxide (AlOOH) was shown to have a significant effect on particulate and fibrous debris beds of more than 15 g/FA. In those tests, conditions were noted that resulted in reduction of flow through the test loop below that required to make up for core boil-off.

This effect has only been shown under controlled test conditions where a uniform bed has developed and the surrogate AlOOH is used. As has been discussed elsewhere in this report, it is not likely that a uniform debris bed will form at the core inlet. Without a uniform bed, any chemical precipitates that form will not have the deleterious effect seen in the controlled test environment. Further, the actual chemical precipitates that form will likely consist of other forms besides AlOOH (Volume 6), and AlOOH has been shown to produce higher pressure drops compared to other precipitates that might form (Reference 10-2).

Therefore, the use of only AlOOH on an assumed uniform and contiguous bed at the core inlet of any debris amount ensures conservative results.

### **10.2.3 Cladding Temperature**

For the HLB evaluation, a cladding temperature of 800°F is used as an acceptance criterion to ensure that decay heat continues to be removed (Section 3.7). The basis for this value is discussed in detail in Reference 10-1, Appendix A. In summary, long-term autoclave testing demonstrated that the increase in



oxide thickness and hydrogen loading was limited when exposed to temperatures of less than 800°F for periods of 30 days. With limited corrosion and hydrogen pickup, the impact on cladding mechanical performance is not significant. Therefore, no significant degradation in cladding properties would occur due to 30-day exposure at 800°F. Further, a top-skewed axial power profile was analyzed (Assumption 12) such that if the core uncovered and heated-up, the cladding temperature response would be maximized.

To meet the acceptance criterion, the cladding temperatures in the TH analyses (Volume 4) were kept below 800°F for all times after SSO in the final cases. Sensitivity studies showed a cladding heatup above 800°F (but well below 2200°F) for approximately 500-800 seconds resulted in a decrease in  $t_{block}$  of approximately 20-25 percent and an increase in  $K_{max}$  of approximately 20 percent. This relatively mild temperature excursion, lasting no more than 20 minutes in a small section of the core, demonstrates the significant conservatism inherent in the derivation of  $t_{block}$  and  $K_{max}$ .

#### 10.2.4 Bounding Thermal-Hydraulic Analyses

The TH analyses described in Section 6.1 and Volume 4 used a combination of core power and BB flow resistance that bound all plants in a given category. As a result, the values obtained for  $K_{max}$  and  $t_{block}$  are conservative for most plants. When calculating  $K_{max}$  and  $t_{block}$ , a conservatively high value for the BB resistance was used. Reducing the BB resistance will increase  $K_{max}$  (i.e., allow more debris to be captured at the core inlet) and decrease  $t_{block}$  (i.e., allow complete core inlet blockage earlier). Recovering this margin is most easily done by performing a plant-specific analysis using the approach described in Volume 4.

The TH analyses in Volume 4 also demonstrated that a higher value of  $K_{max}$  and an earlier time for  $t_{block}$  was calculated at higher ECCS flow rates. In other words, the  $K_{max}$  and  $t_{block}$  developed at minimum ECCS flow are conservatively applied to all flow rates in the HLB methodology described in Section 6.5. Accounting for the effects of various ECCS flow rates on  $K_{max}$  and  $t_{block}$  would increase the total amount of fiber that could be tolerated in the RV.

#### 10.2.5 Subscale Test Facility Design

The subscale test facility described in Volume 6 was designed to ensure conservative results. Design features include (1) assuring that a well-developed, uniform flow and uniform distribution of debris was delivered to the test section; (2) no obstructions between the debris injection point and the test section were included (i.e. no lower plenum structures); and (3) the middle section of the lower end filter was used such that the lower core plate did not alter the flow patterns. These design features ensured that debris captured uniformly across the core inlet or spacer grid.

In reality, the flow patterns approaching the core inlet will not be uniform, nor is the region free of obstructions. Before the ECCS reaches the core inlet, it must travel down the downcomer and turn 180 degrees along the lower hemisphere of the RV to begin the upward progression towards the core inlet. In this region, there are a number of internal structures that impede and direct the flow. Further, the holes in the core support plate will redirect flow. Consequently, debris will likely be delivered to the core in a non-uniform manner, leading to a non-uniform distribution of debris at the core inlet. As has been

discussed elsewhere in this report, if the debris does not build a uniform bed at the core inlet, then the effects of the limiting quantities of debris calculated with the method herein will be less than predicted.

Licensees may wish to perform additional testing (either in the subscale facility or in an equivalent) to recover these margins.

### 10.2.6 Particulates Used in Testing

A number of parameters related to the particulates used in testing were selected to ensure that the most limiting result was obtained. In particular, the particulate-to-fiber (p:f) ratio was varied until a limiting result was obtained, and the particulate size distribution used was conservatively skewed. The conservative effects of these selections are discussed here.

It is not expected that a single size particulate will preferentially pass through the sump strainer. Instead, some distribution of sizes is expected. Any filtering bed at the sump strainer will preferentially capture larger particulates due in part to the bed morphology. Test data show that large particulates are present past the sump strainer, but the testing caps the largest particulate size to [ ]<sup>a,c</sup> Some subscale testing with particulate size distributions that contained particulates larger than [ ]<sup>a,c</sup> improved the results.

Not only are the particulate parameters used in testing conservative, but the degree of conservatism is significant and the likelihood of these parameters existing in the most conservative combination is very unlikely. Figures 5-22 and 5-23 of Volume 6 demonstrate why the degree of conservatism is considered significant. [ ]<sup>a,c</sup>

### 10.2.7 Flow Rates Used in Testing

Testing showed that the most limiting debris beds were developed under minimum ECCS flow rates; therefore, the final head loss correlations were developed under these conditions (see Section 6.3). However, the TH analyses and HLB methodology do not credit the benefits of a higher ECCS flow rate even when such flows are analyzed. At higher flow rates, the subscale testing (Volume 6) demonstrated that multiple debris beds formed, which allows for a higher debris limit. The TH analyses (Volume 4) demonstrated that a higher value of  $K_{max}$  and an earlier time for  $t_{block}$  was calculated at higher ECCS flow rates. In other words, the correlations developed at minimum ECCS flow are conservatively applied to all flow rates in the HLB methodology described in Section 6.5.

### 10.2.8 Geometry Used in Testing

The core inlet geometries tested represent the most restrictive geometries currently produced by each vendor. The tested geometries represent fuel for a 17x17 bundle that is intended to be used in Westinghouse 3- and 4-loop plant designs. The openings through the RFA bottom nozzle (for Westinghouse fuel) and the **FUELGUARD™** filter (for AREVA fuel) are smaller than similar hardware

FUELGUARD is a trademark of its respective owner. Other names may be trademarks of their respective owners.

used in the CE, B&W, and Westinghouse 2-loop plant designs. Larger openings will collect less debris and allow for higher debris limits. In this manner, the results from the 17x17 bundle are conservatively applied to all fuel designs currently in production.

### 10.2.9 Reactor Vessel Fiber Limits

The maximum fiber limit allowed in the RV is [ ]<sup>ac</sup> (Section 6.5.5). This limit corresponds to the maximum allowed debris limit in the heated core and assumes that no debris is captured at the core inlet. Assuming that no debris will capture at the core inlet is very conservative given the geometry of the core inlet structures. Further, the subscale program demonstrated that debris will accumulate to some level at either the lower end fitting (LEF) or the first spacer grid for a wide range of conditions, which imply that some debris will accumulate in these locations. Therefore, it is conservative to assume that none will collect at the core inlet and set a maximum limit to that which can be tolerated in the heated core.

## 10.3 COLD LEG BREAKS

A number of conservatisms inherent in the CLB approach are outlined in Volume 3, Section 3.3.1. A few of the items related to debris transport and accumulation are discussed in Section 7. The remaining items are reiterated here for completeness.

The CLB methodology is designed to maximize the prediction of debris at the core inlet. A number of assumptions are made to support this effort. First, the minimum sump water volume is assumed. This assumption delivers the highest concentration of fiber to the RCS. More debris delivered earlier results in more debris at the core inlet.

The earliest time of sump recirculation is assumed. Further, the prevailing core power uncertainty is used along with a 20 percent increase in the core decay heat. These inputs and assumptions ensure a conservatively high core decay heat and core boil-off rate. Since the core boiling rate defines the flow rate to the core and the flow rate defines the debris delivery rate, these inputs and assumptions over-predict the amount of debris that reaches the core inlet. On top of this, the amount of fiber entering the core is increased by 20 percent.

A limiting single failure in the ECCS and CSS is assumed. Since the flow to the core is fixed by the core boil-off rate, this assumption minimizes the fraction of ECCS that exits the break and thus minimizes the amount of debris that exits the break and returns to containment to be re-filtered.

The latest HLSO time maximizes fiber capture in the core.

## 10.4 REFERENCES

- 10-1 WCAP-16793-NP-A, Rev. 2, "Evaluation of Long-Term Cooling Considering Particulate, Fibrous and Chemical Debris in the Recirculation Fluid," July 2013.

- 10-2 B. B. Banh, K. E. Kasza, and W. J. Shack, "Technical Letter Report on Follow-on Studies in Chemical Effects head-Loss Research; Studies on WCAP Surrogates and Sodium Tetraborate Solutions," Argonne National Laboratory, NRC Contract N6100.

## 11 SUMMARY AND CONCLUSION

The PWROG has undertaken a comprehensive test and analysis program as part of the resolution to GSI-191 to increase the fibrous debris limits per FA. This report documents the methodology that member utilities can use to assess the time-dependent collection of fibrous debris in the RV, which can then be used for final closure of NRC GL 2004-02 and GSI-191. This work provides an alternative approach to the method detailed in WCAP-16793-NP-A, Rev. 2 for defining an in-vessel fibrous debris limit and provides a means for increasing the currently established in-vessel fibrous debris limit of 15 g/FA.

This volume consolidates the results of five separate, but interrelated elements of the PWROG program. The individual program elements are described in detail in separate volumes, the collection of which, including the present volume (Volume 1), constitute WCAP-17788. These respective program elements include a PIRT (Volume 2), a CLB evaluation method (Volume 3), TH analyses for a HLB (Volume 4), autoclave testing for chemical effects (Volume 5), and subscale head loss testing for HLB (Volume 6).

This program is applicable to Westinghouse, CE, and B&W PWR NSSS plants. The methodology for calculating the in-vessel debris limits described in this report are plant-specific and depend on inputs for each plant (or group of identical plants). The general approach for all plants is to separately assess the debris limits for the CLB and HLB scenarios. Both break locations must be considered given the large difference in system response and the relative effects on core cooling and mixing between them.

This report further divides the plants into those that initially begin sump recirculation with ECCS recirculation flow to the cold legs and those that initially begin with ECCS recirculation flow to the upper plenum (UPI plants). Section 5 identifies the major assumptions used in the methodology for both types of plants. For plants that initially start with cold side recirculation, Section 4.2 outlines the methodology for HLB and Section 4.3 outlines the methodology for CLB. Sections 6 and 7 provide the details of the methods for calculating the amount of fiber delivered to the RCS for HLB and CLB, respectively. For UPI plants, Section 8 provides the methodology for both break locations. For the spectrum of large breaks, this methodology can be used to ascertain that the amount of debris generated in containment does not ultimately result in an excessive amount of debris (fiber and particulate) delivered to the RV such that LTCC is compromised.

Results obtained using the methods described herein will result in a conservative calculation of the amount of debris that can be tolerated in the RV and sump. Details of the conservatisms and margins in the method and supporting calculations are detailed in Section 10.

## **APPENDIX A – PHENOMENA IDENTIFICATION AND RANKING**

To support the assessment of chemical reaction products on the acceptable fibrous debris limit per FA, the Phenomena Identification and Ranking Table (PIRT) process was initiated. The objective of the PIRT process is to identify and rank phenomena that are important to chemical effects, TH and transport associated with the post-accident operation of the ECCS in the recirculation mode over the time period of interest. The ranking considers the relative importance of the respective phenomena, and the associated state of knowledge (SoK). Volume 2 documents the efforts of the panel of experts convened to develop a PIRT to support the comprehensive test and analysis program undertaken by the PWROG to increase the currently established fiber limits. This PIRT was developed so that it applies to all U.S. PWR designs, regardless of vendor.

### **A.1 PIRT SCENARIO IDENTIFICATION, PHASES, AND PERIODS**

The scenarios of high importance for chemical effects in the recirculating coolant path post-accident are those accidents that:

1. Introduce debris into the coolant.
2. Require the plant to recirculate coolant from the reactor containment building sump.

To maximize the debris generation, and to provide for the evolution of the ECCS and CSS to evolve from injecting coolant from the RWST to recirculating coolant from the pool of spilled and debris-laden coolant on the containment building floor, an LBLOCA was considered for development of the PIRT.

Two scenarios were used for constructing these PIRT:

1. Large DEG HLB
2. Large DEG CLB

For the purposes of the development of the PWROG GSI-191 PIRT, the accident, regardless of break location, was divided into five phases. The phases and their durations were selected to be consistent with events of significance associated with both the DEG HLBs and CLBs. The phases selected and their durations selected are identified in Table A-1.

A listing and description of significant events that occur in each phase of the hypothetical DEG CLB are listed in Volume 2, Table 6-2. A similar listing and description of significant events that occur in each phase of the hypothetical DEG HLB are listed in Volume 2, Table 6-3.

<b>Table A-1 PIRT Scenario Phases and Phase Duration</b>		
<b>Phase</b>	<b>Duration</b>	<b>Description</b>
P1	0 to 30 seconds	Initial depressurization of the RCS (i.e., blowdown)
P2	30 seconds to start of sump recirculation	1. Injection of the RWST/BWST into the RCS 2. Initiation of containment spray
P3 <sup>(1)</sup>	Start of sump recirculation to 12 hrs	1. Beginning of LTCC 2. Realistic time when core flushing is needed
P4	12 hrs to 1 day (24 hrs)	1. Maintain LTCC 2. Cooldown and depressurization of reactor containment building
P5	1 day to 30 days	1. Maintain LTCC 2. Long-term containment building cooldown
<b>Notes:</b> 1. The time when core flushing for B&W plants or hot leg switchover (HLSO) for CE and Westinghouse plants occurs is a plant-specific parameter that can vary from as little as one to two hours after the LOCA occurs to as long as about 14 hours after the LOCA occurs for most plants. A value of 12 hours was chosen to be representative of the time duration that recirculation from the sump may occur without evolving to core flushing or HLSO. However, it is possible that the core flushing flow may be initiated prior to 12 hours or possibly not at all if the core exit subcooling is reestablished for some plants		

## A.2 DEVELOPMENT APPROACH FOR THE PWROG GSI-191 PIRT

The time period of interest for the debris entering the RCS within the PWROG GSI-191 PIRT begins with period P3, the time of switchover from injecting from the RWST. During Period P3, the recirculation of debris laden coolant from the sump can enter the RCS and flow to the core with the ECCS flow (for UPI plants, this debris-laden flow is injected directly into the RV UP).

For plants that inject ECCS flow on the cold side of the core, the core coolant flows down the downcomer and into the bottom of the core. Under these flow conditions, there is a potential for debris to collect and form a debris bed at the core inlet and within the core that would challenge LTCC.

The initiation of active boron dilution actions mitigates the build-up of boric acid in the core for postulated CL breaks by either reversing the flow in the core (for CE and Westinghouse plants) or providing another flow path to duct coolant from the core to the sump (HL letdown for B&W plants). Both of these processes provide for the flushing of concentrated boron from the core before boron solubility limits are reached. This flushing will also have the effect of diluting post-accident chemical products that are collected and concentrated in the core during periods P2 and P3 due to the boiling associated with core cooling of a CL break.

At the beginning of period P3 following a DEG CL break, the core power is capable of generating sufficient steam that coolant injected into the HL may not readily reach the core and be effective in matching the core decay heat and initiating a core flushing flow for Westinghouse and CE plant designs. Hence, time periods P1 (i.e., blowdown), P2 (i.e., injection from the RWST) and P3 (i.e., initial recirculation of spilled coolant from the containment recirculation sump until active boron dilution; 12 hours is provided as a representative time before active boron dilution is initiated in this PIRT activity) are critical for debris generation and transport, which are the focus of this PIRT. However, the PIRT panel unanimously agreed that time periods P4 (12 hours to 1 day – cool down of the core and reactor

containment building) and P5 (1 day to 30 days – LTTC) should also be included in this PIRT activity for completeness because these are the periods during which the effects of chemical products become more important. Hence, the PIRT addresses time periods P1 through and including P5, although periods P1 through P3, and particularly P3, are of primary interest for this PIRT.

The PIRT panel recognized that both chemical effects and TH phenomena have the potential to collectively contribute to the overall consequences of post-accident chemical effects on LTCC. Thus, the PIRT panel chose to account for both chemical and TH mixing phenomena in the development of a PIRT for this project.

The chemical effects PIRT is presented in Volume 2, Section 7. The TH PIRT is presented in Volume 2, Section 8. Variations in phenomena related to break location (HLB versus CLB), when they are evaluated to occur, are identified in the PIRT. A discussion of the high ranked phenomenon is provided in Volume 2, Section 9.

### **A.3 PIRT RECOMMENDATIONS AND DISPOSITION**

The PIRT tables provide guidance for the PWROG comprehensive test and analysis effort to close GSI-191. The PIRT panel advanced the following recommendations for consideration by the PWROG upon completion of identifying the phenomena, the ranking of the importance of the phenomena and the assigning of a SoK to the phenomena. Those phenomena and processes that are ranked “H” in importance and “L” for a SoK are candidates for additional study to improve the SoK associated with that phenomena or process. The following details those specific related phenomena and processes identified by the PIRT and the disposition of each within the WCAP-17788 program.

- Radiation-induced debris bed chemical reactions. Concentration of radionuclides leads to locally high radiation fields and changes in dissolution and precipitation processes.
  - Program disposition – Radiation impacts were beyond the scope of the current program. Given the conservatism and margins built into the entire GSI-191 evaluation process, this is deemed acceptable, as this is unlikely to result in earlier chemical effects than those found without radiation.
- For a CL break, fibrous debris collecting on fuel elements alters flow patterns and mixing volumes, changing the risk of precipitation due to boiling concentration.
  - Program disposition – Regarding BAP, such effects are considered in Volume 1, Section 9.2.2. Regarding chemical effects, the limits imposed on debris at the core inlet for CL breaks are small enough that filtering debris beds are not formed, and therefore, there is no mechanism to catch sufficient chemical effects to impact cooling flow through the core.
- For a CL break, chemical products in combination with fibrous debris collecting on fuel elements alter flow patterns and mixing volumes, changing the risk of precipitation due to boiling concentration.
  - Program disposition – Regarding BAP, such effects are considered in Section 9.2.2. A uniform bed will not be formed and maintained under CLB conditions at the fiber limits



---

established, so the impact of chemical effects is negligible. Since open regions still exist at the core inlet, communication continues, and mixing pattern alteration is minimal.

- For a HL break, chemical products in combination with fibrous debris collecting on fuel elements alter flow patterns and mixing volumes, changing the risk of precipitation due to boiling concentration.
  - Program disposition – The TH analysis (Volume 4) assumes complete core inlet blockage with the arrival of chemical effects. Analysis showed that mixing patterns are altered but not to the point that BAP would be expected to occur. Core mixing is dominated by boiling, which in turn keeps core region concentrations uniform. Liquid carryover remains sufficient such that core region remain below the boric acid solubility limit. Regarding chemical effects, the autoclave tests were integrated effects tests. They included fiber both in the autoclave and in the drain time samples. The samples were cooled, giving the opportunity for supersaturation and deposition on fibers.
- Impact of kinetics of precipitation. Non-equilibrium effects are a benefit as they may delay precipitation.
  - Program disposition – The autoclave testing was performed in a prototypic fashion and was not forced to be in equilibrium. Therefore, non-equilibrium effects were captured by the testing.
- Particulate settling in the reactor. Particulate settling may occur due to relatively low, upwards flow (for CL recirculation for CL breaks) within reactor.
  - Program disposition – Particulate settling was not investigated because it is conservatively assumed that all debris that enters the vessel collects at core inlet or transports to the core proper. Both the subscale fuel testing and the autoclave testing took measures to limit or eliminate settling to remain conservative in this regard.
- Deposition. Chemical products formed during all periods may deposit on other surfaces.
  - Program disposition – Some level of chemical product deposition on autoclave walls and materials may have occurred, but if so, this is representative of what happens in the plants' sumps and on their strainers and on other structures and components inside containment. If no chemical remains suspended in the sump fluid to reach the core, the chemical effect on the core is negligible. If it does remain suspended in the sump fluid, then it will be transported to the core and potentially impact debris bed pressure drop; the same happens in the drain time measurements, where the primary available surface for precipitation is the filter (representative of the debris bed on the fuel). Therefore, this has been appropriately represented.

## **APPENDIX B - REQUESTS FOR ADDITIONAL INFORMATION AND RESPONSES**

The RAIs addressed herein were provided to the Pressurized Water Reactor Owners Group (PWROG) via the following documents for Volumes 1 and 3. Note that the Volume 3 RAIs are included herein as many of the RAIs were associated with Volume 1 content, and no revisions are being made to Volume 3.

NRC Correspondence, "Request for Additional Information Related to Volume 1 of Pressurized Water Reactor Owners Group Topical Report WCAP-17788 'Comprehensive Analysis and Test Program for GSI-191 Closure,'" April 2016, ADAMS Accession No. ML16078A166.

NRC Correspondence, "Request for Additional Information RE: Pressurized Water Reactor Owners Group Topical Report WCAP-17788 'Comprehensive Analysis and Test Program for GSI-191 Closure' (TAC No. MF6536)," August 2016, ADAMS Accession No. ML16102A357.

**RAI-1.1**

The method to define debris limits provided in the submittal is said to apply to all fuel designs in production by Westinghouse and Areva as of January 2015, except for Areva fuel with the TRAPPER fine mesh filter. This design was not tested as part of the program even though it is still used in some plants.

The submittal states:

“The use of the TRAPPER fine mesh filter fuel design in limited quantities would not alter the limits defined by the methodology.”

- a. Provide justification that the limits in this methodology would not be altered if the TRAPPER fine mesh filter fuel design is in use. Provide any pertinent limitations regarding the presence of fuel assemblies with this filter in the reactor core.

***Response***

As identified in WCAP-17788, Volume 1, Section 4, the **TRAPPER™** fine mesh filter is no longer in production and was therefore not tested as part of the WCAP-17788 program. However, fuel assembly designs with the fine mesh filter may still be present in spent fuel pools of some utilities. While this fuel design will not be used in any batch implementation, individual assemblies may be re-inserted into cores in lower power locations as may be defined by the core energy requirements and the cycle design. No more than eight assemblies with the **TRAPPER** fine mesh filter would be included in the core at any given time. The use of the **TRAPPER** fine mesh filter fuel design in these limited quantities would not alter the in-vessel limits defined by the WCAP-17788 methodology as described in the following discussion.

The **TRAPPER** fine mesh filter was used on assemblies that refueled Westinghouse 3- and 4-loop, and Babcock & Wilcox (B&W) plant designs. The assemblies used in Westinghouse plants had rod arrays of 17x17, and B&W plants used assemblies with rod arrays of 15x15. The intermediate spacer grid designs in the assemblies were of a standard, “egg-crate” design. The **TRAPPER** fine mesh filter was not used in Combustion Engineering (CE) or Westinghouse 2-loop (i.e., upper plenum injection) plant designs. Therefore, this RAI response does not apply to CE or Westinghouse upper plenum injection (UPI) plants.

As described in WCAP-17788, Volume 1, Section 4.1, debris transported to the reactor vessel (RV) is assumed to accumulate in one of two locations: at the core inlet and/or in the heated core region (in-core). The in-core debris limit is unaffected by the use of the fine mesh filter. The dimensions and configuration of the fuel assembly above the lower end fitting (LEF) (i.e., rod diameters, pin and assembly pitches, number of fuel rods and control rod guide tubes) are the same for fuel designs that use the **TRAPPER** or **FUELGUARD™** LEF in any given plant. Testing described in WCAP-17788, Volume 6 showed that debris capture and head loss at spacer grids used in assemblies with the same

TRAPPER is a trademark or registered trademark of AREVA. Other names may be trademarks of their respective owners.

FUELGUARD is a trademark or registered trademark of AREVA. Other names may be trademarks of their respective owners.

flow area were similar. For example, 17x17 fuel assemblies use either the RFA grid type of the **HMP™** grid type. The RFA grid type has a single piece of metal forming the grid strap, whereas [

] <sup>a,c</sup> forming the grid strap. The results of the grid capture discussed in WCAP-17788, Volume 6, Section 5.2.5 indicate a similar pressure drop for these two different grid designs. Therefore, only debris accumulation at the core inlet need be considered in this evaluation.

At the core inlet, testing described in WCAP-17788, Volume 6 showed that the limiting scenario occurred when debris accumulated at the leading edge of the LEF. Figure RAI-1.1-1 and Figure RAI-1.1-2 show the **FUELGUARD** (which was tested) and the **TRAPPER** fine mesh filter (which was not tested) as seen from below, which is the direction that debris would approach. From this perspective, both LEFs are flat screens with rectangular or square openings. The openings in the **TRAPPER** fine mesh filter are [

] <sup>a,c</sup> The openings in the **FUELGUARD** LEF are [

] <sup>a,c</sup>



**Figure RAI-1.1-1 Photograph of FUELGUARD Lower End Fitting**

HMP is a trademark of AREVA. Other names may be trademarks of their respective owners.



**Figure RAI-1.1-2 Photograph of TRAPPER Fine Mesh Filter**

Debris accumulation at the core inlet can be divided into two time frames; before chemical precipitate formation (i.e., the debris bed is composed of fiber and particulates only) and after chemical product formation. The methodology in WCAP-17788 assumes that complete core inlet blockage occurs once chemical products have formed regardless of how much debris has accumulated on the LEF. The use of either the **TRAPPER** fine mesh filter or the **FUELGUARD** will not affect the evaluation after chemical product formation. Therefore, only the time before chemical product formation need be examined in detail.

The subscale testing in WCAP-17788, Volume 6 indicated that only a small amount of fiber penetrates through the core inlet during the early stages of debris bed development ( [ ]<sup>a,c</sup>

WCAP-17788, Volume 6, Section 5.2.8). Testing done with the **FUELGUARD** LEF indicated similar results; during the initial phases of debris introduction, a small amount of fiber will pass through the core inlet. However, the fiber capture efficiency at the core inlet becomes nearly 100 percent after a small amount of fiber accumulates. Consequently, the majority of the fiber that reaches the core inlet is captured by the **FUELGUARD**. Since the **TRAPPER** fine mesh filter has smaller openings than the **FUELGUARD**, it is expected that it will capture the same or only slightly more fiber than the **FUELGUARD** LEF.

Subscale testing also determined that capture geometry has a strong influence on the pressure drop across the debris bed. The **TRAPPER** and **FUELGUARD** can both be considered flat screens, which would suggest similar pressure drops under similar debris loads. But, since the open area through the **TRAPPER** fine mesh filter is different from that of the **FUELGUARD** LEF, the following calculations

determine the resulting pressure drop difference through the fiber and particulate debris bed that collects on the leading edge of the fine mesh filter relative to the **FUELGUARD**.

WCAP-17788, Volume 1, Equation 6-1 calculates the equivalent form-loss coefficient for a given fiber mass:

$$K_{test} = \frac{2g_c dP}{\rho v^2}, \quad \text{WCAP-17788, Volume 1, Equation 6-1}$$

where  $v$  is the average superficial velocity through the debris bed as defined by WCAP-17788, Volume 1, Equation 6-2:

$$v = \frac{\left(\frac{Q}{A_{column}} + \frac{Q}{A_{BN}}\right)}{2}, \quad \text{WCAP-17788, Volume 1, Equation 6-2}$$

Rearranging and solving for  $dP$ , the ratio of pressure drop through the **FUELGUARD** ( $dP_{test,FG}$ ) to the expected pressure drop through the **TRAPPER** fine mesh filter ( $dP_{test,fine mesh}$ ) for the same fiber mass yields:

$$\frac{dP_{test,fine mesh}}{dP_{test,FG}} = \frac{\left(\frac{1}{A_{column}} + \frac{1}{A_{fine mesh}}\right)^2}{\left(\frac{1}{A_{column}} + \frac{1}{A_{FG}}\right)^2}.$$

As reported in WCAP-17788, Volume 1, Section 6.3.3,  $A_{column}$  is 16 in<sup>2</sup> and  $A_{FG}$  is [ ]<sup>a,c</sup>. While the **TRAPPER** fine mesh filter was not tested, the LEF flow area of a similar test piece would be [ ]<sup>a,c</sup>. Substituting these values into the above equation,

$$\left[ \right]^{a,c}$$

This result indicates that the expected pressure drop across a debris bed on the **TRAPPER** fine mesh filter is approximately [ ]<sup>a,c</sup> than the pressure drop across a debris bed on the **FUELGUARD** for the same fiber mass. This, of course, assumes that the flow rate through the fine mesh filter remains the same as that through the **FUELGUARD** during the debris accumulation period. This means that for the same pressure drop across the core inlet, smaller amounts of fiber will accumulate on the **TRAPPER** fine mesh filter relative to the **FUELGUARD** LEF. The reduction in fiber mass at core inlet locations with the **TRAPPER** fine mesh filter can be approximated by using the equations in WCAP-17788, Volume 1, Section 6.3.3 for fiber load as a function of  $K_{test}$  and  $K_{eq}$  for AREVA fuel.

WCAP-17788, Volume 1, Figure 6-13 shows the fiber load as a function of  $K_{eq}$  for AREVA fuel. WCAP-17788, Volume 1, Table 6-4 identifies the equations for the curve fits shown on WCAP-17788, Volume 1, Figure 6-13 as a series of three linear fits. In order to obtain the maximum fiber load for a plant category,  $K_{eq}$  from the subscale testing is set to  $K_{max}$  from the WCAP-17788, Volume 4 thermal-hydraulic (TH) analyses, and the linear equations are rearranged to solve for fiber mass. The results are shown in WCAP-17788, Volume 1, Table 6-5.

For the **TRAPPER** fine mesh filter,  $K_{eq}$  is reduced as described above. To obtain an acceptable core inlet fiber load for the fine mesh filter,  $K_{max}$  is reduced by a similar amount and the linear equations are solved. For Westinghouse upflow barrel/baffle plants, this process is as follows:

$$\left[ \begin{array}{c} \\ \\ \end{array} \right]_{a,c}$$

The maximum acceptable fiber load falls within Regime 2, so:

$$\left[ \begin{array}{c} \\ \\ \end{array} \right]_{a,c}$$

Similarly, for Westinghouse downflow barrel/baffle plants:

$$\left[ \begin{array}{c} \\ \\ \end{array} \right]_{a,c}$$

The maximum acceptable fiber load falls within Regime 2, so:

$$\left[ \begin{array}{c} \\ \\ \end{array} \right]_{a,c}$$

For B&W plants:

$$\left[ \begin{array}{c} \\ \\ \end{array} \right]_{a,c}$$

The maximum acceptable fiber load falls within Regime 3, so:

$$\left[ \begin{array}{c} \\ \\ \end{array} \right]_{a,c}$$

However, [ ]<sup>a,c</sup> is larger than the maximum amount of fiber tested, which was [ ]<sup>a,c</sup>

The new fiber loads and the limited number of assemblies can be used to estimate the decreased fiber load when up to eight fuel assemblies with the **TRAPPER** fine mesh filters are included in a core. For the Westinghouse 4-loop plants, there are 193 fuel assemblies in the core. For Westinghouse 3-loop plants, there are 157 fuel assemblies in the core. For B&W plants, there are 177 fuel assemblies in the core. Using the smaller number will result in a larger fraction of fine mesh assemblies and a more conservative fiber load. Therefore, eight of these assemblies would be **TRAPPER** and 149 would be **FUELGUARD**.

Using the maximum fiber loads from WCAP-17788, Volume 1, Table 6-5 for the **FUELGUARD** assemblies and the above values for the fine mesh assemblies, the core average debris load for Westinghouse upflow plants would be:

$$\left[ \right]_{a,c}$$

which is a decrease of [ ]<sup>a,c</sup> compared to a core that contains only **FUELGUARD** assemblies.

Similarly, for Westinghouse downflow plants, the core average debris load would be:

$$\left[ \right]_{a,c}$$

which is a decrease of [ ]<sup>a,c</sup> compared to a core that contains only **FUELGUARD** assemblies.

Since the B&W core can tolerate more debris than was tested, the core average reduction would be on the same order of magnitude or smaller.

Based on the above calculations, it is clear that including up to eight fuel assemblies with the **TRAPPER** fine mesh filter would have a negligible effect on the limits defined by the methodology described in WCAP-17788, Volume 1. Therefore, a core loading pattern can be designed with up to eight fuel assemblies with the **TRAPPER** fine mesh filter without needing to account for them explicitly.

- b. Provide a list of fuel types and designs that were tested as part of the program.

### ***Response***

A variety of grid and fuel inlet components were tested as part of this program. The selected test geometries are representative of the fuel products currently in use. The tested fuel features, as summarized in WCAP-17788 Volume 6, Table 3-2, are provided below.



Westinghouse Manufactured Fuel Components:

- Tested Bottom Nozzle (BN) Designs: RFA Debris Filter Bottom Nozzle / Protective grid (P-grid)
- Tested Grid Designs: RFA, OFA, and UFA

AREVA Manufactured Fuel Components:

- Tested Lower End Fitting Design: **FUELGUARD**
- Tested Grid Design: High Mechanical Performance Fuel Assembly Grid (**HMP**)

- c. Provide a list of fuel designs that the method in this submittal applies to. Include identification and description of the fuel types, bottom nozzle designs, and spacer grid designs.

***Response***

The NRC reviewer is requesting additional information that justifies how the tested fuel designs bound the untested designs. Additionally, information is provided to explain how a fuel assembly with a pitch not equal to the tested value of [ ]<sup>ac</sup> is scaled to determine an equivalent fibrous debris loading in units of grams per fuel assembly (g/FA).

In the original response to this question (Reference RAI-1.1-1), a list of Westinghouse and AREVA fuel designs that the WCAP-17788 in-vessel debris methodology applies to was provided. Table RAI-1.1-1 repeats the list of Westinghouse fuel for convenience. Table RAI-1.1-2 repeats the list of AREVA fuel for convenience (note that Table RAI-1.1-2 is updated to include the fuel assembly pitch in lieu of the rod pitch).

Table RAI-1.1-1      Applicable Westinghouse Fuel Designs					
Fuel Array	Fuel Assembly Pitch (in)	Fuel Assembly Flow Area (in <sup>2</sup> )	Fuel Rod OD (in)	Bottom Nozzle Hole Dia. (in)	Debris Grid Filter Design
14x14 422V+					NA
15x15 UFA					P-Grid
16x16 STD					Guardian
16x16 CE					Guardian
16x16 NGF					Guardian
17x17 OFA					P-Grid
17x17 RFA					P-Grid
17x17 XL RFA					P-Grid
17x17 NGF					P-Grid

Table RAI-1.1-2 Applicable AREVA Fuel Designs							
Fuel Assembly Type	Plant Type	Lattice	FA Pitch (in)	Rod Diameter (in)	Intermediate Grid Type	Bottom Grid Type	Lower End Fitting
Mark-B-HTP-1	B&W	15x15					
Advanced W17 HTP	Westinghouse	17x17					
W17HTP	Westinghouse	17x17					
W17HTP	Westinghouse	17x17					
W15HTP	Westinghouse	15x15					
CE16HTP	CE	16x16					
CE15HTP	CE	15x15					
CE14HTP	CE	14x14					

a,c

Not all fuel designs listed in Tables RAI-1.1-1 and RAI-1.1-2 were explicitly tested in the WCAP-17788 subscale head loss test program. The subscale head loss program tested the Westinghouse 17x17 RFA bottom nozzle with a Protective Grid (P-grid) and the AREVA **FUELGUARD™** lower end fitting to define the WCAP-17788 core inlet debris limits.

The testing determined that formation of a single debris bed on the bottom nozzle surface resulted in the limiting head loss, compared to a situation in which the fibrous debris is distributed across multiple debris beds at different locations within the fuel assembly. With regard to head loss across a debris bed formed on the bottom nozzle, it was determined that bottom nozzle hole diameter was the critical geometric parameter. Smaller hole sizes resulted in increased fiber capture and head loss. Therefore, the RFA bottom nozzle was selected to define the subscale final limits for Westinghouse supplied fuel since it had the smallest bottom nozzle hole diameter.

As shown in Table RAI-1.1-1, the tested bottom nozzle hole size of [ ]<sup>a,c</sup> is equal to or smaller than the bottom nozzle hole sizes of all fuel types except the 14x14 422V+ design. This fuel design is only used in Westinghouse 2-loop upper plenum injection (UPI) plants. As described in Section 8 of WCAP-17788, Volume 1, the in-vessel debris methodology for Westinghouse UPI plants does not rely on testing results from the subscale head loss test program. Rather, UPI plants use the approved 15 g/FA core inlet fibrous debris limit defined in WCAP-16793-NP-A, Rev. 2 (Reference RAI-1.1-2). As such, justification of this fuel type is not required since the subscale testing results are not used to define the core inlet debris limit.

FUELGUARD is a trademark or registered trademark of its respective owner. Other names may be trademarks of their respective owners.

The entrance gap for the AREVA FUELGUARD is identical for all fuel designs described in Table RAI-1.1-2. Therefore, the tested design is applicable to all of the AREVA supplied fuel.

The fuel assembly pitch is another factor that needs to be considered when justifying the applicability of the WCAP-17788 debris limits to fuel designs not tested. The tested fibrous debris loads, and associated limits defined in WCAP-17788 are presented in units of g/FA. The tested debris loads were scaled to a full-area fuel assembly assuming an assembly pitch of [ ]<sup>a,c</sup>. If the assembly pitch is different, the fibrous debris load must be adjusted to account for this difference. Table 3-7 of WCAP-17788, Volume 6 reports the scaling factor for the tested bottom nozzles (fuel assembly pitch [ ]<sup>a,c</sup>) to be [ ]<sup>a,c</sup>.

If the fuel design has a different fuel assembly pitch, the first step is to determine the appropriate scaling factor,  $R_m$ :

$$R_m = \frac{R}{A_s} (P_{FA})^2 = \left[ \right]^{a,c} \quad \text{Eq. RAI-1.1-1}$$

Where,

$R$  = the scaling factor applied in WCAP-17788, Volume 6.

$A_s$  = the subscale test column flow area.

$P_{FA}$  = the pitch of the fuel assembly being scaled.

Using Eq. RAI-1.1-1, the fibrous debris limits reported in WCAP-17788 can be scaled to a fuel assembly pitch that is different than the tested pitch of [ ]<sup>a,c</sup>.

$$M_{sd} = M_d \times R_m \left[ \frac{g}{FA} \right] \quad \text{Eq. RAI-1.1-2}$$

Where,

$M_{sd}$  = the scaled debris load in units of g/FA for a fuel assembly with pitch,  $P_{FA}$ .

$M_d$  = the debris load in units of g/FA reported in WCAP-17788.

$R_m$  = the scaling factor determined from Eq. RAI-1.1-1.

Review of Tables RAI-1.1-1 and RAI-1.1-2 indicates that the Babcock and Wilcox (B&W) and Combustion Engineering (CE) fuel products have a different fuel assembly pitch than what was used to determine the WCAP-17788 fibrous debris limits presented in units of g/FA. As such, the fibrous debris limits for these fuel products need to be determined from the scaling approach defined above.

For example, the scaling factor  $R_m$  for 16x16 STD and 16x16 NGF fuel products is calculated as:

$$R_m = \left[ \frac{\text{Core Inlet Fibrous Debris Limit for 16x16 STD or 16x16 NGF fuel}}{\text{Core Inlet Fibrous Debris Limit for 17x17 fuel}} \right]^{a,c}$$

This value is then applied to the fibrous debris loads reported in WCAP-17788. For example, per Table 6-3 in WCAP-17788, Volume 1, a CE plant with Westinghouse fuel has a reported core inlet fibrous debris limit of [ ]<sup>a,c</sup>. If the plant has 16x16 STD or 16x16 NGF fuel, this value must be scaled using the calculated  $R_m$  value of [ ]<sup>a,c</sup> which results in a scaled core inlet fibrous debris limit of [ ]<sup>a,c</sup> for these fuel types.

In conclusion, the WCAP-17788 in-vessel debris methodology is applicable to all Westinghouse fuel products listed in Table RAI-1.1-1 and the AREVA fuel products listed in Table RAI-1.1-2 provided that the appropriate scaling is made to the debris limits presented in WCAP-17788 to account for any difference in fuel assembly pitch. If the fuel assembly pitch is different than [ ]<sup>a,c</sup>, Eq. RAI-1.1-1 is used to calculate a scaling factor which is applied to the debris limits defined in WCAP-17788 to adjust the debris limit to a specific fuel assembly pitch.

Updates will be made to WCAP-17788, Volume 1, Sections 6.3 and 6.5 to identify and explain this additional step.

- d. What are the evaluation criteria for applicability of this method to fuel designs developed after January 2015?

### **Response**

As described in WCAP-17788, Volume 1, Section 4, the debris limits defined can be applied directly to fuel assembly designs that are in production by Westinghouse and AREVA as of January 2015. A list of applicable fuel assembly designs is provided in the response to RAI-1.1.c. However, fuel assembly designs are continuously evolving and changing in order to improve fuel reliability and increase performance during both normal operation and postulated accidents. The majority of design changes are small, incremental changes to existing fuel assembly components. Occasionally, the changes are significant enough such that they result in a “new” fuel assembly design.

As the fuel assembly designs evolve and change, the following question must be answered regardless of the extent of the design change(s), “*Will the proposed change affect the in-vessel debris limits calculated using the method described in WCAP-17788?*” This question will have to be answered by the licensee and/or fuel vendor in accordance with applicable regulatory guidance and regulations, including 10CFR50.59. An overview of the evaluation process, including specific criteria that should be considered when evaluating fuel assembly design changes or new fuel assembly designs when applying the WCAP-17788 methodology (i.e., answering the above question), is provided below. The evaluation can include: (1) an analytical assessment, (2) additional testing, or (3) some combination of both. The details of the evaluation process will be defined by each utility and/or fuel vendor.

As described in WCAP-17788, Volume 1, the primary concern related to in-vessel debris is the accumulation of debris on fuel assembly components (e.g., bottom nozzle/lower end fitting or spacer

grids). Changes to fuel assembly components that have the potential to affect the debris accumulation characteristics are of primary importance. Changes that affect the fuel assembly loss coefficient can be an indicator of such changes. While a change in the fuel assembly loss coefficient is normally not a significant concern for post-LOCA conditions (the post-LOCA flow rates are too low to register a meaningful pressure drop across these components without debris), a change in the fuel assembly loss coefficient (or steady-state pressure drop) may be indicative of a change that should be investigated relative to the ability to capture debris.

#### **Bottom Nozzle/Lower End Fitting Changes**

The bottom nozzle/lower end fitting is an important fuel assembly component relative to GSI-191. The subscale testing documented in WCAP-17788, Volume 6 determined that for a given fibrous debris mass, the limiting fuel assembly pressure drop occurred when a single debris bed formed on the bottom nozzle/lower end fitting (as opposed to a condition in which debris is distributed in multiple beds at several locations within the bundle). The subscale testing considered two distinct bottom nozzle/lower end fitting designs. The results of this testing may be used to evaluate bottom nozzle/lower end fitting changes relative to their ability to capture debris. If the changes are too extensive to provide an analytical assessment (i.e., too unlike the designs tested), testing may be required to justify the WCAP-17788 limits or to define new debris limits for the bottom nozzle/lower end fitting design change.

#### **Spacer Grid Changes**

The spacer grids are also important fuel components relative to the GSI-191 issue as they can result in the capture of debris due to their complex geometry and small flow areas. While typically not limiting for GSI-191, if the changes to the spacer grid designs are extensive, the fuel assembly testing conclusions reached in WCAP-17788, Volume 6 could be affected. The results of previous testing may be used to evaluate new spacer grid designs relative to their ability to capture debris. If an analytical assessment cannot be made, testing may be required to provide new data for the spacer grid changes.

#### **Top Nozzle/Upper End Fitting Changes**

The top nozzle/upper end fitting is not a limiting fuel component relative to the GSI-191 issue and specifically with respect to the capture of debris in the fuel assembly. Unless there is a significant change, such as increasing the component loss coefficient such that the fuel assembly pressure drop is significantly increased, most changes to this fuel component could be evaluated as having no adverse impact on the GSI-191 issue. The results and conclusions of WCAP-17788 would remain valid and bounding in this case.

#### **Fuel Rod, Guide Tube and Instrument Tube Changes**

The fuel rod, guide tube, and instrument tube designs are typically not limiting fuel components relative to the GSI-191 issue and specifically with respect to the capture of debris in the fuel assembly. Unless there is a significant design change, such as increasing the fuel rod and/or tube diameter or adding more guide tubes to the fuel assembly, most changes to these fuel components

could be evaluated as having no adverse impact on the GSI-191 issue. The results and conclusions of WCAP-17788 would remain valid and bounding in this case.

### **Summary and Conclusion**

In general, most changes to fuel assembly designs tend to fall into the category of minor manufacturability/design changes which are small improvements to existing designs. These types of changes can generally be evaluated to be bounded by the testing and analyses presented within WCAP-17788. However, certain changes may have an uncertain or potentially significant effect on the GSI-191 in-vessel debris limits, and they must be more extensively evaluated to ensure that the WCAP-17788 limits continue to be applicable.

It is important that cumulative effects also be considered. That is, any new evaluation of a fuel assembly component change needs to consider any prior evaluations of other component changes related to the GSI-191 issue. While a single design change may not have a significant impact on the GSI-191 issue, a combination of changes of relatively small magnitude may have a larger cumulative effect.

Plants that use the WCAP-17788 methodology to determine in-vessel debris limits must evaluate fuel assembly design changes in accordance with applicable regulatory guidance and regulations. The evaluation of a fuel assembly design change can include: (1) an analytical assessment, (2) additional testing, or (3) some combination of both. The details of this evaluation process will be defined by each utility and/or fuel vendor.

### **References**

- RAI-1.1-1 PWR Owners Group Correspondence, ADAMS Accession No. ML17069A174, "Submittal of Responses to NRC Requests for Additional Information (RAIs) and Revisions to Topical Report WCAP-17788-P/WCAP-17788-NP, Revision 0, "Comprehensive Analysis and Test Program for GSI-191 Closure" related to Volume 1 and Volume 6 in Support of the Closure of GSI-191 (PA-SEE-1090)," March 8, 2017.
- RAI-1.1-2 WCAP-16793-NP-A, Revision 2, "Evaluation of Long-Term Cooling Considering Particulate, Fibrous and Chemical Debris in the Recirculation Fluid," July 2013.

**RAI-1.2**

The trends in Figures 6-4, 6-6, and 6-8 show that as the resistance at the core inlet ( $K-K_{split}$ ) increases, the flow through the alternate flow paths increases for various emergency core cooling system (ECCS) recirculation flow rates.

- a. As seen in Figure 6-4, there is a nearly vertical ramp in the fraction of ECCS flow through the upper head spray nozzles (UHSN) at  $K-K_{split}$  of about 10,000 for a flow rate of 40 gallons per minute (gpm) per fuel assembly (FA). What is the reason for this sudden increase in the UHSN flow fraction amounting to about 15 percent of the maximum observed value?
- b. Figure 6-6 shows results of the Combustion Engineering analysis. Explain why the results are widely scattered compared to those depicted in Figures 6-4 and 6-8 where the results show less data scatter for each ECCS recirculation flow rate. Describe the reason for the observed behavior of the 12.5 gpm/FA results in Figure 6-8 associated with a change in the exhibited trends and a steep increase in the barrel/baffle flow fraction for  $K-K_{split}$  between 5,500 and 6,000. Explain why the results in Figure 6-8 contain a significant amount of data points that are considerably different from the general trends, especially in the 2000-4000  $K-K_{split}$  range.

**Response**

- a. WCOBRA/TRAC uses flow regime maps to describe two-phase flow patterns and subsequent calculations for interfacial heat and mass transfer, interfacial drag, and wall drag. These calculations are dependent on the flow regime identified by the flow regime maps. Before selecting a flow regime for a given mesh cell, WCOBRA/TRAC performs a check to assure that the local flow regime is consistent with the global flow pattern. This is done by checking the void fraction difference between two axial mesh cells. These checks are described in WCAP-16009-P-A, Section 3-2-1 (Reference RAI-1.2-1). If a large void gradient is calculated, certain ramps are applied and the void fractions used in the calculations of the interfacial quantities to determine flow regime transitions for the mesh cell are redefined using averaging schemes that depend on the specific condition. When a large void gradient between two cells is not present, the void fractions at the momentum cell center are assumed to be [ ]<sup>a,c</sup>

When resistance due to the accumulation of debris is simulated in the downflow plant model, liquid provided by the ECCS fills the downcomer and cold leg piping. Eventually, the downcomer liquid level reaches the UHSN nozzles and liquid begins to fill the upper head region. When the upper head liquid level reaches the upper guide tube elevation liquid begins to drain into the upper plenum. As the upper guide tubes are initially highly voided, the resulting flow pattern is an inverted pool with a large void gradient between the upper head region and the upper guide tubes. The sudden increase in the UHSN flow fraction is related to the WCOBRA/TRAC logic used to determine the void fraction at the upper head and guide tube interface and the subsequent calculations for the interfacial drag and wall drag. The void fraction logic to determine the local flow regime at this interface transitions between averaging schemes at this point, and the global two-phase flow pattern changes as a result.

This behavior was only observed in the 40 gpm/FA case because this was the only case that had an UHSN flow large enough to fill the upper head region to nearly liquid solid. In the other cases the

UHSN flow was lower and the switch in void fraction logic did not occur. It is also noted that the revised 40 gpm/FA downflow plant  $K_{split}/m_{split}$  calculations presented in the response to RAI-4.20 do not experience this effect because the UHSN resistance was increased as described in the response to RAI-4.2. The increase in UHSN resistance limited the flow into the upper head such that the volume did not fill with liquid to the same level observed in the original 40 gpm/FA flow case.

- b. Figure 6-6 from WCAP-17788, Volume 1 was developed from the thermal-hydraulic analyses presented in WCAP-17788, Volume 4. As part of the RAI responses for Volume 4, this figure will be revised and replaced based on additional CE analyses that will be developed in response to RAI 4.20 and 4.21.

Figure 6-8 from WCAP-17788, Volume 1 was developed from the thermal-hydraulic analyses presented in WCAP-17788, Volume 4. As part of the RAI responses for Volume 4, this figure will be revised and replaced based on an updated understanding of the role the alternate flow path plays in the B&W analyses. The reader is directed to the response to RAI 4.20 and 4.21 for the new figure and discussion.

#### Reference

RAI-1.2-1 WCAP-16009-P-A, "Realistic Large-Break LOCA Evaluation Methodology Using the Automated Statistical Treatment Of Uncertainty Method (ASTRUM)," January 2005.



**RAI-1.3**

On page 6-24, the particulate to fiber (p:f) ratio is calculated.

- a. The TR states that the calculated particulate to fiber (p:f) ratio represents the limiting case and the expected p:f ratios are less than the calculated result. What assumptions were used in the calculation to ensure it is the limiting result?
- b. Provide references and/or further justification to show the ratios expected are less than the calculated result.
- c. Section 6.4.3.2 discusses sources in open literature that indicate the addition of suspended particulates in a fluid will improve heat transfer. Were the results of these experiments based on mass or volume? Justify the applicability of these results to the expected core conditions considering quantitative particulate characteristics such as shape, size, and density along with their distributions as appropriate.

**Response**

- a. As stated in Response 1.3c below, WCAP-17788, Volume 1, Section 6.4.3.2 will be updated to reflect the information provided therein. The discussion no longer includes a p:f ratio. Therefore, no response is required to this RAI.
- b. As stated in Response 1.3c below, WCAP-17788, Volume 1, Section 6.4.3.2 will be updated to reflect the information provided therein. The discussion no longer includes a p:f ratio. Therefore, no response is required to this RAI.
- c. There are two aspects to this clarification question: Hot leg break (HLB) and cold leg break (CLB). The HLB issue relates to WCAP-17788, Volume 1, Section 6.4.3.2 (Reference RAI-1.3-1). The CLB issue relates to Volume 1, Section 7.1.2 in the erratum submitted in November of 2015 (Reference RAI-1.3-2). Both the HLB and CLB must address the issue of debris concentration within the heated region of the core. The following response discusses the aspects of the break locations separately.

**Hot Leg Break**

Under large HLB conditions, break flow is approximately equal to the flow supplied by the emergency core cooling system (ECCS) less boil-off and the liquid needed to account for the slow inventory increase in the reactor vessel due to the diminishing decay heat. Under this condition, the mechanisms for particulate retention in the reactor vessel are limited. Some fraction of particulate entering the reactor vessel may settle out of the flow in the lower plenum, and some fraction of particulate is expected to be captured within any fibrous debris beds that may have formed at or near the core inlet. There are no mechanisms for particulates to concentrate in the suspended fluid since there is a continuous throughput of liquid from the ECCS injection points to the break. Particulates that do not settle out, penetrate, or bypass any fibrous debris beds will continue to transport with the

liquid through the reactor vessel and out the break. As such, the concentration of particulates in the reactor vessel liquid will be less than or equal to the particulate concentration within the sump pool.

When unrealistic assumptions are made regarding the arrival time and accumulation rate of debris at the core inlet, it is possible to retard the throughput of liquid from the ECCS injection points to the break. Under this condition, particulate could concentrate in the reactor vessel liquid inventory. However, the WCAP-17788, Volume 4 thermal-hydraulic analyses, which applied these unrealistic assumptions, demonstrated that any reduction in liquid throughput due to debris accumulation at the core inlet would be temporary. As such, the resulting concentration buildup of particulate would also be temporary and would not result in significant increases in the reactor vessel particulate load.

Given that there is no mechanism for debris concentration in the core following a HLB, the effect of particulates on the core TH response following a HLB will be bounded by the effects of a CLB where, much a like a boric acid precipitation scenario, debris can concentrate (see the CLB discussion for details). That is, plant-specific analyses performed to evaluate and justify the CLB response can be used to justify the HLB scenario as well.

WCAP-17788, Volume 1, Section 6.4.3.2 will be revised to reflect the above discussion.

### **Cold Leg Break**

In-vessel particulate debris load is defined as the amount of particulate that can transport to the reactor vessel and remain suspended in the liquid. Under large cold leg break conditions, it is possible to concentrate particulate debris in the core region liquid because there is no significant liquid carryover, and thus, particulate carryover from the reactor vessel to the break.

The in-vessel particulate debris loading is plant-specific and is determined by particulate generation and transport evaluations. In many cases these evaluations make simplifying assumptions that contain significant conservatism, and if these loadings are applied to the in-vessel particulate evaluations, the resulting particulate load can be unrealistically high leading to the potential for unacceptable conclusions regarding the effects of suspended particulate on long-term decay heat removal. Under more realistic conditions, less particulate debris would be generated and transported to the containment sump strainer, some fraction of particulate would capture on the strainer, and some fraction would settle within the emergency core cooling system (ECCS) and reactor vessel lower plenum. When plant-specific refinements are made to the particulate debris generation, transport, and strainer penetration assumptions, the maximum in-vessel particulate load is expected be less than [ ]<sup>a,c</sup> by mass for the U.S. pressurized water reactor (PWR) fleet. Plant-specific validation of in-vessel particulate loading may be required and is not part of this RAI response. It is expected that plants will provide this validation as part of resolution of GSI-191 and response to GL 2004-02.

Suspended particulate flows less than [ ]<sup>a,c</sup> by mass are commonly referred to as dilute particulate flows and these types of flows have been studied extensively for industrial applications such as pneumatic conveying of dry powders, transport of liquid-solid slurry flows, and fluidized beds used in the chemical industry. For the particulate types and sizes expected to transport and remain suspended in the reactor vessel liquid under typical large cold leg break conditions, the Stokes number is on the order of  $10^{-5}$  to unity. This result indicates that the particle and liquid phase

velocities will be nearly equal (dynamic equilibrium). As such, the particulate and liquid phases in the reactor vessel can be reasonably approximated as a single phase flow with modified fluid properties.

The introduction of solid particles into a fluid stream has a direct effect on the heat transfer and hydrodynamic characteristics of the multiphase flow. Under dilute particle loads; the available experimental and analytical research generally concludes that the addition of solid particles into a fluid stream causes additional mixing and turbulence. As a result, the heat transfer coefficients and friction factors of particle flows become greater than those of single phase flows. Information collected from the open literature demonstrates that the effects of suspended particulate at, or below, a [ ]<sup>g</sup>/cc particulate mass loading are not expected to significantly impact the heat transfer and hydrodynamic characteristics of the flow. As such, the ability to adequately remove decay heat from the reactor core is expected with up to a [ ]<sup>g</sup>/cc by mass loading of particulates suspended in the reactor vessel liquid-phase.

WCAP-17788, Volume 1, Section 7.1.2 will be revised to reflect the above discussion, and a detailed evaluation to support the [ ]<sup>g</sup>/cc by mass particulate loading assumption is provided in the following sections.

### IN-VESSEL PARTICULATE DEBRIS SOURCES

For the purposes of this evaluation, in-vessel particulate load is defined as the amount of particulate that can be transported to the reactor vessel and remain suspended in the liquid-phase. A postulated high energy line break (HELB) may generate both particulate and fibrous debris. The types of particulate debris sources considered in the in-vessel particulate evaluation include the following:

- Reflective Metallic Insulation (RMI)
- Protective Coatings both Inside and Outside the Break Zone of Influence (ZOI)
- Latent Containment Debris
- Insulation and Fire Barrier Materials

In addition to the quantity of particulate debris generated and transported to the reactor vessel, the particulate debris type and size characteristics are also important.

The quantity of particulate debris generated and transported to the reactor vessel is a plant-specific parameter, and plant-specific values are not considered in this evaluation. Instead, a maximum particulate debris quantity of [ ]<sup>g</sup>/cc by mass is assumed. It may be necessary for plants to verify that their plant-specific in-vessel particulate debris loading is less than or equal to the assumed [ ]<sup>g</sup>/cc loading.

The particulate debris type and size characteristics, to some extent, are also plant-specific; however, information regarding the particulate debris type and characteristics are necessary for this evaluation. The determination of appropriate particulate debris characteristics for each particulate debris source considered in this evaluation are presented below. Plants may also need to verify that their specific particulate debris types and characteristics are represented by this

evaluation. If the plant has different particulate debris sources, or sources with different characteristics, then additional justification may be required.

### **Reflective Metallic Insulation**

Testing has been performed to investigate the debris characteristics of RMI when subjected to saturated water jets and saturated steam jets. These tests are summarized in NUREG/CR-6808, Section 3.2.2.4, "Siemens Metallic Insulation Jet Impact Tests (MLJITs)," (Reference RAI-1.3-3). Although the data from these tests is not publically available, for a saturated jet, the following was observed:

The degree of destruction caused by saturated water jets was much less than that caused by saturated steam jets. Damage tended to take the form of crumpling the RMI panels rather than fragmenting them into smaller pieces. Panel disintegration was observed (with water jet only) only when the target became stuck in the mounting trestle and remained in the core of the jet during the 30 second blowdown. In this case, a small percentage of the panel was fragmented.

The NRC conducted a single debris generation test to generate representative RMI debris. The debris was analyzed with respect to size distribution. The overall size distribution for the total recovered debris mass is shown in NUREG/CR-6808, Figure 3-7 (Reference RAI-1.3-3). It is noted that the RMI size distribution shown in the figure is based on 91% recovery of the RMI debris. Generally unrecovered debris material from testing is assigned to the smallest size category because smaller debris is the most difficult to recover. Following this practice, an additional 9% would be added to the smallest debris size bin shown in the figure.

The transport of debris towards a simulated containment strainer has also been experimentally studied in the University of New Mexico Integrated Debris Transport Test Program as reported in Section 5.2.6 of (Reference RAI-1.3-3). The summary related to RMI debris transport was summarized as follows:

RMI debris transport tests indicated that the most important aspect of evaluating RMI debris transport is probably the transport during the pool fill-up phase, when the transport velocities associated with the fast-spreading flows can effectively push substantial RMI debris in the direction of the flow. Both stainless-steel RMI and aluminum RMI debris was pushed readily either toward the outlet screen or away from it, depending on the test configuration. After the tank became sufficiently flooded to slow water flows, the RMI did not substantially transport at the tank velocities normally tested. Pieces of RMI debris that were dropped into an established steady-state pool sometimes floated a significant distance before sinking because air was trapped within the debris.

In the plant, the water pool forms on the containment floor before the ECCS pumps begin to draw suction from the sump. Thus, although fluid velocities in the plant may vary somewhat from those in the test, RMI debris is not expected to be drawn to the containment sump. Therefore, the only source of RMI debris considered at the containment sump should be 13.3% (4.3% recovered

plus 9% unrecovered) of the total RMI debris mass generated with a characteristic size of < 0.25 inch.

This is further justified by the fact that replacement sump strainers generally are considered to have flow passages with a nominal dimension of 1/8 inch or less. As such, even if larger pieces of RMI could be transported to the sump strainer, the pieces would not be able to penetrate the strainer.

### **Protective Coatings**

There are three classifications of coatings that may be present in the containment building:

1. DBA Qualified and DBA Acceptable Coatings – these coatings have been evaluated to have successfully undergone testing to either appropriate ASTM standards (DBA Qualified) or ANSI standards (DBA Acceptable).
2. Indeterminate Coatings – these coatings cannot be determined to have undergone testing to either appropriate ASTM or ANSI standards.
3. DBA Unqualified and DBA Unacceptable Coatings – these coatings have been evaluated to have undergone testing to either appropriate standards with unacceptable results, or have not been evaluated per one of the appropriate standards.

For DBA Qualified and DBA Acceptable coatings, the guidance of NEI 04-07 (Reference RAI-1.3-4), states that coatings debris generated within the ZOI will have characteristic dimension of the coating pigment, or about 10  $\mu\text{m}$  – 50  $\mu\text{m}$  (about  $4 \times 10^{-4}$  inches –  $2 \times 10^{-3}$  inches). For the purposes of in-vessel debris evaluations, smaller particulate size will have a higher probability of reaching the reactor vessel and remaining suspended in the coolant. Therefore, all DBA Qualified and DBA Acceptable coatings are assumed to be spherical with a diameter of 10  $\mu\text{m}$ .

All DBA Unqualified and DBA Unacceptable coatings inside and outside the ZOI are assumed to fail. Epoxy and epoxy phenolic coating failure outside the ZOI will result, in all likelihood, in debris that are relatively larger, highly cohesive, and no smaller in the worst case than 25  $\mu\text{m}$ .

Savannah River testing, summarized in (Reference RAI-1.3-5), subjected qualified coatings to effects of radiation and thermal stresses and then submerged the coating samples in water at 200°F. The results of the tests shows that the coatings failed by delamination, resulting in debris particulates ranging from 0.25 inch to the pigment size (~10  $\mu\text{m}$ ). Although these tests were completed with qualified coatings, and due to the lack of applicable debris size data from tests completed with unqualified coatings, the size range for unqualified coating debris outside the ZOI is assumed to be 10  $\mu\text{m}$  to 0.25 inch. Unqualified coatings within the ZOI are assumed to fail to the pigment size (~10  $\mu\text{m}$ ).

Testing performed by EPRI and reported at an NRC Public Meeting (Reference RAI-1.3-5) confirm that OEM Unqualified Coatings fail by delamination (when they fail). Coating failures were generally less than 100% and the majority of tested samples showed failures less than 5%.

Although this testing did not include particulate size characterization, it did confirm that the failure mechanism was consistent with that reported by Savannah River (Reference RAI-1.3-5). This gives some indication that the particulate size distribution would be similar, and assuming that unqualified coatings fail at this size range is acceptable for this evaluation; however, plant-specific consideration of unqualified coating failure rates and size characteristics would require additional justification.

### Latent Particulate

Latent particulate was characterized in NUREG/CR-6877 (Reference RAI-1.3-6) using physical samples from three plants, and the overall average of the particulate size distribution is shown in Table RAI-1.3-1. Insights were also gained into the fraction of the  $< 75 \mu\text{m}$  particulates that might actually fall into the  $< 10 \mu\text{m}$  range. Analysis of the  $< 75 \mu\text{m}$  particulates from Plant-A showed that 51% of the particulate was between  $10 \mu\text{m}$  and  $75 \mu\text{m}$  while 49% was  $< 10 \mu\text{m}$ . These results are rough approximations, and Plant-A results are only considered because (Reference RAI-1.3-6) reports that Plant-A results may yield the best approximation since no mass correction was required to compensate for the presence of residual trapped fiber.

Table RAI-1.3-1 Overall Plant Average Latent Particulate Size Distribution Results (Ref. RAI-1.3-6)			
$> 2 \text{ mm}$	$500 \mu\text{m} - 2 \text{ mm}$	$75 \mu\text{m} - 500 \mu\text{m}$	$< 75 \mu\text{m}$
22.0%	21.6%	27.4%	28.9%

Based on the data shown in Table RAI-1.3-1, the latent particulate size distribution assumed at the sump strainer for the model will include three size classes; fine, medium, and course:

- 37% mass are particulates  $< 75 \mu\text{m}$
- 35% mass are particulates  $\geq 75 \mu\text{m} < 500 \mu\text{m}$
- 28% mass are particulates  $\geq 500 \mu\text{m} < 2 \text{ mm}$

This size distribution is consistent with the recommended surrogate size distribution for latent debris as reported in NUREG/CR-6877 (Reference RAI-1.3-6). The  $> 2\text{mm}$  particulate size group was not included on the basis that particulate of this size would be much less likely to transport to the sump strainer. The size distribution shown in Table RAI-1.3-1 was normalized to the three size groups to determine the appropriate mass fractions in each group.

### Insulation and Fire Barrier Materials

This debris source includes particulate debris generated from insulation and fire barrier material. NEI 04-07 (Reference RAI-1.3-4) recommends a mean particulate size of  $5 \mu\text{m}$  for calcium silicate particulate, and a size of  $< 0.2 \mu\text{m}$  for microtherm particulate. Based on this NEI 04-07 (Reference RAI-1.3-4) recommendation, it is assumed that all particulate debris from these sources will fail with a characteristic length of  $< 10 \mu\text{m}$ .

## **PARTICULATE SETTLING IN THE LOWER PLENUM**

The ability of the ECCS flow to lift particulates into the core has been generically evaluated in WCAP-16406-P-A, Rev. 1 (Reference RAI-1.3-7). The evaluation considered debris having a spherical geometry with a specific gravity of 1.6. For the maximum flow conditions into the core (two trains of ECCS operating and a hot leg break) and using a conservatively small flow area representing the region below the core support plate, the maximum debris size that could be lifted into the core region was evaluated to be about 400  $\mu\text{m}$  – 500  $\mu\text{m}$ . Particulate larger than this will not remain suspended in the liquid phase and will not be considered as part of the in-vessel particulate debris load.

### **Reflective Metallic Insulation Debris**

RMI used in containment buildings resembles the cross-section of a corrugated cardboard box. The corrugated material is either aluminum or stainless-steel sheeting, and an inner and outer sheaths are stainless-steel. The density of aluminum is about 171  $\text{lbm}/\text{ft}^3$ , and the density of stainless-steel is about 489  $\text{lbm}/\text{ft}^3$ . The densities of both aluminum and stainless steel give specific gravities considerably in excess of the 1.6 values used in the generic settling evaluation (Reference RAI-1.3-7). Therefore, the small amount of RMI that could potentially pass through the sump strainer and transport to the reactor vessel is evaluated to settle in the lower plenum and will not remain suspended.

### **Protective Coating Debris**

Since DBA Qualified and DBA Acceptable coatings that fail within the break ZOI are assumed to fail as 10  $\mu\text{m}$  spheres, this particulate debris is not subject to lower plenum settling. However, unqualified coatings that fail outside the ZOI are subject to lower plenum settling. Unqualified coatings have a material density of 94  $\text{lbm}/\text{ft}^3$  (Reference RAI-1.3-4), which results in a specific gravity of approximately 1.6. Thus, unqualified coating particulate debris greater than about 400  $\mu\text{m}$  will settle in the lower plenum.

### **Latent Particulate Debris**

Latent particulate was characterized in NUREG/CR-6877 (Reference RAI-1.3-6) using physical samples from three plants, and the average density of the latent particulate was found to be 169  $\text{lbm}/\text{ft}^3$  (2.7  $\text{g}/\text{cm}^3$ ). This density results in calculating a specific gravity greater than 1.6. Thus, latent particulate debris that penetrates that sump strainer is subject to settling in the reactor vessel lower plenum, and particulates greater than about 400  $\mu\text{m}$  would be expected to settle.

### **Insulation and Fire Barrier Particulate Debris**

Since it is assumed that all particulate debris from these sources will fail with a characteristic length of < 10  $\mu\text{m}$ , this debris is not subject to lower plenum settling.

## SUMMARY OF IN-VESSEL PARTICULATE DEBRIS SOURCES

Table RAI-1.3-2 provides a summary of the in-vessel particulate debris sources, and additional information for each source is provided below.

Table RAI-1.3-2 Summary of In-Vessel Particulate Debris Sources			
Debris Source	Characteristic Size	Characteristic Shape	Basis
Qualified Coatings	10 $\mu\text{m}$	Spheres	Qualified coatings within the break ZOI will fail at the constituent pigment size (Ref. RAI-1.3-4).
Unqualified Coatings	10 $\mu\text{m}$ – 400 $\mu\text{m}$	Spheres (inside ZOI) Chips (outside ZOI)	Unqualified coatings outside the ZOI fail through delamination and will remain in the form of larger chips (Ref. RAI-1.3-5). Inside the ZOI, unqualified coatings are assumed to fail at the pigment size. Particulate greater than 400 $\mu\text{m}$ will settle in the lower plenum (Ref. RAI-1.3-7).
Latent Debris	< 10 $\mu\text{m}$ – 400 $\mu\text{m}$	Spheres and Chips	Latent debris characterization is based on the analysis of plant samples collected during containment walkdowns (Ref. RAI-1.3-6). Particulate greater than 400 $\mu\text{m}$ will settle in the lower plenum (Ref. RAI-1.3-7).
Insulation and Fire Barrier	< 10 $\mu\text{m}$	Spheres	Based on this NEI 04-07 (Ref. RAI-1.3-4) recommendation, it is assumed that all particulate debris from these sources will fail with a characteristic length of < 10 $\mu\text{m}$ .

### Reflective Metallic Insulation Debris

RMI generated debris consists of large shards with a high specific gravity. Considering this, only a small fraction (~13.3% maximum) is expected to transport to the sump strainer. As larger pieces will collect on the strainer, even a smaller fraction is expected in the downstream fluid stream. What RMI can be transported to the reactor vessel is expected to settle within the lower plenum due to the high specific gravity of RMI. For these reasons, RMI particulate debris is not included as part of the in-vessel debris source term.

### Protective Coating Debris

DBA qualified and DBA acceptable coatings within the break ZOI will fail as 10  $\mu\text{m}$  spheres, making them readily transportable to the sump strainer. Also, the small size of this debris indicates that it will not be subject to settling within the lower plenum.



Unqualified coatings fail over a range of sizes, and a large fraction of the unqualified coating debris is expected to fail with a characteristic size greater than 400  $\mu\text{m}$ . Based on the generic lower plenum settling assessment (Ref. RAI-1.3-7), unqualified coating debris greater than 400  $\mu\text{m}$  will settle in the lower plenum. As such, only a small fraction with a size less than 400  $\mu\text{m}$  provides a particulate source for in-vessel considerations.

### Latent Particulate Debris

Similar to unqualified coatings, latent particulate debris has a broad size distribution, with 28% of the latent particulate debris having a characteristic length greater than 500  $\mu\text{m}$ . This fraction of the latent debris cannot be lifted in the core region and will settling in the lower plenum. The remaining 72% of latent particulate debris provides a source for in-vessel evaluations.

### Insulation and Fire Barrier Particulate Debris

This debris source includes particulate debris generated from insulation and fire barrier material. Since it is assumed that all particulate debris from these sources will fail with a characteristic length of < 10  $\mu\text{m}$ , this debris provides a source of particulate for in-vessel evaluations.

### STOKES NUMBER

The Stokes number is an important parameter in fluid-particle flows. The Stokes number related to the particle velocity is defined as:

$$St_v = \frac{\tau_v}{\tau_F} \quad \text{Eq. RAI-1.3-1}$$

where  $\tau_v$  is the momentum response time and  $\tau_F$  is some time characteristic of the flow field. For continuous liquid flow through rod bundle geometry, the characteristic time may be  $D_{sub}/U$  where  $D_{sub}$  is the subchannel hydraulic diameter and  $U$  is the flow velocity. The Stokes number then becomes:

$$St_v = \frac{\tau_v U}{D_{sub}} \quad \text{Eq. RAI-1.3-2}$$

If  $St_v \ll 1$ , the response time of the particles is much less than the characteristic time associated with the flow field. Thus the particles will have ample time to respond to changes in the flow velocity. Thus the particle and fluid velocities will be nearly equal (dynamic equilibrium). On the other hand, if  $St_v \gg 1$ , then the particle will have essentially no time to respond to the fluid velocity changes and the particle will have essentially no time to respond to fluid property changes and the particle velocity will not be significantly affected by the flow velocity.

The momentum response time for a spherical particle is defined as (Reference RAI-1.3-8):

$$\tau_v = \frac{\rho_d D^2}{18\mu_l} \quad \text{Eq. RAI-1.3-3}$$

where  $\rho_d$  is the particle material density,  $D$  the particle diameter, and  $\mu_l$  the liquid viscosity. The viscosity of pure saturated water at atmospheric conditions is  $1.89 \times 10^{-4}$  lbm/ft-s. As discussed above, in-vessel particulate can have a size range on the order of  $10 \mu\text{m} - 400 \mu\text{m}$  and material densities ranging from  $94 - 169 \text{ lbm/ft}^3$ .

Table RAI-1.3-3 provides the calculated momentum response times for a range of particulate sizes and densities that bound the expected in-vessel particulate characteristics. As the table shows, the momentum response time,  $\tau_v$ , varies from approximately  $3.0 \times 10^{-5}$  to  $8.6 \times 10^{-2}$  and increases with increasing particulate density and size.

<b>Table RAI-1.3-3 Momentum response times calculated for spherical particles representative of in-vessel particulate debris</b>		
<b>Particulate Density (lbm/ft<sup>3</sup>)</b>	<b>Particulate Diameter (<math>\mu\text{m}</math>)</b>	<b><math>\tau_v</math> (1/s)</b>
94	10	$3.0 \times 10^{-5}$
94	200	$1.2 \times 10^{-2}$
94	400	$4.8 \times 10^{-2}$
169	10	$5.3 \times 10^{-5}$
169	200	$2.1 \times 10^{-2}$
169	400	$8.6 \times 10^{-2}$

A fuel assembly with a fuel rod diameter of 0.374 inches and a rod pitch of 0.496 inches has a typical subchannel hydraulic diameter,  $D_{sub}$ , of 0.464 inches. The continuous liquid velocity in a subchannel under large cold leg break conditions is on the order of several inches per second. Using a typical subchannel hydraulic diameter and a range of liquid velocities from 1 in/s to 1 ft/s, the Stokes number is calculated for the minimum and maximum particle momentum response times provided in Table RAI-1.3-3.

The results of these calculations are given in Table RAI-1.3-4. As the table shows, the Stokes number over the range of conditions analyzed is on the order of  $10^{-5}$  to unity. This result indicates that the particle and liquid phases will be nearly equal (dynamic equilibrium). As such, the particulate and liquid phases in the core region can be reasonably approximated as a single phase flow with modified fluid properties.

<b>Table RAI-1.3-4 Stokes number calculated for spherical particles representative of in-vessel particulate debris</b>		
<b>Flow Velocity (ft/s)</b>	<b><math>\tau_v</math> (1/s)</b>	<b><math>St_v</math></b>
1/12	$3.0 \times 10^{-5}$	$6.4 \times 10^{-5}$
1	$3.0 \times 10^{-5}$	$7.7 \times 10^{-4}$
1/12	$2.1 \times 10^{-2}$	$4.6 \times 10^{-2}$
1	$2.1 \times 10^{-2}$	0.6
1/12	$8.6 \times 10^{-2}$	$1.8 \times 10^{-1}$
1	$8.6 \times 10^{-2}$	2.2

## ASSESSMENT OF IN-VESSEL PARTICULATE DEBRIS

For the purposes of in-vessel debris evaluations, the maximum particulate debris load, defined as the amount of particulate debris that can transport to the core region and remain suspended in the liquid volume is [ ]<sup>a,c</sup> by mass. If all the particulates suspended in the core liquid volume are assumed to have a density of 94 lbm/ft<sup>3</sup>, the equivalent volume fraction is [ ]<sup>a,c</sup> which is approximately an order of magnitude lower than the 30% volume concentration originally discussed in Section 6.4.3.2 of WCAP-17788-P, Volume 1. As particulate density increases, the equivalent volume fraction reduces. For example, applying a particulate density of 169 lbm/ft<sup>3</sup> to the [ ]<sup>a,c</sup> mass fraction results in a volume fraction of approximately [ ]<sup>a,c</sup>

Suspended particle flows at, and below, a [ ]<sup>a,c</sup> particulate load are commonly referred to as dilute particle flows and these types of flows have been studied extensively for industrial applications such as pneumatic conveying of dry powders, transport of liquid-solid slurry flows, and fluidized beds used in the chemical industry. The introduction of solid particulates into a fluid stream has a direct effect on the heat transfer and hydrodynamic characteristics of the multiphase flow. Under dilute particulate loads; the available experimental and analytical research concludes that the addition of solid particles into a fluid stream causes additional mixing and turbulence. As a result, the friction factors and heat transfer coefficients of particulate flows become greater than those of single-phase flows (References RAI-1.3-9 and RAI-1.3-10). Further, it is commonly accepted that a fluid-particle flow with a Stokes number approaching zero, which is the case for the suspended particulate flow in the core during a large cold leg break scenario, is characterized by velocity equilibrium and can be regarded as a single phase flow with modified properties (Reference RAI-1.3-8). Therefore, showing that the effect of a [ ]<sup>a,c</sup> particulate loading has only a minimal effect on the bulk fluid properties of the flow is sufficient to conclude that the heat transfer and hydrodynamic characteristics will not change significantly.

The majority of particle-liquid flow studies have focused on vertical and horizontal pipe flow with experimental data available for both laminar and turbulent flows over a broad range of particulate sizes, types, and concentrations. Little research has been done on dilute particulate flows in rod bundle geometries, with the only known experimental study being the WCAP-17360-P (Reference RAI-1.3-11) rod bundle boiling tests. Since this experiment was completed using a relatively small particulate loading (on the order of 1% by mass), it cannot be used in of itself to justify that a dilute particulate flow with a particulate loading of [ ]<sup>a,c</sup> will be acceptable. The remainder of this section is devoted to demonstrating that in-vessel particulate debris loadings of [ ]<sup>a,c</sup> by mass, or less, are not expected to have a significant impact on the heat transfer and hydrodynamic characteristics of the flow.

### Heat Transfer

In this section relevant experimental studies that investigated the heat transfer characteristics of particle-laden flows are presented. Studies focusing on convective and nucleate boiling heat transfer in channel and pool flows with similar particulate characteristics and concentrations as those expected in the core following a large cold leg break are considered. Table RAI-1.3-5 provides a summary of experimental studies and includes the heat transfer regime, channel geometry, particulate characteristics, and the flow condition. All the experiments except the

WCAP-17360-P (Reference RAI-1.3-11) rod bundle experiments were conducted with pure water. The WCAP-17360-P (Reference RAI-1.3-11) experiments were conducted with unbuffered and buffered boric acid solutions.

All of the experimental studies shown in Table RAI-1.3-5 demonstrate, in general, that the heat transfer is enhanced under conditions with dilute particulate flows. By comparing the particulate characteristics shown in Table RAI-1.3-5 to the in-vessel particulate characteristics provided in Table RAI-1.3-2 it can be seen that the experimental data set includes particulates that are representative of the in-vessel particulate. It is also shown in Table RAI-1.3-5 that the particulate loadings used in the experiments cover the range of particulate concentrations expected in-vessel. As such, the experimental dataset reasonably represents the condition expected following a large cold leg break scenario, and it is expected that the heat transfer in the reactor core would be enhanced due to the presence of suspended particulates, consistent with the experimental observations.

**Table RAI-1.3-5 Summary of Experimental Studies of the Heat Transfer Characteristics of Particulate-Laden Flows**

Researcher	Heat Transfer Regime	Channel Geometry	Channel Hydraulic Diameter	Particle Type	Particle Density (lbm/ft <sup>3</sup> )	Particle Size	Volume Conc. (%)	Reynolds Number
WCAP-17360-P (Ref RAI-1.3-11)	Nucleate Boiling	3x3 Rod Bundle	0.94 cm	Silicon Carbide	193	10 $\mu$ m	0.31	141 <sup>1</sup>
Ozbelge (Ref RAI-1.3-12)	Forced Convection	Vertical Annulus	10 cm	feldspar	150	64 $\mu$ m - 230 $\mu$ m	0.3 - 2.3	800 - 20,000
Ku (Ref RAI-1.3-13)	Forced Convection	Horizontal Pipe	--	Fly Ash	141.4	4 $\mu$ m - 78 $\mu$ m	0 - 50	4000 - 11,000
Yang (Ref RAI-1.3-14)	Nucleate Boiling	Pool with a horizontal cylindrical heating element	3.2 mm diameter heating element	Al <sub>2</sub> O <sub>3</sub> powders	232.2	0.05 $\mu$ m - 1 $\mu$ m	0.1 - 0.5	—

<sup>1</sup> Reynolds number is calculated based on the steaming rate

## Pressure Drop

In the work of Ozbelge and Beyaz (Reference RAI-1.3-12), the flow characteristics of solid-water mixtures were investigated experimentally at steady-state conditions, and the relationship between the axial two-phase frictional pressure drop and the radial concentration distribution of solids in the test section was determined for the vertical upward flows of these mixtures in a concentric annulus at different operating conditions. The experimental conditions including particulate type, size, and concentration are presented in Table RAI-1.3-5. The flow velocity investigated in these tests was on the order of inches per second, which is consistent with the velocities expected in the reactor vessel under large cold leg break conditions.

The highest two-phase frictional pressure drop from tests completed with 64  $\mu\text{m}$  particulate at a volume fraction of 2% occurred at a mixture velocity of 6 cm/s (2.4 in/s) and was approximately 1300 Pa (0.19 psi). Using the 165  $\mu\text{m}$  particulate, a two-phase frictional pressure drop of approximately 1700 Pa (0.25 psi) at a mixture flow velocity of 10 cm/s (3.9 in/s) and a volume concentration of 2%. A similar two-phase frictional pressure drop was observed using 230  $\mu\text{m}$  diameter particulate at a volume concentration of 1.8%.

From this experimental study, it can be concluded that the additional frictional pressure drop due to the presence of suspended particulate will be minimal at loadings at or below [ ]<sup>a,c</sup> by mass.

### Fluid Properties

In this section, the effect of suspended particulate on the fluid physical properties will be discussed. The focus will be on the mixture density and effective viscosity of a dilute particulate flow with a loading of [ ]<sup>a,c</sup> by mass.

#### Density

When the flow is in dynamic equilibrium, the particulate loading,  $Z$ , and mass ratio,  $C$ , have the same value (Reference RAI-1.3-8):

$$Z = \frac{\bar{\rho}_p u}{\bar{\rho}_l u} = C \quad \text{Eq. RAI-1.3-4}$$

where  $\bar{\rho}_p$  is the particulate bulk density,  $\bar{\rho}_l$  the bulk liquid density, and  $u$  the mixture velocity.

The mixture density can then be written as:

$$\rho_m = \bar{\rho}_p + \bar{\rho}_l = \bar{\rho}_l(1 + Z) = \rho_l \alpha_l(1 + Z) \quad \text{Eq. RAI-1.3-5}$$

where  $\rho_l$  is the density of water and  $\alpha_l$  the liquid fraction of the particulate-liquid mixture.

At a particulate loading of [ ]<sup>a,c</sup> by mass and 30,000 lbm of water, the particulate load is [ ]<sup>a,c</sup>. If the density of the particulate is 169 lbm/ft<sup>3</sup>, the resulting particulate volume is approximately [ ]<sup>a,c</sup>. Assuming a water density of 60 lbm/ft<sup>3</sup>, the volume of water is approximately 500 ft<sup>3</sup>. The liquid fraction of the mixture is:

$$\alpha_l = \frac{V_l}{V_t} \quad \text{Eq. RAI-1.3-6}$$

Where  $V_l$  is the liquid volume (500 ft<sup>3</sup>) and  $V_t$  [ ]<sup>a,c</sup> the total mixture volume, resulting in a liquid fraction of [ ]<sup>a,c</sup>. Using Eq. RAI-1.3-5, the mixture density is calculated to be:

$$\left[ \right]^{a,c}$$

This is approximately [ ]<sup>a,c</sup> higher than that of pure water assuming a density of 60 lbm/ft<sup>3</sup>, which is close to the density of saturated water at atmospheric conditions.

It is noted that if the particulate loading is fixed at [ ]<sup>a,c</sup> the mixture density calculated using Eq. RAI-1.3-5 is independent of the assumed liquid mass. In other words, the same mixture density would be calculated if a water mass of 60,000 lbm were assumed.

A lower particulate density would result in a smaller calculated mixture density. For example, a particulate density of 94 lbm/ft<sup>3</sup> would result in a mixture density of [ ]<sup>a,c</sup> keeping all other values fixed.

Since the liquid fraction is near unity, the calculation in terms of percent increase of the mixture density from the density of pure water is not sensitive to the assumed value of water. For example, assuming a water density of 62 lbm/ft<sup>3</sup> results in a calculated mixture density of [ ]<sup>a,c</sup> or an approximate [ ]<sup>a,c</sup> increase.

Considering the above discussion, the mixture density of a particulate-liquid mixture at a particulate loading of [ ]<sup>a,c</sup> does not significantly increase above that of the liquid phase.

### Viscosity

For very dilute flows, the effective viscosity,  $\mu$ , is commonly taken as predicted by the well-known Einstein (Reference RAI-1.3-15) relation:

$$\frac{\mu}{\mu_0} = 1 + 2.5\phi \quad \text{Eq. RAI-1.3-7}$$

where  $\mu_0$  is the viscosity of pure water without particles and  $\phi$  is the particle volume fraction. The relation is valid for dilute spherical particle flows and loses its accuracy when the volume fraction is greater than 0.02, when the effective viscosity starts to increase much more rapidly than the Eq. RAI-1.3-7 prediction (Reference RAI-1.3-16).

At a 0.02 volume fraction, the effective viscosity of the particle-laden liquid is calculated to be 5% greater than that of pure water without particles. At a particulate mass fraction of [ ]<sup>a,c</sup> the resulting volume fraction is on the order of [ ]<sup>a,c</sup>. Based on Eq. RAI-1.3-7, the viscosity of the liquid in the core with suspended particles is not expected to change dramatically, and it can be concluded that the hydrodynamic characteristics of the flow will not change significantly.

### References

- RAI-1.3-1 WCAP-17788-P, Revision 0, "Comprehensive Analysis and Test Program for GSI-191 Closure (PA-SEE-1090)," July 2015.
- RAI-1.3-2 OG-15-439, "Transmittal of Additional Information in Support of WCAP-17788, 'Comprehensive Analysis and Test Program for GSI-191 Closure (PA-SEE-1090)'," November 30, 2015 (NRC Accession Number ML15342A067).

- RAI-1.3-3 NUREG/CR-6808, "Knowledge Base for the Effects of Debris on Pressurized Water Reactor Cooling Performance," February 2003.
- RAI-1.3-4 NEI 04-07, "Pressurized Water Reactor Sump Performance Evaluation Methodology," December 2004.
- RAI-1.3-5 NRC Meeting Summary, "September 26, 2000 Meeting Summary," ADAMS Accession No. ML003758107.
- RAI-1.3-6 NUREG/CR-6877, "Characterization and Head-Loss Testing of Latent Debris from Pressurized-Water-Reactor Containment Buildings," July 2005.
- RAI-1.3-7 WCAP-16406-P-A, Rev. 1, "Evaluation of Downstream Sump Debris Effects in Support of GSI-191," March 2008.
- RAI-1.3-8 Crowe, C., Sommerfeld, M., Tsuji, Y., *Multiphase Flows with Droplets and Particles*, CRC Press LLC, 1998.
- RAI-1.3-9 Eraslan, A.N., Ozbelge, T.A., Assessment of flow and heat transfer characteristics for proposed solid density distributions in dilute laminar slurry upflows through a concentric annulus, *Chem. Eng. Science* 58 (2003) 4055-4069.
- RAI-1.3-10 Michaelides, E.E., Heat transfer in particle flows, *Int. J. Heat Mass Transfer* 29 No. 2 (1986) 265-273.
- RAI-1.3-11 WCAP-17360-P, "Small Scale Unbuffered and Buffered Boric Acid Nucleate Boiling Heat Transfer Tests with Sump Debris in a Vertical 3x3 Rod Bundle," May 2012.
- RAI-1.3-12 Ozbelge, T.A., Beyaz, A., Dilute solid-liquid upward flows through a vertical annulus in a closed loop system, *Int. J. Multiphase Flow* 27 (2001) 737-752.
- RAI-1.3-13 Ku, J-H., Cho, H-H., Koo, J-H., Yoon, S-G., Lee, J-K., Heat transfer characteristics of liquid-solid suspension flow in a horizontal pipe, *KSME Int. Journal* 14 No. 10 (2000) 1159-1167.
- RAI-1.3-14 Yang, Y.M., Maa, J.R., Boiling of Suspension of Solid Particles in Water, *Int. J. Heat Mass Transfer* 27 No. 1 (1984) 145-147.
- RAI-1.3-15 Einstein, A., A new determination of molecular dimensions, *Ann. Phys.* 19 No. 4 (1906) 289-306. Correction: A. Einstein, A new determination of molecular dimensions, *Ann. Phys.* 34 (1911) 591-592. See also A. Einstein, *Investigations on the theory of Brownian movement*, Dover NY, 1956.
- RAI-1.3-16 Abedian, B., Kachanov, M., On the effective viscosity of suspensions, *Int. J. Eng. Science* 48 (2010) 962-965.

**RAI-1.4**

For the hot leg break (HLB) methodology, it is assumed that all fiber that enters the reactor vessel (RV) remains in the RV and any fiber diverted to the containment spray system will return to the sump. Given these assumptions, Equations 6-16 through 6-19 are simplified to equations 6-20 through 6-23, accordingly. The TR states a utility may use “information about these parameters” instead of taking these assumptions. Under what conditions would alternate assumptions be used if plant-specific information is available? What would this information include? Provide an example calculation where a utility uses plant-specific information for these parameters instead of the assumptions provided to solve the system of differential equations.

***Response***

The terms  $\zeta$  and  $\gamma$  in Equations 6-16 through 6-19 of WCAP-17788, Volume 1 are defined as the bypass fraction through the reactor vessel (RV) to the break and the bypass fraction of fiber that transfers from the containment spray system (CSS) to the sump, respectively. The calculation process defined in WCAP-17788 sets  $\zeta$  to zero and  $\gamma$  to one to provide additional conservatism in the calculation of the final debris limits by specifying that no debris exits the break and no debris is held up in the CSS. These assumptions are then used along with the assumptions that ECCS flow after sump switchover and the sump strainer bypass efficiency are constant to solve Equations 6-16 through 6-19.

While the above approach produces conservative results, utilities may be able to justify different values for the terms  $\zeta$  and  $\gamma$  either through engineering analysis or testing. If they choose to do so, then they will have to develop and provide the basis in a plant-specific application. Further, a utility may wish to provide time-dependent values for ECCS flow rate,  $\eta$ ,  $\zeta$  or  $\gamma$  as well. Along with justification for the time dependence, the solution to Equations 6-16 through 6-19 must also be resolved to provide appropriate equations for implementation in the method. At present, the PWROG is not aware of any utility that may desire to credit debris out the break or hold up in the CSS. However, the option should remain for them to take this path, provided that it can be justified and subsequently accepted by the NRC staff.

In order to clarify the above discussion in WCAP-17788, Volume 1, the following changes are provided to Section 6.5.3, pg. 6-33, third paragraph:

With the assumption of  $\zeta$  equal to zero,  $\gamma$  equal to 1.0, constant ECCS flow rate after sump switchover and constant strainer efficiency, the general equations used to govern fiber transport are simplified into equations 6-20 through 6-23.



**RAI-1.5**

For upper plenum injection plants that utilize cold leg recirculation to control boric acid concentration within the core, provide an example of how the debris quantity entering the cold side of the reactor coolant systems (RCS) is calculated and checked against the core inlet fibrous debris limit. In the example include how the calculation is performed, each step of the calculation, and how the outcome is used.

**Response**

The tracking of debris through the reactor vessel for upper plenum injection (UPI) plants is calculated in accordance with the methodology defined generically in WCAP-17788, Volume 1, Section 8.1.3.

Upper plenum injection flow is treated consistent with hot leg recirculation flow as described in the generic methodology; therefore, it is assumed that all fiber suspended in the incoming UPI recirculation flow is delivered to the heated core region of the vessel. For a 2-loop UPI plant, cold leg recirculation is provided by the high head safety injection (HHSI) pumps. This can give rise to a simultaneous injection period during which low head safety injection (LHSI) is delivered to the upper plenum and HHSI is delivered to the cold leg. The incoming cold leg recirculation flow is assumed to deposit all suspended fiber at the core inlet, as no alternate flow paths are credited for UPI plants.

The mass of fiber within the emergency core cooling system (ECCS) recirculation flow is calculated as a function of the ECCS flow rate, sump strainer bypass fraction, containment spray flow rate, and total system liquid mass.

Figure RAI-1.5-1 provides the results of a sample calculation for a UPI plant hot leg break case. The significant input parameters for this case are summarized in Table RAI-1.5-1. Figure RAI-1.5-1 shows that fiber is only being collected in the heated core region prior to the initiation of simultaneous injection to the cold legs, consistent with the methodology outlined in WCAP-16793-NP-A, Revision 2 (Reference RAI-1.5-1). As simultaneous injection to the cold legs is initiated at 19,800 seconds, all of the fiber being carried with the cold leg flow begins to collect at the core inlet. The core inlet fiber concentration is compared directly to the UPI plant core inlet limit of [ ]<sup>a,c</sup>. This limit is selected such that the formation of chemical products does not result in the total blockage of the core inlet (Reference RAI-1.5-1); therefore, the time at which chemical products form (referred to as  $t_{chem}$ ) is not of significance for UPI plants. If the resulting fiber concentration at the core inlet remains below this limit, then adequate flow is provided to the core to support decay heat removal and boric acid precipitation control.

<b>Table RAI-1.5-1 Input for Sample 2-Loop UPI Hot Leg Break Calculation</b>	
Initial Sump Fiber Loading	1240 gram/Fuel Assembly
Upper Plenum Injection Flow Rate	1400 gpm
Cold Leg Recirculation Flow Rate	1000 gpm
Simultaneous Injection Switchover Time	19,800 sec (5.5 hr)

Table RAI-1.5-1 Input for Sample 2-Loop UPI Hot Leg Break Calculation	
Sump Volume	550,000 gallons
Number of Fuel Assemblies	121
Fuel Vendor	Westinghouse
Plant Type	Westinghouse UPI
Strainer Bypass Fraction	5 percent

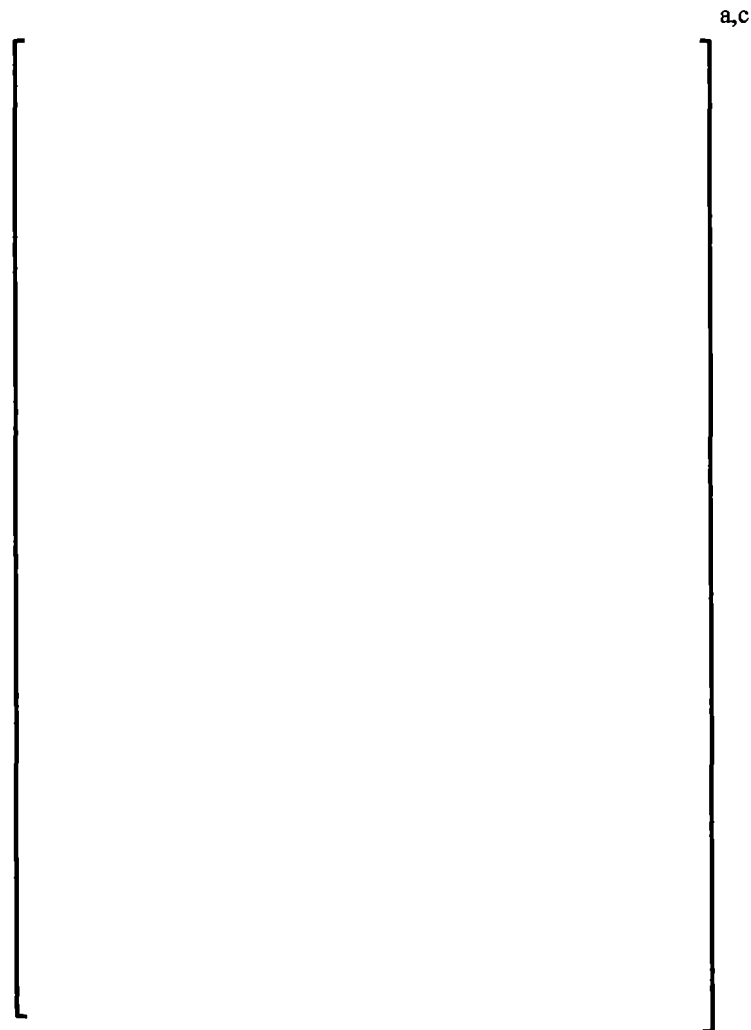


**Figure RAI-1.5-1 2-Loop UPI Plant Sample Case**

#### References

RAI-1.5-1 WCAP-16793-NP-A, Revision 2, "Evaluation of Long-Term Cooling Considering Particulate, Fibrous and Chemical Debris in the Recirculation Fluid," July 2013.

**RAI-1.6**

Do the thermal hydraulic evaluations that calculate peak cladding temperature consider the effects evaluated in the loss-of-coolant-accident (LOCA) deposition model, (e.g., crud deposition on the fuel, fiber buildup at the spacer grids)? If not, would the effects be significant?

***Response***

The thermal hydraulic analyses performed do not consider the effects evaluated in the LOCA deposition model (LOCADM), such as crud deposition on the fuel or fiber buildup at the spacer grids. The thermal hydraulic simulations provided in WCAP-17788, Volume 4 have demonstrated that if a debris-induced secondary heatup occurs, it is expected to occur early in the transient before a significant quantity of fibrous debris has reached the heated core region. This is because the debris-induced heatup is driven by debris collection at the core inlet prior to activation of the alternate flow path (AFP). As such, only fibrous debris that penetrates the core inlet reaches the heated core region. Head loss testing presented in WCAP-17788, Volume 6 demonstrates that the quantity of fibrous debris penetrating the core inlet is small and significant fibrous debris quantities are not available to collect within the spacer grids. When the AFP is activated, chemical precipitates have not formed as demonstrated in WCAP-17788, Volume 5. As such, the deposition of chemical products in the heated region of the core will not occur before or during the debris-induced secondary heatup predicted by the thermal hydraulic analysis. Given that the timing of debris deposition in the heated core region occurs after the debris-induced secondary heatup due to debris buildup at the core inlet, the thermal hydraulic analysis results are not impacted by LOCADM evaluations.

**RAI-1.7**

In Section 4 of the TR, the timing for chemical effects is not clearly described. Volume 5 recognizes six hours as the default timing. Section 4 states 24 hours is the maximum timing. Just above the 24 hour timing it is stated that approximately four to six hours is assumed. Section 5, "Major Assumptions," also states 24 hours. Clarify what the timing of chemicals is and the reason for the listed discrepancies in the TR.

**Response**

The time at which chemical precipitates form is plant specific, and to better understand the timing of precipitate formation, significant autoclave testing was completed as part of this program. The autoclave testing described in WCAP-17788, Volume 5 determined the earliest time at which chemical precipitates are expected to form. This time is defined as  $t_{chem}$  and is an input parameter to the method for calculating the hot leg break in-vessel debris limit. The autoclave testing took fluid samples at 2, 4, 6, 8, and 24 hours and analyzed the samples to determine if chemical precipitates had formed. Overall, only one plant group showed chemical effects in the 6 hour fluid sample, meaning that chemical products may have formed just after 4 hours for this plant group. All other plant groups showed chemical effects only after 6 hours and in many cases chemical effects were not identified at the final sampling time of 24 hours.

In WCAP-17788, Volume 1, Section 4, it is stated that the hot leg break method assumes that chemical precipitates form at 24 hours if they didn't form earlier. This assumption is required because the autoclave testing ended at 24 hours. Since the autoclave testing did not determine the time of chemical effects beyond 24 hours, the hot leg break method assumes chemical precipitate formation, and complete core inlet blockage at 24 hours, since applying an earlier time (i.e., 24 hours instead of > 24 hours) for the occurrence of complete core inlet blockage is conservative. This is consistent with the statement made in WCAP-17788, Volume 1, Section 5, Major Assumptions, regarding the timing of chemical effects.

In WCAP-17788, Volume 1, Section 4, it is also stated that the method assumes that all chemical precipitates are sufficiently delayed and do not form until after a critical point where sufficient cooling occurs as a result of flow directed through the alternate flow paths (AFPs). Total core blockage due to debris and or chemical effects after this point (approximately 4 to 6 hours) is assumed. The 4 to 6 hour time period is provided as an indicator of the earliest possible time that chemical effects are expected. Since the autoclave testing took fluid samples at 4 and 6 hours, if chemical effects were identified in the 6 hour sample, it must be assumed that chemical effects could have occurred just after the 4 hour sample was taken.

To provide clarity regarding the discussion on chemical effects timing, the last paragraph on page 4-1 in WCAP-17788, Volume 1, Section 4 will be revised as follows:

*Formation of chemical precipitates must also be considered. As described previously, the in-vessel fiber evaluations documented in WCAP 16793-NP-A Rev. 2 (Reference 4-1) demonstrated significant head loss in the presence of the chemical precipitate surrogate used during testing, thereby limiting the fiber quantities. In the present effort, the method assumes that all chemical precipitates are sufficiently delayed and do not form until after a critical point where sufficient cooling occurs as a result of flow directed through the AFPs. Based on autoclave testing described in Volume 5, the earliest time that total core*

*blockage due to chemical effects is expected to occur is 4 hours. In all cases, this method assumes that chemical precipitates form at 24 hours if they don't form earlier.*

**RAI-1.8**

The discussion in Section 4.3 of the TR states that the maximum fiber limit defined in Section 7.1 is based on the following facts: 1) fiber loads at or below the limit will not form a contiguous bed at the core inlet, 2) the pressure drop through the regions of the core inlet with a fiber and particulate bed is negligible, and 3) the addition of chemical precipitates will not further impede flow into the core. Questions related to Fact 1 will be included in requests for additional information for Volume 3. Reference 4-1 did not explore what the head loss across a debris bed might be without the consideration of chemical effects. The head losses for cold leg break flows, measured with chemical effects and 18 grams of fiber, were significant when compared to the available driving head. Please describe how it was determined that the pressure drop across the core inlet is negligible as stated in Fact 2 above.

**Response**

The statement that the pressure drop across regions of the core inlet with a fiber and particulate bed is negligible is based on experimental head loss data performed at low flow conditions. The head loss testing reported in WCAP-17057-P, Revision 1 (Reference RAI-1.8-1) to support WCAP-16793-NP-A, Revision 2 (Reference RAI-1.8-2) did explore head loss due to fiber and particulate debris under low flow conditions representative of large cold leg break scenarios. Table G-2 in Reference RAI-1.8-2 indicates that five Westinghouse tests were completed using 18 g of fibrous debris per fuel assembly (g/FA) at a constant flow rate of 3 gpm and varying particulate loads. These tests are CIB29, CIB30, CIB31, CIB32, and CIB33. The order of debris addition in these tests was particulate, followed by fiber, then chemical products. Since the fiber and particulate bed was allowed to form before the addition of chemical precipitates, the measured head loss just before the chemical product addition is representative of a fiber and particulate composite debris bed. Head loss results before chemical product addition from the tests identified above are provided in Table RAI-1.8-1. As the table shows, debris bed head loss before the addition of chemical products is small.

A similar test was performed by AREVA. Specifically, Test 2-FG-FPC was conducted with 18 g of fibrous debris, 810 g of particulate (45:1 p:f ratio), and a constant flow rate of 3 gpm. The total assembly pressure drop before the addition of chemical products was [ ]<sup>a,c</sup>

<b>Table RAI-1.8-1 Fiber and Particulate Debris Bed Head Loss from Fuel Assembly Testing under Low Flow Conditions</b>		
<b>Test No.</b>	<b>Pressure Drop (psid)</b>	
CIB29		a,c
CIB30		
CIB31		
CIB32		
CIB33		

In addition to the Reference RAI-1.8-2 head loss test results, results from the subscale head loss testing documented in WCAP-17788, Volume 6 support the statement that fiber and particulate debris beds will

lead to negligible head loss under low flow conditions. WCAP-17788, Volume 6, Figure 5-47 shows debris bed pressure drop results from the Westinghouse core inlet geometry tests plotted as a function of cumulative fiber load. These tests were conducted with a flow rate of approximately 12.4 gpm/FA when a fiber bed of approximately [ ]<sup>a,c</sup> had formed at the core inlet. Pressure drop results from these tests are provided in Table RAI-1.8-2. As the table shows, the pressure drop across a debris bed of approximately [ ]<sup>a,c</sup> of fiber is negligible even at this flow rate, which is 4 times higher than those expected under prototypic cold leg break conditions. The other subscale test results from low flow test conditions show similar trends.

Table RAI-1.8-2 Fiber and Particulate Debris Bed Head Loss from Subscale Testing at a Fiber Load of Approximately 15 g/FA			
Test Series / Test No.	Pressure Drop (psid)		
57 / T165			a,c
57 / T167			
57 / T176			
59 / T173			
59 / T174			
59 / T175			
60 / T177			

### References

- RAI-1.8-1 WCAP-17057-P, Revision 1, "GSI-191 Fuel Assembly Test Report for PWROG," September 2011.
- RAI-1.8-2 WCAP-16793-NP-A, Revision 2, "Evaluation of Long-Term Cooling Considering Particulate, Fibrous and Chemical Debris in the Recirculation Fluid," July 2013.

**RAI-1.9**

How is the flow area used in the thermal hydraulics analysis to simulate resistance due to a debris bed ( $A_{TH}$ ) calculated in Equation 6-3?

***Response***

The flow area used in the thermal hydraulic analysis for Westinghouse, Combustion Engineering (CE), and Babcock & Wilcox (B&W) nuclear steam supply system (NSSS) designs are presented in Sections 6.1, 6.2, 6.3, and 6.4 of WCAP-17788-P, Volume 4, respectively. This flow area is a function of the method used to apply the resistance in the thermal hydraulic model used in the analysis of each NSSS type. The CE and B&W flow areas correspond to the [ ]<sup>a,c</sup> and the Westinghouse flow area corresponds to the [ ]<sup>a,c</sup>

Westinghouse NSSS Flow Area

Westinghouse NSSS plants utilize a [ ]<sup>a,c</sup> These holes have an inner diameter of [ ]<sup>a,c</sup> Therefore, the per fuel assembly flow area of the [ ]<sup>a,c</sup> is calculated as:

$$\left[ \right]^{a,c}$$

CE NSSS Flow Area

For the plant used in the CE analysis, the flow area in the active core is calculated using the cold dimensions of each assembly. For a single assembly, the calculation is as follows. In one assembly there are 236 fuel rods (OD = [ ]<sup>a,c</sup>) for a cross-sectional area of:

$$\left[ \right]^{a,c}$$

four guide tubes (OD = [ ]<sup>a,c</sup>) for an area of:

$$\left[ \right]^{a,c}$$

and one instrument tube (OD = [ ]<sup>a,c</sup>) for an area of:



$$\left[ \right]^{a,c}$$

The assembly envelope is the assembly pitch [ ]<sup>a,c</sup> squared, or:

$$\left[ \right]^{a,c}$$

Subtracting the rod area from the envelope area gives the hot assembly flow area of [ ]<sup>a,c</sup>  
 Note that an area of [ ]<sup>a,c</sup> is reported and used in WCAP-17788, Volume 1, which is [ ]<sup>a,c</sup>  
 percent smaller than the value calculated here. The use of the smaller area will have a negligible effect on  
 the calculations where it is used in WCAP-17788, Volume 1. Since each of the 217 assemblies in core have  
 these dimensions, the full core flow area is calculated to be [ ]<sup>a,c</sup>

#### B&W NSSS Flow Area

A similar calculation is performed for the B&W plants. However, for the B&W plant model, the control  
 volumes reflect a hot geometry by using the hot, diametrically expanded dimensions. In one assembly there  
 are 208 fuel rods (OD = [ ]<sup>a,c</sup>) for a cross-sectional area of:

$$\left[ \right]^{a,c}$$

sixteen guide tubes (OD = [ ]<sup>a,c</sup>) for an area of:

$$\left[ \right]^{a,c}$$

and one instrument tube (OD = [ ]<sup>a,c</sup>) for an area of:

$$\left[ \right]^{a,c}$$

The assembly envelope is the assembly pitch [ ]<sup>a,c</sup> squared, or:

[ ]<sup>a,c</sup>

Subtracting the rod area from the envelope area gives the hot assembly flow area of [ ]<sup>a,c</sup>  
 Note that an area of [ ]<sup>a,c</sup> is reported in WCAP-17788, Volume 1, which is [ ]<sup>a,c</sup>  
 larger than the value calculated here. The use of the slightly larger area will have a negligible effect on  
 the calculations where it is used in WCAP-17788, Volume 1. Since each of the 177 assemblies in core  
 have these dimensions, the full core flow area is calculated to be [ ]<sup>a,c</sup>

In the original response to this question (Reference RAI-1.9-1), the Combustion Engineering (CE) and  
 Babcock & Wilcox (B&W) flow areas calculated were slightly different than the values reported in  
 WCAP-17788. The response stated that the differences were negligible and did not require revisions to  
 WCAP-17788 to reflect the recalculated flow areas.

The NRC reviewer has requested that WCAP-17788 be updated to reflect the new flow areas. As such,  
 the original response to this question is being revised to state that the CE and B&W flow areas used in the  
 thermal hydraulics analysis to simulate resistance due to a debris bed will be updated to be consistent with  
 the flow areas calculated in the original response to this question. The updated CE fuel assembly flow  
 area is [ ]<sup>a,c</sup> Since each of the 217 assemblies in the core have these dimensions, the full core  
 area is calculated to be [ ]<sup>a,c</sup> The updated B&W fuel assembly flow area is [ ]<sup>a,c</sup> Since  
 each of the 177 assemblies in the core have these dimensions, the full core flow area is calculated to be  
 [ ]<sup>a,c</sup>

WCAP-17788, Volumes 1 and 4 will be updated to reflect these areas.

### Reference

RAI-1.9-1 PWR Owners Group Correspondence, ADAMS Accession No. ML17069A174, "Submittal  
 of Responses to NRC Requests for Additional Information (RAIs) and Revisions to Topical  
 Report WCAP-17788-P/WCAP-17788-NP, Revision 0, "Comprehensive Analysis and Test  
 Program for GSI-191 Closure" related to Volume 1 and Volume 6 in Support of the Closure  
 of GSI-191 (PA-SEE-1090)," March 8, 2017.

**RAI-1.10**

In Section 6.4.3.2 of the TR, provide the basis for assuming a void fraction of 50 percent.

***Response***

As stated in Response 1.3c above, WCAP-17788, Volume 1, Section 6.4.3.2 will be updated to reflect the information provided therein. The discussion no longer includes a void fraction assumption. Therefore, no response is required to this RAI.

**RAI-1.11**

In Section 6.5.2.5 of the TR, does the initial sump fiber load include erosion of larger pieces?

***Response***

The methodology pertains to the smaller fines within the sump that have the potential to pass through the sump strainer and be delivered to the vessel. Determining the initial sump fiber load is a plant-specific endeavor. The calculation of the initial sump fiber load must be justified by the utility or vendor that performed the calculations, including, if necessary, the effects of erosion of larger pieces into fines that can potentially be drawn through the sump strainer. The details of the erosion of larger pieces of debris, as they pertain to determining the initial load of fines within the sump, are beyond the scope of the methodology provided in WCAP-17788.

**RAI-1.12**

In Section 9.1.2 of the TR, "BAP (Boric Acid Precipitation) Control," what is the specified void fraction and why is it appropriate for this application?

***Response***

The method for calculating the effective mixing volume utilizes the modified Yeh correlation (Reference RAI-1.12-1) to calculate the void fraction in the two-phase region. Using this correlation, the core average void fraction is calculated at various points in time which is then used to calculate the time varying effective mixing volume. The volume in the upper plenum to the bottom of the hot leg is assumed to be voided at the same value as the core exit. The analysis assumes that the upper plenum region above the bottom of the hot leg is completely voided. The core and upper plenum average void fraction from the simulation summarized in WCAP-17788, Volume 1, Section 9.1.2 is shown in Figure RAI-1.12-1.

As described in Reference RAI-1.12-1, the modified Yeh correlation has been shown to adequately predict void fraction data obtained from applicable rod bundle geometries under low-pressure boil-off conditions prototypic of those expected during the long-term core cooling (LTCC) period following a large break loss-of-coolant accident (LOCA). The modified Yeh correlation is used by Westinghouse to perform licensing basis post-LOCA boric acid precipitation control analyses, using methodology that has been reviewed and accepted by the NRC previously (e.g., Reference RAI-1.12-2).

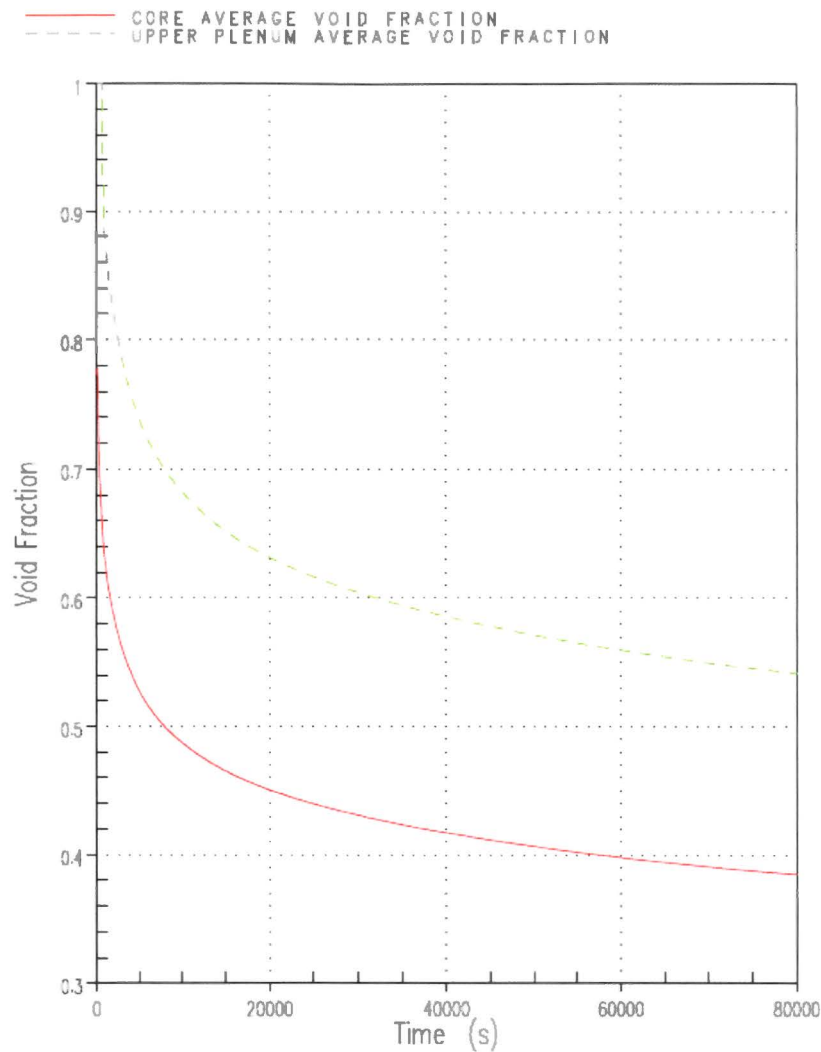


**Figure RAI-1.12-1 Core and Upper Plenum Below Bottom of Hot Leg Average Void Fraction Calculated using the Modified Yeh Correlation**

#### References

- RAI-1.12-1 Yeh, H. C., "Modification of Void Fraction Correlation," Proceedings of the 4th International Topical Meeting on Nuclear Thermal Hydraulics, Operations and Safety, Vol. 1, Taipei, Taiwan, April 5-9, 1994.
- RAI-1.12-2 FENOC to NRC Correspondence, L-05-112, "Beaver Valley Power Station, Unit Nos. 1 and 2 BV-1 Docket No. 50-334, License No. DPR-66 BV-2 Docket No. 50-412, License No. NPF-73 Responses to a Request for Additional Information in Support of License Amendment Request Nos. 302 and 173," July 8, 2005, ADAMS Accession No. ML051940575.

**RAI-1.13**

Assumptions regarding BAP are listed on page 9-2. One of them states: "The initial core boron concentration is equal to the sump mixed mean concentration. The mixed mean concentration is determined by taking all the possible sources of liquid in containment (i.e., Refueling Water Storage Tank (RWST), accumulators, RCS, and Boron Injection Tank) and assuming that they are homogenously mixed within the associated control volumes (RV and sump)." The RWST, and accumulators have set concentrations but the LOCA can occur anytime during a cycle so that the boron concentration in the RCS can vary from zero at the end-of-cycle to a certain maximum value at the beginning-of-cycle. Is the assumption that the RCS boron concentration is at the maximum value at the beginning of the operating cycle for BAP evaluations? If not, explain why.

***Response***

In boric acid precipitation (BAP) evaluations, the reactor coolant system (RCS) boron concentration is equal to or greater than, the maximum RCS boron concentration that could occur over the entire operating cycle. The maximum RCS boron concentration typically occurs early in the fuel cycle.

**RAI-1.14**

Please provide details of how the velocity averaging scheme in Section 6.3.1 of the TR was developed and how the test results were used to validate it.

- a. Provide the assumptions regarding the velocity averaging.
- b. What were the geometric conditions of the testing?
- c. How were the various fuel inlet geometries considered?
- d. How are the form-loss coefficients ( $K_{\text{test}}$  and  $K_{\text{eq}}$ ) values validated for the range of conditions to which they are applied?

**Response**

- a. The subscale head loss final limits testing used a prototypic core inlet geometry consisting of a fuel bottom nozzle (lower end fitting) with a fuel bundle positioned above the bottom nozzle. Figure RAI-1.14-1 provides an illustration of the subscale facility used for the final limits head loss testing. As shown in the figure, the fluid stream contracts during its passage through the bottom nozzle holes, which impacts the upstream velocity profile through the debris bed. As discussed in WCAP-17788, Volume 6, Section 2.2.1, pressure loss through a debris bed can take the general form for one-dimensional flow through porous media (WCAP-17788, Volume 6, Equation 2-1). The porous media formation is dependent on the superficial fluid velocity which can be related to the interstitial velocity as follows:

$$U_i = \frac{U}{\varepsilon}$$

WCAP-17788, Volume 6, Equation 2-8

Niven (Reference RAI-1.14-1) describes additional factors that can influence the relationship between the interstitial velocity and the superficial velocity. Geometric effects and the porous media composition can influence the fluid stream through the debris bed that changes the relation shown in WCAP-17788, Volume 6, Equation 2-8. Similarly, the presence of the bottom nozzle, which creates a flow restriction, is also expected to influence the interstitial velocity relation.

The discussion above provides the basis for the velocity averaging scheme developed in WCAP-17788, Volume 1, Section 6.3.1 as it is expected that the upstream superficial velocity based on the subscale column flow area will result in poor predictions of the subscale final limits head loss data due to the fluid stream contraction. The mean interstitial velocity through the debris bed is a more appropriate value, which will be greater than the upstream superficial velocity. As shown in Figure RAI-1.14-1, the velocity at the inlet of the debris bed is chosen to be the superficial velocity based on the column flow area and the velocity at the exit is chosen to be the superficial velocity based on the bottom nozzle flow area. The mean interstitial velocity is the average of these two values.



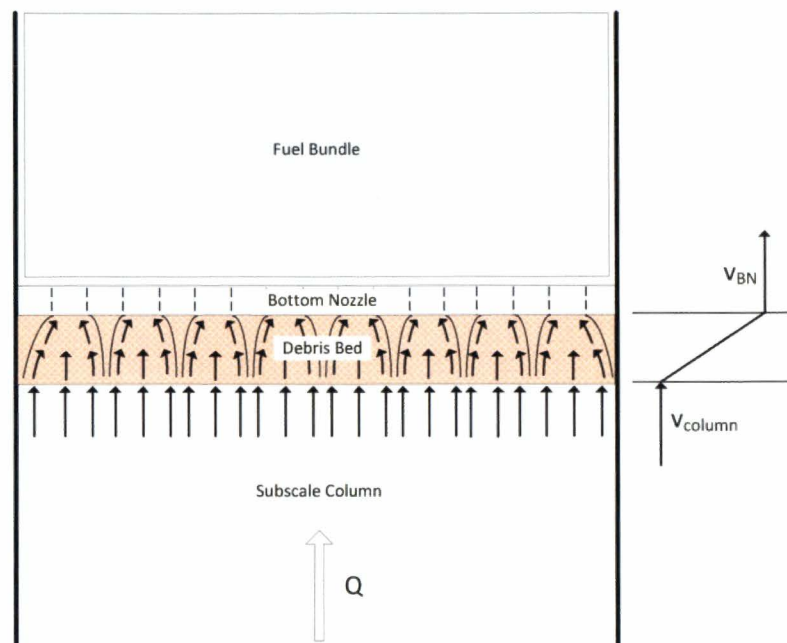


**Figure RAI-1.14-1 Pattern of Flow through Debris Bed**

- b. The geometric conditions important to the subscale final limits testing that are used to determine the average velocity described in WCAP-17788, Volume 1, Section 6.3.1 include the subscale test column and the bottom nozzle geometries. WCAP-17788, Volume 6, Section 3.4 provides the geometry of the subscale test column, and the bottom nozzle geometries used for the final limits testing are described in WCAP-17788, Volume 6, Sections 3.5.3 and 3.5.4.
- c. The velocity averaging scheme is used in the determination of  $K_{test}$ . As such, the two fuel geometries that were tested for the final limits head loss testing were considered. These geometries represent bottom nozzle flow areas that are less than or equal to all fuel inlet geometries utilized by the pressurized water reactor (PWR) fleet, which results in the highest pressure drop, and thus, highest resistance.
- d. The values for  $K_{test}$  and  $K_{eq}$  bound the range of conditions for which they are applied. The subscale final limits head loss testing varied the flow rate and determined that a [
 
$$J^{a,c}$$

## References

- RAI-1.14-1 Niven, R. K., "Physical Insight into the Ergun and Wen & Yu Equations for Fluid Flow in Packed and Fluidised Beds," Chemical Engineering Science 57 (2002) 527 – 534, Elsevier Science Ltd., 2002.

**RAI-3.4**

The example summarized in Table 7-1 of Volume 1 of WCAP-17788-P assumes that recirculation begins at 45 minutes. Is this a bounding assumption? Historically, it is assumed that sump recirculation begins at 20 minutes for limiting cases. How do the results of the evaluation change if it is assumed that recirculation starts at 20 minutes?

***Response***

As described in Table 7-1 of WCAP-17788 Volume 1, the example models the emergency core cooling system (ECCS) performance assuming an active failure of a train of safety injection. As such, the injection phase of the accident transient is extended with time, and the 45 minute sump switchover time does not bound the earliest possible sump switchover time that could occur for this plant.

The purpose of the example summarized in Table 7-1 of WCAP-17788 Volume 1 is to demonstrate the flow patterns expected at the core inlet following a large cold leg LOCA. After complete core quench, the example shows a strong circulation pattern at the core inlet with upflow in the higher power assemblies in the central region of the core and downflow in the lower power assemblies around the core periphery. As the transient progresses, and decay heat reduces, circulation at the core inlet tends to decay and the flow distribution becomes more uniform with less downflow at the periphery of the core inlet. Since it is expected that areas of the core inlet experiencing downflow will not collect debris, assuming a later debris arrive time (i.e., a later sump switchover time) could lead to a higher fraction of the core inlet forming a debris bed. For this reason, the example summarized in Table 7-1 of WCAP-17788 Volume 1 applies a late entry into sump recirculation for a large break LOCA to delay the arrival of debris. This is a realistic entry into sump recirculation when failure of a train of safety injection is considered.

The expected behavior following an earlier entry into sump recirculation can be inferred from the result of the evaluation. When transfer to sump recirculation occurs, there is little change in the core inlet flow distribution. The higher power assemblies are experiencing predominately upflow, while the peripheral assemblies are experiencing predominately downflow. If the transfer to sump recirculation were to occur at 20 minutes post-LOCA, the core inlet flow distribution is also not expected to change significantly. A 20 minute sump switchover time would require two trains of ECCS to be functioning, which would result in more flow to the reactor coolant system (RCS). However, since this example considers a large CLB, the amount of ECCS flow reaching the core inlet is still only that required to replace boil-off (ECCS flow in excess of boil-off spills from the break). At 20 minutes post-LOCA, the circulation pattern at the core inlet is stronger with more downflow. As a result, the fraction of the core inlet expected to collect debris would be smaller.

Based on the above discussion, it is not necessary to bound the earliest sump switchover time. The purpose of the example is to demonstrate the flow patterns at the core inlet under a large CLB scenario, which are not significantly influenced by sump switchover time.

**RAI-3.5**

Section 7.1.1 of Volume 1 states that for regions where flow is upward, debris may collect at the core inlet.

- a. As the debris collects, will flow shift to other areas of the core inlet or does the pressure differential remain low enough that flow is not significantly affected?
- b. How does the evaluation account for the diversion of flow and debris to areas of the core where debris has not collected?
- c. Can a relatively uniform debris bed build at the core inlet as flow is redirected to areas of less debris resistance? If so, how would this affect the conclusions of the evaluation?

***Response***

- a. Debris head loss testing, as described in the response to RAI-3.27, shows that the pressure differential (dP) is low such that the flow distribution is not significantly affected.
- b. The assessment in Section 7.1.1 of WCAP-17788 Volume 1 does not consider diversion of flow and is intended to illustrate the flow condition prior to and during the initial phase of debris arrival.
- c. Under these conditions, a uniform debris bed cannot form at the core inlet. As debris begins to arrive, and potentially accumulate on regions of the core inlet with upflow, the dP is not large enough to significantly influence the redirection of flow. As the transient progresses, other processes (e.g., buoyancy-driven convection) will generate secondary flows that preclude formation of a uniform debris bed.

**RAI-3.6**

Section 7.1.1 of Volume 1 states that the quality of the steam exiting the vessel remains low enough to limit the buildup of boron in the core. How was it determined that maintaining steam quality below 0.8 ensures carryover that will adequately limit the buildup of boron solutes in the core? What is the maximum allowable quality that will ensure excessive boron concentrations will not occur? Provide the basis for this value.

**Response**

The effect of entrainment on core region boric acid concentration can be estimated with a calculation based on a control volume encompassing the lower plenum, core region and upper plenum. Boric acid will come into the control volume through boiloff makeup at the Refueling Water Storage Tank (RWST) or sump boric acid concentration. Boric acid will leave the control volume via entrainment at the core region boric acid concentration. The core region boric acid concentration will stop increasing when:

$$CORE_{BCMAX} = BOILOFF\ MAKEUP_{BC} \times \left[ \frac{1}{(1 - x)} \right]$$

Where reactor vessel (RV) exit steam quality,  $x$ , is defined as:

$$x = \frac{\dot{m}_v}{\dot{m}_v + \dot{m}_l}$$

And,

$\dot{m}_v$  = vapor phase mass flow rate,

$\dot{m}_l$  = liquid phase mass flow rate.

In terms of Entrainment,  $E$ :

$$CORE_{BCMAX} = BOILOFF\ MAKEUP_{BC} \times \left[ \frac{1}{(E)} \right]$$

Where Entrainment is defined as:

$$E = \frac{\dot{m}_l}{\dot{m}_v + \dot{m}_l}$$

The SKBOR code has the ability to model entrainment out of the core region and therefore SKBOR is a suitable tool for examining the effect on RV exit steam quality on the ultimate core region boric acid concentration. A base model for this study was Case 1 in Table 7-2 from Section 7.1.1.3 of WCAP-17788, Volume 1.

Starting with Case 1, a series of SKBOR runs were made with various levels of constant entrainment throughout the transient. For these cases, the boiloff makeup was assumed to be at a boron concentration of 2500 ppm (actual sump boron concentrations would be much lower). Table RAI-3.6-1 and Figure RAI-3.6-1 show the results of these runs. The results show that 95% RV exit steam quality (5% entrainment) will limit the core region's boric acid concentration to a level below the boric acid solubility limit of 29.27 wt% at 14.7 psia. As expected, the SKBOR results closely match theoretical limit calculated by the above equations.

The calculational mixing volume will affect the initial rate of buildup of boric acid in the core region, but will not significantly affect the ultimate limit for the core region boric acid concentration. This is demonstrated in Figure RAI-3.6-2 where the 90% RV exit quality case was rerun with a 25% reduction in the lower plenum and core region mixing volume. Figure RAI-3.6-2 demonstrates that when the core region boric acid concentration is controlled by liquid entrainment out of the reactor vessel, the core region mixing volume is not a factor.

While the ultimate limit for the core region boric acid concentration is controlled by the longer term RV exit steam quality, early entrainment will significantly delay the buildup of boric acid. This is demonstrated in a case where the long term RV exit steam quality of 98% was decreased to 96% at 50,000 seconds, 94% at 10,000 seconds, and 92% at 1000 seconds. This schedule for early entrainment extended the time to reach the boric acid solubility limit from 8 ½ hours to 20 hours when compared to the constant 98% constant RV exit steam quality case, as shown in Figure RAI-3.6-3.

Results from this sensitivity study justify the statement made in Section 7.1.1 of Volume 1 that the quality of the steam exiting the vessel remains low enough to limit the buildup of boron in the core, because it is shown that a steam quality of 80% results in a maximum theoretical boron solute concentration build-up of less than 7.2 wt% (Case 10, Table RAI-3.6-1). Steam qualities below 80% will result in a lower concentration build-up. The maximum allowable quality that will ensure excessive boron concentrations will not occur is approximately 95% (Case 6, Table RAI-3.6-1) for a boric acid solubility limit of 29.27 wt% at 14.7 psia.

<b>Table RAI-3.6-1 Entrainment Sensitivity Study</b>				
<b>Case</b>	<b>Steam Quality</b>	<b>48 hr BAC wt%</b>	<b>Theoretical Max (wt%) =2500*(1/(100-x))/1748.4*100</b>	<b>29.27 wt% HLSO Time (hr)</b>
1	100	> 100	> 100	6.10
2	99	74.19	> 100	7.22
3	98	55.20	71.49	8.93
4	97	42.43	47.66	11.95
5	96	33.75	35.75	19.36
6	95	27.71	28.60	NA
7	93	20.15	20.43	NA
8	90	14.19	14.30	NA
9	85	9.49	9.53	NA
10	80	7.13	7.15	NA

## CORE REGION BORIC ACID CONCENTRATION

- CASE 1. 100% Quality  
 CASE 2. 99% Quality  
 CASE 3. 98% Quality  
 CASE 4. 97% Quality  
 CASE 5. 96% Quality  
 CASE 6. 95% Quality  
 CASE 7. 93% Quality  
 CASE 8. 90% Quality  
 CASE 9. 85% Quality  
 CASE 10. 80% Quality

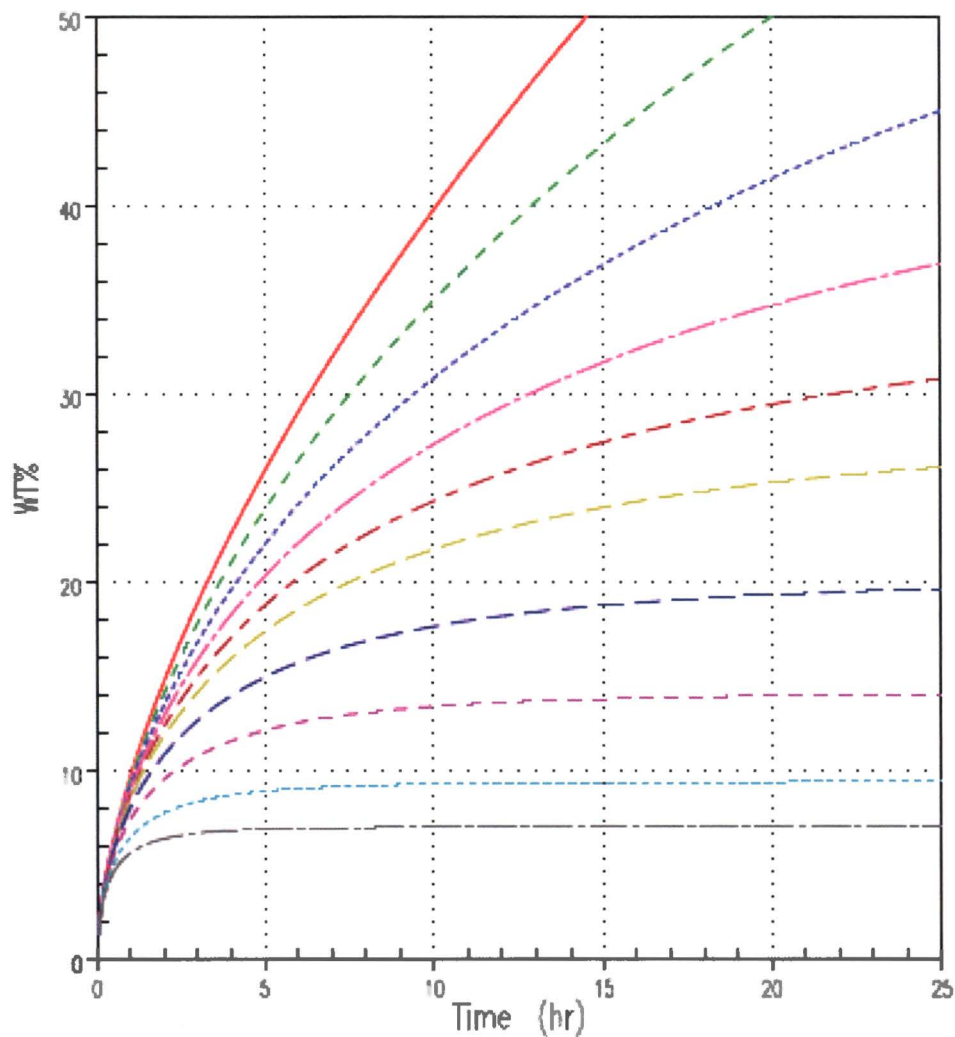
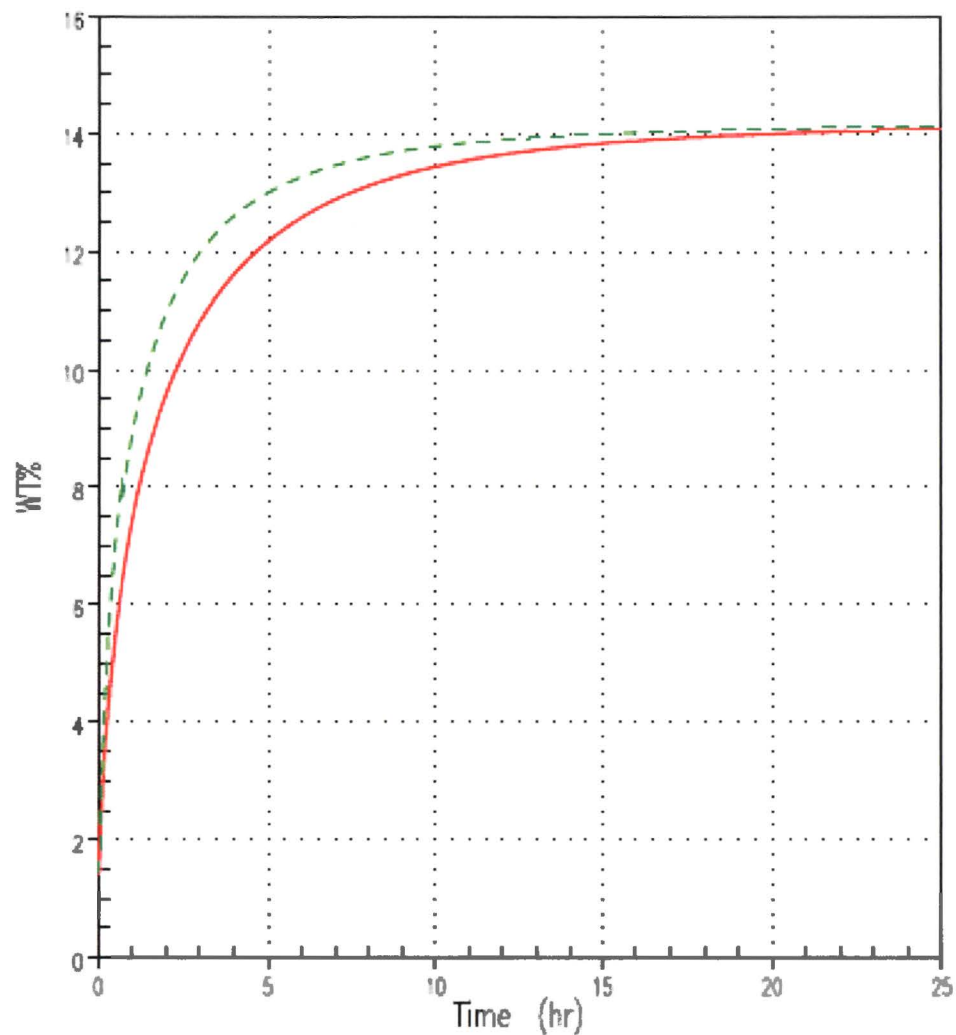


Figure RAI-3.6-1 Effect of Entrainment on Core Region Boric Acid Concentration



## CORE REGION BORIC ACID CONCENTRATION

— 90% Quality  
- - - 90% Quality, 25% Reduced Core, LP Volume



**Figure RAI-3.6-2 Effect of Reduced Mixing Volume on Core Region Boric Acid Concentration**

## CORE REGION BORIC ACID CONCENTRATION

— Constant 98% Quality  
- - Constant 90% Quality  
- - - Increasing Quality, 90-98%

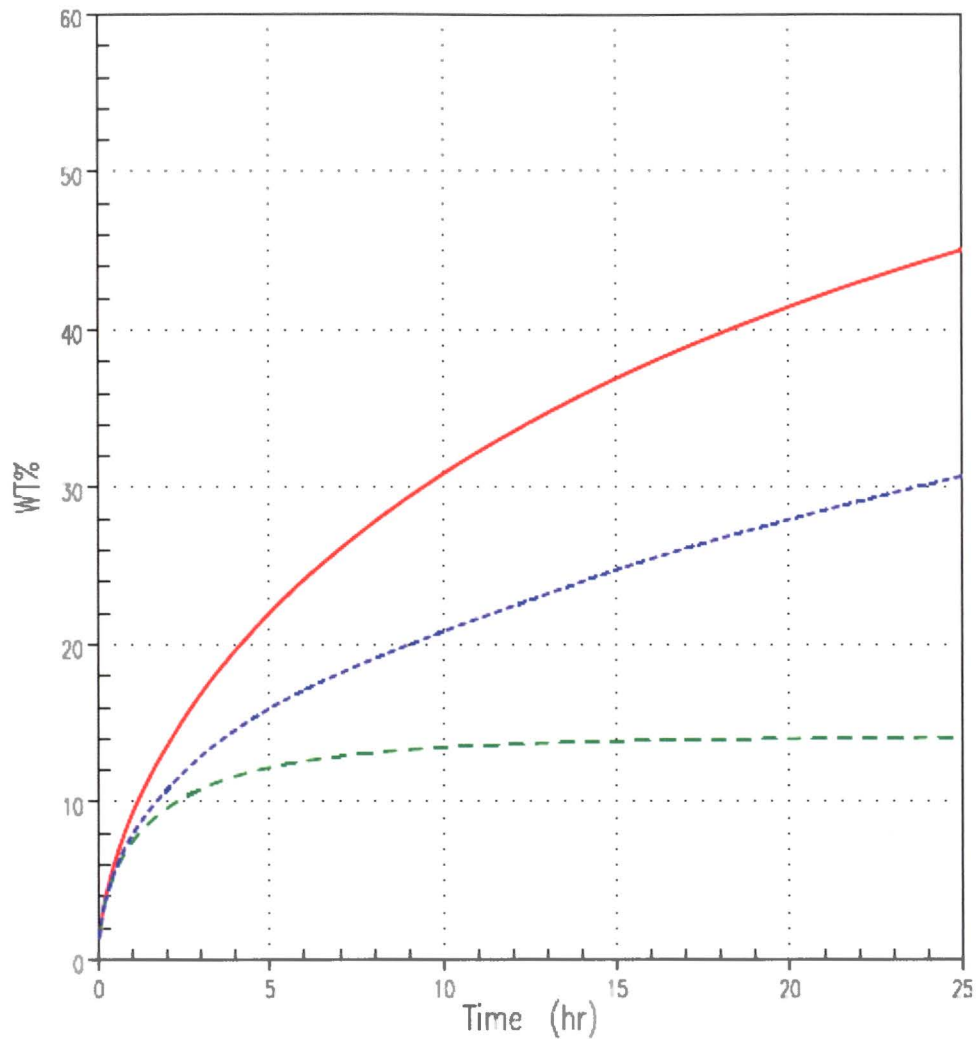


Figure RAI-3.6-3 Effect of Early Entrainment on Core Region Boric Acid Concentration



**RAI-3.7**

In Figure 7-5 of Volume 1, the exit steam quality does not appear to increase significantly at 45 minutes as might be expected when flow to the core is stopped for 2 minutes during swapover. Also, after swapover, the exit quality might be expected to be higher because the temperature of the coolant being injected to the core is assumed to be higher. Discuss the trend in exit quality with respect to these observations. Will these results be used as justification for crediting entrainment?

***Response***

Prior to sump switchover the exit steam quality is increasing because the steaming rate is decreasing as the decay heat drops. Reduced steaming rates lead to less liquid entrainment and reduced liquid carryover from the reactor vessel into the broken loop hot leg. By the time sump switchover occurs the downcomer has had enough time to fill and the collapsed liquid level is near the cold leg elevation, which is approximately 7 ft above the top of the active fuel. As such, the core mixture level remains above the top of the active fuel during the two minute interruption since there is enough excess liquid in the downcomer to replace boil-off during the interruption. At 45 minutes the steaming rate is approximately 50 lbm/s. If this boiling rate continues for 2 minutes, approximately 100 ft<sup>3</sup> of liquid is removed from the core. The downcomer annulus has a flow area of approximately 30 ft<sup>2</sup>. Assuming 100 ft<sup>3</sup> of liquid is removed from the core due to boiling; the downcomer liquid level would reduce by roughly 3 ft, which is still well above the top of the active fuel. For this reason, the exit steam quality is not expected to significantly increase during the two minute interruption. Note that the exit steam quality does increase slightly during the two minute interruption.

During sump switchover the ECCS coolant temperature is increased from 68°F to 150°F. The increase in ECCS coolant temperature increases the enthalpy of liquid entering the core, which increases boiling. Increased boiling produces a higher two-phase mixture level swell, which increases the liquid inventory in the upper plenum region. As such, liquid carryover into the broken loop hot leg increases. Since exit quality is defined as the ratio of vapor mass flow to total mass flow (vapor phase plus liquid phase), an increase in liquid carryover causes the exit quality to decrease.

Licensing basis boric acid precipitation (BAP) analyses currently do not credit liquid carryover into the broken loop hot-side piping. Although the results presented in Section 7.1.1 of WCAP-17788 Volume 1 demonstrate that liquid carryover occurs, at least early in the transient, these results are not presented as justification for crediting liquid carryover (entrainment) in licensing basis analyses. These results are used to support the SKBOR sensitivity studies documented in Section 7.1.1.3 of WCAP-17788 Volume 1. Specifically, sensitivity Case Nos. 6 and 7 which delay the accumulation start time consistent with the expected effect that liquid carryover will delay the accumulation of boron in the inner reactor vessel. See the response to RAI 3.9 for more discussion.

**RAI-3.8**

Section 7.1.1.1 of Volume 1 discusses the results of the brine test program. The section states that the head loss across the debris bed at the core inlet was maintained very low, even with equivalent fiber loading of 22.5 grams of fiber per fuel assembly (g/FA). The stated pressure drop was about an order of magnitude lower than non-chemical results obtained during testing under cold-leg conditions with 18 g/FA for the test program included in TR WCAP-16793-P-A, Rev. 2, "Evaluation of Long-term Cooling Considering Particulate, Fibrous and Chemical Debris in the Recirculating Fluid."

- a. Why are the head loss results for the brine tests significantly different than those reported in WCAP-16793?
- b. Why are the results of the brine test, exclusive of previous testing, applicable to the evaluation in WCAP-17788?
- c. Why should the results from prior testing not be considered in conclusions for WCAP-17788?
- d. The particulate to fiber ratios used during the tests in WCAP-16793 found that the limiting ratios were different for hot and cold leg flow rates. Do the conditions tested during the brine test program provide adequate assurance that particulate has no effect on the test results?

**Response**

- a. The head loss results from the brine testing are different than the WCAP-16793 cold leg break tests because the test procedures were different. In the brine testing, the largest particulate load resulted in a particulate-to-fiber (p:f) ratio of [ ]<sup>a,c</sup> Test CIB30 from the WCAP-16793 test program was conducted with a p:f ratio of [ ]<sup>a,c</sup> The particulate loads are comparable; however, because the particulate was allowed to recirculate during the WCAP-16793 test, the final in-bed particulate load prior to the addition of chemical products was higher. Results from both the subscale head loss and the WCAP-16793 test programs demonstrate that [ ]<sup>a,c</sup> Although there is no way to quantify the in-bed particulate load for Test CIB30, it would be higher than the brine tests conducted with similar particulate loads because the brine testing was conducted with a once-through particulate delivery method.

A comparison of the tests can be made by examining a once-through condition in Test CIB30. As described in the Westinghouse fuel assembly test report for the WCAP-16793 program (Reference RAI-3.8-1), the cold leg break head loss tests were conducted with a flow rate of 3 gpm. The test facility had a liquid volume of 100 gallons. At the cold leg break flow rates, one liquid turnover in the facility is approximately 33 minutes. The Test CIB30 head loss results from the WCAP-16793 program are shown in Figure 6-12 of Reference RAI-3.8-1. As the figure shows, the first fiber addition is added just before 1.5 hours. After approximately one turnover, the measured head loss is less than [ ]<sup>a,c</sup> which is comparable to the brine test head loss results conducted with debris loads similar to Test CIB30.

- b. The brine tests are not intended to be exclusive of previous testing, as applicable to the evaluations in WCAP-17788. The WCAP-16793 test program cold leg break tests also support the assertion that debris bed formation resulting from [ ]<sup>a,c</sup> of fibrous debris, or less, will not lead to high head loss prior to the arrival of chemical effects.
- c. The results of previous testing can be considered in the conclusions of WCAP-17788. As described in the response to RAI-3.27, the WCAP-16793 results support the conclusions made in WCAP-17788 regarding the cold leg break in-vessel debris limit.
- d. Section 7.1.1.1 of WCAP-17788, Volume 1 never states that particulate has no effect on the test results. The supplement states that [

] <sup>a,c</sup> The cold leg break p:f evaluation completed for the WCAP-16793 test program also showed that [

] <sup>a,c</sup> The WCAP-16793 test program conducted cold leg break tests with the Westinghouse fuel assembly at p:f ratios of [

] <sup>a,c</sup> in tests CIB29, CIB30, CIB31, CIB32, and CIB33, respectively. The WCAP-16793 cold leg break p:f study determined that a p:f ratio of [ ] <sup>a,c</sup> resulted in the highest head loss, but all tests measured a head loss of less than [ ] <sup>a,c</sup> before the addition of chemical products. The increased head loss seen in the WCAP-16793 cold leg break p:f study is also magnified because the particulate was allowed to recirculate, giving the particulate multiple opportunities to capture within the debris bed.

The primary objective of the brine test program was to investigate the effect that a debris bed has on the core-to-lower plenum buoyancy-driven exchange process. The test results demonstrated that increasing the particulate load resulted in a [

] <sup>a,c</sup>

The effect of increased particulate load on decreasing debris bed stability was also observed in the WCAP-17788 subscale head loss and the WCAP-16793 test programs. The conditions tested in the brine test program provide adequate assurance that [

] <sup>a,c</sup> This

conclusion is consistent with the WCAP-17788 head loss and WCAP-16793 test programs. From the perspective of buoyancy-driven exchange flow, the brine test results demonstrate that the addition of particulate does not significantly change [

] <sup>a,c</sup>

## Reference

- RAI-3.8-1 WCAP-17057-P, Revision 1, "GSI-191 Fuel Assembly Test Report for PWROG," September 2011.

**RAI-3.9**

Section 7.1.1.3 of Volume 1 provides the SKBOR case study that was performed to study the sensitivity of boron concentration levels in the core and Lower Plenum (LP). The results of the study are informative, but may not provide realistic or bounding results.

- a. Provide a basis for the variables and values chosen for the study.
- b. What are realistic assumptions for the core blockage area and accumulation start time for boron?
- c. Provide the results of boric acid concentration over time for a case using bounding values for the variables in part a so that the behavior under limiting conditions can be understood.
- d. The submittal states that the reactor vessel (RV) steam exit quality remains less than 80% until about 40 minutes after the LOCA. Is this based on a recirculation swapover time of 20 or 45 minutes? What effect does swapover timing have on steam exit quality?

**Response**

- a. The key variables and the basis for their values are summarized in Table RAI-3.9-1. The basis for each value is discussed in detail below.

<b>Table RAI-3.9-1 Summary of key variables and the basis for their value</b>	
<b>Key Variable</b>	<b>Basis for Value</b>
Decay Heat	A high decay heat will maximize steaming rate and minimize liquid mixing volume
Mixing Volume	A smaller mixing volume will maximize the accumulation of boron
Boron Source Concentration	A high boron source concentration will maximize the accumulation of boron
Solubility Limit	A low solubility limit will be reached earlier in the transient
Source Coolant Temperature	A saturated coolant temperature will maximize steaming and increase the accumulation rate of boron
Accumulation Start Time	An early accumulation start time will maximize the accumulation rate of boron

**Table RAI-3.9-1 Summary of key variables and the basis for their value**

Key Variable	Basis for Value
Core Blockage Area	A larger fraction of blocked area will reduce the transport rate of boron from the core to the lower plenum

#### Decay Heat

A larger decay heat value will increase the accumulation rate of boron concentrations in the reactor vessel by increasing the steaming rate and decreasing the liquid mixing volume. The Appendix K decay heat model is selected for the study. The use of Appendix K decay heat in this study is consistent with the decay heat modeling used in current Westinghouse boric acid precipitation licensing basis analyses. Appendix K decay heat bounds all other decay heat models.

#### Mixing Volume

A smaller mixing volume will increase the accumulation rate of boron in the reactor vessel. In the study, the mixing volume is minimized by:

- Accounting for voiding in the core and upper plenum regions. The void fraction in the upper plenum region is assumed to be equal to the core exit void fraction. The use of Appendix K decay heat and a saturated coolant source maximizes the calculated void fraction.
- Assuming that the two-phase mixture level only extends to the bottom of the hot leg (i.e., no liquid in the upper plenum above the bottom of the hot leg).
- No credit for other regions in the reactor coolant system that contain liquid. The barrel baffle region is not considered part of the mixing volume. The hot leg piping is not considered part of the mixing volume. In the base case, only 50% of the lower plenum volume is credited.

#### Boron Source Concentration

A higher boron source concentration increases the accumulation rate of boron in the reactor system. A value of 2500 ppm is selected for the study. This value is the maximum value for the water refueling storage tank and accumulators allowed by technical specifications for the plant selected for the study. Also, the source boron concentration is held constant during the analysis, and the effects of boron dilution in the containment sump are not considered. Including the effects of sump dilution would reduce the source concentration over time and decrease the accumulation rate of boron in the reactor vessel.

#### Solubility Limit

The reactor vessel boron concentration will reach a lower solubility limit earlier in the transient. A solubility limit of 29.27 wt% is selected for the study. This solubility limit is based on an

unbuffered boric acid solution at a pressure of 14.7 psia. The presence of buffering agents increases the solubility limit and is not credited. Elevated pressure in the reactor vessel also increases the solubility limit and is not credited.

#### Source Coolant Temperature

A saturated source coolant temperature will maximize the steaming rate, which increases the accumulation rate of boron in the reactor vessel. A source coolant temperature of 212°F is selected for the study, which corresponds to saturation temperature of pure water at the selected pressure. Subcooling in the source coolant is not credited as the presence of subcooling reduces the steaming rate and increases the effective mixing volume by reducing the void fraction.

#### Accumulation Start Time

An early accumulation start time will maximize the initial accumulation rate of boron in the reactor vessel since decay heat is highest early in the transient. An early accumulation start time will decrease the total time required to reach the solubility limit. A 100 second accumulation start time is selected for most of the sensitivities performed in the study. In Case Nos. 6 and 7 the accumulation start time is varied to understand the sensitivity of the results to accumulation start time.

#### Core Blockage Area

Increasing the fraction of core inlet blockage area will decrease the transport of boron from the core to the lower plenum. The core blockage area is varied as part of the sensitivity study to understand the sensitivity of the results to core blockage area.

- b. Given the relatively low state-of-knowledge with regard to core blockage area under large cold leg break conditions, it is difficult to define a realistic fraction of core inlet area that would accumulate debris. This is the reason for performing the sensitivity study. Considering the prototypic system and the conditions that exist under large cold leg break conditions (i.e., low flow velocities and circulation patterns at the core inlet), a significant fraction of the core inlet is not expected to collect debris.

In this study, the accumulation start time is defined as a means to represent the effects of liquid carryover from the reactor vessel into the hot-side piping. Significant liquid carryover will delay the accumulation of boron in the reactor vessel. Considering the prototypic system and the conditions that exist under large cold leg break conditions, liquid carryover is expected to delay the initial accumulation of boron for hours.

- c. The results from Case No. 1 presented in Section 7.1.1.3 of WCAP-17788 Volume 1 represent the behavior under limiting conditions. The case applies bounding values for the variables presented in Part a. for the specific type of plant used for the study.
- d. As stated in Section 7.1.1.3 of WCAP-17788 Volume 1, the statement that the reactor vessel steam exit quality remains less than 80% until about 40 minutes after the LOCA is based on the WCOBRA/TRAC results presented in Section 7.1.1 of WCAP-17788 Volume 1. Table 7-1 in

WCAP-17788 Volume 1 describes the ECCS performance modeled in the WCOBRA/TRAC simulation and shows that the transfer to sump recirculation begins at 45 minutes.

The timing of sump switchover can impact the steam exit quality because the transfer to sump recirculation can change the ECCS coolant enthalpy. Typically, the ECCS coolant temperature increases following transfer to sump recirculation. As discussed in the response to RAI 3.7, reduced steaming rates lead to less liquid entrainment and reduced liquid carryover from the reactor vessel into the broken loop hot leg. In this case, increasing the coolant enthalpy would increase the steaming rate, and decrease the exit quality.

**RAI-3.10**

PWROG-15091-P, Section 4.2.2, in describing the selection of the working fluid, provides insights into how the trend of viscosity as a function of mass percent of the working fluid is similar to that of boric acid. Figure 4-2 shows the relationship of concentration versus dynamic viscosity for various combinations of boric acid and buffers compared to the studied working fluids. Potassium Bromide (KBr), the working fluid ultimately chosen for the testing, has an opposite trend as the boric acid results. Describe why KBr was chosen as the working fluid despite this apparent difference.

***Response***

As discussed in Section 4.2.2 of PWROG-15091-P, Tritton (Reference RAI-3.10-1) states that when the Grashof number (Gr) is large, viscous forces are negligible compared with the buoyancy and inertial forces. Indeed, Tritton states that for small temperature differences (1°C), the Grashof number for water will be on the order of  $\sim 10^3$ , causing vigorous convection currents to arise. Performing Grashof number calculations for Boric Acid and Potassium Bromide results in values 3 and 2 orders of magnitude greater than that of water, respectively. Therefore, it is shown that discrepancies in viscous effects of the working fluid are negligible and the buoyancy and inertial forces remain dominant.

Additionally, the Froude number (Fr) can be used to reinforce the fact that, so long as the density gradient is equivalent between the salt solution and the boric acid being simulated, the fluid behavior will be similar as well.

Lastly, KBr was also chosen for its practicality. Due to the ability to dispose of KBr in the city sewage system, along with cost, availability, and solute properties at room temperatures to replicate boric acid density gradients, it was selected as the final working fluid.

**References**

RAI-3.10-1 D. J. Tritton, "Physical Fluid Dynamics," Oxford Science Publications, Second Edition, 1988.



**RAI-3.11**

For brine tests without debris injection in PWROG-15091-P, the following table summarizes the discussion in Section 9.

Test	Time onset of exchange flow (sec)	Core Concentration	Average Boric Acid (BA) Concentration	Brine source concentration
T012	50	[ ] weight percent (wt%) BA	lower	49 wt% BA
T032	45	[ ] wt% BA	lower	52 wt% BA
T051	55	[ ] wt% BA	higher	52 wt% BA

- Describe why the core concentration in test T032 is lower than in test T051 at the onset of exchange flow if the brine source concentration is the same between the two tests.
- Test T032 has a water supply temperature of 60.1 degrees Fahrenheit (°F), which is outside the desired range of 64-72°F. Operating outside of the desired range decreases the accuracy of the conductivity probes. How was this aspect taken into account in the results?
- Table 9-2 is used to describe the differences in the table above by comparing temperatures in the water supply to the brine supply for all three tests. The submittal states that the lower water injection temperature of T032 makes it more comparable to T051. However, the lower temperature would mean the density differences are increased, and take longer for exchange to occur, but T032 has the earliest onset of exchange flow. Explain why the lower temperature case has the earliest onset of exchange between the core and LP.
- Explain why the highest core concentration test (T051) has the latest [ ]. Logically, it seems a higher concentration would [ ].

**Response**

- To understand the differences between tests T032 and T051, a review of the water and brine supply temperatures is completed. PWROG-15091-P, Table 9-2 lists the liquid temperatures recorded at the beginning of tests T012, T032, and T051. As seen in the table, the water supply temperature in test T032 is lower than the desired range of 64 - 72°F. This temperature range was defined based on the temperature range that was considered for the conductivity probe calibration. Conductivity is dependent on temperature and lower temperatures result in lower measured conductivities. PWROG-15091-P, Figure 9-10 shows the test column inlet and outlet temperatures measured during test T032. As seen in the figure, the inlet temperature is

approximately 60°F throughout the test duration, consistent with the water supply temperature. The test column outlet temperature increases from approximately 60 to 64°F during the test duration, which is consistent with a 66°F injected brine solution mixing with the colder water in the test column. Given the above discussion, the concentrations seen in test T032 are higher than the measurements suggest due to the lower fluid temperature, which if taken into account, would make test T032 more comparable to test T051.

- b. As described in Part a., the conductivity probes measure a lower concentration as temperature decreases. The additional uncertainty in the conductivity probe measurement due to operation outside their desired temperature range was not quantified as part of the test program; however, tests conducted with fluid temperatures outside the desired temperature range are identified in PWROG-15091-P, Table 7-1.
- c. The submittal states that the lower water injection temperature of T032 makes it more comparable to T051 because the lower temperature results in a lower than expected measured brine concentration. Although it is true that a lower temperature will result in a higher density gradient driven by temperature, the density gradient created by the low injection temperature in test T032 is small compared to density gradients created by variations in brine concentration. For example, the density difference between water at 72°F and 60°F at atmospheric conditions is 0.081 lbm/ft<sup>3</sup>. On the other hand, the density difference between a KBr solution with a 0.5 wt% difference is approximately 0.225 lbm/ft<sup>3</sup> under standard conditions. As the example illustrates, the onset of exchange flow is more sensitive to variations in the brine concentration than variations in the fluid temperature. Considering that the conductivity probes have an accuracy of 0.5 wt% or greater, it is not unreasonable to expect that a test with a lower fluid temperature might produce an earlier onset of exchange flow in the testing.
- d. First, it needs to be clarified that the tests under consideration in this RAI (tests T012, T032, and T051) were performed without debris. The statement made in the RAI, "Logically, it seems a higher concentration would disrupt the debris bed earlier and initiate exchange flow." is not directly applicable to the tests in question. It would be appropriate to state that a higher core concentration would result in an earlier onset of exchange flow. Although the times reported in the submittal indicate that T051 has the latest onset of exchange flow, it is only 5 and 10 seconds later compared to test T012 and T032, respectively. When the variability in the tests is considered, such as the accuracy of the conductivity probes, a 10 second difference in the onset of exchange flow is reasonable.

**RAI-3.12**

In Section 10.3 of PWROG-15091-P, results of tests conducted with 15 wt% KBr are presented. These results show that in the AREVA Inc. (AREVA) tests, [ ] and in the Westinghouse Electric Company (Westinghouse) tests, [ ]. It is stated that the core concentration in the AREVA cases is higher, which could lead to these results. It is also stated that the AREVA inlet geometry is [ ].

- a. How were differences in core geometry addressed when determining the conditions under which [ ] will occur?
- b. Does the core KBr concentration have a higher influence than core geometry on whether or not exchange flow completely stops and on the timing of core breakthrough? Provide a comparison of test results that shows the influence of these factors on the phenomena.

**Response**

- a. Since the conditions under which [ ]<sup>a,c</sup> occurred were determined experimentally, differences in core geometry were explicitly addressed since prototypic core inlet geometries were used in the tests. The time of [ ]<sup>a,c</sup> was determined by analyzing the lower plenum solute concentration trend. The [ ]<sup>a,c</sup> was defined as the time when the lower plenum region solute concentration begins to increase (i.e., exchange flow is reestablished). The conditions under which [ ]<sup>a,c</sup> occurred were then extracted from the experimental data at the specific time.
- b. PWROG-15091-P, Section 10.6 provides results from tests that experienced [ ]<sup>a,c</sup> based on the Froude number. For the Westinghouse core inlet geometry, the Froude number [ ]<sup>a,c</sup> For the AREVA core inlet geometry, the Froude number [ ]<sup>a,c</sup>

The Froude number is calculated using Eq. 4-3 in PWROG-15091-P. Eq. 4-3 shows that the Froude number is a function of superficial velocity, U. Superficial velocity through the bottom nozzle is a function of the flow area. Differences in flow areas between the Westinghouse bottom nozzle and the AREVA lower end fitting (bottom nozzle) were considered when calculating the Froude numbers presented in PWROG-15091-P, Section 10.6. Eq. 4-3 also shows that the Froude number is a function of the core and lower plenum average density, and the density difference, both of which are functions of the core concentration.

The Westinghouse bottom nozzle flow area used in the brine testing is provided in PWROG-15091-P, Table 5-2. The AREVA lower end fitting flow area used in the brine testing is provided in the response to RAI 3.33b. Comparison of the flow areas shows that the AREVA lower end fitting used in the testing has a flow area that is more than double the Westinghouse bottom nozzle flow area. The superficial velocity through the AREVA lower end fitting will be less than half the superficial velocity through the Westinghouse bottom nozzle for the same

volumetric flow rate because the flow area is larger. As such, it is expected that [ ]<sup>a,c</sup> will occur at a lower core concentration when the AREVA lower end fitting is present for the same volumetric flow rate, debris bed, and lower plenum concentration.

As shown in PWROG-15091-P, Table 10-3, Westinghouse Test T025 and AREVA Test T043 were both conducted with a fiber mass of [ ]<sup>a,c</sup> and the volumetric flow rates at the time of [ ]<sup>a,c</sup> were similar; however, the core region concentration at the time of [ ]<sup>a,c</sup> was approximately 23% lower in the AREVA test compared to the Westinghouse test.

Westinghouse Tests T022 and T024 were both conducted with [ ]<sup>a,c</sup> of fibrous debris and the same flow conditions. [ ]<sup>a,c</sup> was observed in both tests. Test T022 was conducted with a KBr source concentration of 10 wt% and Test T024 was conducted with a 15 wt% KBr source concentration. Since Test T024 was conducted with a higher source concentration, the core concentration is expected to be higher, and the time of [ ]<sup>a,c</sup> is expected to be earlier. PWROG-15091-P, Table 10-3 shows the condition at the time of [ ]<sup>a,c</sup> for both tests. As expected, the core region concentration is higher in Test T024, and the time that [ ]<sup>a,c</sup> occurs is earlier. The core inlet flow rate was approximately 9% higher at the time of [ ]<sup>a,c</sup> in Test T024.

Based on the above discussion and the test comparisons, it can be concluded that the core inlet geometry, because of its effect on superficial velocity, has a stronger influence on determining whether or not exchange flow will stop and the time that [ ]<sup>a,c</sup> occurs. This can be confirmed by considering the change to the Froude number. If the superficial velocity is decreased by 20%, the Froude number will also decrease by 20%. If the core concentration is increased by 20%, the Froude number will decrease by less than 10%. Since the AREVA lower end fitting has a larger flow area, the superficial velocity is smaller, making this geometry more prone to [ ]<sup>a,c</sup>. Conditions with higher core concentrations also promote [ ]<sup>a,c</sup> because the potential for exchange flow is increased.

**RAI-3.13**

The timing of [ ] in Figure 10-11 of PWROG-15091-P spans between about [ ]. Explain why the [ ] is so diverse. Include a discussion about whether or not measurement uncertainty was credited in the explanation.

***Response***

PWROG-15091-P, Figure 10-11 shows average core and lower plenum concentrations from four tests completed using the AREVA lower end fitting. Although all four tests are reported as being performed at the same nominal test conditions, tests T041 and T048 had higher source KBr concentrations, which is why the average core concentrations from these two tests are higher in Figure 10-11. The diversity seen in the results from these four tests can be attributed to [ ]<sup>a,c</sup>

[ ]

] <sup>a,c</sup>

With regard to measurement uncertainty, the concentration measurements from tests T041 and T048 are less accurate than the measurements made during tests T052 and T054. The response to RAI-3.18 discusses concentration measurement accuracy. However, citing the increased measurement uncertainty in test T041 and T048 is not necessary to explain the behavior in question.

**RAI-3.14**

In PWROG-15091-P, many brine tests were conducted to understand the effect of particulate on [ ]. Figure 10-8 (tests T036 and T042) shows that particulate delays the timing of [ ]. Figure 10-12 (tests T040 and T049) shows that [ ]. Explain this discrepancy in the results. Justify that the tests conducted without particulate are representative of the behavior that would occur in the plant or state that the results of those tests are not relevant to the conclusions drawn from the testing.

**Response**

PWROG-15091-P, Figure 11-2 (tests T016 and T020) also shows that the test conducted with particulate debris (T020) resulted in an [ ]<sup>a,c</sup> compared to the test run without particulate (T016), which is consistent with the behavior shown in PWROG-15091-P, Figure 10-12. Therefore, Test T036 is the only particulate test that did not lead to [ ]<sup>a,c</sup> when compared to tests conducted at similar conditions without particulate.

The discrepancy in Test T036 is an anomaly and cannot be explained with the available brine testing; although the behavior is likely to be related to debris bed variability. An overall observation from the brine testing was that [ ]

[ ]<sup>a,c</sup> Additionally, three other tests were completed at the same condition as Test T042; Tests T035, T053, and T055. The average core and lower plenum concentrations from these four tests are shown on PWROG-15091-P, Figure 10-7. As the figure shows, [ ]

[ ]<sup>a,c</sup> The discrepancy observed in Test T036, and the inability to explain it with absolute certainty, does not invalidate the conclusions drawn from the brine testing.

**RAI-3.15**

In Figures 7-1 and 7-2 of PWROG-15091-P, it appears that the pressure increases significantly more for the delayed injection tests. Is this an actual result or is Figure 7-1 not showing the extent of the increase? Provide the magnitude of the increase for each test type.

***Response***

PWROG-15091-P, Figure 7-1 is not showing the extent of the pressure increase. Since the start of the brine injection pump was not controlled by the data acquisition system, the start time of brine injection is not always consistent with the start time of the data acquisition system. In the case of test T029

(Figure 7-1), the brine injection pump was started just prior to the start of the data acquisition system.

The column test pressure was recorded manually in the test procedures prior to starting the brine injection pump. The initial column pressure, prior to brine injection, reported for test T029 is 2.92 psi. Based on PWROG-15091-P, Figure 7-1, the maximum pressure achieved after the start of brine injection is approximately 6.3 psi. The magnitude of pressure difference for test T029 is 3.38 psi.

This pressure difference is comparable to test T021. From PWROG-15091-P, Figure 7.2, the pressure prior to brine injection is approximately 2.2 psi and the maximum pressure after brine injection is approximately 5.4 psi. The magnitude of pressure difference for test T021 is 3.2 psi.

**RAI-3.16**

At the bottom of Page 10-8 of PWROG-15091-P, verify that the test that had the lowest core region concentration is T052 instead of T054, as stated.

***Response***

Correct. Test T052 is the test that had the lowest core region concentration.



**RAI-3.17**

In PWROG-15091-P, what caused the flow rate for brine test T018 shown in Figure 10-10 to decrease so quickly at both around 1,800 seconds and at the end of the test? Was this a planned evolution?

***Response***

The reduction of flow for test T018 was a planned evolution. Note that in PWROG-15091-P, Table 6-1, the footnote in the table indicates that for test T018 the flow was manually reduced at the end of the test. At approximately 1800 seconds, the flow was manually reduced from 0.5 gpm to 0.25 gpm. At approximately 2500 seconds, the flow was manually stopped, and the test was terminated.

**RAI-3.18**

Table 5-5 of PWROG-15091-P shows the conductivity probe accuracy. The accuracy after Calibration 2 is significantly higher for all probes. Why is the accuracy much higher after Calibration 2? How was the accuracy accounted for in the overall results of the evaluation?

***Response***

A summary of the conductivity probe calibration is provided in Table RAI-3.18-1. Calibration of the probes was completed using 500 mL standards at KBr concentrations of 1, 5, 10, 15, and 20 wt%. As shown in Table RAI-3.18-1, an original five-point calibration was performed on 2/10/2015 prior to shakedown testing. On 3/2/2015, a three-point calibration check was completed. The check confirmed that the original calibrations were still valid. Then, on 4/8/2015, it was determined that the probe signal had drifted and a recalibration was performed. Finally, at the conclusion of testing on 4/15/2015, a post-calibration was performed which confirmed that the recalibration completed on 4/8/2015 remained valid.

Since multiple calibrations were performed during the duration of the test program, multiple calibration curves, with different accuracies, are needed to reduce the entire dataset. For each conductivity probe, three calibration curves are needed to reduce the data. The raw signal calibration values collected at a given standard concentration were used to create third-order polynomial curve fits that correlate the raw output signal to wt% KBr. The correlation was then applied to the experimental calibration data to determine the accuracy of each calibration curve by comparing the concentration standards to those predicted by the correlation.

As an example, the first calibration curve from probe CP2 is shown in Figure RAI-3.18-1. This calibration curve was generated using the calibration data from 2/10/2015 and 3/2/2015 and is valid for tests performed over that time period. The tests performed over that time period were the shakedown tests and tests T012 – T021. Similar curves were generated for the other seven probes.

The second calibration curve for probe CP2 is shown in Figure RAI-3.18-2. This calibration curve was generated using data from 2/10/2015, 3/2/2015, and 4/14/2015 and is valid for tests performed from 3/3/2015 to 4/7/2015. The tests performed over that time period were T022 – T051. Since drift occurred over this time period, the original calibration data was averaged with calibration data collected after the drift was identified. Because of this, the accuracy of the conductivity probes is significantly less compared to the other sets of calibration curves. Similar curves were generated for the other seven probes.

The third calibration curve for probe CP2 is shown in Figure RAI-3.18-3. This calibration curve was generated using data from 4/8/2015 through 4/15/2015 and is valid for tests completed over that time period. The tests performed over that time period were T052 – T055. Similar curves were generated for the other seven probes.

As described in PWROG-15091-P, Section 7.8, the brine concentrations are volume-averaged based on test geometry to determine a core region and lower plenum region average concentration. PWROG-15091-P, Figure 5-14 shows the axial locations of the conductivity probes as well as the control

volumes that will be used to perform the volume averaging. The physical volumes of each control volume are calculated based on the physical dimensions of the test column. Probes CP3, CP6, and CP7 were used to calculate the core region average concentration and probes CP5, CP1, CP2, and CP4 were used to calculate the lower plenum volume average concentration.

The conductivity probe accuracy was used to calculate the uncertainty in the volume-averaged concentrations by taking the partial derivative of the volume average with respect to each variable, multiplication with the accuracy in that variable, and addition of these individual terms in quadrature. PWROG-15091-P, Equation 7-8 and Equation 7-9 perform this operation for the lower plenum and core regions, respectively. As such, the accuracy of each conductivity probe is accounted for in the uncertainty of the volume-average lower plenum and core region concentrations.

<b>Table RAI-3.18-1 Summary of Conductivity Probe Calibration</b>			
<b>Calibration Date</b>	<b>Description</b>	<b>Number of Calibration Points</b>	<b>Calibration Range (wt% KBr)</b>
2/10/2015	Original calibration of probes CP1 – CP8	5	0 – 20
3/2/2015	Calibration check of probes CP1 – CP8	3	0 – 10
3/17/2015	Original calibration of probe CP1a (CP1 replacement)	5	0 – 20
4/8/2015	Recalibration of probes CP1a – CP8	5	0 – 20
4/14/2015	Calibration check of probe CP8	4	0 – 15
4/15/2015	Post-calibration of probes CP1a – CP8	4	0 – 15

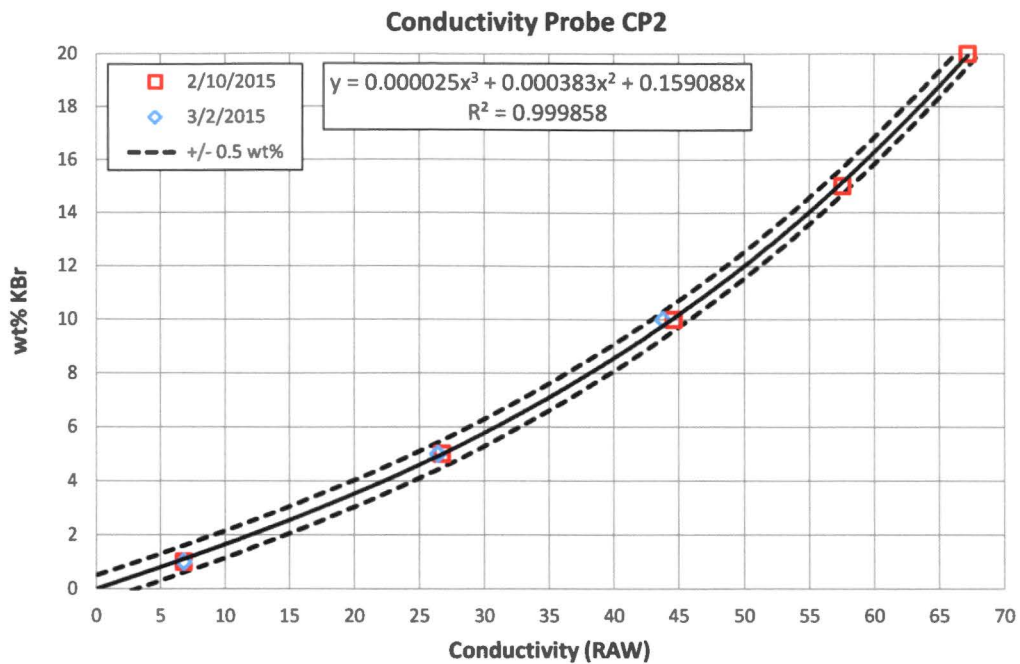


**Figure RAI-3.18-1 Conductivity Probe CP2 Calibration Curve for Experiments Conducted between 2/10/2015 and 3/2/2015**

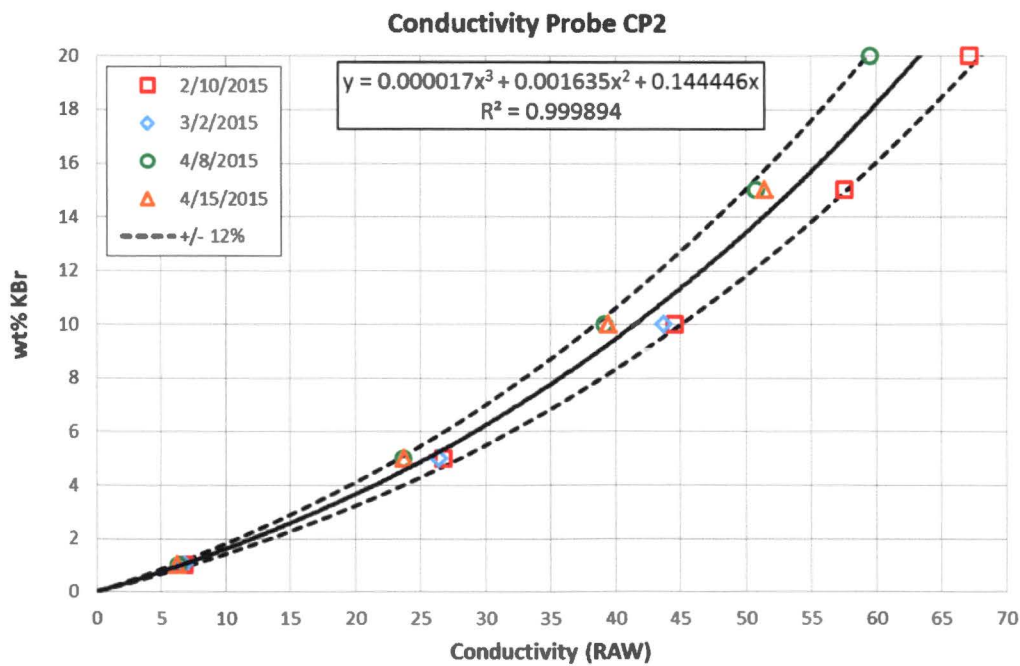


**Figure RAI-3.18-2 Conductivity Probe CP2 Calibration Curve for Experiments Conducted between 3/3/2015 and 4/7/2015**

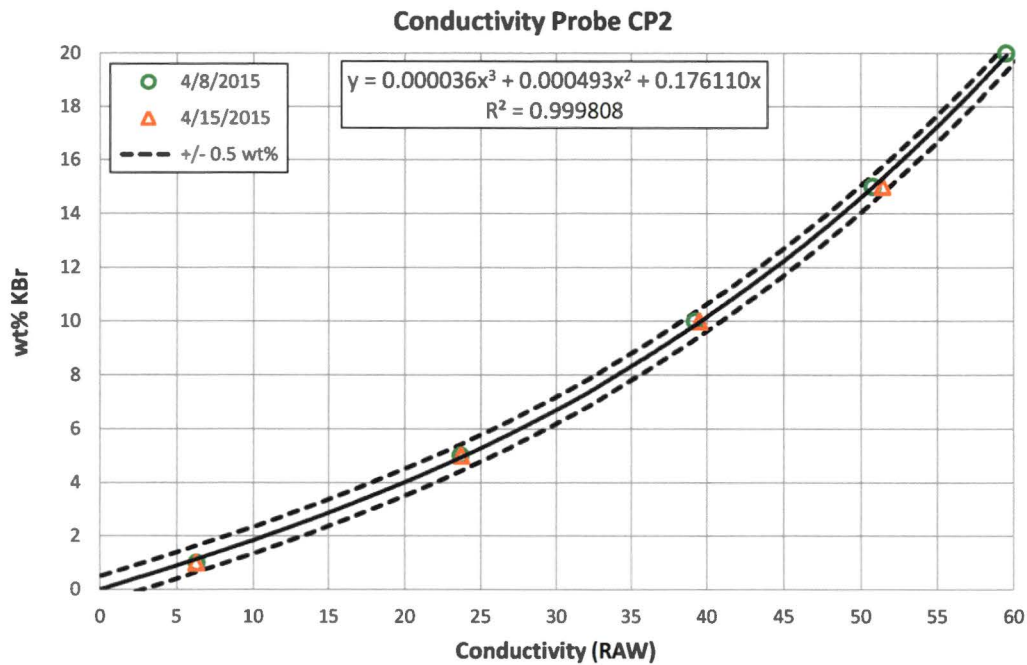


**Figure RAI-3.18-3 Conductivity Probe CP2 Calibration Curve for Experiments Conducted between 4/8/2015 and 4/15/2015**

**RAI-3.19**

In brine test T022 of PWROG-15091-P, [ ]. Can this result be used to predict [ ] for this concentration, debris loading, and core inlet geometry?

***Response***

Yes. As stated in Section 10.2 of PWROG-15091-P, [ ]<sup>a,c</sup> occurred in tests T022 and T018 at similar flow conditions (i.e., upwards flow), as well as similar density gradients. Therefore, these results can be used to predict [ ]<sup>a,c</sup> for this concentration, debris loading, and core inlet geometry.

**RAI-3.20**

Were any brine tests with delayed brine injection in PWROG-15091-P run using the AREVA core inlet geometry? If not, how can the Westinghouse results for tests with delayed brine injection be confidently used for making conclusions with the AREVA inlet geometries?

***Response***

No delayed-injection tests were run with the AREVA inlet geometry. Test results from the delayed-injection tests using Westinghouse geometry were not used to make conclusions about expected performance with regard to AREVA geometry.

In both instances (simultaneous and delayed injection), the test results demonstrate that [

] <sup>a,c</sup>

**RAI-3.21**

In PWROG-15091-P, how does the scaling and operational parameters of the brine test rig affect the results of the testing as compared to the plant condition? For example, how does the head of higher density solution in the core compare to the head of higher density solution in the test? In the core there is significant voiding while in the test the assembly is not full height. Justify that the test results or observations from the test can be applied to the plant condition considering the physical differences between the test facility and plant conditions.

***Response***

Global natural circulation through the reactor vessel depends largely upon the single-phase and two-phase gravity head. As the brine test facility is a reduced height adiabatic facility, these parameters are not well-preserved and the global natural circulation in the brine facility would be smaller than the circulation expected in the plant because of the reduced height. However, as described in PWROG-15091-P, Section 3, buoyancy-driven exchange flow between two regions separated by a horizontal partition is governed by the local geometry of the partition; in this case, the core inlet. As the brine test facility utilized prototypic core inlet geometry, the buoyancy-driven exchange flow between the core and lower plenum would be well-preserved.

It is also important to consider differences in fluid properties between brine and boric acid. The Froude number can be used to predict the onset of buoyancy-driven exchange flow by providing the relative importance of inertia to buoyancy forces. The Froude number is a function of the average density between the two fluids in the core and lower plenum and the density gradient between the two regions. This formulation reinforces the fact that so long as the density gradient is equivalent between the brine solution and boric acid, the fluid behavior will be similar. The source concentration of the brine solution used in the brine testing was selected such that the density gradient between the core and lower plenum would be preserved, as compared to actual plant conditions.



**RAI-3.27**

Volume 1 attempts to establish the basis for an in-vessel fiber limit of [ ] for the CLB scenario. Instead of providing a basis for choosing [ ], various aspects are discussed to show why [ ] would not adversely impact Long Term Core Cooling. Testing results from the brine test program and the 3x3 heated rod bundle program are presented to demonstrate that transport between the core and LP will continue in the presence of in-vessel debris without indicating the amount of debris this applies to. Provide a quantitative basis for choosing a debris limit of [ ] for the CLB scenario. Provide justification for why the limit applies to all plant categories in WCAP-17788.

**Response**

WCAP-17788, Volume 1 identifies five items that need to be addressed in order to demonstrate that the CLB in-vessel debris limit will not adversely impact long-term core cooling (LTCC):

1. Debris collection at the core inlet resulting in increased pressure losses through the inner RV such that the two-phase mixture level is reduced below that required to keep the core covered.
2. Debris collection at the core inlet such that the transport of high concentration boron solution from the core to the LP is reduced below that required to maintain adequate Boric Acid Precipitation Control (BAPC).
3. Suspended debris in the liquid-phase within the RV resulting in increased pressure losses through the inner RV due to changes in apparent fluid properties, two-phase flow characteristics, and heat transfer processes.
4. Suspended debris in the liquid-phase within the RV resulting in premature BAP due to a reduction in the two-phase mixture level or liquid inventory, a reduction in liquid carryover, or changes to the precipitation mode or precipitation location.
5. Local collection of debris on spacer grids within the core region resulting in increased frictional resistance through the core region or reduced heat transfer.

With regard to Item 1, head loss testing completed as part of the brine testing demonstrated that the head loss due to debris accumulation at the core inlet under large CLB conditions was significantly low for fibrous debris loads up to [ ]<sup>a,c</sup> The WCAP-16793-NP-A, Rev. 2 (Reference RAI-3.27-1) head loss test program also showed that the head loss was significantly low under large CLB conditions for fibrous debris loads up to [ ]<sup>a,c</sup> (See the response to RAI-3.8).

The largest pressure drop measured across the debris bed from these tests (before chemical product addition) was [ ]<sup>a,c</sup> from test CIB32 (Reference RAI-3.27-2). Under large CLB conditions, the static head in the downcomer is limited by the break elevation, and the available driving head is the difference between the static head in the downcomer and the pressure drop across the core and the broken loop to the break location. Conservative plant calculations show that the available driving head in the downcomer is greater than 1psi, which is [ ]

[ ]<sup>a,c</sup> The discussion in Section 7.1 of WCAP-17788, Volume 1

provides the basis for why a continuous debris bed cannot form at the core inlet under large CLB conditions. If a continuous debris bed does not form at the core inlet, the actual core inlet pressure drop across the debris bed would be less than that measured in the testing. However, even without crediting a non-continuous debris bed at the core inlet, the available driving head in the downcomer is large enough to ensure adequate flow reaches the core to replace boil-off and maintain adequate LTCC. As provided in WCAP-16793-NP-A, Rev. 2 (Reference RAI-3.27-1) the head loss test program is applicable to all plant categories in WCAP-17788. As such, the testing shows that Item 1 is addressed for CLB in-vessel debris loads of up to [ ]<sup>a,c</sup>

With regard to Item 2, the brine testing demonstrated that debris [ ]<sup>a,c</sup> will occur for fibrous debris loads up to [ ]<sup>a,c</sup> such that communication between the core and lower plenum will continue. Note that one test using the Westinghouse core inlet geometry was completed using a fibrous debris load of [ ]<sup>a,c</sup>. This test also demonstrated debris [ ]<sup>a,c</sup> however, the highest fibrous debris loading tested with the AREVA core inlet geometry with brine injection was at [ ]<sup>a,c</sup>. As described in PWROG-15091-P and supplemented by the response to RAI-3.21, the brine test facility preserved the key phenomena related to buoyancy-driven convection, such that the test observations are applicable to all plant categories considered in WCAP-17788. As such, Item 2 can be addressed for CLB in-vessel debris loads of up to [ ]<sup>a,c</sup>. The WCOBRA/TRAC and SKBOR analyses, and the 3x3 testing presented in WCAP-17788, Volume 1 provide additional assurance that communication between the core and the lower plenum will continue at the CLB in-vessel debris limit.

With regard to Items 3 and 4, the 3x3 boiling tests documented in WCAP-17360 (Reference RAI-3.27-3) showed that suspended debris did not significantly impact the two-phase flow characteristics or the heat transfer processes. The tests also showed that the two-phase mixture level, and the timing and location of boric acid precipitation were not significantly impacted by the presence of suspended debris. The 3x3 boiling tests were completed with a fibrous debris loading of [ ]<sup>a,c</sup>. From the perspective of the effects of suspended debris, the 3x3 testing supports a CLB in-vessel fibrous debris limit of [ ]<sup>a,c</sup>. As described in WCAP-17788, the key physical phenomena under consideration in the testing are reasonably scaled to prototypic Pressurized Water Reactor (PWR) conditions, making the tests applicable to all plant categories in WCAP-17788. As such, Items 3 and 4 can be addressed for CLB in-vessel debris loads of up to [ ]<sup>a,c</sup>

With regard to Item 5, WCAP-16793-NP-A, Rev. 2, Section 4.4 (Reference RAI-3.27-1) summarizes cladding heatup calculations performed to demonstrate that localized blockages will not impede LTCC. WCAP-16793-NP-A, Rev. 2 is approved for in-vessel fibrous debris loadings up to 15 g/FA. Sensitivity studies were performed for other PWR fuel designs in WCAP-16793-NP-A, Rev. 2, making the results applicable to all plant categories considered in WCAP-17788 since the same plants were considered in WCAP-16793-NP-A, Rev. 2. The 3x3 boiling tests showed that local debris collection at spacer grid locations was minimized such that resistance due to this local collection would not be significant for fibrous debris loads up to [ ]<sup>a,c</sup>. As such, Item 5 can be met for CLB in-vessel debris loads of 15 g/FA or greater.

Based on the testing and analysis described above, acceptable fibrous debris limits have been quantified that address each of the five items necessary to demonstrate adequate LTCC. Since all five items need to be addressed, the minimum acceptable quantity of fibrous debris is chosen for the WCAP-17788 CLB in-vessel debris limit; [ ]<sup>a,c</sup> which is applicable to all plant categories in WCAP-17788.

**References**

- RAI-3.27-1      WCAP-16793-NP-A, Rev. 2, "Evaluation of Long-Term Cooling Considering Particulate, Fibrous and Chemical Debris in the Recirculating Fluid," July 2013.
- RAI-3.27-2      WCAP-17057-P, Revision 1, "GSI-191 Fuel Assembly Test Report for PWROG," September 2011.
- RAI-3.27-3      WCAP-17360-P/NP, "Small Scale Unbuffered and Buffered Boric Acid Nucleate Boiling Heat Transfer Tests with Sump Debris in a Vertical 3x3 Rod Bundle," May 2012.

**RAI-3.28**

Section 7 in Volume 1 states that the subscale brine test program documented in PWROG-15091, states that “the testing considered a broad range of conditions prototypic of those expected to occur following a postulated large CLB LOCA.” Section 7 explains that the flow rate through the test column was scaled “based on the boil-off rate calculated for prototypic post-LOCA conditions.” Specifically, “for tests that had brine injection, the flow rate was reduced during each test consistent with the DH curve” and for tests conducted with debris only (no brine injection) the flow rate was held constant at a value consistent with DH boil-off calculated at 20 minutes post-LOCA. Figure 5-5 in PWROG-15091 shows the two flow curves defined for the brine testing. Figures 7-8, 7-9, 7-10, 8-1, 9-1, and 10-10 show measured flow rates for selected tests. The CLB methodology in Volume 3 will be used to calculate the amount of fiber delivered to the core inlet from the time of initiation of sump recirculation to the time of HL switchover. Provide the following information to assure that the flow rates in the brine testing program are bounding for expected large CLB conditions.

- a. Identify the DH model used to scale the test flow curves in Figure 5-5 and clarify whether the uncertainty in the model was accounted for (e.g., using a 1.2 multiplier).
- b. Justify that the flow rate through the test column (based on boil-off rate post-LOCA) is bounding for all plant categories in the operating fleet. If it cannot be shown as bounding, why is a plant with a flow rate outside the bounds of the test able to apply the test results?
- c. What is the accuracy of the flow rate through the test column?
- d. What is the accuracy of the brine injection flow rate?
- e. Considering the variability in both the time of initiation of sump recirculation and the time of HL switchover among individual plant units using this methodology, explain how the experimentally attained test flow conditions were prototypic. Specifically, provide justification with regard to plant units that have shorter time of initiation of sump recirculation and/or switchover to HL injection. The concern is that earlier times of initiation of sump recirculation and/or switchover to HL injection will have higher flow rates compared to the test flow rates so the bed break-through may occur in the plant at different times than observed in testing.
- f. Volume 3 explains “to allow for uncertainties, the fluid volume entering the fuel is assumed to be 1.2 times the boil-off flow rate requirement based on the decay heat at any given time in the transient starting at recirculation initiation.” Explain how the test flow condition in the brine test program accounts for the uncertainty of this parameter.

**Response**

- a. Appendix K decay heat (1.2 times the values for infinite operating time in the ANS 1971 Standard) was used to define the test flow curves.
- b. The objective of the brine testing was to determine the condition under which debris [ ]<sup>a,c</sup> occurs. In the tests, a debris bed was formed for a given brine injection source concentration. In the tests completed with higher debris loads [ ]<sup>a,c</sup> Selection of the brine flow control curve was determined based on the plant boil-off rate to ensure that the

range of flow rates used in the brine testing were representative of those expected to occur in the prototypic system, and it was not necessary to bound all flow rates in the system at all times.

- c. The accuracy of the flow rate through the test column is discussed in the response to RAI-3.29.
- d. The accuracy of the brine injection flow rate is discussed in the response to RAI-3.29.
- e. As discussed in the response to RAI-3.30, the brine tests cannot be scaled with time. Instead of simulating a transient condition in which the solute concentration in the core region is continually increasing, the strategy taken for the brine testing is to create a series of quasi-steady-state conditions in which buoyancy-driven exchange flow will occur in the subscale facility. For this reason, the time of [ ]<sup>a,c</sup> will occur at different times in the plant than observed in the testing. The brine testing determines the condition under which debris [ ]<sup>a,c</sup> is predicted to occur, and it is not necessary to preserve the time scale.
- f. There is no direct relationship between what is assumed in Volume 3 and what is used as a boundary condition in the testing. The brine testing determines under what conditions debris [ ]<sup>a,c</sup> will occur, which is independent of the assumptions made in the Volume 3 methodology.

**RAI-3.29**

Section 7.4 of PWROG-15091, "Test Column Flow Rates," states that "the outlet flow rate, which is the combination of inlet and brine injection flow rates, is measured during each experiment." The test report lists an accuracy of "0.258% rate" and a range from 0 to 100 gpm for this device.

The maximum main flow rate in all tests was 0.8 gpm equating to 0.8% of the flow meter upper range limit. The minimum flow rate in the tests using Flow Control 1 was [ ] of the flow meter upper range limit and about [ ] in the tests using Flow Control 2. Even with the addition of the brine solution injection flow of 0.5 gpm, the corresponding total flow rates and fractions are [ ]. These measured flow rates represent very small quantities compared to the upper range limit of 100 gpm of the flow meter.

- a. Clarify whether the accuracy of the magnetic flow meter provided in Table 5-4 as "0.258% rate" is valid for the entire specified range from 0 to 100 gpm or it is based on the upper range limit of 100 gpm.
- b. Provide the accuracy for the brine injection flow rate relative to setting the speed of the positive displacement pump in order "to achieve the prescribed brine injection flow rate of 0.5 gpm."
- c. Provide the calculation for the error in the main flow rate used in the tests. Justify the applied main flow rates taking into consideration the applicable measurement error. Taking into consideration that "for all brine testing, the primary flow rate was set ... to follow a predetermined flow rate curve based on decay heat," the justification should substantiate the applicability of the test results on the basis of adequate representation of DH and its uncertainty.

**Response**

- a. The instrument measurement accuracy provided in PWROG-15091-P, Table 5-4 accounts for instrument accuracy and data acquisition system accuracy. One Rosemount flow meter was used to measure the test section outlet flow rate. The instrument accuracy from the manufacturer is  $\pm 0.25\%$  of the measurement for the entire span of the instrument. The NI 9203 mA input card used to acquire signals from the Rosemount flow meter has an accuracy of  $\pm 0.04\%$  times the measured current  $\pm 0.0043$  mA. The combined accuracy of the flow meter and analog input card reported was calculated using the square root sum of squares (SRSS) of the NI 9203 analog input module and the flow meter sensor accuracy. To simplify the analysis, the analog input module accuracy is evaluated at the instrument span (100 gpm) to be equal to  $\pm 0.062\%$  ( $0.0004 + 0.0043\text{mA}/20\text{mA}$ ) of the reading. For flow meter F1, the accuracy is then  $\pm 0.258\%$  of the reading  $(0.062^2 + 0.25^2)^{0.5}$ . Since this accuracy was calculated at the instrument span (100 gpm), it bounds the accuracy of the instrument at lower readings. At the maximum flow rate used in the testing (1.3 gpm), the combined accuracy is  $\pm 0.0034$  gpm ( $0.00258 \times 1.3$  gpm).

The flow meter was calibrated to within the manufacturer's tolerance, down to 0.390 gpm, by Alden Research Lab prior to its use in the brine test facility.

- b. The manufacturer accuracy for the brine injection pump is  $\pm 1\%$  of the reading.
- c. The inlet flow rate (main flow rate) used in the brine testing was calculated by subtracting the prescribed brine injection flow rate from the measured outlet flow rate:

$$Q_{inlet} = Q_{outlet} - Q_{brine} \quad \text{Eq. RAI-3.29-1}$$

Both quantities have individual accuracies, as provided in the responses to Items a. and b. The uncertainty in the calculated inlet flow rate can be determined using the square root sum of squares method:

$$\delta Q_{inlet} = [(\delta Q_{outlet})^2 + (\delta Q_{brine})^2]^{0.5} \quad \text{Eq. RAI-3.29-2}$$

Where  $\delta Q_{outlet}$  is the accuracy of the measured outlet flow rate, and  $\delta Q_{brine}$  is the accuracy of the brine injection flow rate. At the maximum outlet flow rate used in the testing (1.3 gpm), the uncertainty in the calculated inlet flow rate is  $\pm 0.006$  gpm  $(0.0034^2 + 0.005^2)^{0.5}$ . Compared to the measured flow rates, the uncertainty in the calculated inlet flow rate due to the flow meter and brine pump accuracy is very small.

The error between the calculated inlet flow rate and the predetermined flow rate is the difference between the two values divided by the predetermined flow rate:

$$E = \frac{Q_{test} - Q_P}{Q_P} \quad \text{Eq. RAI-3.29-3}$$

Where  $Q_{test}$  is the calculated inlet flow rate from the test, and  $Q_P$  is the predetermined flow curve based on decay heat. The error is calculated for brine test T029. The measured outlet flow rate, brine injection flow rate, and calculated inlet flow rate from this test are shown in Figure 7-8 of PWROG-15091-P. The predetermined flow curve for this test is Flow Control 2 shown in Figure 5-5 of PWROG-15091-P. The uncertainty associated with the inlet flow rate ( $\pm 0.006$  gpm) is not included in the error calculation since it is small compared to the inlet flow rate. Figure RAI-3.29-1 shows the error between the test inlet flow rate and the predetermined flow curve used in the testing for brine test T029. As the figure shows, the majority of inlet flow data points fall within a range of +20% and -30% of the predetermined flow curve.

Although the error between the calculated inlet flow rate from the brine testing and the predetermined flow curve is not negligible, it is acceptable. As described in the response to RAI-3.28, the brine testing determined the conditions under which a continuous debris bed could not form at the core inlet and represented those conditions in the form of Froude number. In determining the Froude number, the inlet velocity was taken from the test data, and not the predetermined flow curve. As shown above, the uncertainty associated with the test inlet flow rate is very small ( $< 0.006$  gpm) such that the uncertainty in the velocity is small. For example, for an inlet flow rate of 0.8 gpm, the velocity through the Westinghouse bottom nozzle used in the brine testing is  $0.0619 \pm 0.0005$  ft/s. The predetermined flow curve based on Appendix K decay heat was used to establish the range of inlet flow rates that was representative of the prototypic large cold leg break scenario, but since the condition under which a continuous debris bed cannot

form was determined from the test data, it was not required that the flow rate used in the testing followed the predetermined flow curve with great accuracy.

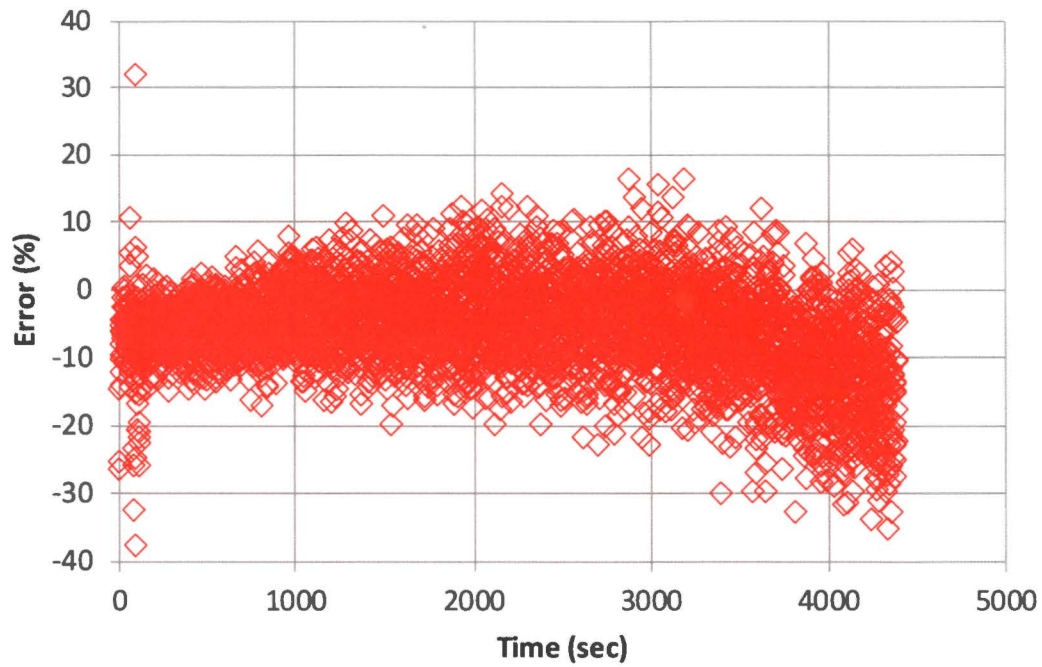


Figure RAI-3.29-1 Error in Brine Test Inlet Flow Rate from Test T029



**RAI-3.30**

A brine injection flow rate of 0.5 gpm was used in all tests described in PWROG-15091. The source concentration of KBr in the injection solution, while kept constant for each test, was set at several different concentration levels for different tests. Based on the test matrix for the Westinghouse core inlet geometry in Table 6-1, the concentrations were equal to 5, 10, and 15 wt%. As both the rate of fluid injection and the concentration of the solute in the fluid were constant in each individual test, the rate of solute injected into the test column was constant.

The scalability of the tests with regard to time is in question. The relation between the timing in the tests and the timing of the process of solute accumulation in the prototype system is not established in the test report. It is not clear how the real time scale can be transposed relative to the experimental time scale at each source concentration level used in the tests. Provide the scaling basis for the applied process of brine solute injection in the tests so that the relevance of the timing aspect of the observed processes can be related to the behavior of the prototype system.

***Response***

The design of the subscale facility makes it impossible to scale the tests with regard to time. Instead of simulating a transient condition in which the solute concentration in the core region is continually increasing, the strategy taken for the brine testing is to create a series of steady-state conditions in which buoyancy driven exchange flow will occur in the subscale facility. Figure RAI-3.30-1 shows the control volume defined for the test scenario. As the figure shows, brine will be injected into control volume 1 (V1) several inches above the test section geometry. As the brine concentration builds within V1 a density gradient will develop between V1 and control volume 2 (V2). Once the density gradient is large enough to overcome the upward flow through the flow column, buoyancy driven mass transport will begin.

Prior to starting the brine testing, simulations were performed to help define appropriate boundary and initial conditions for the testing. Applying the transport model discussed in Section 3.3 of PWROG-15091-P to the subscale system shown in Figure RAI-3.30-1, the concentration buildup and exchange flow can be estimated for various brine injection flow rates and concentrations. Figure RAI-3.30-2 shows the predicted concentration buildup in the subscale flow column using a fixed source injection concentration of 20 wt% KBr. Note, a source concentration of 20 wt% KBr was not used in the testing because it was determined that the equivalent boric acid concentration would be near the solubility limit. However, the conclusions drawn from the subscale system analysis discussed here would not change based on the value of the source concentration chosen. Figure RAI-3.30-2 shows the onset of mass transport occurs much earlier compared to the prototypic system prediction shown in Figure RAI-3.30-3. The prototypic system predicts the onset at half an hour while the subscale prediction is before 100 seconds for the four injection flow rates analyzed.

Since the time scale associated with the onset of mass transport between the core region and the lower plenum region of the subscale flow column cannot be preserved, the time at which brine is injected relative to debris was varied within the test matrix. Two brine injection times were chosen. The first time, concurrent with brine and debris injection, was chosen to represent a condition in which the onset of buoyancy driven convection had occurred consistent with the time of debris arrival. The second time,

delayed brine injection, was chosen to represent a condition in which a debris bed had begun to form prior to the onset of buoyancy driven convection.

Figure RAI-3.30-4 shows the exchange flow transient from the prototypic system, predicted from the transport model. The exchange flow begins at zero and increases over time. At 4 hours the exchange flow through the core inlet is approximately 6 lbm/sec. Scaling this value to the subscale geometry results in an exchange flow rate of approximately 0.07 gpm. Figure RAI-3.30-5 shows the estimated exchange flow rate for the subscale geometry with a 20 wt% KBr source injection concentration and various injection flow rates. The figure shows that an injection flow of 0.75 gpm results in an exchange flow rate of approximately 0.07 gpm. Although the exchange flow rate is preserved, it is only for a given point in time for a specific plant condition. For these reasons the source concentrations were varied within the test matrix in order to create a range of exchange flow rates.

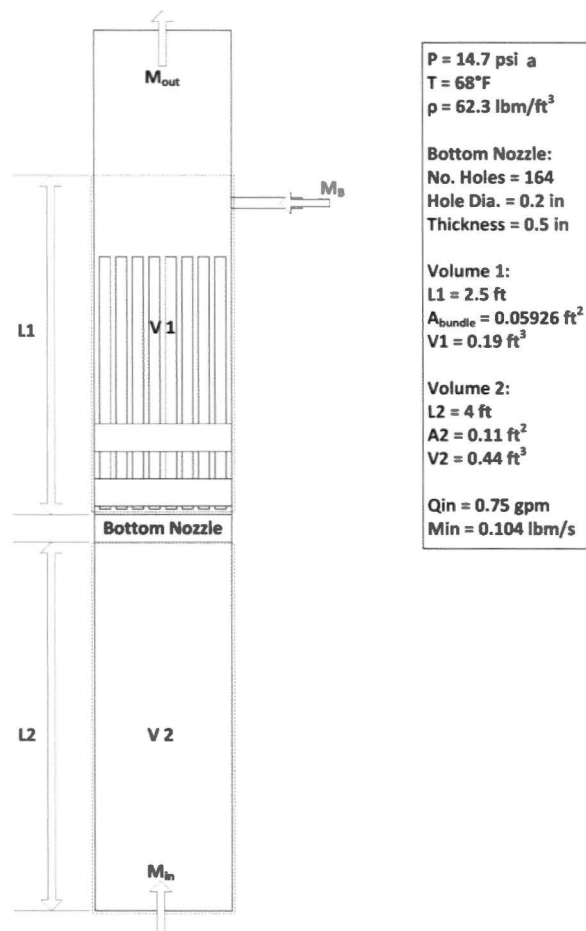


**Figure RAI-30.3-1 Subscale Test Facility Control Volume for Brine Testing**

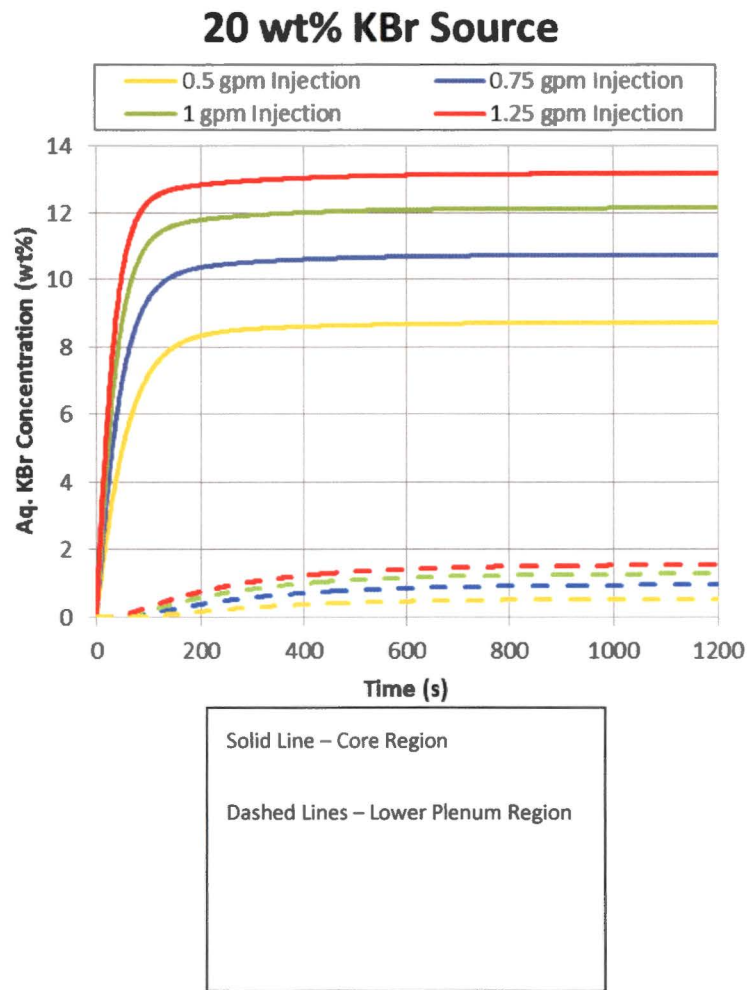
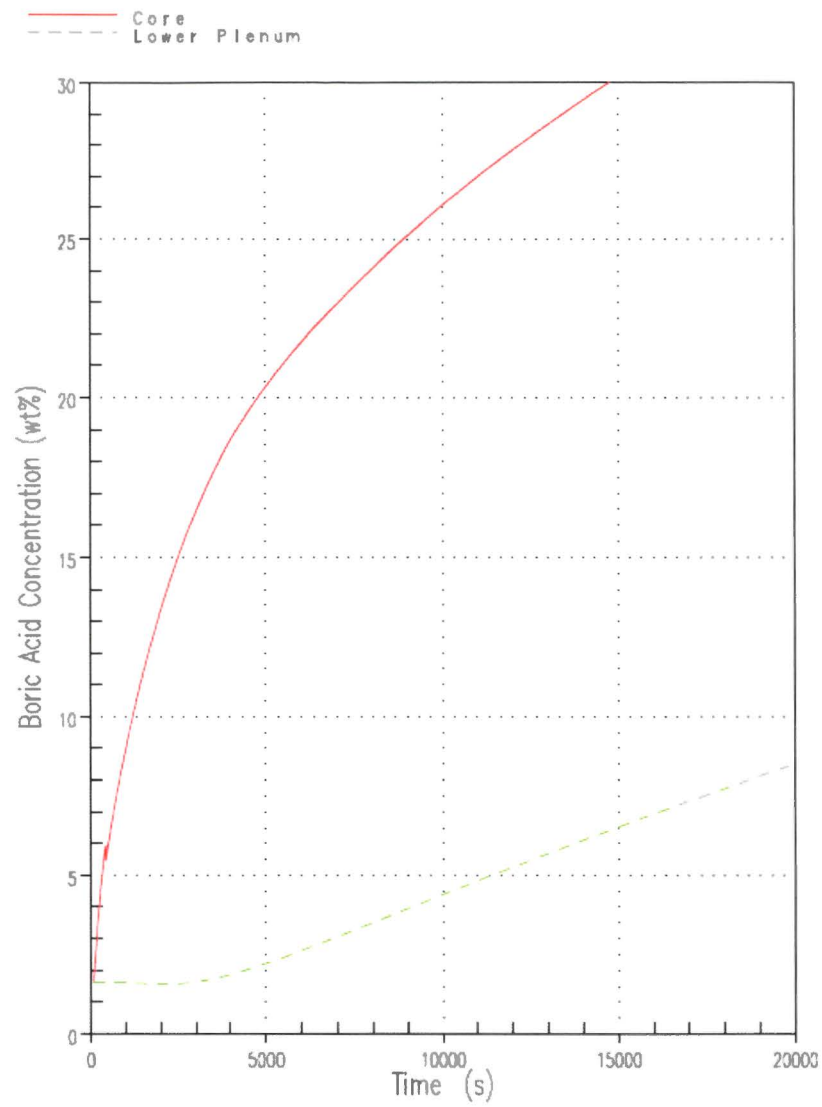
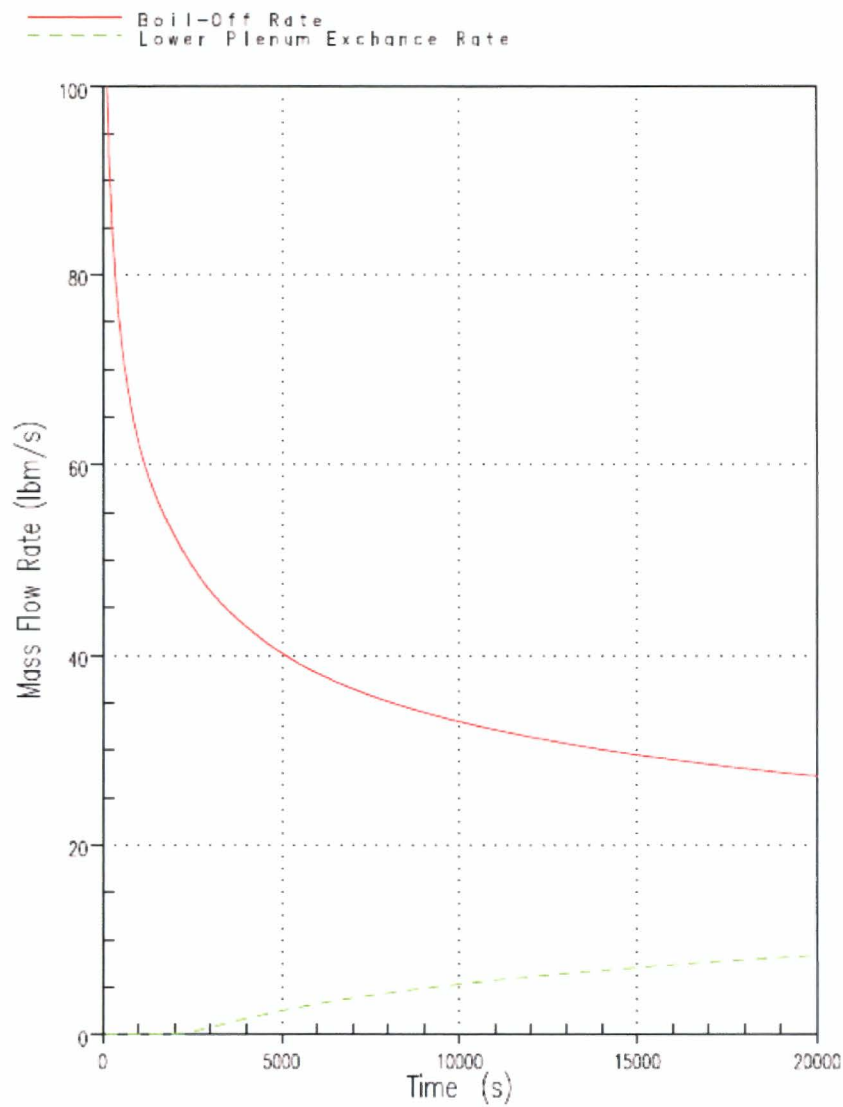


Figure RAI-3.30-2 Estimated Concentration Buildup in Brine Test



**Figure RAI-3.30-3 Predicted Boric Acid Concentration Build-Up from Boron Transport Model**



**Figure RAI-3.30-4 Boil-off Rate Compared to the Core-to-Lower Plenum Exchange Flow Rate Predicted by the Boron Transport Model**

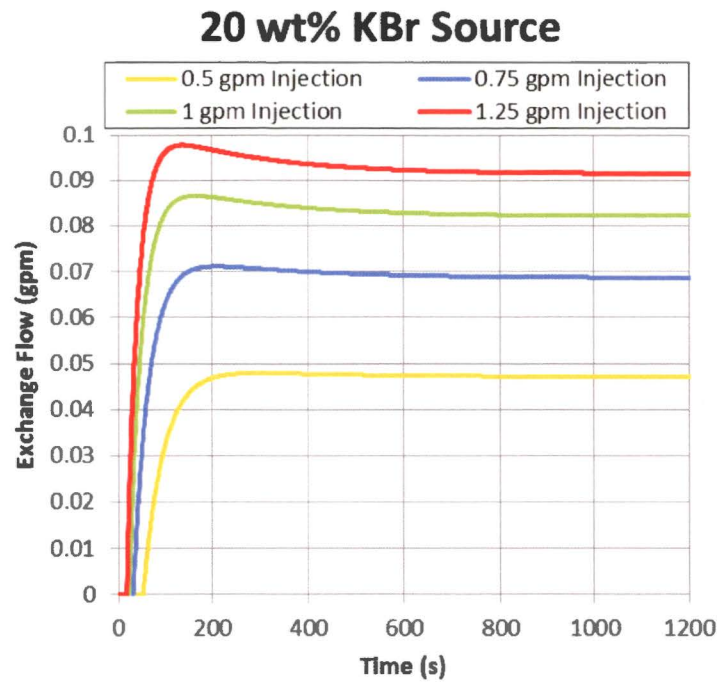


Figure RAI-3.30-5 Estimated Exchange Flow in Brine Test



**RAI-3.31**

Section 5.3 in PWROG-15091 describes the sparger pipe used for injecting the brine solution into the test section. The resulting average fluid exit velocity at the applied brine injection rate of 0.5 gpm was 0.97 feet per second (ft/sec) (29.5 centimeters per second). Based on the sketch in Figure 5-14, the holes were located along the axial length of the sparger so that the flow velocity through the hole(s) farthest from the blocked end of the sparger should have been noticeably larger than the average injection velocity of 0.97 ft/sec.

Section 5.3 explains that a brine solution injection velocity of 1.94 ft/sec corresponding to an injection rate of 1 gpm "is sufficient to induce mixing in the subscale core region but is low enough to minimize any impact on the buoyancy-driven process being studied." Section 7.1, describing the pressure response observed in the tests, states in part that "the pressure trends seen throughout the test program include a small pressure spike corresponding to the start of brine injection..." Figure 7-2 shows the pressure record for Test T021 with delayed brine injection, which is described "typical" for all tests with delayed brine injection. The initiation of brine injection caused a significant jump of about 3 pounds per square inch (psi) gauge in the system pressure. Presumably, the measurement was taken from the upstream pressure transducer, shown in Figure 5-1, which had an accuracy of plus or minus 0.289 psi based on Table 5-4. A similar effect is also seen in Figure 7-1 for Test T029 with no brine injection delay.

Provide justification that jetting did not have an impact on the test results including the timing of the testing observations. Justify that the major findings from the tests relevant to WCAP-17788 are not affected.

***Response***

Shakedown testing was performed for two different sparger hole sizes and orientations. The first sparger design utilized 6 holes all with a diameter of 3/16 inches. Upon testing this design it was observed that the brine distribution through the holes was not uniform. As a result, the hole diameters were adjusted to correct for this effect. The revised design utilized holes that progressively get smaller in 1/32 inch increments to create a more uniform brine injection. Visual inspection during shakedown testing confirmed that the brine injection is uniform across the flow area of the test section.

With regard to sparger orientation, two different orientations were considered. The first orientation had the sparger holes pointing downward while the second had the sparger holes pointing upward. Testing showed that regardless of orientation, the brine distribution and transport rates were comparable and independent of sparger design as shown in Figure RAI-3.31-1. Regardless of this outcome, the orientation with the sparger holes pointing upward was chosen to ensure that any inertia due to the injection will not influence the transport process at the core inlet or disrupt the debris bed.

As shown in PWROG-15091-P, Figures 7-1 and Figure 7-2, the test column pressure increases when the brine injection is initiated. There was a concern that this pressure spike would influence the debris bed that had formed prior to the start of brine injection in the delayed brine injection tests. This is only a concern in the delayed brine injection tests since a debris bed had not formed in the tests conducted without brine injection delay.

During the delayed brine injection tests, the debris bed was observed closely to visually determine if the initialization of brine injection led to any change to the debris bed. In all the brine injection tests, no change in the debris bed was observed when the brine injection was started. The pressure drop measured across the debris bed was also monitored when brine injection was initiated. No significant changes in the measured pressure drop were noted.

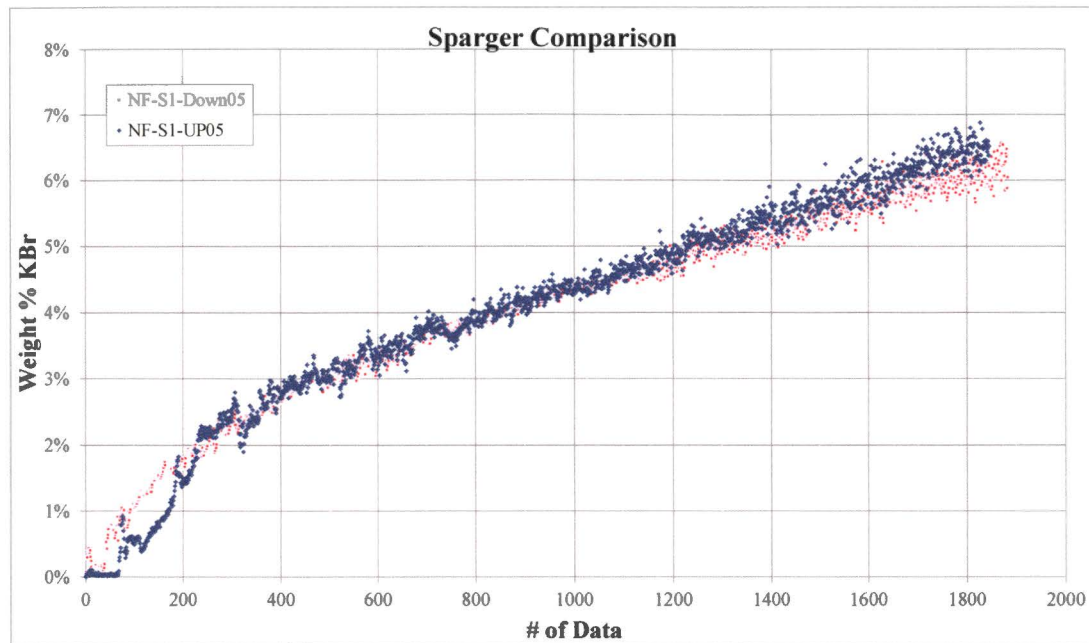


**Figure RAI-3.31-1 Comparison of KBr Concentration below Core Inlet following Injection from the Two Sparger Orientations (Holes Pointing Down vs. Holes Pointing Up)**



**RAI-3.32**

Section 3.5 “Equations,” explains that the equations for calculating the amount of fiber delivered to the core inlet are solved explicitly as a difference from time step to time step and that they can be easily solved by hand. In addition, Section 3.5.8, “Suggested Time Step Interval,” states in part that “for this evaluation, a time step of one minute is suggested.”

Section 6.5 of Volume 1, Subsection 6.5.2.1, “Time Step,” also discusses time steps for the hot leg break (HLB) methodology. The HLB method states that an iterative solution with respect to time is necessary and recommends that time step sensitivity be performed. The method suggests that the time step should be small enough to ensure that the important processes behave linearly over each time step. A starting time step value of 100 seconds is recommended.

- a. Provide results for an example case analyzed with the CLB method to illustrate the effect of the time step size. Provide the results from two calculations performed with time step sizes of 1 second and 10 seconds and compare the results from the calculation using the recommended time step size of 60 seconds.
- b. Provide results for an example case analyzed with the HLB method to illustrate the effect of the time step size. Provide the results from two calculations performed with time step sizes of 1 second and 10 seconds and compare the results from the calculation using the recommended time step size of 100 seconds.
- c. Provide quantitative criteria for assuring that the results from a calculation performed with both the CLB and HLB methods produce “stable results” along with justification as to how these criteria will be assured. State how the proposed process assures that an appropriate time step size will be applied to the proposed methods.

***Response***

- a. The method described in Section 3 of Volume 3 of WCAP-17788 calculates the mass of fibrous debris collected on the sump screen and in the reactor vessel for a large cold leg break scenario. The method uses an explicit solution technique for the calculation scheme, which implies that the error in calculated solution from the previous time step is sufficiently small that it has negligible effect on the calculations performed for the next time step, and so on. An explicit calculation scheme works well when changes in the governing parameters of interest are small from time-step to time-step.

The method description in Section 3 of Volume 3 of WCAP-17788 suggests the use of a one minute (60 second) time step to calculate the change in accumulated fibrous debris on the sump screen and in the vessel, as well as a change in fibrous debris concentration remaining in the coolant inventory of the reactor containment building sump. This approach approximates the integral of the rate of fibrous debris captured on the sump screen and in the vessel, as well as the rate of depletion of the fibrous concentration in the sump fluid inventory. There are several factors that favor the use of a one minute time interval, one of which is that minutes are a common unit of time measure for many of the input parameters (e.g., time of sump recirculation (minutes), initiation and termination of ECCS and the CSS (minutes), Hot Leg switchover (hours or minutes), and ECCS and CSS flow (gallons per minute)).

Using a constant time step for explicit calculations may be likened to the application of trapezoidal rule for integrating the area under a curve. As is the case with the trapezoidal rule, the use of successively smaller time steps in the method of Section 3 of Volume 3 of WCAP-17788 may be expected to provide for an increasingly accurate approximation of the area under a curve (i.e., the integral of the amount of fibrous debris capture on the sump screen and in the vessel, as well as the depletion of the concentration of fibrous debris in the sump inventory).

It is noted that the initial debris concentration in the sump inventory is relatively small when compared to the mass of the coolant inventory. During the long-term cooling period associated with recirculation of sump fluid by the ECCS and CSS of a plant, all plant parameters affecting the ECCS and CSS flows, and hence fibrous buildup at screens and depletion in the sump inventory, are either constant or slowly changing relative to the size of the suggested one minute (60 second) time step.

- 1) ECCS and CSS flows are constant.
- 2) At this time during the transient, the decay heat is decreasing in a slow and gradual manner.

Also, as the decay heat slowly decreases, the mass of coolant needed to match boil-off also decreases, thereby minimizing the delivery of debris-laden coolant to the core while increasing the mass of water returned to the sump inventory through the break and re-filtered by the sump screen, further decreasing the fibrous debris concentration supplied to the vessel in the next time step.

To demonstrate the acceptability of a one minute or 60 second time step, sensitivity calculations were performed for three different time step sizes; the recommended one minute (60 second) time step, a ½ minute (30 second) time step, and a 1 second time step. For these sensitivity calculations, calculation inputs were representative of a large 4-loop PWR. Specific inputs to the calculations were:

- 1) The time of switch-over from injection from the RWST to recirculation from the inventory of the sump was assumed to be at 25 minutes after initiation of the LOCA.
- 2) The ECCS and CSS flow rates were taken to be 3800 gpm and 3000 gpm, respectively.
- 3) The active volume of coolant in the reactor containment building sump was taken to be 47,343.93 ft<sup>3</sup>. At the ECCS and CSS flow rates used in the calculations, the coolant inventory in the sump was turned over once every 52.08 minutes.
- 4) The initial amount of fibrous debris in the reactor containment sump fluid is 20.4 ft<sup>3</sup>, or, assuming a density of 2.4 lbs/ft<sup>3</sup>, 49.44 lbs. of fibrous debris. As there are 193 fuel assemblies in a Westinghouse 4-loop PWR, this mass equates to a fibrous debris loading of 116.2 grams/fuel assembly upstream of the sump screen.
- 5) A capture efficiency of 55% was assumed for the sump screen. This provided for a maximum of 52.3 grams of fibrous debris per fuel assembly to be available immediately downstream of the sump screen (assuming a single-pass of the initial sump coolant volume through the vessel).

- 6) For the purposes of this sensitivity evaluation, the decay heat was held constant at its 25 minute value. This assumption maximized the flow to the core for the duration of interest for the calculation and therefore maximizes the amount of debris calculated to collect in the vessel which, in turn emphasizes the difference in calculated debris deposition in the vessel as a function of the size of the time step used in the calculation.

The calculations were run for 12 hours of problem time after initiation of recirculation from the reactor containment building sump. The results of the sensitivity calculations are shown in Figure RAI-3.32-1. Time  $t=0$  of the plot is to be taken as the start of recirculation; 25 minutes after initiation of the LOCA. A green line with green triangles as markers represents the results using a 60 second time step, a red line with red squares as markers represents the results of the 30 second time step, and a light blue line with solid diamonds as markers represents the results of the 1 second time step (see the legend on the right-hand side of Figure RAI-3.32-1). The difference between the results of the three time step durations are sufficiently small that they overlay one another on the plot of Figure RAI-3.32-1 and are indiscernible.

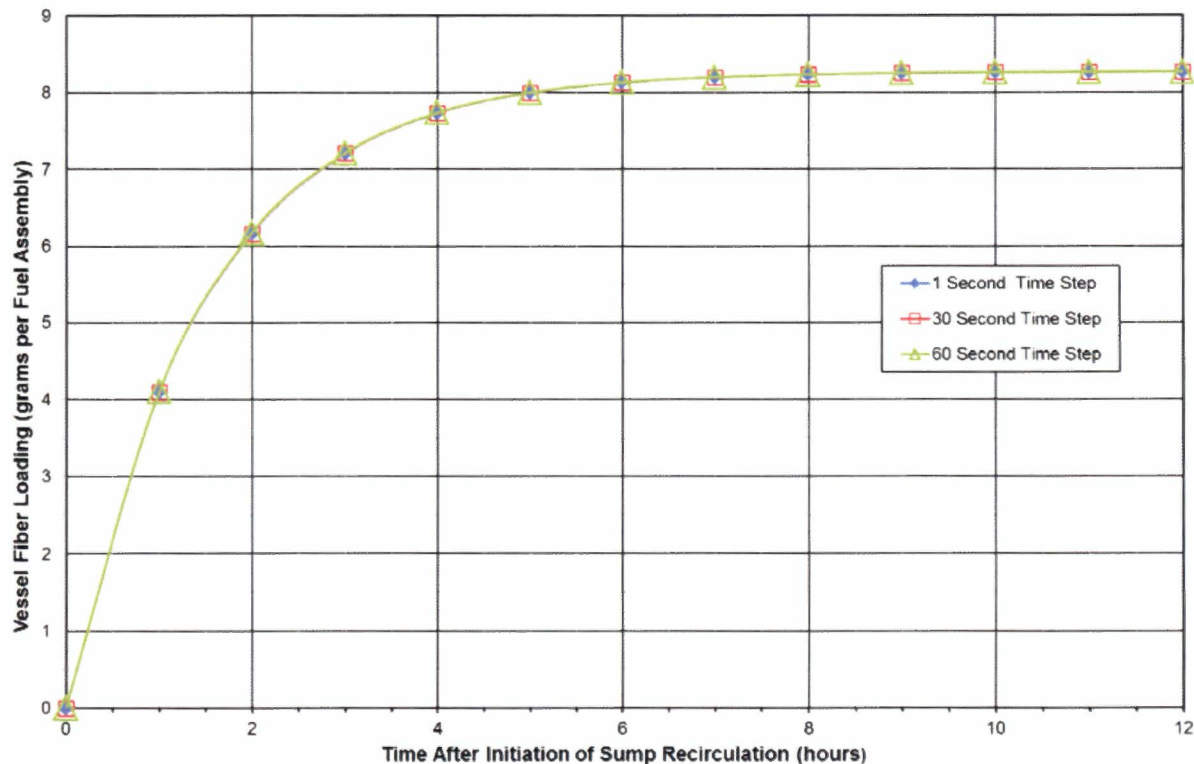


**Figure RAI-3.32-1 Reactor Vessel Fibrous Debris Collection as a Function of Time Step Selection**

From the plot of Figure RAI-3.32-1, it is concluded that following initiation of recirculation from the reactor containment building sump (time = 0), there is negligible difference between the three sets of results using three different time steps.



The hour-by-hour differences between the calculations performed using the three time steps are summarized in Table RAI-3.32-1.

**Table RAI-3.32-1 Comparison of Reactor Vessel Fibrous Debris Collection as a Function of Time Step Size**

Time (hours)	Fibrous Debris Collected (grams per fuel assembly)			Comparison	
	1 Second Time Step	30 Second Time Step	60 Second Time Step	Absolute Difference (60 sec - 1 sec)	Percent Difference
0	0.0000	0.0000	0.0000	0.0000	0.0000
1	4.0869	4.0948	4.1029	0.0160	0.3920
2	6.1528	6.1608	6.1690	0.0162	0.2628
3	7.1972	7.2032	7.2094	0.0122	0.1701
4	7.7251	7.7291	7.7333	0.0082	0.1065
5	7.9920	7.9945	7.9972	0.0052	0.0649
6	8.1269	8.1284	8.1300	0.0031	0.0386
7	8.1951	8.1960	8.1969	0.0018	0.0226
8	8.2295	8.2300	8.2306	0.0011	0.0130
9	8.2470	8.2472	8.2476	0.0006	0.0073
10	8.2558	8.2559	8.2561	0.0003	0.0041
11	8.2602	8.2603	8.2607	0.0005	0.0058
12	8.2625	8.2625	8.2626	0.0001	0.0012

From the tabular listing given in Table RAI-3.32-1, the following observations are made:

- 1) Using a smaller time step for the calculations results in a slightly smaller amount of fibrous debris collection in the reactor vessel.
- 2) Over the range of time steps studied, the maximum difference in calculated debris collection is less than 0.4% at 1 hour after initiation of recirculation from the reactor containment building sump.
- 3) At the time range of most interest, from 3 to 6 hours after initiation of recirculation from the reactor containment building sump, the difference in calculated fibrous debris collected is:
  - a. Less than 0.2% at 3 hours, and,
  - b. Less than 0.04% at 6 hours.
- 4) At 12 hours after initiation of recirculation from the reactor containment building sump, there is essentially no difference in the calculation of fibrous debris collection for any of the three time steps considered.

This small variation is expected for the following reasons; the majority of the ECCS coolant, along with all of the CSS flow (approximately 93% of the total of the ECCS and CSS flow), is recirculated back to reactor containment building sump inventory where it is again filtered by the sump strainer before being made available to enter the core, and the governing parameters in the calculation are changing slowly.

Although this exercise is performed to evaluate the impact of time step on the calculated debris collection in the vessel, the assumptions made for this comparison are conservative as they maximize the differences between calculated fibrous debris collection for the following reasons:

- 1) The decay heat was held at a constant value equal to the decay heat at the time of switchover from RWST (volume of borated water outside of the reactor containment building) injection to sump recirculation for the 12 hour duration of the calculations. As the decay heat remained high, the flow drawn into the core remained high, maximizing the deposition of fiber in the reactor vessel.
- 2) The coolant inventory of the reactor containment sump will cool down as the event progresses. The time step evaluation presented here conservatively neglects this cooldown, thereby also neglecting the increase in sensible heating of the coolant entering the core that is required before steam is generated. The assumption of maintaining the high temperature of the coolant in the sump at the time of switchover from injection from the RWST to recirculation from the reactor containment building sump maximizes the steaming rate, and consequently the mass of coolant delivered to the core during the time step assessment.
- 3) Conservative methods are used to estimate the amount of fibrous debris that is generated and transported to the sump during the initial blowdown from a large cold leg break and the washdown of that debris into the sump fluid during the drain down of the RWST (no credit is taken for the deposition of fibrous debris on intervening structures in the flow of spilled coolant as it flows to the sump screen). This provides for a conservatively large initial debris concentration of fibrous debris in the sump fluid.
- 4) The evaluation of fibrous debris accumulation in the vessel is based on the time to switchover from cold leg injection to hot leg recirculation which ranges from about 2 to 3 hours to about 6 to 8 hours for most plants with a 2 or 3 plants possibly extending to about 12 hours. However, the amount of fibrous debris used to calculate an initial fibrous debris concentration is the 30 day limit used to evaluate sump screen performance, which also accounts for erosion for those plants that generate fiberglass debris. This is an additional conservatism in the CLB calculation method.

Considering the above, the use of a one minute time step, or smaller, used in the calculation method of Section 3 of Volume 3 of WCAP-17788 to estimate the delivery of fibrous debris to the reactor vessel for a cold leg break will result in essentially the same result. Therefore, a time step of one minute (60 second) or less is reasonable and appropriate for this calculation method.

- b. WCAP-17788, Volume 1, Section 6.5 describes the method for calculating a fiber limit following a hot leg break (HLB) for any given plant. This methodology provides an analytical solution to the fiber distribution throughout the system. Because of this, errors are not introduced with each time step as they would be in a numerical solution where the differential equations are approximated. This means that the time step is not as important as it is in many thermal-hydraulic (TH) codes. While the time step does not affect the solutions to the equations, it is necessary for two other reasons: capturing the time dependent

boundary conditions such as hot leg switchover and checking the stopping criteria. For both of these needs, the time step should be small enough such that these important events are not missed by a significant amount of time.

WCAP-17788, Volume 1, Section 6.5.6 provides two example calculations for the HLB methodology. As stated therein, these cases can be used to verify an implementation of this methodology. However, the inputs for these cases are not intended to reflect realistic plant conditions; rather, they are intended to test implementation of the methodology. To that end, generic time step sensitivity studies of the nature requested would be of little value.

As described in WCAP-17788, Volume 3, an analytic solution is also used to determine the amount of fiber that reaches the core following a CLB. The solution does not rely on a numerical solution where the differential equations are approximated. The time step sensitivity study performed for the CLB solution confirmed that this calculation method is insensitive to the time step size selected (see Response 3.32a above). Since the HLB method uses a similar mathematical solution as the CLB method, variations in the time step used for the HLB evaluation are not expected to affect the solution to the equations. Therefore, a time step sensitivity study is not required for the HLB methodology described in WCAP-17788, Volume 1, Section 6.5.

- c. The acceptability of a one minute (60 second) time step for the cold leg break calculation method has been established in the response to RAI 3.32 (a). In fact, a one minute (60 second) time step provides slightly conservative calculation of fuel assembly debris loading compared to a 1 second time step.

As described in the response to Item (b) of this RAI, generic time step sensitivity studies of the nature requested for the hot leg break method are of little value. For plant-specific applications, it is recommended that each utility perform a time-step sensitivity study as part of their analysis. This process would include selecting a base time step of 100 seconds as described in Section 6.5.2.1 of WCAP-17788, Volume 1. Additional cases should be run in which this time step is varied until it can be demonstrated that the time step used is stable. Stability would be demonstrated by a change of less than one percent in final results.

***Proposed Revision to Volume 1:***

Given the above response, WCAP-17788, Volume 1, Section 6.5.2.1 is revised and expanded to read as follows:

**6.5.2.1 Time Step**

Because this problem contains time varying boundary conditions, specifically the core inlet resistance and ECCS configuration, an iterative solution with respect to time is necessary. While a time step sensitivity study is not required, the time step selected should be small enough such that the important processes (such as the timing of activation of the AFP, initiation of HLI, or stopping criteria) are captured appropriately. Therefore, a value of 100 seconds or less is recommended.

***Proposed Revision to Volume 3:***

WCAP-17788, Volume 3, Section 3.5.8 "Suggested Time Step Interval" will be revised as follows:

For this evaluation, a time step of one minute is suggested for the following reasons:

- The mass of fluid inventory in the recirculation sump is large compared to the mass of the ECCS and CSS over a one minute time step. The one minute time step provides for a relatively slow "clean up" of fibrous debris by both the recirculation sump screen and the core. The results of the calculations are therefore insensitive to variations in time step sizes around the one minute value.
- The use of a one minute time step provides for small changes in the decay heat curve from time step to time step in the time period of start of recirculation from the sump and beyond. This provides for an accurate calculation of core boil-off mass needed for long-term core cooling.
- The use of a one minute time step is convenient for the calculations as the ECCS and CSS flow rates are generally defined in units of gallons per minute.
- The use of time steps smaller than one minute have been evaluated and determined to have a negligible impact on the calculated results.

Thus, for the reasons noted above and from a practical consideration, a one minute time step for this calculation is suggested. This recommendation, however, does not preclude the use of a smaller time step

**RAI-3.33**

Section 7 in Volume 1 states that the subscale brine test program documented in PWROG-15091 "considered both Westinghouse and AREVA core inlet geometries by using prototypic fuel components." Provide the following clarifying information regarding the test rig geometry.

- a. Explain how the value of [ ], provided in: Table 5-2 in PWROG-15091 for the ratio of test column inlet flow area to installed FA inlet flow area, was calculated (the value differs from the open flow area ratio of [ ] in the same table, which is based on the flow area of [ ] holes).
- b. Table 5-2 pertains to the tests for the Westinghouse bottom nozzle. Provide a similar table for the tested AREVA fuel nozzle.
- c. For both tested fuel geometries, provide the distance between the test column wall inner surface and the closest point on the surface of the peripheral fuel rod elements for all four sides of the square test column. In addition, provide the fuel rod pitch and the fuel assembly pitch for each fuel assembly as well as the types of the prototypical fuel assemblies considered (e.g., 17x17).
- d. Was the gap between the peripheral fuel rods and the column wall measured and controlled during the test program? It appears from Figure 5-9 in PWROG-15091 that the gap on the "west" side of the depicted square is larger than the gaps on the remaining three sides (due to the location of the thimble tubes). Provide the flow area in the fuel bundle test region (Figure 9-11 in Volume 1) and the corresponding flow area of the represented region of the fuel bundle. Provide information for both Westinghouse and AREVA tests fuel bundles.
- e. Provide assurance that the test findings using the tested fuel bundle geometries remain valid for other fuel types.

**Response**

- a. The ratio of [ ]<sup>a,c</sup> is based on the bottom nozzle flow area of [ ]<sup>a,c</sup> compared to the total test column flow area (excluding fuel) of [ ]<sup>a,c</sup>. The ratio of [ ]<sup>a,c</sup> is based on the test column cross-sectional flow area of [ ]<sup>a,c</sup> compared to the total assembly flow area (excluding fuel) of [ ]<sup>a,c</sup> based on a fuel assembly pitch of [ ]<sup>a,c</sup>.
- b. Table RAI-3.33-1 shows the important dimensions of the tested lower end fitting **FUELGUARD™**.

FUELGUARD is a trademark or registered trademark of AREVA. Other names may be trademarks of their respective owners.



**Table RAI-3.33-1 Summary of Tested AREVA Bottom Nozzle FUELGUARD**

	Value	Units
Flow Openings	[ ] <sup>a,c</sup>	in
Total open flow area	[ ]	in <sup>2</sup>
Test column flow area	[ ]	in <sup>2</sup>
Open flow area ratio	[ ]	%
Ratio of test column inlet flow area to installed FA inlet flow area <sup>1</sup>	[ ]	%
<b>Note 1:</b> This value is used to scale results from the test geometry to a full-area fuel assembly.		

- c. The following gaps between the rods and the wall are given in reference to Figure 3-23 of WCAP-17788 Volume 6, re-presented below as Figure RAI-3.33-1. The grid strap in the center of the image is centered at 2 in. in a 4 in. channel. The fuel rod diameter of [ ]<sup>a,c</sup> and fuel rod pitch of [ ]<sup>a,c</sup> results in a gap of [ ]<sup>a,c</sup>. The gap on the left side, determined by the thimble tubes with a diameter of [ ]<sup>a,c</sup>, is [ ]<sup>a,c</sup>. The remaining fuel information requested is in Table 3-3 of WCAP-17788 Volume 6.
- d. The gaps were not measured. During the test program, visual inspection was performed to ensure the rods were not touching the walls. The design of the assembly insert also assured control of the gap space. Indeed, the gaps on the “west” side of the housing that had the thimble tubes were smaller, as the thimble tubes have a larger OD than the fuel rods. The flow area in the fuel bundle (excluding grids) for both fuel types is [ ]<sup>a,c</sup>.
- e. The brine testing was completed in order to demonstrate that buoyancy driven convection due to density gradients between the core and lower plenum regions is an effective process for disrupting debris bed formation at the core inlet. For buoyancy driven convection to occur, the potential force created by the density gradient must be strong enough to overcome the upward flow of liquid from the lower plenum into the core region. The fuel bottom nozzle geometries tested were selected because they have the smallest flow areas and therefore bound all other fuel bottom nozzles. The bottom nozzle geometries used for the brine testing are the same as those used in the subscale head loss final limits testing documented in WCAP-17788 Volume 6. These geometries were used in the final limits head loss testing because they have the smallest flow areas and therefore bound all other fuel bottom nozzles. Buoyancy driven convection through bottom nozzle designs with larger flow areas would be increased, for the same density gradient, since the flow velocity through these bottom nozzle designs would be less.

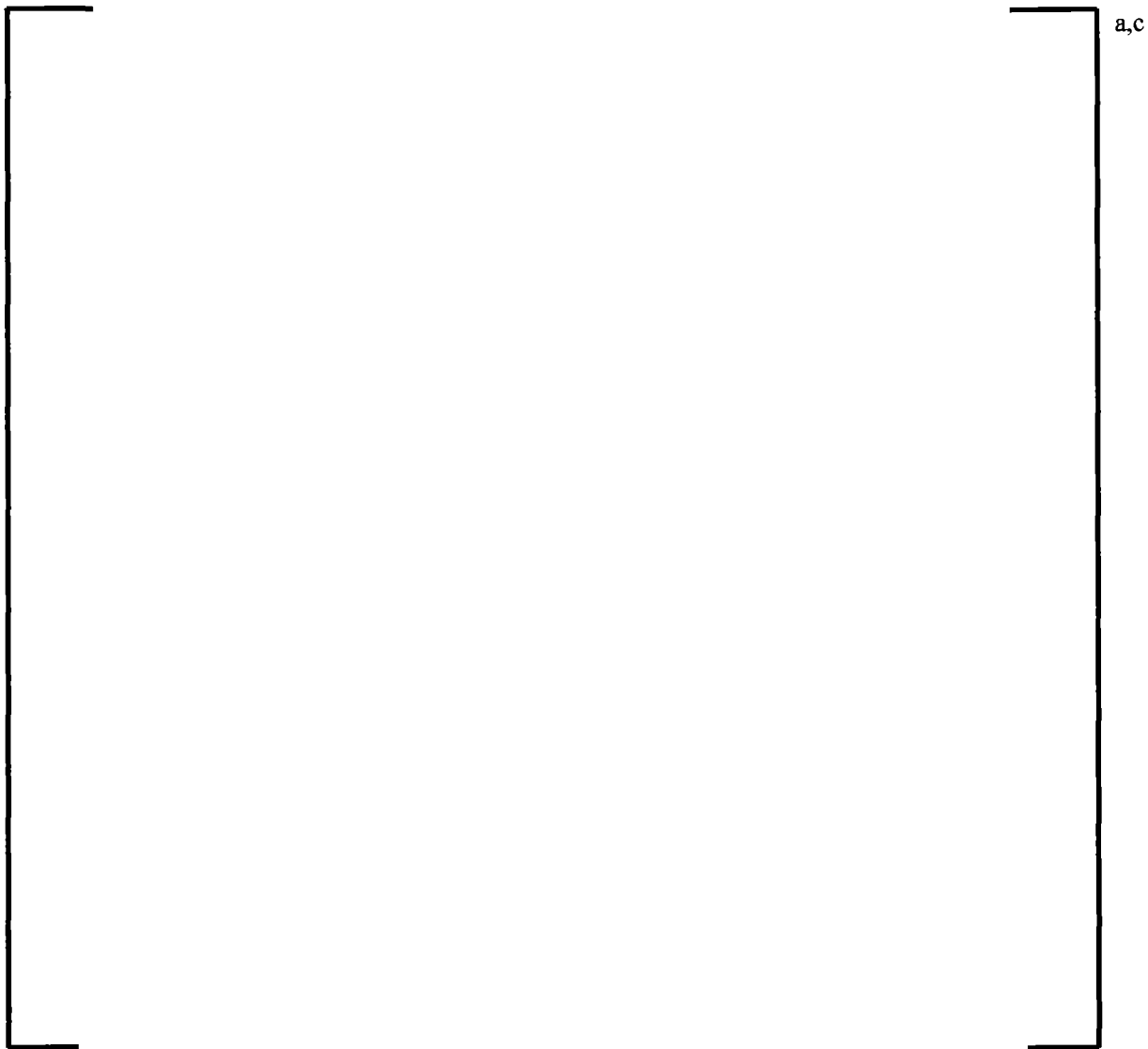


**Figure RAI-3.33-1 Test Section Top View Showing Bottom Nozzle Flow Holes with Respect to Simulated Fuel Rods**

**RAI-3.34**

Provide a sectional breakdown of PWROG-15091-P, listing the sections unrelated to the review and approval of WCAP-17788. Also list those sections needing review by the U.S. Nuclear Regulatory Commission (NRC) and explain how that determination was made. Provide any additional clarification to aid the NRC staff in the review.

***Response***

In the supplement of WCAP-17788 Volume 1, a number of processes are identified that preclude uniform debris accumulation at the core inlet. The brine test report is referenced to demonstrate that one of the processes (i.e., buoyancy-driven countercurrent exchange flow) that generate secondary flows at the core inlet is sufficient to preclude uniform debris bed formation at the fuel inlet. Secondary flows, driven by processes like buoyancy-driven exchange flow, create circulation patterns and flow oscillations at the core inlet that lead to non-uniform debris accumulation. The intent of the brine testing is to provide a demonstration that the buoyancy-driven process is sufficient to preclude uniform debris accumulation.

The Brine Test Program Report, PWROG-15091-P, is a comprehensive test report that includes a review of previous buoyancy-driven exchange flow work, a description of the test facility design and operation, the test matrix, an overview of the test results, data analysis, model development and predictions, and conclusions. Since this report is not being reviewed by the NRC staff for approval, only certain aspects of the brine test report need to be considered. Since conclusions from the summary of previous works are not considered in the supplement of WCAP-17788 Volume 1, NRC review of Section 3 of the report is not necessary. Further, any discussion related to model development and predictions contained in Sections 9, 10, and 11 do not require approval since the supplement of WCAP-17788 Volume 1 relies solely on the test observations and conclusions contained in the brine test report.

Provided below is the Table of Contents (TOC) for PWROG-15091-P. Sections deemed by the PWROG to be unrelated to the review and approval of WCAP-17788 are struck-through. The sections not struck-through are related to the test facility design and operation, test matrix, test results, and conclusions. The PWROG believes that NRC review of these sections is sufficient to conclude that the brine testing is adequate to demonstrate that buoyancy-driven countercurrent exchange flow is capable of precluding uniform debris accumulation at the core inlet under prototypic CLB conditions, which is the key piece of information referenced by WCAP-17788.

## TABLE OF CONTENTS

LIST OF TABLES .....	x
LIST OF FIGURES .....	xi
1 EXECUTIVE SUMMARY .....	1-1
2 INTRODUCTION .....	2-1
2.1 BACKGROUND .....	2-1
2.2 PROTOTYPIC SCENARIO .....	2-2
2.3 POST-LOCA BORIC ACID PRECIPITATION ANALYSIS METHODOLOGY .....	2-3
2.4 REFERENCES .....	2-3
3 REVIEW OF PREVIOUS WORK .....	3-1
3.1 BUOYANCY DRIVEN EXCHANGE FLOW THROUGH SMALL OPENINGS IN A HORIZONTAL PARTITION .....	3-1
3.2 COMBINED BUOYANCY DRIVEN EXCHANGE FLOW AND FORCED FLOW THROUGH SMALL OPENINGS IN A HORIZONTAL PARTITION .....	3-3
3.3 CORE-TO-LOWER PLENUM BORON TRANSPORT MODEL .....	3-4
3.3.1 Model Equations .....	3-6
3.3.2 Inception Criteria .....	3-7
3.3.3 Plant Simulation .....	3-7
3.4 REFERENCES .....	3-11
4 SELECTION OF WORKING FLUID .....	4-1
4.1 INTRODUCTION .....	4-1
4.2 WORKING FLUID PROPERTIES .....	4-1
4.2.1 Density .....	4-1
4.2.2 Dynamic Viscosity .....	4-3
4.2.3 Electrical Conductivity .....	4-6
4.3 CONCLUSIONS .....	4-7
4.4 REFERENCES .....	4-8
5 TEST FACILITY DESCRIPTION .....	5-1
5.1 OVERVIEW .....	5-1
5.2 DEBRIS INTRODUCTION .....	5-2
5.2.1 Debris Constituents .....	5-5
5.3 BRINE INTRODUCTION .....	5-6
5.4 FLOW CONTROL .....	5-7
5.4.1 Main Flow .....	5-7
5.4.2 Brine Injection Flow .....	5-8
5.5 TEST COLUMN .....	5-8
5.6 TEST GEOMETRY .....	5-10
5.6.1 Westinghouse Core Inlet Geometry .....	5-10
5.6.2 AREVA Core Inlet Geometry .....	5-10
5.7 DEBRIS FILTRATION .....	5-13
5.8 WATER CHEMISTRY .....	5-14
5.8.1 Main Coolant Supply .....	5-14
5.8.2 Brine Solution .....	5-14
5.9 POST-TEST INSPECTION AND CLEANUP .....	5-15

5.10	INSTRUMENTATION .....	5-15
5.10.1	Concentration Measurement .....	5-18
5.11	REFERENCES .....	5-21
6	TEST MATRIX .....	6-1
6.1	TEST SERIES 1 .....	6-1
6.2	TEST SERIES 2 .....	6-1
7	OVERVIEW OF TEST RESULTS .....	7-1
7.1	TEST COLUMN PRESSURE .....	7-1
7.2	TEST COLUMN INLET AND OUTLET TEMPERATURE .....	7-3
7.3	DEBRIS INJECTION SYSTEM TANK LIQUID LEVELS .....	7-7
7.4	TEST COLUMN FLOW RATES .....	7-8
7.5	CUMULATIVE FIBER MASS .....	7-11
7.6	PRESSURE DROP ACROSS FUEL COMPONENTS .....	7-12
7.7	TEST COLUMN AND BRINE TANK CONCENTRATIONS .....	7-15
7.8	VOLUME-AVERAGED CONCENTRATIONS .....	7-16
8	TESTS WITHOUT BRINE INJECTION .....	8-1
9	TESTS WITHOUT DEBRIS INJECTION .....	9-1
9.1	CALCULATION OF EXCHANGE FLOW RATE .....	9-8
9.2	PREDICTION OF EXCHANGE FLOW RATE .....	9-10
10	TESTS WITH CONCURRENT BRINE AND DEBRIS INJECTION .....	10-1
10.1	TESTS CONDUCTED WITH 5 WEIGHT PERCENT POTASSIUM BROMIDE SOURCE CONCENTRATION .....	10-2
10.2	TESTS CONDUCTED WITH 10 WEIGHT PERCENT POTASSIUM BROMIDE SOURCE CONCENTRATION .....	10-5
10.3	TESTS CONDUCTED WITH 15 WEIGHT PERCENT POTASSIUM BROMIDE SOURCE CONCENTRATION .....	10-11
10.4	CALCULATION OF EXCHANGE FLOW RATE .....	10-14
10.5	PREDICTION OF EXCHANGE FLOW RATE .....	10-16
10.6	PREDICTION OF DEBRIS BED BREAK THROUGH .....	10-17
11	TESTS WITH DELAYED BRINE INJECTION .....	11-1
11.1	MODEL PREDICTIONS OF DELAYED BRINE INJECTION TESTS .....	11-4
12	SUMMARY OF RESULTS AND CONCLUSIONS .....	12-1